Cellular specificities of Jasmonate repressors in *Arabidopsis thaliana* roots

Dissertation

zur Erlangung des

Doktorgrades der Naturwissenschaften (Dr. rer. nat.)

vorgelegt der

Naturwissenschaftlichen Fakultät I – Biowissenschaften

Martin-Luther-Universität Halle-Wittenberg

von Andreas Schenke

Gutachtende:

I: Prof. Dr. Steffen Abel

II: Prof. Dr. Sascha Laubinger

III: PD Dr. Susanne Berger

Tag der öffentlichen Verteidigung: 22.08.2024

Summary

Plants, as sessile organisms, are constantly exposed to various challenges from both abiotic and biotic stress factors. To acclimate to their environment, plants have evolved intricate systems that regulate development and stress responses throughout their life cycle. One crucial regulator is the phytohormone (+)-7-*iso*-jasmonoyl-L-isoleucine (JA-Ile). JA-Ile plays a pivotal role in governing diverse processes, including defense responses, fertility development, and vegetative growth. While basal levels of JA-Ile are typically low during normal growth, its biosynthesis is rapidly induced by external stimuli, primarily stressors like mechanical damage. The perception of JA-Ile in plants relies on a sophisticated system where JA-Ile triggers the degradation of transcriptional repressors known as JASMONATE ZIM DOMAIN PROTEINS (JAZs). This degradation leads to the release of transcription factors (TFs), which subsequently mediate JA-Ile responses. Remarkably, JA-Ile is the sole known bioactive hormone, but regulates numerous Jasmonate (JA) responses, precisely tailoring them based on the unique functions of different cell types. Despite our comprehensive understanding of the fundamental components of JA-Ile perception and signalling, the precise way this individual molecule can induce unique responses in diverse cell types, as well as how these responses are finely regulated within the cells, remains uncertain. In this thesis, I have gathered data suggesting that the JAZ protein family plays an essential role in modulating cellular specificities. Using transcriptional and translational reporters, I have demonstrated that the 13 Arabidopsis JAZs exhibit cell-specific expression patterns. Through phenotype analysis of single and multiple order *jaz* knockout (KO) mutants, lacking the expression of JAZs, I have shown that JAZs act to repress cell-specific JA signalling within the context of their expression sites. Furthermore, in this project I revealed for the first time, that JAZs have different ligand-dependent turnover rates *in planta* when expressed under their native promoters, suggesting that JAZ proteins are crucial for modulating JA-Ile responses. Collectively, my results provide new insights into how JA-Ile modulates cellular specificities and fine-tunes responses to enable plants to adapt effectively to diverse environmental challenges.

Zusammenfassung

Pflanzen sind als sessile Organismen ständig verschiedenen Herausforderungen durch abiotische und biotische Stressfaktoren ausgesetzt. Um sich an ihre Umgebung anzupassen, haben Pflanzen komplexe Systeme entwickelt, die die Entwicklung und Stressantworten während ihres Lebenszyklus regulieren. Ein entscheidender Regulator ist das Phytohormon (+)-7-*Iso*-Jasmonoyl-L-Isoleucin (JA-Ile). JA-Ile spielt eine entscheidende Rolle bei der Steuerung verschiedener Prozesse, einschließlich Abwehrreaktionen, Fruchtbarkeitsentwicklung und vegetativem Wachstum. Während die JA-Ile Level während des normalen Wachstums in der Regel niedrig sind, wird seine Biosynthese schnell durch externe Reize, hauptsächlich Stressoren wie mechanische Schäden, induziert. Die Wahrnehmung von JA-Ile in Pflanzen beruht auf einem ausgefeilten System, bei dem JA-Ile den Abbau von Transkriptionsrepressoren auslöst, die als JASMONATE ZIM DOMAIN PROTEINS (JAZs) bekannt sind. Dieser Abbau führt zur Freisetzung von Transkriptionsfaktoren (TFs), die anschließend die JA-Ile-Reaktion vermitteln. Bemerkenswert ist, dass JA-Ile das einzige bekannte bioaktive Hormon ist, aber zahlreiche Jasmonat (JA)-Antworten reguliert und sie präzise an die einzigartigen Funktionen verschiedener Zelltypen anpasst. Trotz unseres umfassenden Verständnisses der grundlegenden Komponenten der JA-Ile-Wahrnehmung und -Signalgebung bleibt der genaue Weg, auf dem dieses einzelne Molekül einzigartige Reaktionen in verschiedenen Zelltypen auslösen kann, sowie wie diese Reaktionen innerhalb der Zellen fein reguliert werden, unklar. In dieser Arbeit sammelte ich Daten, die darauf hinweisen, dass die JAZ-Proteinfamilie eine wesentliche Rolle bei der Modulation zellspezifischer Eigenschaften spielt. Unter Verwendung von transkriptionellen und translationellen Reportern habe ich gezeigt, dass die 13 Arabidopsis JAZs zellspezifische Expressionsmuster aufweisen. Durch Phänotyp-Analysen von einzel- und mehrfachen *jaz* Knockout (KO) Mutanten, welche die Expression von JAZs nicht aufweisen, habe ich gezeigt, dass JAZs dazu dienen, zellspezifische JA-Signalgebung im Zusammenhang ihrer Expressionsorte zu unterdrücken. Darüber hinaus habe ich in diesem Projekt erstmals gezeigt, dass JAZs unterschiedliche Liganden-abhängige Umsatzraten *in planta* aufweisen, wenn sie unter ihren nativen Promotoren exprimiert werden, was darauf hindeutet, dass JAZ-Proteine entscheidend sind, um JA-Ile-Reaktionen fein abzustimmen. Insgesamt liefern meine Ergebnisse neue Erkenntnisse darüber, wie JA-Ile zellspezifische Eigenschaften moduliert und Reaktionen fein abstimmt, um es Pflanzen zu ermöglichen, sich effektiv an vielfältige Umweltbedingungen anzupassen.

Experimental work from this thesis was conducted at the Leibniz Institute of Plant Biochemistry (Halle, Germany), Department of Molecular Signal Processing in the research team 'Jasmonate Signaling' led by Dr. Debora Gasperini, from Nov 2018 to Dec 2022

Publications arising from my Doctoral work:

- **Schenke A**, Mielke S, Zimmer M, Gasperini D (in preparation). In vivo expression and turn-over specificities of Jasmonate repressors.

  - Contributions: Generated and analysed data presented throughout the thesis

- Bartrina I, Werner S, **Schenke A**, Gasperini D, Schmuelling T (in revision at Plant Phys) Root-derived cytokinin regulates flowering time in *Arabidopsis thaliana* through components of the age pathway.

  - Contributions: For this research article I assessed the plastochrone of grafted plants with affected CK responses. This part was in addition to my thesis and is not presented herein, but allowed me to gain more experience in phytohormone research.

Table of contents

List of abbreviations

Throughout this thesis the amino acid one-letter or three-letter code is used according to IUPAC-IUB (recommendations 1983).

α-LeA	α-linolenic acid
4,5-didehydrojasmonate	4,5-ddh-JA
11-HPHT	11(*S*)-hydroperoxy-hexadecatrienoic acid
13-HPOT	13(*S*)-hydroperoxy-octadecatrienoic acid
13-LOX	13-LIPOXYGENASE
35Sp	Overexpressing promoter from Cauliflower mosaic virus
A	Adenine
aa	Amino acid
ABBA	Abscisic acid
ABI5	ABA INSENSETIVE 5
ACC	Aminocyclopropane-1-carboxylic acid
AFU	Arbitrary fluorescence units
AGP30	ARABINOGALACTAN PROTEIN 30
ANOVA	Analysis of variance
AOC	ALLENE OXIDE CYCLASE
AOS	ALLENE OXIDE SYNTHASE
ARF	AUXIN RESPONSE FACTOR
ARGONAUTE 18	AGO18
ARGIS	Arabidopsis Gene Regulatory Information Server
ASK1	ARABIDOPSIS-LIKE SKP1
ATP	Adenosintriphosphat
AUX/IAA	AUXIN/INDOLE-3-ACETIC ACID
bHLH	Basic helix loop helix
BiFC	Bimolecular fluorescence complementation
BR	Brassinosteroid
C	Cytosine
C-terminal	Carboxy-terminal position of a peptide or protein
Cas9	CRISPR-ASSOCIATED PROTEIN 9
cDNA	Complementary DNA
CIT	CITRINE
CK	Cytokinin
CMID	Cryptic MYC domain
co	Cortex

COI1	CORONATINE INSENSITIVE 1
Col-0	Columbia 0
COR	CORONATINE
CRISPR	Clustered Regularly Interspaced Short Palindromic Repeats
CTS	COMATOSE
CUL1	CULLIN 1
Cys	Cysteine
DAD1	DEFECTIVE IN ANTHER DEHISCENCE 1
DEG	Differentially expressed gene
DELLAs	(Aspartic acid–Glutamic acid–Leucine–Leucine–Alanine), a group of repressors of the GA pathway
DEPC	Diethyl pyrocarbonate
DLL	DAD1-LIKE LIPASE
DZ	Differentiation zone
dn-OPDA	Dinor-oxo-phytodienoic acid
DNA	Deoxyribonucleic acid
dNTP	Deoxynucleotide Triphosphate
do	days old
E1	Ub-activating enzyme
E2	Ub-conjugating enzyme
E3	Ub-ligase
e.g.	*exempli gratia* (=for example)
EDTA	Ethylenediamine tetraacetic acid
EDZ	Early differentiation zone
EGL3	ENHANCER OF GLABRA
EIL1	EIN3-LIKE 1
EIN3	ETHYLENE INSENSITIVE 3
en	Endodermis
ep	Epidermis
ERF1	ETHYLENE RESPONSE FACTOR 1
ET	Ethylene
EZ	Elongation zone
F-Box	Protein motif for Protein-Protein interaction
FAR1	FAR RED-IMPAIRED RESPONSE 1
FHY3	FAR-RED ELONGATED HYPOCOTYL3
Fig.	Figure
Fig. S	Supplemental Figure
G	Guanine
G-Box	DNA motif for DNA-Protein interaction
GA	Gibberellin

GAI	GIBBERELLIC ACID INSENSITIVE
GFP	Green Fluorescent Protein
GL	GLABRA
GO	Gene ontology
GRP2	GLYCINE RICH PROTEIN 7
GUS	Beta-glucuronidase
h	Hour(s)
HDA	HISTONE DEACETYLASE
HSD	Honest significant difference
IAA	Auxin
IAR3	IAA-ALANINE RESISTANT 3
ICE	INDUCER OF CBF EXPRESSION
Ijas9	insensitive jas9 degron
ILL6	IAA-LEUCINE RESISTANT-LIKE 6
InsP	Inositol phosphate
ITC	Titration calorimetry
IVU	*In vitro* ubiquitylation assay
JA	Jasmonate
JA-Ile	(+)-7-*iso*-jasmonoyl-L-isoleucine
JAO	JASMONATE-INDUCED OXYGENASE
JAR1	JASMONATE RESISTANT 1
Jas	Jasmonate associated motif
JASSY	Export transporter of OPDA from the chloroplast
JAZ	JASMONATE ZIM DOMAIN PROTEIN
jazNB	*jaz* non-basally mutant (*jaz7-1 jaz8-v jaz10-1 jaz13-1*)
jazQ	*jaz* quintuple mutant (*jaz1-2 jaz3-4 jaz4-1 jaz9-4 jaz10-1*)
jazT	*jaz* triple mutant (*jaz1-3 jaz2-6 jaz3-4*)
JGP	*JAZ10p:GUSPlus*
JID	JASMONATE INTERACTION DOMAIN
JMT	JASMONIC ACID CARBOXY METHYL TRANSFERASE
JNV	*JAZ10p:NLS-3xVEN*
JOX	JASMONIC ACID OXIDASE
K	Rate constant
KEG	KEEP ON GOING
K_D	Dissociation constant
KO	knock-out
KOR1	KORRIGAN 1
LCI	Luciferase complementation imaging

LCMD	Laser Capture Microdissection
LDZ	Late differentiation zone
logFC	Logarithmic fold change
LRRs	Leucine-rich repeats
LSM	Laser scanning microscope
MED25	MEDIATOR OF RNA POLYMERASE II TRANSCRIPTION SUBUNIT 25
MeJA	Methyl-JA
MES	2-(N-morpholino)ethanesulfonic acid
MG132	A reversible proteasome inhibitor
MGDG	Monogalactosyldiacylglycerol
min	Minute(s)
mRNA	Messenger ribonucleic acid
MS	Murashige and Skoog media
MYB	MYB-DOMAIN PROTEIN
MYC	Basic-helix-loop-helix transcription factor
MZ	Meristematic zone
N	Nucleotide
N/A	Not available
n.a.	Not analysed
n.d.	No data available
N-terminal	Amino-terminal position of a peptide or protein
NaOAc	Sodium acetate
NASC	Nottingham Arabidopsis Stock Centre
NGS	Next generation sequencing
NINJA	NOVEL INTERACTOR OF JAZ
NLS	Nuclear localisation signal
OPDA	12-oxo-phytodienoic acid
OPR	OXOPHYTODIENOATE REDUCTASE
p	Promoter
PCC1	PATHOGEN AND CIRCADIAN CONTROLLED 1
PCR	Polymerase chain reaction
PD	Pull-down
PDF	PLANT DEFENSIN
PE	Paired-end
pe	Pericycle
PEG	Polyethylenglycol
Phe	Phenylalanine
PhyB	Phytochrome B
PIF	PHYTOCHROME INTERACTING FACTOR

PI	Propidium iodide
pLDDT	per-residue model confidence score
PLT	PLETHORA
QC	Quiescent centre
qRT-PCR	Real-time quantitative reverse transcription PCR
rat.	ratiometric
RBX	RING BOX-LIKE PROTEIN 1
rc	Root cap
RDH6	ROOT HAIR DEFECTIVE 6
RFP	RED FLUORESCENT PROTEIN
RGA	REPRESSOR OF GA
RGL1	RGA-LIKE1
RNA	Ribonucleic acid
RNA POLY II	RNA POLYMERASE II
RSL1	RDH6-LIKE1
RT-PCR	Reverse transcription-PCR
SA	Salicylic acid
SAT	Saturation binding assay
SCF	SKP1/CULLIN/F-Box complex
SD	Standard deviation
SDS	Sodium lauryl sulfate
sec	Second(s)
SEM	Standard error of the mean
sgRNA	Single guide RNA
SKP1	S-PHASE KINASE-ASSOCIATED PROTEIN 1
SL	Strigolactone
SMXL	SMAX1-LIKE
st	Stele
ST2A	SULFOTRANSFERASE 2A
t	time point
T	Thymine
TBE	Tris-Borate-EDTA Buffe
T-DNA	Transfer-DNA
Tab.	Table
Tab. S	Supplemental table
TAD	Transcriptional activation domain
TAIR	The Arabidopsis information resource
TBE	Tris-borate-EDTA
TF	Transcription factor
TIC	TIME FOR COFFEE
TIR1	TRANSPORT INHIBITOR RESPONSE 1

TOE	TARGET OF EAT
TOM	TOMATO (nucleus localizing)
TPL	TOPLESS
TPR	TOPLESS-RELATED
TSAP	Thermosensitive alkaline phosphatase
TT8	TRANSPARENT TESTA 8
Ub	UBIQUITIN
UBC21	UBIQUITIN-CONJUGATING ENZYME 21
UBQ10	UBIQUITIN 10
UTR	Untranslated region
v (as for *jaz8-v*)	*Vash-1* (assession of *Arabidopsis thaliana*)
VEN	VENUS
VSP	VEGETATIVE STORAGE PROTEIN
WT	Wild-type
WRKY57	WRKY DNA-BINDING PROTEIN 57
WUS	WUSCHEL
Y2H	Yeast-two-hybrid
ZIM	JASMONATE ZINC FINGER INFLORESCENCE MERISTEM

Section I - Introduction

Phytohormones

Plants regulate developmental processes, as well as responses to external stimuli through small molecules known as plant hormones or phytohormones (Dharmasiri, 2013; Gilroy & Breen, 2022; Santner & Estelle, 2009). To date, several small molecules have been identified as essential phytohormones, including Auxins (IAAs), Abscisic acid (ABA), Brassinosteroids (BRs), Cytokinins (CKs), Gibberellins (GAs), Ethylene (ET), Strigolactones (SLs), Salicylic acid (SA), and Jasmonates (JAs) (Dempsey et al., 2011; Dharmasiri, 2013; Gilroy & Breen, 2022; Gomez-Roldan et al., 2008; Santner & Estelle, 2009; Umehara et al., 2008; Wasternack & Hause, 2013). Plant hormones have traditionally been classified as "growth-regulating" hormones (IAAs, CKs, GAs, BRs, and SLs) and "stress/defense-response" hormones (ABA, ET, SA, and JAs) (Gilroy & Breen, 2022). However, this simplified classification has evolved thanks to intense research efforts describing extensive crosstalk during development, growth, and stress responses (Gilroy & Breen, 2022). In fact, some plant hormones can act synergistically, while others exhibit more antagonistic functions depending on their concentration and cellular context (Gilroy & Breen, 2022; Hirose et al., 2008; Mockaitis & Estelle, 2008; Symons et al., 2008; Wasternack & Hause, 2013; Yamaguchi, 2008; Zhao, 2008). For instance, synergistic crosstalk between GA and JA has been demonstrated for stamen development (Cheng et al., 2009; Song et al., 2011), while these phytohormones act antagonistically in terms of plant growth and defense responses (Hou et al., 2010; Kazan & Manners, 2012; Yang et al., 2012).

The effect of phytohormones results in transcriptional reprogramming in plants, resulting in significant changes in terms of growth, development, and acclimation (Dharmasiri, 2013; Gilroy & Breen, 2022; Santner & Estelle, 2009). Remarkably, some phytohormones, such as GAs, SLs, IAAs, and JAs, achieve rapid transcriptional reprogramming by degrading repressors of transcription factors (TFs) (Fig. 1A) (Aziz et al., 2022; Gupta & Chakrabarty, 2013; Mashiguchi et al., 2021; Mockaitis & Estelle, 2008; Wasternack & Hause, 2013). During this process, three essential enzyme systems (the ATP-consuming Ub-ACTIVATING ENZYME [E1], Ub-CONJUGATIING ENZYME [E2], and Ub-LIGASE [E3]) conjugate the target repressors with single or multiple Ubiquitins (Ubs), eventually leading to rapid repressor degradation by the proteasome (Fig. 1B) (Hershko & Ciechanover, 1998; Kelley & Estelle, 2012; Santner & Estelle, 2010; Vierstra, 2009; Voges et al., 1999). For instance, in the case of Auxin/INDOLE-3-ACETIC ACID 4 (IAA4) and IAA6 in pea, two repressors of IAA signalling, studies have demonstrated half-lives of approximately 6 and 8 minutes, respectively, at a concentration of 20 µM IAA (Abel et al., 1994; Aziz et al., 2022; Mockaitis & Estelle,

2008). Hence, the rapid degradation of transcriptional repressors by phytohormones enables prompt responses through an "activation by degradation" process (Guilfoyle, 1986; Kelley & Estelle, 2012). Notably, the specificity for various protein targets is determined by the wide diversity of E3 ligases (Vierstra, 2009).

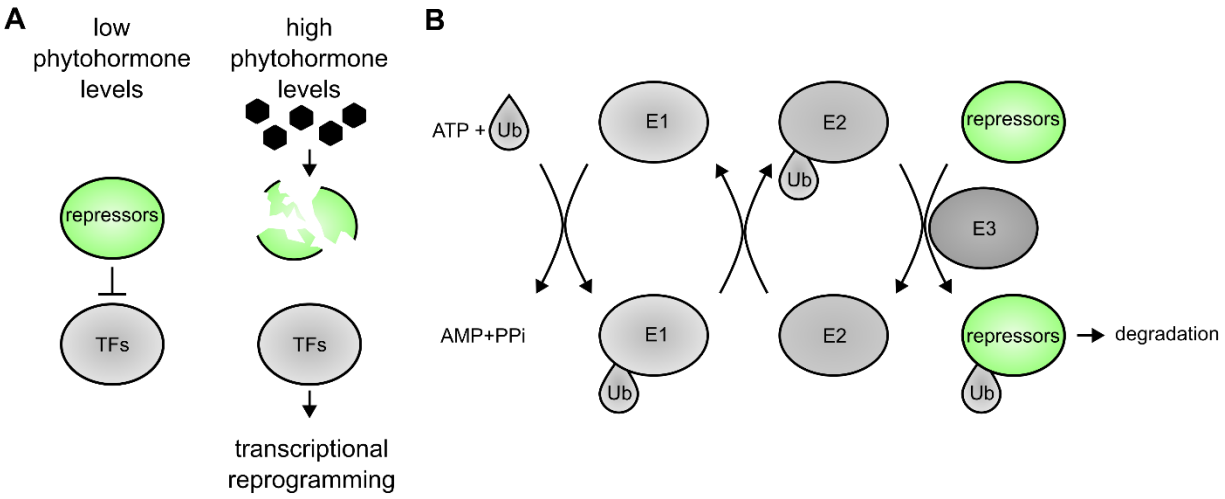

Figure 1. Schematic model of transcriptional reprogramming via repressor degradation. (**A**) Several phytohormones (including Auxins [IAAs], Gibberellin [GAs], Strigolactones [SLs], and Jasmonates [JA]) induce transcriptional reprogramming by facilitating the degradation of transcription factor (TF) repressors. Under low levels of these phytohormones, repressors inhibit the transcriptional activity of TFs. In contrast, the presence of these phytohormones triggers the degradation of these repressors, thereby releasing TFs to orchestrate transcriptional reprogramming within the plant. (**B**) Repressor degradation involves a series of ubiquitylation steps, carried out by three enzyme systems. In the initial step of targeted ubiquitylation, UBIQUITIN (Ub) binds to the UBIQUITIN ACTIVATING ENZYME (E1) with the consumption of Adenosine-triphosphate (ATP). Ub is then transferred to E2 UBIQUITIN CONJUGATING ENZYME (E2). Eventually, the UBIQUITIN LIGASE (E3) enables the transfer of Ub from the E2 to a lysine residue on the target protein, in this case, a transcriptional repressor). This process can be iterated, resulting in poly- or multiubiquitylation of one or more targets. Eventually, the ubiquitylated substrates are earmarked for degradation by the proteasome.

The phytohormone Jasmonate-isoleucine (JA-Ile) and its functions

The phytohormone JA Ile (+)-7-*iso*-jasmonoyl-L-isoleucine, commonly known as JA-Ile, stands out as it governs a broad spectrum of signalling responses in higher plants, such as stress responses and development regulation (Dennis & Norris, 2015; Wasternack & Feussner, 2018). Given that the transcriptional, proteasomal, and metabolic reprogramming is energetically costly, the system is typically kept repressed under basal conditions (Barto & Cipollini, 2005; Zavala & Baldwin, 2006).

As reviewed in (Browse & Wallis, 2019), JA-Ile is crucial for male fertility in *Arabidopsis thaliana* (Arabidopsis), as JA-Ile promotes stamen filament elongation, anther dehiscence, and viability of pollen grains. Hence, Arabidopsis plants that are unable to synthesise or sense JA-Ile display male sterility (Browse & Wallis, 2019). In the case of JA-Ile-deficient mutants, such as loss-of-function mutants of JA-Ile

biosynthesis gene *ALLENE OXIDE SYNTHASE* (*AOS*), these defects can be rescued by the exogenous application of JA to flower buds (McConn & Browse, 1996; Park et al., 2002). In contrast, mutants with impaired JA signalling exhibit resistance to external JA treatment and, consequently, remain sterile (Feys et al., 1994). Notably, while JA-Ile governs the development of male reproductive organs in Arabidopsis, it regulates also female fertility and seed development in tomato (Dobritzsch et al., 2015; Li et al., 2004; Schubert, Dobritzsch, et al., 2019; Schubert, Grunewald, et al., 2019). This highlights that, despite sharing the same JA core signalling pathway, the outcomes can be specific to organs and species (Browse & Wallis, 2019).

Moreover, JA-Ile plays a crucial role in safeguarding plants against herbivorous insects, necrotrophic pathogens, and wounding (Wasternack & Feussner, 2018). Arabidopsis mutants deficient in JA-Ile production or signalling exhibit heightened susceptibility to larvae of herbivorous insects such as *Bradysia impatiens*, *Pieris rapae*, and *Spodoptera littoralis* (Bodenhausen & Reymond, 2007; McConn et al., 1997; Reymond et al., 2004). Additionally, the JA pathway regulates responses to necrotrophic pathogens, as JA-deficient mutants are more vulnerable to oomycetes (*Pythium jasmonium*) and fungal pathogens, such as *Alternaria brassicicola* and *Botrytis cinerea* (Kachroo & Kachroo, 2009; Manners et al., 1998; Penninckx et al., 1996; Vijayan et al., 1998) compared to the wilde type (WT). Similar susceptibility patterns have been reported in several other plant species besides Arabidopsis (e.g., tobacco and tomato), indicating a general role of JA-Ile in plant defense responses (Halitschke & Baldwin, 2003; Howe et al., 1996).

Transcriptome analysis comparing WT plants with JA-deficient plants exposed to insect herbivory led to the identification of over 100 JA-specific transcripts (Reymond et al., 2000). These transcripts include genes involved in indole glucosinolate metabolism, resource reallocation (e.g., *VEGETATIVE STORAGE PROTEIN 2* [*VSP2*]), and insecticidal activity (e.g., Lectins) (Jander et al., 2001; Lambrix et al., 2001; Peumans & Van Damme, 1995; Rask et al., 2000; Reymond et al., 2004; Strauss & Agrawal, 1999). Interestingly, transcriptional profiles of plants subjected to specialist herbivores (e.g., *Pieris rapae*) or generalist herbivores (e.g., *Spodoptera littoralis*) exhibited nearly identical patterns (Reymond et al., 2004). Furthermore, comparisons between plants fed on by insects and mechanically wounded plants revealed that wounding serves as an excellent elicitor of JA responses and is a valuable model for studying defense against herbivores, as the transcriptomes were highly similar (Reymond et al., 2000).

Remarkably, studies have also demonstrated that JA-Ile plays a role in antiviral defense responses, as reviewed in (Yan & Xie, 2015). However, its precise role remains controversial, as reports suggesting that JA-Ile can either positively or negatively regulate plant antiviral defense mechanisms (Lozano-Duran et al., 2011; Oka et al., 2013; Wu et al., 2017; Yan & Xie, 2015; Yang et al., 2008; Zhang et al., 2016). A recent study has revealed that JA-Ile levels increase in rice upon infection with *Rice stripe virus* (Yang et al., 2020). This increase in JA-Ile levels enhances the transcription of a core RNA silencing component called *ARGONAUTE 18* (*AGO18*) in rice, subsequently promoting RNA silencing defense responses against the virus (Yang et al., 2020).

JA-Ile is also pivotal for regulating abiotic stress responses (Howe et al., 2018). This implies stress reactions to high salinity, drought, and significant temperature fluctuations (Hu et al., 2013; Kazan, 2015; Kim et al., 2017; Toda et al., 2013). Studies have shown that Arabidopsis plants with impaired JA signalling exhibit heightened sensitivity to salt, drought, and temperature stresses, as reviewed in (Kazan, 2015).

Additionally, it was shown that enhanced JA signalling impedes the growth of developing organs, triggers an increase in trichome numbers, and promotes higher anthocyanin accumulation (Yan et al., 2007; Yoshida et al., 2009; Zhang & Turner, 2008). The application of exogenous JA hampers both root and shoot growth by restricting cell division and elongation (Chen et al., 2011) and by inhibiting cell proliferation in leaves (Noir et al., 2013). Therefore, plant mutants with constantly elevated JA-Ile levels, such as the quintuple loss-of-function mutant of the *JASMONATE ZIM DOMAIN* (*JAZ*) family named *jaz1 jaz3 jaz4 jaz9 jaz10* (*jazQ*), exhibits severe vegetative growth reduction (Campos et al., 2016). In contrast, the *jazQ* mutant consistently displays heightened defense responses (Campos et al., 2016). It is hypothesized that the observed "growth/defense trade-off" that occurs during JA signalling is attributed to resource allocation for defense responses with the cost of reduced growth (Barto & Cipollini, 2005; Zavala & Baldwin, 2006). However, this hypothesis has faced recent challenges, as an additional loss-of-function mutation in *Phytochrome B* (*phyb*) within the *jazQ* mutant restores the WT growth phenotype while sustaining consistently increased defense responses (Campos et al., 2016). Furthermore, it has been demonstrated that defense in Arabidopsis can be enhanced without impeding growth using a laboratory-designed ligand called *O*-phenyl oxime. This ligand triggers the COI1-dependent degradation, specifically targeting only 2 (JAZ9 and JAZ10) out of the 13 JAZs in Arabidopsis (Takaoka et al., 2018). These promising results hold significant potential for the development of future strategies in crop improvement.

JA-Ile biosynthesis and metabolism

JA-Ile biosynthesis occurs during various developmental processes, including regulatory mechanisms associated with reproduction, and can also be initiated by environmental stresses such as wounding, as reviewed in (Wasternack & Feussner, 2018). In the context of environmental stresses, several elicitors associated with herbivores, microbes, plant viruses, damage, and osmotic regulations have been suggested to initiate JA-Ile biosynthesis (Campos et al., 2014; Mielke & Gasperini, 2019; Mielke et al., 2021; Yan & Xie, 2015). However, how precisely these events are connected to the initiation of biosynthesis remains largely unknown (Campos et al., 2014; Mielke & Gasperini, 2019).

Interestingly, the synthesis of JA-Ile after injury is a rapid process, with detectable JA-Ile levels emerging within just 60 seconds (Glauser et al., 2009.) As previously reviewed, the initial steps of JA-Ile biosynthesis take place within plastids (Fig. 2) (Wasternack & Strnad, 2018). Within these organelles, lipases play a pivotal role in breaking down polyunsaturated fatty acids, particularly α-linolenic acid (α-LeA) and hexadecatrienoic acid. Before this cleavage, these fatty acids are stored as monogalactosyldiacylglycerols (MGDGs) in the inner plastid membrane and thylakoid membranes (Li & Yu, 2018; Wasternack & Strnad, 2018). Notably, the lipase DEFECTIVE IN ANTHER DEHISCENCE (DAD1), primarily expressed in flowers, plays a specific role in regulating JA biosynthesis during male fertility development but not in vegetative tissues (Ishiguro et al., 2001). Over recent years, accumulating data have suggested that DAD1-LIKE LIPASES (DALLs) participate in regulating the initiation of JA biosynthesis in vegetative tissues (Ellinger et al., 2010; Kimberlin et al., 2022; Lin et al., 2016; Rudus et al., 2014; Ryu, 2004; Seo et al., 2009; Wang et al., 2018; Yang et al., 2007). Recent research has highlighted the essential role of DALL2 in the rapid synthesis of JA-Ile and JA-Ile precursors downstream of MGDGs, particularly in the veins distal to wounds (Morin et al., 2023). These findings strongly suggest that DALL2 functions as a crucial lipase in the primary vasculature. After cleavage from MGDGs, α-LeA and hexadecatrienoic acid carbon chains are oxygenated by the 13-LIPOXYGENASES (13-LOXs) (Bannenberg et al., 2009). The arising products, 13(*S*)-hydroperoxy-octadecatrienoic acid (13-HPOT) and 11(*S*)-hydroperoxy-hexadecatrienoic acid (11-HPHT), serve as substrates for AOS, which generates unstable allene oxides (Laudert et al., 1996). These unstable allene oxides are then cyclized by ALLENE OXIDE CYCLASES (AOCs) into 12-oxo-phytodienoic acid (OPDA) and dinor-oxo-phytodienoic acid (dn-OPDA), respectively (Stenzel et al., 2003). The next step involves the export of OPDA and dn-OPDA from plastids through the JASSY transporter followed by its import into peroxisomes facilitated by the putative COMATOSE (CTS) transporter (Guan et al., 2019; Theodoulou et al., 2005).

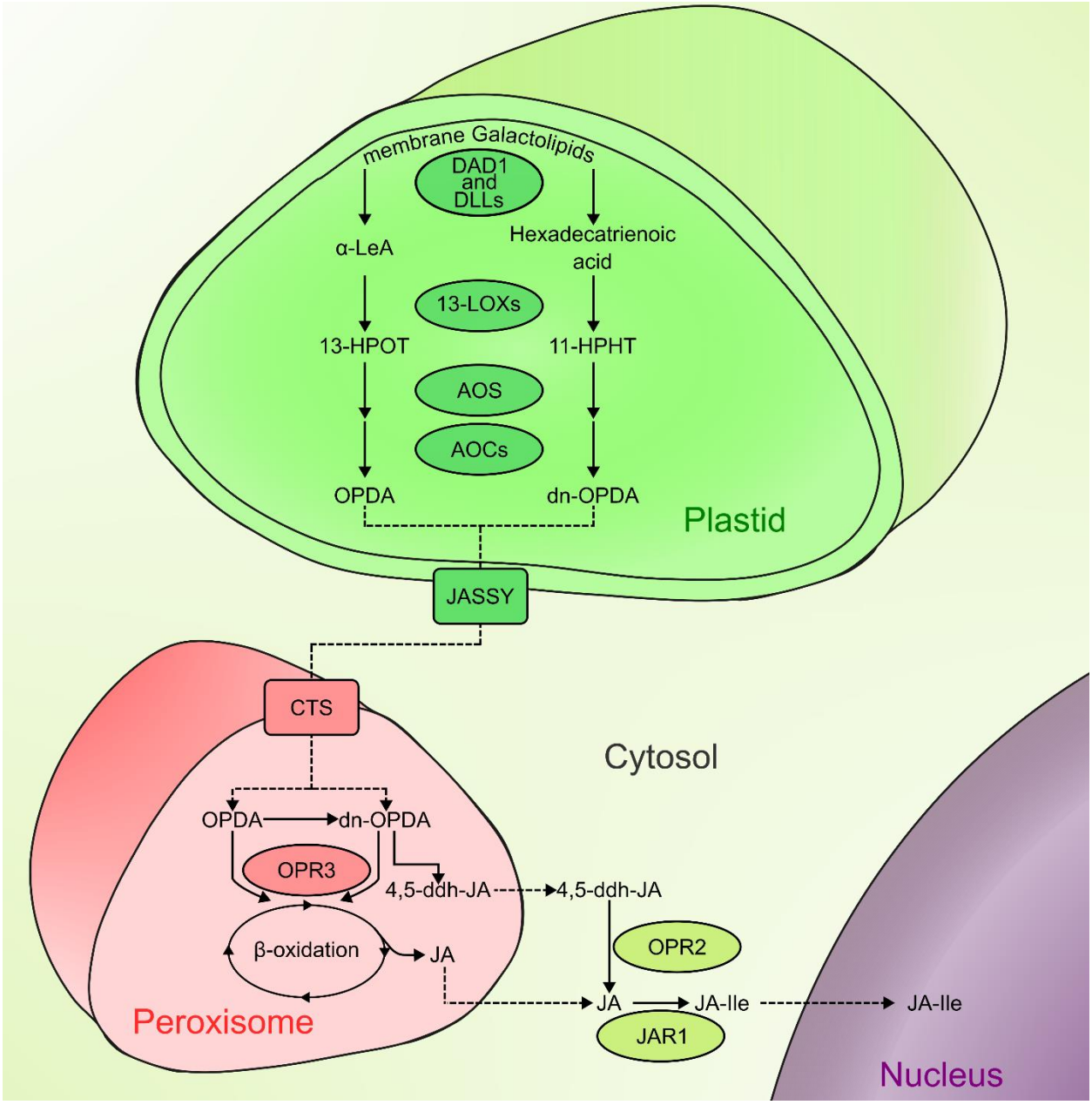

Figure 2. The JA-Ile biosynthesis pathway in *Arabidopsis thaliana*. Overview of JA-Ile biosynthesis in Arabidopsis. In plastids, membrane lipases, such as DEFECTIVE IN ANTHER DEHISCENCE (DAD1) and DAD1-like lipases (DALLs), cleave galactolipids, resulting in the formation of α-linolenic acid (α-LeA) and hexadecatrienoic acid. These compounds serve as substrates for 13-lipoxygenases (13 LOXs), which synthesize 13(*S*)-hydroperoxy-octadecatrienoic acid (13-HPOT) and 11(*S*)-hydroperoxy-hexadecatrienoic acid (11-HPHT). The enzymes ALLENE OXIDE SYNTHASE (AOS) catalyses the conversion of 13-HPOT and 11-HPHT, leading to the production of 12-oxo-phytodienoic acid (OPDA) and dinor-oxo-phytodienoic acid (dn-OPDA), respectively. Subsequently, ALLENE OXIDE CYCLASES (AOCs) further process these intermediates. Relocation of OPDA and dn-OPDA from the plastid to the peroxisome is facilitated by JASSY and COMATOSE (CTS). Within the peroxisomes, OPDA and dn-OPDA undergo additional transformations, including the action of 12 OXOPHYTODIENOATE REDUCTASE 3 (OPR3) and subsequent rounds of β-oxidation, resulting in the formation of (+)-7-*iso*-jasmonic acid (JA). Alternatively, OPDA can be directly converted to dn OPDA, which is then converted to JA. In the cytosol, the JASMONATE RESISTANT 1 enzyme (JAR1) conjugates JA to form (+)-7-*iso*-jasmonoyl-L-isoleucine (JA-Ile). Additionally, dn-OPDA can be transformed into 4,5-didehydrojasmonate (4,5-ddh-JA), which is subsequently converted into JA by OPR2 in the cytosol. Black arrows represent catalytic reactions, while dashed arrows represent transport processes.

Within the peroxisomes, OPDA and dn-OPDA undergo reductions catalysed by OXOPHYTODIENOATE REDUCTASE 3 (OPR3), followed by several β-oxidation rounds, resulting in the production of (+)-7-*iso*-jasmonic acid (JA) (Breithaupt et al., 2006; Delker et al., 2007; Li et al., 2005). In an alternative pathway, OPDA can undergo direct conversion to dn-OPDA and subsequently to 4,5-didehydrojasmonate (4,5-ddh-JA), which is ultimately reduced to JA by the OPR2 in the cytosol (Chini et al., 2018). Following the conversion of OPDA to JA, JA is eventually conjugated in the cytosol to form bioactive JA-Ile by the enzyme JASMONATE RESISTANT 1 (JAR1) (Staswick et al., 1992; Staswick & Tiryaki, 2004; Westfall et al., 2012). Ultimately, JA-Ile is perceived in the nucleus to initiate JA signalling (Perez & Goossens, 2013; Santner & Estelle, 2009).

Eventually, JA-Ile undergoes catabolism overt two alternative routes. One the one hand JA-Ile can be converted into 12-hydroxy-JA-Ile and 12-carboxy-JA-Ile through the activity of cytochrome P450-monooxygenases belonging to the CYP94 family (Heitz et al., 2012; Kitaoka et al., 2011; Koo et al., 2011). Alternatively, JA-Ile can be re-transformed into JA by the amidohydrolases IAA-ALANINE RESISTANT 3 (IAR3) and IAA-LEUCINE RESISTANT-LIKE 6 (ILL6) (Widemann et al., 2013).

Besides of JA-Ile, it is known that JA also possesses other derivatives, reviewed in (Heitz et al., 2019; Koo, 2018). For instance, JA can be hydroxylated to 12-hydroxy-JA by JASMONIC ACID OXIDASE (JOX) / JASMONATE-INDUCED OXYGENASE (JAO), sulfated to 12-HSO4-JA by SULFOTRANSFERASE 2A (ST2A), or methylated to Methyl-JA (MeJA) by JASMONIC ACID CARBOXY METHYL TRANSFERASE (JMT) (Caarls et al., 2017; Gidda et al., 2003; Seo et al., 2001; Smirnova et al., 2017). The precise biological functions of these JA derivates remain uncertain, although it is proposed that their possible function as catabolites involved in regulating JA levels (Heitz et al., 2019; Koo, 2018). In the context of MeJA, it can be converted into the bioactive JA-Ile by an esterase, thereby activating JA signalling (Stitz et al., 2011; Stuhlfelder et al., 2004; Tamogami et al., 2008; J. Wu et al., 2008).

JA-Ile perception and signalling

As indicated before, JA signalling is kept inhibited under basal conditions (Fig. 3A) (Barto & Cipollini, 2005; Zavala & Baldwin, 2006). In particular, JA-dependent TFs, such as MYC2, MYC3, MYC4, and MYC5 are maintained in a repressed state by a component-based repressor complex consisting of JAZ proteins (Boter et al., 2004; Cheng et al., 2011; Chini et al., 2009; Chini et al., 2007; Fernandez-Calvo et al., 2011; Figueroa & Browse, 2015; Kazan & Manners, 2013; Lorenzo et al., 2004; Qi et al., 2015). JAZ repressors,

either individually or in conjunction with the NOVEL INTERACTOR OF JAZ (NINJA) adaptor protein, recruit the transcriptional repressor TOPLESS (TPL) and TPL-RELATED proteins (TPRs) (Acosta et al., 2013; Pauwels et al., 2010; Shyu et al., 2012). TPL and TPRs on the other hand bind deacetylases like HISTONE DEACETYLASE 6 (HDA6) or HDA19 to suppress JA-responsive genes (K. Wu et al., 2008; Zhou et al., 2005; Zhu et al., 2011). It is predicted that the main transcriptional repressor complex consists of homo- and heterodimers of MYC transcription factors, where each MYC monomer recruits a hetero- or homodimer of JAZ, respectively (Chini et al., 2009; Chung & Howe, 2009; Geerinck et al., 2010). Additionally, it is hypothesized that the TPL co-repressors are recruited as homo- and heterodimers as well, resulting in an approximately 1 Megadalton (MDa) repression complex (Fig. 3B) (Geerinck et al., 2010).

Upon an elevation in JA-Ile levels, this phytohormone is translocated into the nucleus by the ABCG type JASMONATE TRANSPORTER1 (JAT1) (Li et al., 2017). Within the nucleus, JA-Ile serves as a molecular glue, promoting the interaction between the co-receptor CORONATINE INSENSITIVE 1 (COI1) and JAZ repressors (Fig. 3C) (Fonseca, Chico, et al., 2009; Sheard et al., 2010; Xie et al., 1998). COI1 represents the F-box component of the E3 Ubiquitin ligase of the SKP1/CULLIN/F-Box (SCF) complex (SCF^{COI1}), which targets JAZ repressors for ubiquitylation, resulting in their degradation by the proteasome (Blazquez et al., 2020; Chini et al., 2007; Thines et al., 2007). The degradation of JAZ proteins triggers the liberation of TFs, facilitating the recruitment of transcriptional mediator complexes, such as MEDIATOR OF RNA POLYMERASE II TRANSCRIPTION SUBUNIT 25 (MED25), which subsequently promotes the transcription of JA-responsive genes (Cevik et al., 2012; Fernandez-Calvo et al., 2011; F. Zhang et al., 2015). After an elevation in JA-Ile levels, the expression levels of early JA-responsive genes, such as *MYC2* and *JAZ* transcripts, experience a rapid induction within 5min and peak within 1h (Chung et al., 2010; Hickman et al., 2017). Concurrently, newly synthesized JAZ repressors establish a negative feedback loop to re-inhibit the system (Thines et al., 2007; Yan et al., 2007).

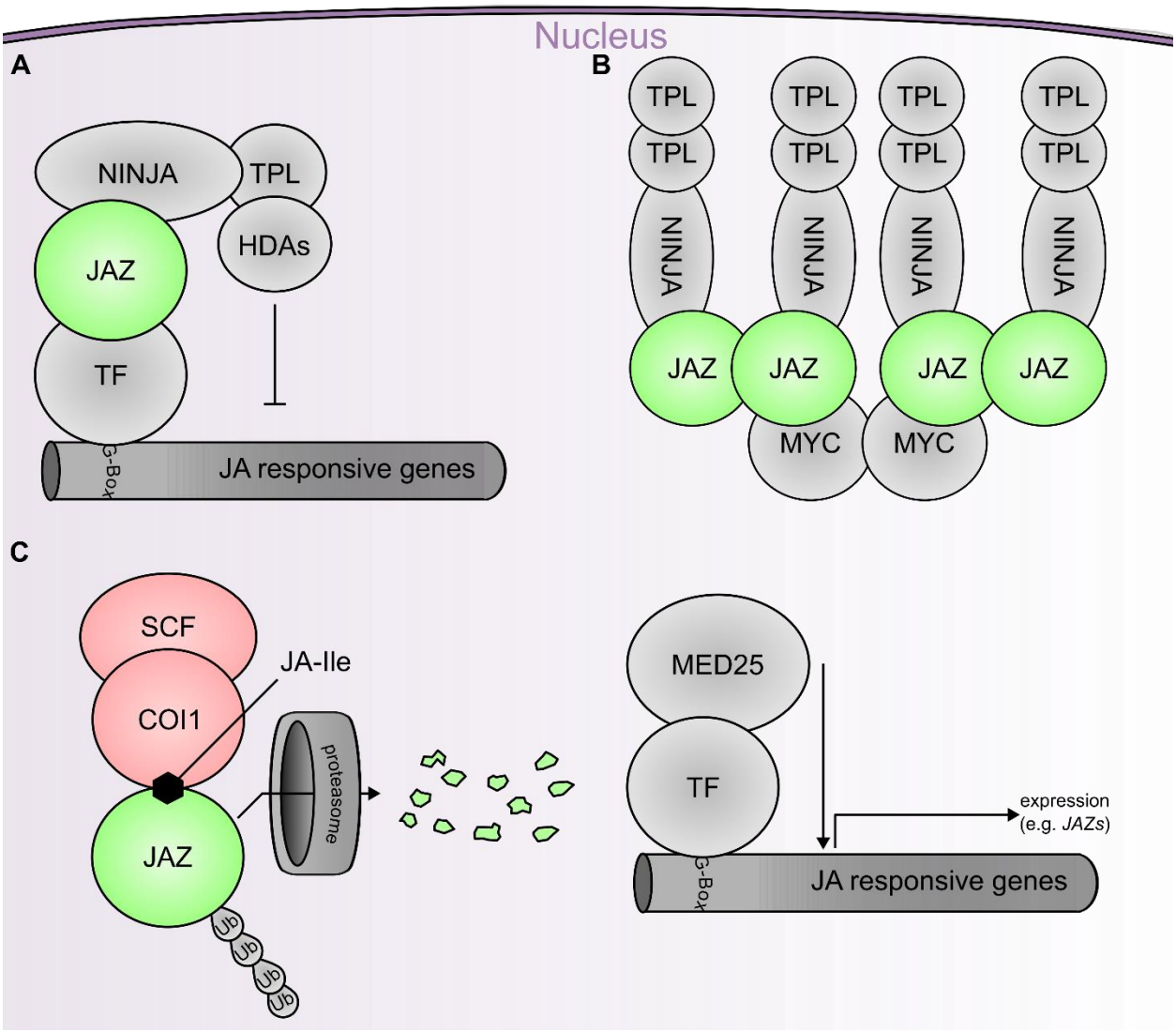

Figure 3. JA-Ile perception and signalling. Model of JA signalling repression and JA-Ile perception in the nucleus. (**A**) Under basal conditions (low JA-Ile levels): In the nucleus the JAZ-NINJA-TPL repressor complex inhibits the binding of G-Box binding TFs like MYC2, MYC3, and MYC4. (**B**) The proposed model of the JA repressor complex is based on stoichiometry derived from tandem affinity purification (TAP) experiments. (**C**) In the presence of JA-Ile (high JA-Ile levels), the hormone facilitates the direct interaction between JAZ co-repressors and the F-Box protein COI1, a component of an E3 Ubiquitin ligase of the SCF type. This interaction leads to the degradation of JAZ repressors by proteasomes and consequently enables the release of TFs and the recruitment of MEDIATOR OF RNA POLYMERASE II TRANSCRIPTION SUBUNIT 25 (MED25). Eventually, the expression of JA-responsive genes is initiated, which includes expression of *JAZs* genes to establish a negative feed-back loop.

After the induction of early JA-responsive genes, mid-term genes, including genes involved in JA-Ile biosynthesis, such as *AOS*, *LOX3*, *LOX4*, and *OPR3*, exhibit their highest expression between 2h and 4h after the onset of the response (Chung et al., 2008). As time progresses beyond 4 hours after response initiation, several canonical JA-dependent defense response genes, such as *VSP1*, *VSP2*, and *PLANT DEFENSIN 1.2* (*PDF1.2*), reach their maximum expression levels (Chung et al., 2008; Kilian et al., 2007; Shin

et al., 2012). Overall, the JA-dependent signalling pathway is tightly regulated, and its induction occurs primarily when necessary.

Although JA-Ile serves as the bioactive derivative of JA, COI1-JAZ interaction in Arabidopsis can also be initiated by a mimic of JA-Ile, called CORONATINE (COR), which is synthesized by the bacterial plant pathogen *Pseudomonas syringae* (Feys et al., 1994; Fonseca, Chini, et al., 2009; Sheard et al., 2010; Staswick & Tiryaki, 2004). During interactions between *Pseudomonas* and plants, COR functions as a pathogen effector that induces JA signalling, subsequently suppressing the accumulation of SA required for mounting defense responses against this biotrophic pathogen (Kloek et al., 2001; Zheng et al., 2012).

As described above, JA-Ile plays an essential role in regulating diverse responses (Dennis & Norris, 2015; Wasternack & Strnad, 2018). The significance of JA-Ile becomes even more pronounced considering that it stands as the sole recognized bioactive derivative of JA with the capability to induce JA signalling in Arabidopsis (Fonseca, Chini, et al., 2009). This prompts the question of how this singular molecule orchestrates such a broad spectrum of responses. The modulation of JA signalling appears to be facilitated by proteins responsible for JA Ile perception, forming a crucial link between the phytohormone and the initiation of JA responses.

The F-Box protein COI1

COI1, as a single copy gene in *Arabidopsis thaliana*, encodes for the F-box protein COI1 that enables JAZ degradation (Chini et al., 2007; Feys et al., 1994; Thines et al., 2007; Xie et al., 1998; Yan et al., 2007). *COI1* null mutants are completely insensitive to JA-Ile or COR, underscoring its essentiality in inducing JA signalling (Feys et al., 1994; Xie et al., 1998). *COI1* exhibits constitutive expression in all tissues and developmental stages while subcellular localization studies have revealed its presence in the nucleus (Klepikova et al., 2016; Withers et al., 2012).

Molecularly, COI1 possesses an F-box motif that directly links it to ARABIDOPSIS-LIKE SKP1 (ASK1), which in turn forms together with CULLIN1 (CUL1) and RING BOX-LIKE PROTEIN 1 (RBX), the core component of the SCF type E3 Ub ligase family (Fig. 4) (Bai et al., 1996; Devoto et al., 2002; Skowyra et al., 1997; Xie et al., 1998). Previous studies have demonstrated the essential role of ASK1 in maintaining COI1 stability, suggesting a coordinated expression of ASK1 and COI1 (Yan et al., 2013; Yang et al., 1999; Zhou et al., 2013).

COI1 contains 16 imperfect leucine-rich repeats (LRRs) that enable the direct interaction of COI1 with JAZ repressors, mediated by the bioactive JA-Ile or COR acting as a bridging ligand (Fig. 3C; Fig. 4) (Fonseca, Chico, et al., 2009; Katsir et al., 2008; Sheard et al., 2010). Consequently, JAZ proteins undergo ubiquitylations mediated by E2, which is recruited by RBX (Fig. 4) (Sheard et al., 2010; Smalle & Vierstra, 2004). Interestingly, COR exhibits an even stronger interaction with COI1 than bioactive JA-Ile, as indicated by the dissociation constant (K_D) values for COR and JA-Ile (Fonseca, Chico, et al., 2009; Katsir et al., 2008; Sheard et al., 2010).

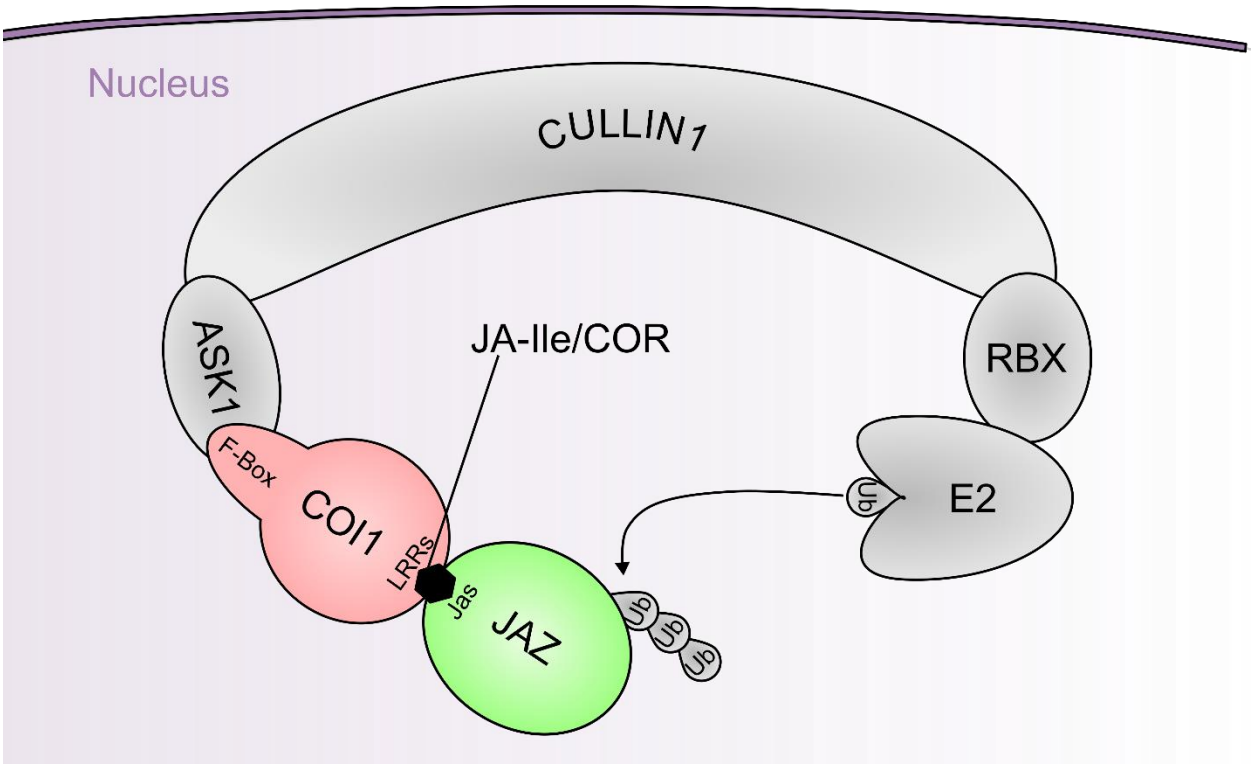

Figure 4. JAZ ubiquitylation is mediated by the SKP/CULLINF/F-BOX/COI1 (SCF^{COI1}) complex. Schematic model of the SCF^{COI1} complex. In the nucleus COI1 interacts with ASK1 through the F-Box motif and forms together with CULLIN1 and RING-BOX-like protein 1 (RBX1) the E3-Ub-ligase complex. In the presence of the ligand, COI1 binds to the Jas degron of JAZ through a leucine-rich (LRR) motif, using JA-Ile or CORONATINE (COR) as a molecular glue. RBX1 binds to the E2, which subsequently transfers Ub molecules to the JAZ proteins.

Inositol phosphates (InsPs) also contribute to COI1 functionality (Sheard et al., 2010). InsP acts as an allosteric cofactor of COI1 and is located adjacent to the bottom of the ligand-binding pocket, thereby enhancing the formation of the COI1-JAZ complex (Sheard et al., 2010). While Inositol pentakisphosphate ($InsP_5$) was previously implicated in JA-Ile perception (Laha et al., 2015; Mosblech et al., 2011; Sheard et al., 2010), it does not globally activate COI1 function in Arabidopsis, indicating that it is not the bioactive

InsP (Laha et al., 2015). Instead, $InsP_8$ exhibits higher COI1 specificity than InsP5 and InsP6 (Cui et al., 2018; Laha et al., 2016), suggesting that $InsP_8$ functions as the allosteric cofactor of COI1.

Although COI1 plays a significant role in JA-Ile perception, its widespread expression as a single copy gene suggests that COI1 may be less involved in the specificity of JA signalling (Klepikova et al., 2016).

The JAZ repressors

JAZ proteins function as repressors of JA signalling by binding MYCs and generally by recruiting NINJA/TPL/TPR (Fig. 3A and B) (Chini et al., 2007; Fernandez-Calvo et al., 2011; Pauwels et al., 2010; Thines et al., 2007; Yan et al., 2007). At low levels of JA-Ile, the JA associated motif (Jas degron) and/or the cryptic MYC domain (CMID) directly interact with MYCs (Cheng et al., 2011; Chini et al., 2009; Chini et al., 2007; Fernandez-Calvo et al., 2011; Goossens et al., 2015; Moreno et al., 2013; Niu et al., 2011; Thireault et al., 2015; Zhang et al., 2017). The JASMONATE ZINC FINGER INFLORESCENCE MERISTEM (ZIM) domain recruits the mediator NINJA, which in turn binds TPL or TPR proteins, resulting in the repression of JA-responsive genes (Fig. 3A and B) (Acosta et al., 2013; Chini et al., 2007; Pauwels et al., 2010; Thines et al., 2007; Yan et al., 2007).

In the presence of JA-Ile, the Jas degron directly interacts with JA-Ile and COI1 (Fig. 3C; Fig. 4;) (Chini et al., 2007; Sheard et al., 2010; Thines et al., 2013). The previously identified SLX2FX2KRX2RX5PY sequence of the Jas degron (Chung & Howe, 2009; Melotto et al., 2008) is responsible for the direct interaction with COI1 (Chung & Howe, 2009; Fonseca, Chico, et al., 2009; Melotto et al., 2008; Sheard et al., 2010).

Notably, researchers have recognized the advantages of the diverse binding features of JAZ repressors, leading to their utilization in the development of valuable research tools. For example, researchers have created a modified JAZ9 peptide that represses MYCs (MYC2, MYC3, and MYC4), while being unable to bind COI1 (Suzuki et al., 2021). As a result, this peptide exerts inhibitory effects on MYC-facilitated gene expression in Arabidopsis following JA treatment (Suzuki et al., 2021). Hence, the modified JAZ9 peptide has the potential to be a valuable tool for studying MYC-related JA signalling pathways (Suzuki et al., 2021). Moreover, researchers designed a hormone biosensor, that is based on the Jas degron of JAZ9, coupled to a VENUS (VEN) fluorophore (Larrieu et al., 2015). The sensor undergoes degradation in response to JA-Ile and COR, hence serving as a tool to measure spatiotemporal JA-Ile distribution during plant responses to both abiotic and biotic stresses (Larrieu et al., 2015).

Although single KO mutations of *JAZ* genes do not result in obvious phenotypes at least under basal conditions, the existence of 13 different JAZ proteins in the Arabidopsis genome suggests structural differences (Fig. 5) and variation in their binding capabilities to canonical and non-canonical JA-Ile perception components, as reviewed in (Howe et al., 2018).

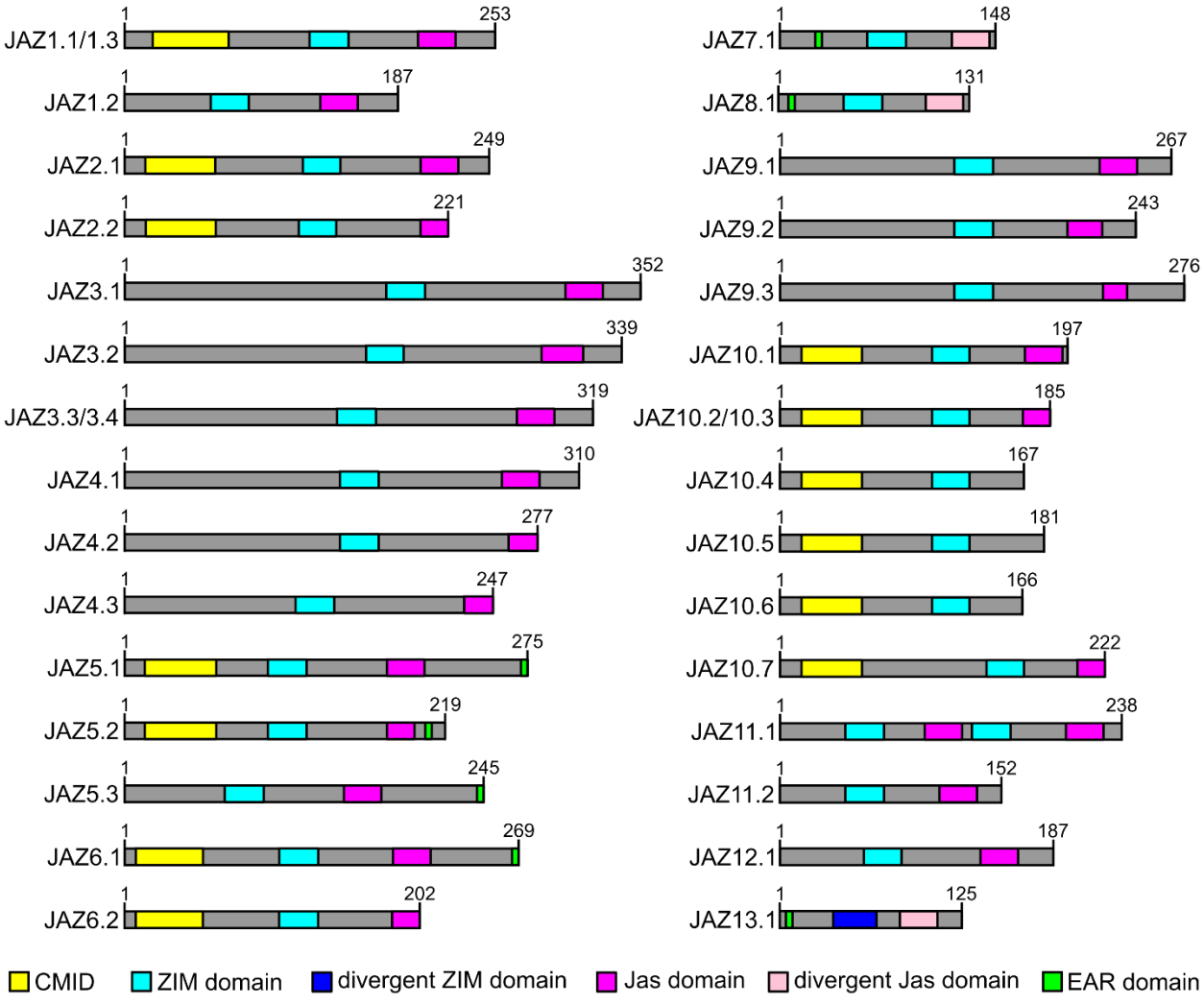

Figure 5. JAZ proteins and their splicing variants display structural variabilities. Schematic representation of all potential protein splicing variants encoded by the 13 *JAZ* genes in Arabidopsis (www.tair.org). JAZ proteins exhibit structural variabilities, including different binding domains, which can significantly impact their binding capabilities (CMID: interaction with MYCs; ZIM domain: interaction with JAZs and NINJA; Jas domain: interaction with COI1 and MYCs; EAR domain: interaction with TPL and TPR).

The discovery of interactions between specific JAZs and components of other pathways has enhanced our understanding of how JA signalling is interconnected with other signalling processes. For example, JAZ1 and JAZ4 interact with bHLH type transcription factors INDUCER OF CBF EXPRESSION 1 (ICE1) and ICE2 to

regulate JA-dependent freezing tolerance (Hu et al., 2013). Furthermore, studies have shown that DELLAs, the repressors of the GA pathway, can engage in competitive interactions with JAZs, leading to the initiation of JA signalling (Hou et al., 2010; Qi et al., 2014). In this context, it has been shown that the balance between plant growth and defense is partially regulated by the interactions between some of the JAZs and DELLAs, which integrate the signalling pathways of JA-Ile and GA. Specifically, increased GA levels enhance the repression of defense by JAZs, while elevated JA-Ile levels enhance the DELLA mediated suppression of growth (Hong et al., 2012; Qi et al., 2014). Furthermore, recent studies have demonstrated the interaction of certain JAZs with FAR-RED ELONGATED HYPOCOTYL 3 (FHY3) and FAR RED-IMPAIRED RESPONSE 1 (FAR1), proteins involved in regulating shade avoidance mechanisms (Liu et al., 2019). These findings highlight the important role of JAZs in responding to changes in light quality, such as shade avoidance, by promoting growth over defense mechanisms. (Chico et al., 2014; Leone et al., 2014; Liu et al., 2019). Previous research has revealed multiple other interactions between JAZs and mediators of other signalling pathways, demonstrating their involvement in linking various signalling processes to JA signalling, including flowering regulation, ABA, IAA and ET signalling, anthocyanin regulation, trichome initiation, root hair development, male fertility, and seed germination (Han et al., 2020; Hou et al., 2010; Jiang et al., 2014; Mei et al., 2023; Pauwels et al., 2015; Zhai et al., 2015; Zhu et al., 2006; Zhu et al., 2011). It is noteworthy that not all JAZs interact with non-canonical intermediates in the same way; there are variations in the binding preferences of different JAZs for specific interactors. A comprehensive overview of JAZ interactions with canonical and non-canonical intermediates can be found in Table S1.

Interestingly, JAZs also exhibit varying binding capabilities towards canonical interactors. In fact, *in vivo* and *in vitro* assays have revealed the ability of JAZ proteins to form homodimers or heterodimers, a process mediated by the ZIM domains (Chini et al., 2009; Chung & Howe, 2009). It is suggested that JAZ dimerization is crucial for the formation of the 1 MDa repression complex mentioned before, ensuring the precise repression of JA-responsive genes (Geerinck et al., 2010). Additionally, studies have demonstrated that JAZ7, JAZ8 and JAZ13 are unable to bind NINJA (Pauwels et al., 2010; Thireault et al., 2015). In case of JAZ13 it was shown, that its inability to bind NINJA stems from the presence of a divergent Jas motif within the JAZ13 structure (Thireault et al., 2015). However, it is predicted that these JAZs are still capable of repressing JA signalling, as genome-wide analysis and interaction assays indicate that JAZ7, JAZ8, and JAZ13, as well as JAZ5 and JAZ6, possess an ERF-associated amphiphilic repression (EAR) domain that allows them to recruit TPL and TPR directly (Causier et al., 2012; Kagale et al., 2010; Shyu et al., 2012; Thatcher et al., 2016; Thireault et al., 2015). Interestingly, other JAZs, such as JAZ1, JAZ3, and JAZ9 can

also directly recruit HDA6 to repress gene expression of JA-responsive genes through epigenetic modifications (Zhu et al., 2011). Furthermore, publications have reported variations in the interactions between JAZ proteins and the canonical transcription factors MYC2, MYC3, MYC4 and MYC5 (Cheng et al., 2011; Chini et al., 2009; Chini et al., 2007; Fernandez-Calvo et al., 2011; Niu et al., 2011; Qi et al., 2015; Thireault et al., 2015), as well as between JAZ proteins and R2R3-MYBs, such as MYB DOMAIN PROTEIN 21 (MYB21) and MYB24 (Song et al., 2011). JAZ proteins have also shown different binding affinities to the co-receptor COI1 (Chung & Howe, 2009; Sheard et al., 2010). For example, in vitro radioligand binding assays have demonstrated higher binding affinity between COI1 and the degron of JAZ1 in the presence of COR (K_D = 48 nM) compared to the binding between COI1 and the degron of JAZ6 (K_D = 68 nM) (Sheard et al., 2010). Further interaction studies have revealed that JAZ8 exhibits lower binding affinity to COI1 in the presence of COR (K_D = 91.4 nM) compared to the JAZ10 splicing variant JAZ10.1 (K_D =7.0 nM) (Shyu et al., 2012). Another example involves the splicing variants *JAZ10.3* and *JAZ10.4* (Chung & Howe, 2009). JAZ10.3 contains a truncated Jas motif, while JAZ10.4 lacks the Jas motif entirely, resulting in weak or no interaction with COI1, respectively (Chung & Howe, 2009). Furthermore, it has been demonstrated that the splicing variant JAZ4.2, which lacks the conserved proline and tyrosine residues at the C-terminus of the degron, exhibits higher COI1/ligand-dependent stability compared to JAZ4.1 due to reduced interaction with COI1 (DeMott et al., 2021).

In total, Arabidopsis has the potential to encode 30 different JAZ proteins, including splicing variants (Fig. 5). The fact that even JAZ splicing variants exhibit different binding capabilities greatly expands the range of potential hormone sensitivities and the activation of downstream responses (Chung et al., 2010).

In addition to variations in binding capabilities, JAZ proteins have been shown to fulfil specific functions and contribute to specific phenotypes. For instance, transgenic lines expressing JAZs lacking the degron motif (JAZ1Δjas, JAZ3Δjas, and JAZ9Δjas) have been studied (Chini et al., 2007; Thines et al., 2007; Withers et al., 2012). While transgenic lines expressing JAZ9Δjas exhibits root growth inhibition as a JA response, plants expressing JAZ1Δjas and JAZ3Δjas display insensitivity to JA (Chini et al., 2007; Thines et al., 2007; Withers et al., 2012). Another example is the *JAZ10* loss-of-function mutant (*jaz10-1*), which shows increased susceptibility to herbivory and JA treatment in terms of root growth inhibition, while displaying no obvious phenotypes under basal conditions (Demianski et al., 2012; Moreno et al., 2013). Interestingly, it has been observed that the hypersensitive JA responses in terms of root growth inhibition exhibited by *jaz10-1* can be further amplified by introducing additional loss-of-function mutations of *JAZ7*, *JAZ8*, and

JAZ13 (Thireault et al., 2015). Recently, it has been demonstrated that JAZ4 plays a role in various processes, including growth, development, elevated plant defense (DeMott et al., 2021; Han et al., 2020; Oblessuc et al., 2020). In this context, it was shown that the loss-of-function mutant *jaz4-1* displays a higher susceptibility towards the infection with *Pseudomans syringae*, while transgenic plants over-expressing JAZ4 lacking the degron (JAZ4Δjas) variants exhibit increased resistant against the bacterium (Oblessuc et al., 2020). In the same study, it was revealed that the expression of JAZ4Δjas to increased root elongation, petiole length, and hypocotyl length. In a later study, it was demonstrated that the overexpression of both JAZ4.1 and JAZ4.2 splicing variants individually leads to increased root growth (DeMott et al., 2021). Other research has demonstrated that JAZ4 and JAZ8 play pivotal roles in root hair development, as Arabidopsis lines overexpressing JAZ4 and JAZ8 lacking the Jas degron exhibited compromised root hair elongation (Han et al., 2020). Additionally, it was shown that JAZ4 is involved in the regulation of ET- and IAA-mediated root processes (DeMott et al., 2021). In this context, it was observed that *jaz4-1* mutants display reduced sensitivity to aminocyclopropane-1-carboxylic acid (ACC), a precursor of ET, as well as IAA, with respect to the reduction in root growth (DeMott et al., 2021). The study revealed that several ET and IAA marker genes, such as *ETHYLENE RESPONSE FACTOR 1 (ERF1)* and *PHYTOCHROME INTERACTING FACTOR 4 (PIF4)*, are upregulated in *jaz4-1* mutants, suggesting a dependence of ET and IAA signalling on JAZ4. As previously mentioned, it has been also demonstrated that the laboratory-designed ligand *O*-phenyl oxime, which specifically induces COI1-dependent degradation of JAZ9 and JAZ10, enhances plant defense without affecting growth (Takaoka et al., 2018). These findings suggest that JAZ9, JAZ10, or both in combination may primarily govern defense responses rather than growth. Moreover, specific JAZs have been identified to play key roles in defining biological and cellular processes. For instance, studies have demonstrated that *JAZ2* is expressed in stomatal guard cells and plays a role in regulating stomatal opening during bacterial infection (Gimenez-Ibanez et al., 2017). However, since most of the single order *jaz* mutants do not exhibit noticeable phenotypes under basal conditions, it is commonly suggested that most JAZ*s* function redundantly (Chini et al., 2007; Thines et al., 2007).

The abundance of JAZ proteins, their binding capability variations, and the manifestation of specific phenotypes indicate that JAZs may serve as key modulators of JA signalling. However, the precise mechanisms by which JAZs are involved in JA modulation still require further investigation.

The MYC transcription factors

MYCs play a crucial role in the transcriptional regulation of JA-responsive genes (Boter et al., 2004; Chini et al., 2007; Fernandez-Calvo et al., 2011; Kazan & Manners, 2013; Lorenzo et al., 2004; Major et al., 2017). Plants with dysfunctional *MYCs* display reduced sensitivity to JA, highlighting the crucial role of MYCs as enhancers of JA signalling (Boter et al., 2004; Fernandez-Calvo et al., 2011; Lorenzo et al., 2004).

MYC TFs contain a bHLH domain, which comprises approximately 15-20 mostly basic amino acids (Abe et al., 1997; Boter et al., 2004; Lorenzo et al., 2004). This bHLH domain plays a crucial role in facilitating the binding of MYCs to the T/G box AACGTG motif, commonly referred to as the G-Box (Fig. 3C) (Abe et al., 1997; Boter et al., 2004). The G-Box motif is found in the promoter regions of target genes regulated by MYCs (Carretero-Paulet et al., 2010; Toledo-Ortiz et al., 2003). In the absence of JA-Ile, MYCs interact with JAZ proteins through the C-terminal JASMONATE INTERACTION DOMAIN (JID), leading to the inhibition of MYC's transcriptional activation function (Fig. 3A and B) (Chini et al., 2009; Fernandez-Calvo et al., 2011). However, in the presence of JA-Ile, MYCs are released from JAZ proteins and recruit MED25 via their N-terminal transcriptional activation domain (TAD) (Cevik et al., 2012; Chen et al., 2012). Interestingly, recent studies have demonstrated that a short motif within MED25, closely related to the JAZ CMID, is essential for the interaction between MED25 and MYC (Takaoka et al., 2022). Following MED25 recruitment, MED25 binds to RNA POLYMERASE II (RNA POLY II), initiating the transcription of target genes (Amoutzias et al., 2008; An et al., 2017; Cevik et al., 2012; Chen et al., 2012; Flanagan et al., 1991; Kelleher et al., 1990).

Although MYC2, MYC3, MYC4, and MYC5 mediated JA responses are presumed to exhibit partial redundancy, they interact differently with non-canonical JA perception components, establishing connections to other signalling pathways, such as the GA pathway or the light signalling pathway (Chico et al., 2014; Fernandez-Calvo et al., 2011; Figueroa & Browse, 2015; Hong et al., 2012; Ortigosa et al., 2020; Qi et al., 2015; Schweizer et al., 2013; Song et al., 2017). Furthermore, more recent data suggest that individual MYC proteins have distinct functions (Fernandez-Calvo et al., 2011; Johnson et al., 2023; D. D. Wang et al., 2021). For instance, forward genetic approaches have unveiled that MYC3 and MYC4 act as key regulators of JA-induced tryptophan metabolism (Johnson et al., 2023).

Similar to JAZs (Chini et al., 2009; Chung & Howe, 2009), MYC2, MYC3, and MYC4 can form homo- and heterodimers, with varying strengths of interaction observed among different MYC combinations

(Fernandez-Calvo et al., 2011). Moreover, MYCs exhibit differences in their DNA binding specificities, with MYC2 and MYC3 binding to nearly identical DNA clusters, while MYC4 recognizes a slightly different subset of target genes (Fernandez-Calvo et al., 2011; Godoy et al., 2011; Zander et al., 2020).

In addition to variations in the binding capabilities of MYC proteins, *MYC* genes also display distinct global expression patterns, and show cell layer-specific expression domains (Fernandez-Calvo et al., 2011; Gasperini et al., 2015). In terms of the root, it was shown that *MYC2* exhibits expression in the endodermis and epidermis of the elongation zone (EZ), as well as in the endodermis, in the lateral root cap, and in the columella cells of the root meristematic zone (MZ) (Gasperini et al., 2015). Meanwhile, *MYC3* showed expression in the endodermis, cortex, and epidermis of the EZ and differentiation zone (DZ) (Gasperini et al., 2015). In contrast, *MYC4* expression was confined to the outer layers of the columella and lateral root cap (Gasperini et al., 2015). These differences among *MYCs* and their coding proteins may explain the partial redundancy observed among them raising questions about the specific involvement of MYCs in JA specificity (Boter et al., 2004; Fernandez-Calvo et al., 2011; Gasperini et al., 2015; Lorenzo et al., 2004; Schweizer et al., 2013).

How is JA signalling modulated?

As previously reviewed (Couvreur et al., 2018; Kiba & Krapp, 2016; Su et al., 2017), the root plays a pivotal role in essential plant functions such as water absorption, nutrient uptake, and gravitropism. Over the past years, it was shown that various processes in the root are regulated by plant hormones, including IAA, ET, ABA, GA, CK, SL, BR, and JA (Pacifici et al., 2015; Qin et al., 2019). The phytohormone JA-Ile has been identified as a crucial player in root processes, such as root growth reduction and root hair development, as reviewed in (Han et al., 2023). However, the modulation of JA signalling at cellular resolution remains elusive. For instance, JA-dependent inhibition of root growth is caused by cell number and cell elongation in the DZ and EZ, as well as by reduced cell division in the MZ (Chen et al., 2011). However, this raises the question once again of how cell-specific JA signalling is modulated in a context-specific manner. Specifically: how does JA-Ile selectively repress cell proliferation in the root meristem while influencing cell number and elongation in the EZ and DZ? Another example is the formation of root hairs: Studies have demonstrated that JA regulates root hair development (Han et al., 2020; Zhu et al., 2006; Zhu et al., 2011), a process restricted to epidermal cells that overlie with two underlying cortical cells (Dolan et al., 1994; Galway et al., 1994; Ishida et al., 2008; Schiefelbein et al., 2009). To date, the root poses open questions concerning the modulation of cell-specific JA signalling that warrant further

investigation. Answering these questions could provide insights that contribute to a better understanding of broader cell-specific modulations in research.

As suggested earlier, potential players in JA signalling modulation may be among the JA-Ile perception components. The regulation of JA signalling by COI1, encoded by a single gene, may have limitations (Feys et al., 1994; Xie et al., 1998). However, other components involved in JA-Ile perception, such as JAZs and MYCs, likely offer extended possibilities for modulation (Boter et al., 2004; Chini et al., 2007; Lorenzo et al., 2004; Thines et al., 2007; Yan et al., 2007). Hence, modulation of JA signalling could be achieved through the transcriptional regulatory functions of the MYCs and/or the repressive capacities of the JAZs. In this context, JAZs are particularly notable. The presence of 13 *JAZs* in Arabidopsis, potentially giving rise to 30 distinct repressor proteins (www.tair.org) with diverse binding capabilities that affect JAZ protein stabilities interactions with other pathway intermediates, and the formation of repressor complexes (Howe et al., 2018), suggests the potential involvement of JAZs in modulating cellular JA signalling (Fig. 5; Tab. S1).

Preparatory work

At the start of this project, there was limited information on the 13 *JAZ* promoter (*JAZp*) activities in Arabidopsis vegetative tissues. Transcriptional reporter lines were only available for *JAZ1*, *JAZ2* and *JAZ10* (Acosta et al., 2013; Gimenez-Ibanez et al., 2017; Grunewald et al., 2009). In this context, the *JAZ1p* was active in lateral roots and at the lateral root bases, as well as in vascular system of the root differentiation zone (Grunewald et al., 2009). For *JAZ2p*, activity was observed in guard cells (Gimenez-Ibanez et al., 2017). In contrast, under basal conditions *JAZ10p* was mostly inactive (Acosta et al., 2013). However, as *JAZ10* is readily inducible after wounding or JA treatment, this transcript is commonly used as a JA marker (Acosta et al., 2013; Mielke et al., 2021).

As a results of the limited knowledge of *JAZp* activities, it was unknown which JAZ proteins were involved in forming the basal repression complex. To visualize the expression sites of *JAZ* promoters, transcriptional reporters of all 13 Arabidopsis *JAZ* promoters driving the expression of the β-GLUCORUNIDASE (GUS) reporter (*JAZp:GUS*) were designed and transformed in wild-type (WT) plants (cloning, transformation and imaging by Dr. Debora Gasperini and Dr. Stefan Mielke). Resulting *JAZp:GUS* reporters revealed that under basal conditions, *JAZ* promoters can be grouped as basally active (*JAZ1p*, J*AZ2p*, *JAZ3p*, *JAZ6p*, *JAZ9p*, and *JAZ10p*) or basally weak/inactive (*JAZ5p*, *JAZ7p*, *JAZ8p*, *JAZ11p*, *JAZ12p*, and *JAZ13p*) in 5-day old (5-do)

seedlings (Fig. 6; Fig. S1A). Notably, promoter activities of the majority of *JAZs* can be induced by cotyledon-wounding, except for *JAZ4p* and *JAZ11p* (Fig. S1).

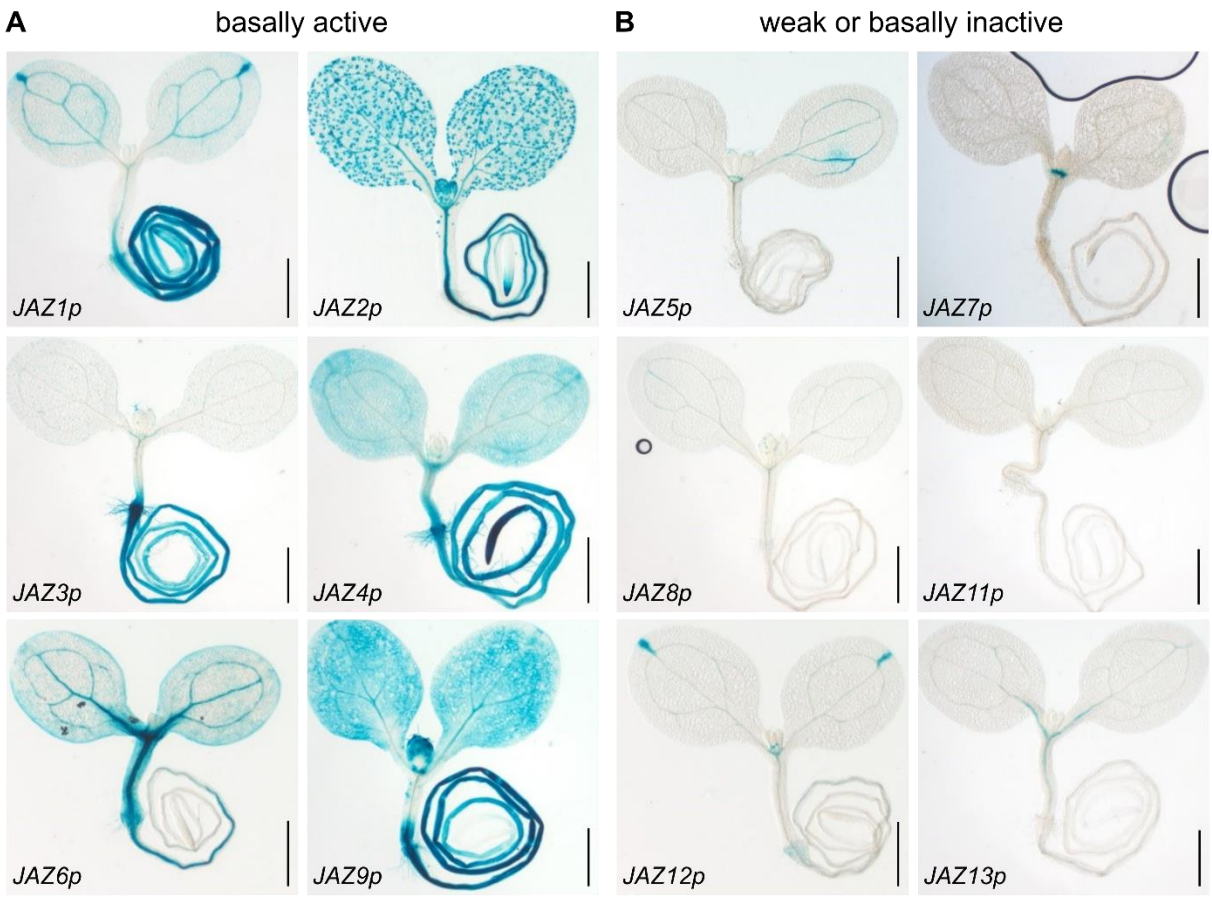

Figure 6: Basal expression of *JAZp:GUS* lines in 5-days old (do) Arabidopsis seedlings. (**A**) *JAZp:GUS* reporters with basal promoter activities in shoots and roots (*JAZ1p*, *JAZ2p*, *JAZ3p*, *JAZ4p*, *JAZ6p*, *JAZ9p*). (**B**) *JAZp:GUS* reporter with no or weak basal promoter activities in shoots and roots (*JAZ5p*, *JAZ7p*, *JAZ8p*, *JAZ11p*, *JAZ12p*, *JAZ13p*). See Figure S1A for the published *JAZ10p:GUS* expression profile. Scale bars in (A) and (B) = 0.5 mm.

Basally active *JAZ* promoters also differ in terms of tissue-specific expression (Fig. 6A). *JAZ1p* activity was observed in the cotyledon veins and in the hydathodes, as well as in the vascular system of the hypocotyl. In contrast with previous findings (Grunewald et al., 2009), *JAZ1p* activity was present throughout the entire root. The difference in expression patterns may be attributed to various experimental conditions, such as different developmental stages of the used transgenic lines. In accordance with earlier reports, *JAZ2p* activity was in the cotyledons, predominantly in guard cells (Gimenez-Ibanez et al., 2017). Furthermore, *JAZ2p* activity was observed in the vascular system of the hypocotyl and in the vascular system of the root. In the root, *JAZ2p* activity ranged from the root-hypocotyl transition zone (collet) to the central region of the root and was also detected in the root tip. *JAZ3p* activity was faintly visible in the

hypocotyl and cotyledons but prominently present throughout the entire root, gradually diminishing towards the root tip, yet still subtly observable there. *JAZ4p* activity was visible in most parts of the cotyledons, hypocotyl, and root. *JAZ6p* activity was detected in the cotyledons, primarily in the veins, as well as in the hypocotyl, predominantly within the vascular system. In addition, *JAZ6p* activity was detected in the upper portions of the root, ranging from the collet to the middle of the root. For *JAZ9p*, promoter activity was primarily observed in the cotyledons, as well as in the root starting at the collet region and reaching to approximately the middle of the root. As described previously (Acosta et al., 2013), *JAZ10p* activity was weak and limited to the hypocotyl and to the cotyledons (Fig. S1A). Therefore, *JAZ10p* was defined as basally inactive in root tissues which agrees with previous reports (Acosta et al., 2013). Among the *JAZp:GUS* reporters that were classified as "weak or basally inactive", only *JAZ7p*, *JAZ12p*, and *JAZ13p* displayed faint promoter activities.

The development of additional tools was initiated before I joined this project, including:

- transcriptional reporter lines expressing NUCLEAR LOCALIZATION SIGNAL linked to 3xVENUS (NLS-3xVEN) under the control of *JAZ* promoters (*JAZp:NLS-3xVEN*) to characterize promoters of basally active *JAZs* at the cellular level (unpublished data, cloning by Dr. Debora Gasperini; plant transformation and selection of *JAZ1p:NLS-3xVEN, JAZ3p:NLS-3xVEN, and JAZ10p:NLS-3xVEN* by Dr. Stefan Mielke. All remaining reporters were transformed and selected by me).
- several non-ratiometric translational reporters under native *JAZp* promoters driving the expression of JAZ proteins fused to CITRINE (CIT) (*JAZp:JAZ-CIT)* to determine the cell-specific localization of JAZ proteins (unpublished data, cloning of translational reporter of JAZ1, JAZ2, JAZ3, JAZ4, JAZ6, and JAZ9 by Dr. Debora Gasperini and Adina Schulze). The remaining non-ratiometric translational reporter lines of JAZ8, JAZ10, and JAZ11 were generated by me.
- generation of full knockout (KO) *jaz* mutants using the CRISPR/Cas9 system following the protocol described in (Pauwels et al., 2018) (unpublished data, cloning and plant transformation by Henrikje Smits. Mutant selections were done by me).

Aims and objectives

Although molecular components involved in JA signalling are known, reviewed in (Howe et al., 2018), knowledge on how JA signalling is regulated in a cell-specific manner remains limited. Several studies have suggested that *JAZ* genes have a redundant function, as most single order *jaz* mutants display no obvious phenotypes (Chini et al., 2007; Chini et al., 2016; Howe et al., 2018; Thines et al., 2007). However, JAZ

proteins exhibit structural variations, such as different binding domains, as reviewed in (Howe et al., 2018) (Fig. 5). These diversities in binding domains can influence the interaction with other JA signalling proteins and eventually affect biochemical features between different JAZs and the COI1 co-receptor (Tab. S1) (Howe et al., 2018). Furthermore, our preliminary analysis indicates that *JAZ* promoters can be classified as "basally active" and "basally weak or inactive" in the primary root, and that "basally active" *JAZ* promoters display tissue-specificities (Fig. 6, Fig. S1A).

I therefore hypothesize that basally active *JAZ* promoters express JAZ proteins that are essential for the basal JA signalling repression complex formation. Moreover, *JAZs* that are active in specific tissues and cell types might repress JA signalling at those specific locations. Therefore, tissue- and cell-specific JA signalling processes may be regulated by the different expression sites of basally active *JAZs* and via different biochemical properties among the different JAZs, such as JA-Ile-dependent stability. Since cellular modulation of JA signalling is poorly understood in the root, I will mainly focus on the root. To test my hypothesis, I have set up several objectives:

Objective I: Are basally active *JAZ* promoters expressed in cell type-specific manners?

While the *JAZp:GUS* reporters revealed tissue-specificities of *JAZ* promoters, we lack cellular resolution. Therefore, additional transcriptional *JAZp:NLS-3xVEN* reporter lines for basally active *JAZ* promoters were designed to visualize cell type-specific promoter activities by live-cell imaging. I next used the *JAZp:NLS-3xVEN* reporter lines to generate maps projecting the frequencies of cell type-specific *JAZp* activities in the primary root.

Objective II: Can JA signalling be activated in a cell type-specific manner?

To investigate whether JAZs repress JA signalling based on their cell-specific promoter activity, I aimed to study *jaz* mutant phenotypes in a cell type-specific context. My plan was to generate multiple order *jaz* mutants based on *JAZp:NLS-3xVEN* expression maps to determine the JAZ repressor composition in each cell type, and test if it is possible to activate JA signalling at specific locations only. New CRISPR/Cas9 *jaz* mutants were generated in cases where T-DNA insertion lines were not available. I then performed several analyses to determine molecular and physiological phenotypes of single and multiple order *jaz* mutants. My hypothesis is that JAZs with basal promoter activity express JAZ repressors, contributing to the formation of the basal JA repression complex.

Objective III: Can JAZ repressors be visualized *in vivo*?

The cell type-specific transcriptional reporters provide information on the potential localization of JAZ repressors. However, the activity of a promoter and the localization of its corresponding protein may not always correlate due to regulation of turnover and localization. To address this issue, *JAZp:JAZ-CIT* reporter lines for all *JAZs* with basal promoter activity were designed, as well as some reporters of *JAZs* with no basal promoter activity as negative controls. Using live cell imaging, I analysed the JAZ-CIT localization of these reporters in the primary root. This approach provided a more comprehensive understanding of the cellular distribution of JAZ repressors, allowing for more accurate interpretation of their regulatory role in JA signalling.

Objective IV: Does ligand-dependent turnover rate vary between different JAZ repressors?

Cell type-specific modulation may be regulated by both defined JAZ expression patterns and other protein features, such as different COI1/ligand-dependent turnover rates. Previous studies have shown that JAZs exhibit differences in ligand-dependent COI1 binding *in vitro* (Sheard et al., 2010), suggesting these differences may be also pertinent *in vivo*. To measure JAZ-CIT turnover rates *in planta*, I generated and analysed ratiometric *JAZp:JAZ-CIT* reporters.

Section II - Results

Basally active *JAZ* promoters display cell type-specific root expression patterns

The *JAZp:GUS* reporters showed that *JAZs* with basal promoter activity display tissue-specific expression patterns (Fig. 6). However, to gain insight into their cellular expression, I selected stable T_3 *JAZp:NLS-3xVEN* transcriptional reporters of basally active *JAZp* and visualized their expression via live cell imaging in primary roots. I next generated their respective expression frequency maps by assessing the presence of reporter activity across root cell files (epidermis, cortex, endodermis, and pericycle cells across different root zones) by evaluating 10 individual roots per 2-3 independent T_3 lines for each construct (Fig. 7).

JAZ1p and *JAZ3p* were broadly expressed, almost throughout the entire root (Fig. 7). *JAZ1p* was active in almost all cell types, except for central cell layers of the root meristem, while *JAZ3p* signal was localized in most cell types except for endodermis and pericycle of the apical meristem. *JAZ2p* displayed activity in the root cap of the division zone, columella cells, epidermis of the root meristem, as well as in endodermis, pericycle, and stele of the late differentiation zone. *JAZ4p* was expressed in endodermis and cortex of both early differentiation zones (EDZ, 900-1215um from quiescent centre [QC]) and late differentiation zones (LDZ, 5000-5315um from QC), as well as in some cells of the stele localized in the early differentiation zone. *JAZ6p* exhibited reporter activity in cortex cells of the division zone, in the endodermis and cortex of both EDZs and LDZs, as well as in endodermis of the LDZ. *JAZ9p* was expressed in vascular initials and some cells of the columella, as well as in endodermis and pericycle cells of the LDZ. Overall, basally expressed *JAZp* show both overlapping and cell type-specific expression (Fig. 8).

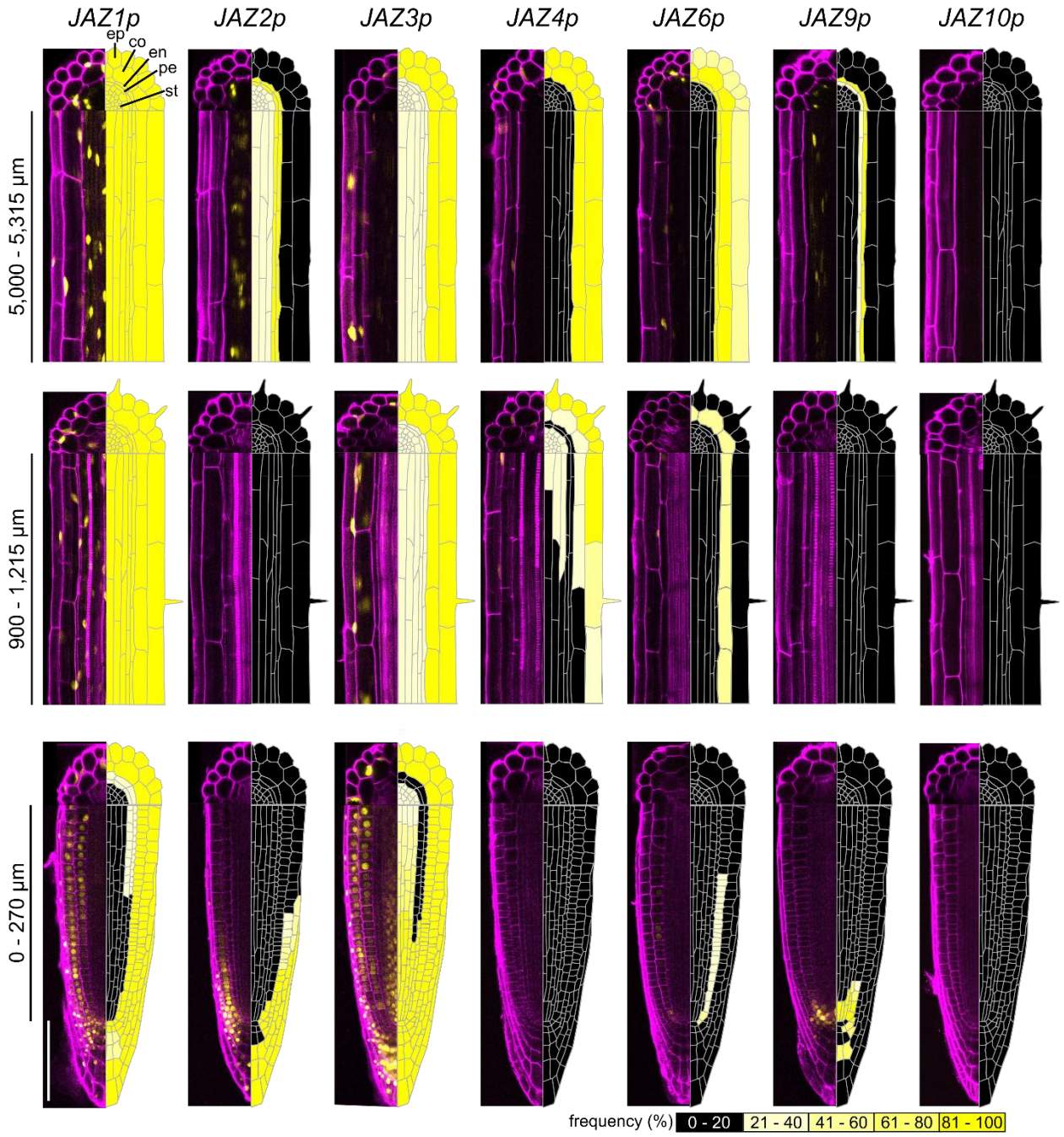

Figure 7: Basally active *JAZ* promoters diplay cell-type specific expression patterns. Orthogonal and longitudinal view of *JAZp:NLS-3xVEN* reporter (yellow) from different root zones in 5-do seedlings (left of each panel), and their associated frequency map of cellular reporter frequency (right of each panel) (n=10 roots for each 2-3 T_3 independent line). *JAZ10p:NLS-3xVEN* seedlings were included as negative control (no basal expression in the root). Roots were stained with propidium iodide (PI; magenta). ep, epidermis; co, cortex; en, endodermis; pr, pericycle; st, stele. Black scale bars indicate the distance from the quiescent centre (QC) towards the shoot (0-270 µm: division and elongation zone; 900-1,215 µm: EDZ, early differentiation zone; 5,000-5,315 µm: LDZ, late differentiation zone. Presence or absence of the reporter was evaluated over the indicated root zones along consecutive longitudinal files from n=10 roots for each 2-3 T_3 independent line. The schematic root template was adapted and modified from (De Smet, 2012) with adjustments made to suit the context of this study. Scale bar = 100 µm.

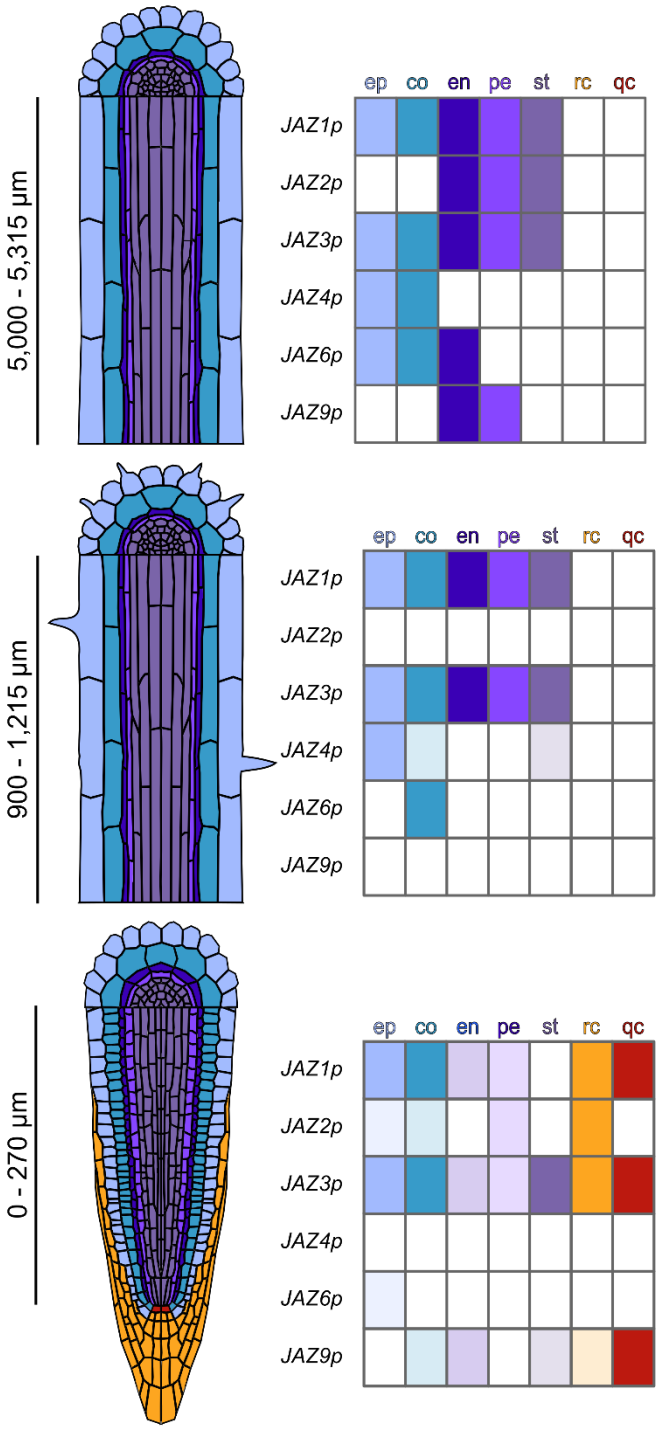

Figure 8: *JAZ* promoter activity map in the primary root. Schematic representation of cell-specific *JAZp* expression in the primary root across different zones. ep, epidermis; co, cortex; en, endodermis; per, pericycle; st, stele; rc, root cap; qc quiescent centre. Black scale bars represent distances from the QC toward the shoot (0-270 µm: division and elongation zone; 900-1,215 µm: EDZ; 5,000-5,315 µm: LDZ). For positions with weaker colour intensities, please refer to the *JAZp:NLS-3xVEN* frequency map (Figure 7). The schematic root template was adapted and modified from (De Smet, 2012) with adjustments made to suit the context of this study.

Characterization of available *jaz* mutants

The *JAZp:NLS-3xVEN* expression maps provide detailed information on the cellular expression patterns of basally active *JAZs* (Fig. 7; Fig. 8). This led me to question whether it is possible to activate cell type-specific JA signalling by using defined *jaz* KO mutations based on the expression map. To test this, I aimed at developing multiple order *jaz* mutants based on their expression pattern rather than as done previously by phylogeny (Campos et al., 2016; Guo et al., 2018).

I therefore analysed *jaz* KO mutants for each Arabidopsis *JAZ* gene except for *JAZ11*. All mutants, except for *jaz8-v*, which included a point mutation in the first exon of *JAZ8*, were T-DNA insertion lines (Campos et al., 2016; Cao et al., 2011; de Torres Zabala et al., 2016; Demianski et al., 2012; Jiang et al., 2014; Pauwels et al., 2010; Sehr et al., 2010; Thatcher et al., 2016; Thines et al., 2007; Thireault et al., 2015) (Fig. 9). After obtaining the homozygous mutant alleles, I tested *JAZ* transcript levels in respective alleles by reverse transcriptase (RT) polymerase chain reaction (PCR) using WT as a positive control. Since not all *JAZp* were basally active, I performed RT-PCR analyses on both untreated and MeJA treated seedlings. *UBIQUITIN CONJUGATING ENZYME 21* (*UBC21*) served as a reference gene, allowing semi-quantitative analyses of the transcripts (Fig. 10).

Results showed that in whole WT seedlings, *JAZ* transcripts with basally active promoters (Fig. 6), such as *JAZ1*, *JAZ2*, *JAZ3*, *JAZ4*, *JAZ6*, *JAZ9*, and *JAZ10*, were detectable by RT-PCR, while *JAZ* transcripts with weak or inactive promoters, such as *JAZ7*, *JAZ8*, *JAZ12*, and *JAZ13*, exhibited weak or absent expression levels (Fig. 10). Interestingly, *JAZ5* and *JAZ12* transcripts were detectable in WT seedlings, despite their promoters appearing to be inactive under basal conditions. MeJA treatment promoted an increase in *JAZ* transcripts in WT plants for most of the *JAZs*, including *JAZ4*, which showed no elevated promoter activity after shoot wounding (Fig. S1). These results mostly correlated with data generated by the *JAZp:GUS* reporters.

As expected, I could not amplify *JAZ* transcripts in most *jaz* mutants under neither basal nor MeJA induced conditions, confirming the validity of these KO alleles as published previously *jaz3-4* (Campos et al., 2016), *jaz4-1* (Jiang et al., 2014), *jaz7-1* (Sehr et al., 2010), *jaz9-1* (Yang et al., 2012), *jaz9-4* (Campos et al., 2016), *jaz10-1* (Sehr et al., 2010), *jaz13-1* (Thireault et al., 2015) (Fig. 10). However, respective *JAZ* transcripts in remaining *jaz* mutants (*jaz1-1*, *jaz1-2*, *jaz2-1*, *jaz2-2*, *jaz3-1*, *jaz5-1*, *jaz6-1*, *jaz6-2*, *jaz6-3*, *jaz12-1*, *jaz12-2*) were detectable under at least one of the tested conditions (Fig. 10).

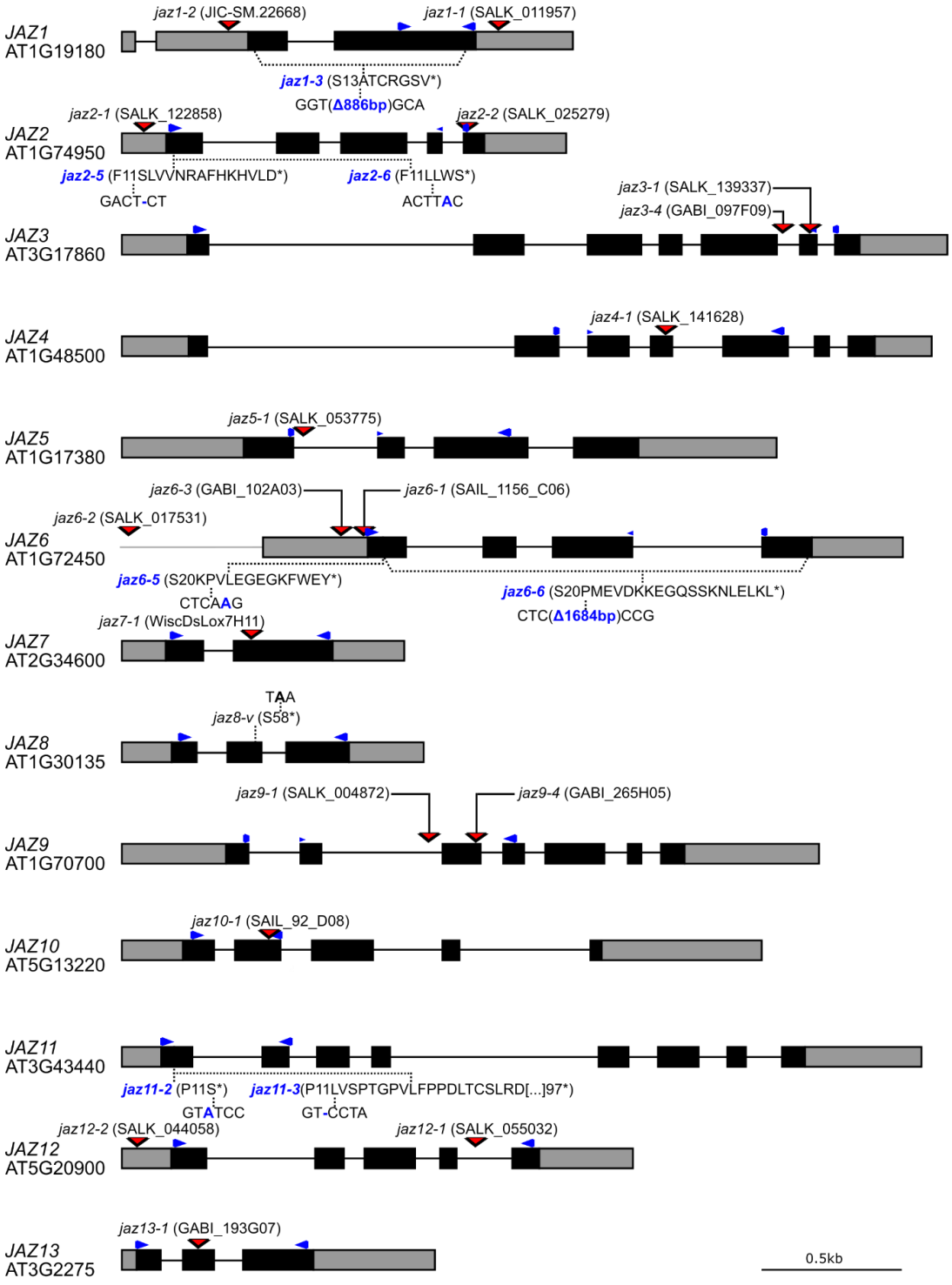

Figure 9: Description of *jaz* mutants used in this work. Schematic representation of all *13 Arabidopsis thaliana JAZ*s genes and respective *jaz* alleles which were tested via RT-PCR. Red triangles indicate T-DNA insertion sites, dotted lines mark all other allele positions I developed with CRISPR/Cas9 (in blue) or which were found in natural populations (*jaz8-v*). Blue arrows denote RT-PCR primers. Black boxes depict exons, grey boxes untranslated regions (UTRs), black straight lines introns, and grey straight lines promoters. Scale bar = 0.5 kb.

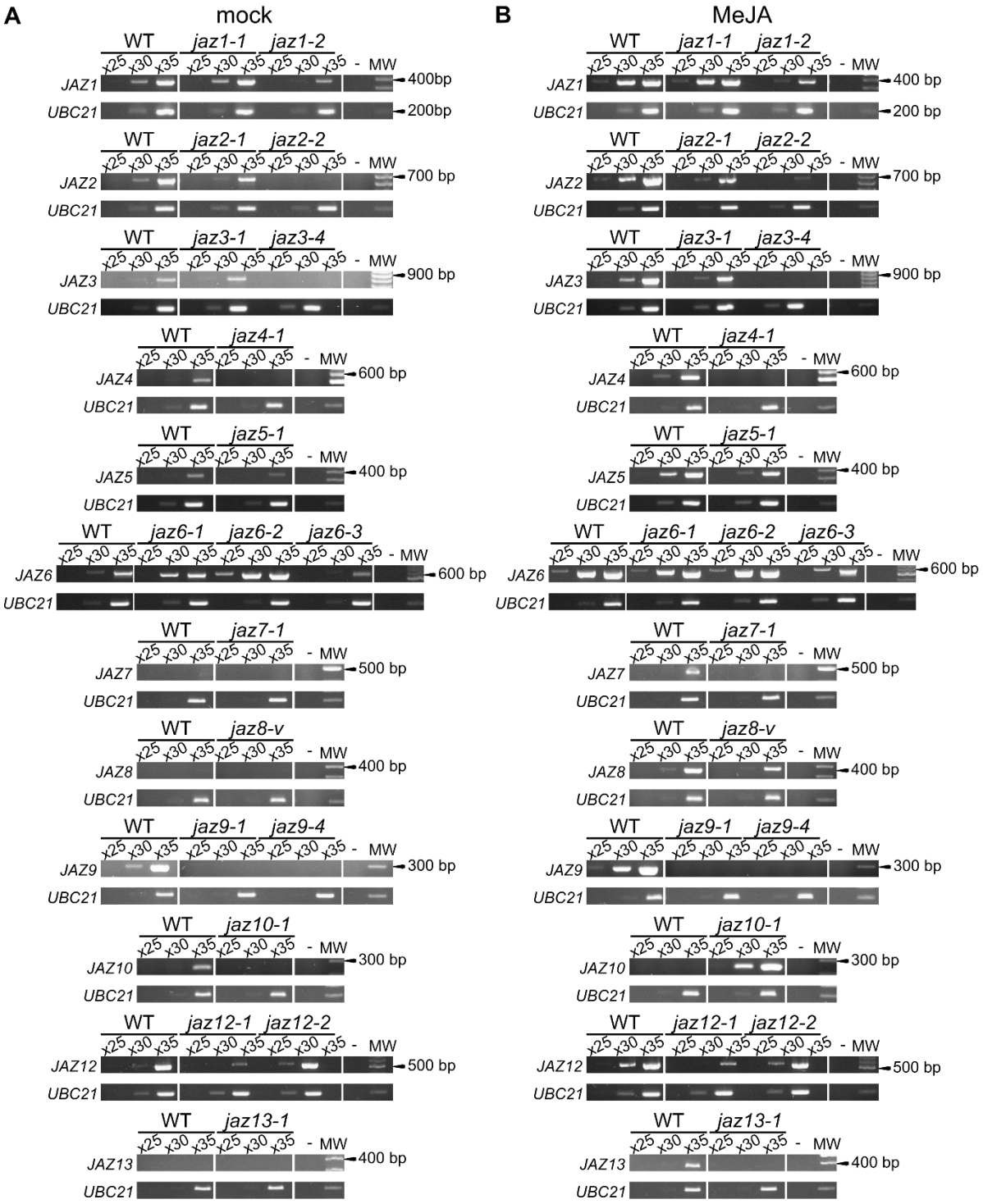

Figure 10: RT-PCR analysis of *JAZ* transcript expression in respective *jaz* mutant alleles at basal or MeJA-induced conditions. (**A,B**) RT-PCR (25, 30, and 35 PCR cycles) of *JAZs* transcripts in indicated 5-do *jaz* and WT seedlings under (**A**) basal (mock) and (**B**) 1h after 10 µM Me-JA induced conditions. The housekeeping gene *UBC21* was used as the reference gene. MW = molecular weight ladder

In the case of *jaz1-1* (Demianski et al., 2012), *jaz1-2* (Campos et al., 2016), *jaz2-1* (Thines et al., 2007), *jaz6-1* (Thatcher et al., 2016), *jaz6-3* (de Torres Zabala et al., 2016), and *jaz12-2* (Thatcher et al., 2016), the T-DNA insertion is specifically located in the untranslated region (UTR) (Fig. 10). This suggests that the transgene is likely to affect post-transcriptional modification regulation processes, such as translation efficiency, as well as transcript transport and stability, but not the open reading frame of the respective transcripts (Bashirullah et al., 2001; Jansen, 2001; Mignone et al., 2002; Srivastava et al., 2018; van der Velden & Thomas, 1999).

The *jaz12-1* allele (Pauwels et al., 2015), harbouring a T-DNA insertion in last intron (Fig. 9), displays *JAZ12* transcripts under both tested conditions (Fig. 10). As reviewed in (Marasco & Kornblihtt, 2023), introns are segments that are excluded from the mature mRNA as a result of alternative splicing. The presence of *JAZ12* transcripts in *jaz12-1* suggests that the T-DNA insertion is excised along with the introns, leading to the formation of functional mature mRNA. It is reasonable to assume that the splicing of *JAZ12* within *jaz12-1* is compromised, as indicated by the observed lower *JAZ12* transcript levels compared to the WT. Nevertheless, the presence of *JAZ12* transcripts suggests that *jaz12-1* is not a complete KO mutant. Furthermore, the *jaz2-2* allele (Thatcher et al., 2016), which has a T-DNA insertion in the last exon (Fig. 9), shows *JAZ2* transcripts after MeJA treatment (Fig. 10B). It is conceivable that the *jaz2-2* allele encodes a predominantly correct protein sequence but might be affected at the C-terminal end. This could potentially impact the Jas domain while leaving earlier motifs, such as CMID and ZIM, unaffected (Fig. 5). As a result, the mutated protein may act as a JA-Ile independent repressor (Thatcher et al., 2016).

Remarkably, *jaz6-2* showed higher-than-WT *JAZ6* expression (Fig. 10). In this case, the T-DNA is localized in the promoter region (Fig. 9), which potentially affects cis-elements and eventually the promoter activity without directly influencing the protein (Schmitz et al., 2022). In the case of *jaz6-2*, the T-DNA insertion appears to enhance the promoter activity, as indicated by the elevated transcript levels observed (Fig. 10). In case of *jaz8-v* (Thireault et al., 2015), *JAZ8* transcripts were also observable (Fig. 10). However, the point mutation in the *jaz8-v* allele causes an early stop codon in the first exon of the *JAZ8* gene, leading to a premature stop codon (Fig. 9) (Cao et al., 2011; Thireault et al., 2015).

Generation of novel *jaz* KO alleles via CRISPR/Cas9

As several T-DNA insertion lines were not confirmed to be loss-of-function *jaz* mutants (Fig. 10), I employed a CRISPR/Cas9 double guide approach to generate novel *jaz* mutant alleles from WT plants

(Pauwels et al., 2018). To do this, CRISPR/Cas9 single guide RNAs (sgRNAs) were designed to excise the first and last exons of each target gene. The aim was to remove major central gene portions, while the border sequences were reconnected by non-homologous end joining (NHEJ). This procedure led to the formation of a non-functional gene that encodes a significantly truncated protein fragment (Pauwels et al., 2018). Alternatively, if CRISPR/Cas9 cuts only once in the target gene, incorrect NHEJ of the cut DNA ends could cause small base pair (bp) insertions or deletions, resulting in frame shifts and early stop codons in the gene sequence (Cong et al., 2013; Doench et al., 2014). Therefore, I screened for *jaz* alleles with large sequence deletions and for single bp indels in the first exon.

Following this approach, I identified one mutant allele for *JAZ1* and two mutant alleles each for *JAZ2*, *JAZ6*, and *JAZ11*, which I named *jaz1-3*, *jaz2-5*, *jaz2-6*, *jaz6-5*, *jaz6-6*, *jaz11-2*, and *jaz11-3* (Fig. 9). *jaz2-5*, *jaz2-6*, *jaz6-5*, *jaz11-2*, and *jaz11-3* are characterized by single bp indels in the first exon of each respective mutant allele (*jaz2-5* and *jaz11-3*: thymine [T] deletion; *jaz2-6*, *jaz6-5*, *jaz11-2*: adenine [A] insertion), while *jaz1-3* and *jaz6-6* alleles imply large sequence deletions (*jaz1-3*: 886 base pairs [bp]; *jaz6-6*: 1648 bp). Despite my efforts, I was unable to identify loss-of-function mutants for *JAZ5* and *JAZ12*. However, since *JAZ5* and *JAZ12* are not basally expressed (Fig. 6B), they were not critical for my further aims.

To characterize *JAZ* transcript levels of the newly generated *jaz* alleles, I performed RT-PCR under basal conditions and after MeJA treatment. WT *JAZ* transcript levels showed the expected basal expression which was further increased by MeJA treatment (Fig. 11). *jaz1-3* and *jaz6-6* did not display detectable *JAZ* transcript levels under any experimental conditions (Fig. 11), indicating that both *jaz1-3* and *jaz6-6* are complete loss-of-function mutants. On the other hand, *jaz2-5*, *jaz2-6*, *jaz6-5*, and *jaz11-2* showed WT levels of respective *JAZ* transcripts (Fig. 11). This is because single base pair indels in the first exon of these alleles resulted in frame shifts in each respective coding sequence, leading to early stop codons (Fig. 9). Therefore, it is expected that translation of these alleles will stop prematurely and produce non-functional protein fragments. *jaz11-3* did not show any transcription under any tested condition, indicating that this allele is likely non-functional (Fig. 11).

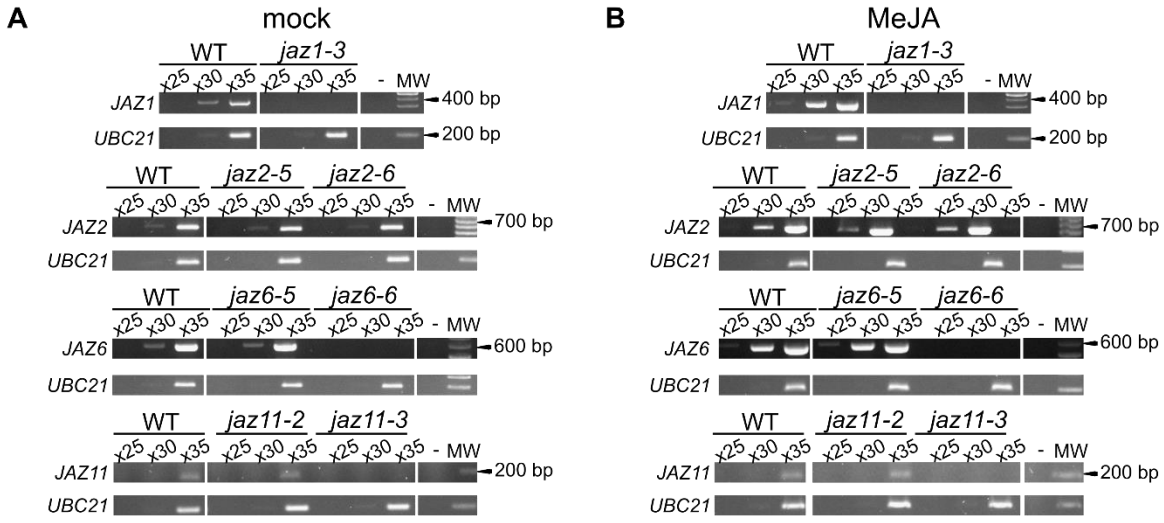

Figure 11: RT-PCR analysis of *JAZ* transcripts in respective CRISPR/Cas9 *jaz* alleles. (**A,B**) RT-PCR of *JAZ* transcripts after 25, 30, and 35 PCR cycles in 5-do WT and newly developed CRISPR/Cas9 *jaz* alleles under (**A**) basal (mock) and following (**B**) 1h after 10 µM MeJA treatment. The housekeeping gene *UBC21* was used reference gene.

JAZ2 represses JA signalling in the root tip

When JAZ repressors with basal promoter activity are not present (as in the case of *jaz* mutants), TFs are released from their repression, mediating the transcription of JA-responsive genes (Chini et al., 2007; Thines et al., 2007; Yan et al., 2007). Constitutive JA signalling can cause severe phenotypes, such as reduced root growth (Huang et al., 2017; Wasternack & Feussner, 2018). As I had at least one loss-of-function *jaz* allele for each basally expressed *JAZ* gene (*jaz1-3*, *jaz2-5*, *jaz2-6*, *jaz3-4*, *jaz4-1*, *jaz6-5*, *jaz6-6*, *jaz9-1*, *jaz9-4*) (Fig. 6; Fig. 7; Fig. 9), I assessed if these single *jaz* mutants show differences in root length compared to WT plants. The *jaz10-1* mutants served as negative control as *JAZ10p* is not basally active in the root (Fig. 7; Fig. S1A).

All single order *jaz* mutants showed no significant differences in root length compared to the WT, indicating that basally active *JAZs* function redundantly to regulate root growth (Fig. 12A). Although I could not observe any obvious root length phenotype, I tested whether the single *jaz* mutants exhibit any molecular JA signalling phenotypes such as a de-repression of JA-responsive genes such as *JAZ10*. I therefore introduced the *JAZ10p:NLS-3xVEN* reporter into *jaz* mutant alleles, which allows JA signalling visualization on a cellular level (Mielke et al., 2021). To avoid confusion, I refer to the *JAZ10p:NLS-3xVEN* reporter as the *JNV* reporter to emphasize its function as a JA signalling marker over that of a transcriptional reporter. Later, I screened for cellular *JNV* reporter activity in *jaz* roots focussing on zones where the *JAZp* under analysis was expected to be active (Fig. 7; Fig. 8; Fig. 12B; Fig. S2).

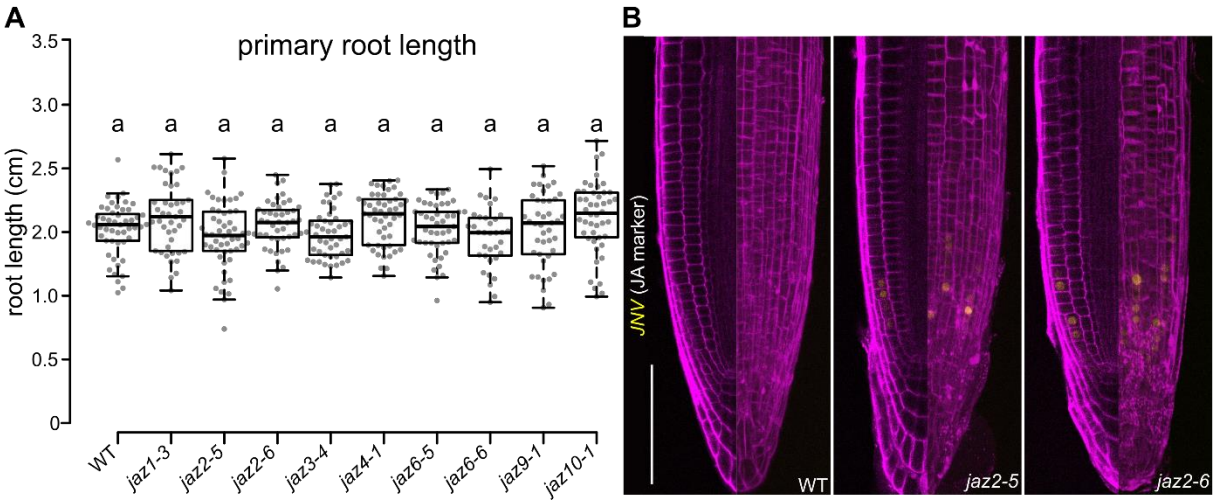

Figure 12: JA signalling is activated in *jaz2* root tips. (**A**) Box plot summary of primary root length of 7-do seedlings in indicated genotypes. Medians are represented inside the boxes by solid lines, circles depict individual measurements (n = 45-60). Letters denote statistically significant differences among samples as determined by One-Way ANOVA analysis followed by Tukey's HSD test ($p<0.05$). Results presented were similar across 3 independent experiments (**B**) *JAZ10p:NLS-3xVEN* (*JNV*; yellow) activity in WT, *jaz2-5*, and *jaz2-6* 5-do root tips. Images represent longitudinal optical sections (left side of each panel) and 3D Z-stack volume renderings (right side of each panel) (n = 10). Samples were counterstained with propidium iodide (magenta). Scale bar = 100 µm.

Interestingly, the *JNV* reporter appeared to be slightly elevated in the epidermal cells of the root meristem and in individual root cap cells of *jaz2-5* and *jaz2-6* mutants, correlating with the expression domains of the *JAZ2p:NLS-3xVEN* reporter (Fig. 7; Fig. 8; Fig. 12B). The *JNV* reporter exhibited no activation in the case of the remaining tested *jaz* alleles (Fig. S2).

JA signalling in the root tip of *jaz2* can be further elevated by disrupting *JAZ1* and *JAZ3*

I next investigated whether the induction of constitutive JA signalling (*JNV*) observed in the root tip of *jaz2* can be further enhanced by deleting additional *JAZ* genes expressed in the same region. I therefore generated multiple order *jaz* mutants by crossing other *jaz* mutants with one of my *jaz2* alleles. Specifically, I chose to use the *jaz2-6* allele over *jaz2-5*, as *jaz2-6* codes for an even earlier stop codon than *jaz2-5* (Fig. 9). According to the *JAZp:NLS-3xVEN* expression map, *JAZ1p:NLS-3xVEN* and *JAZ3p:NLS-3xVEN* have the highest overlapping expression sites with *JAZ2p:NLS-3xVEN* in the root tip (Fig. 7; Fig. 8). Thus, I generated *jaz1-3 jaz2-6* and *jaz2-6 jaz3-4* double mutants, as well as a *jaz1-3 jaz2-6 jaz3-4 triple* mutant (*jazTriple* or *jazT*) by crossing *jaz2-6* with the *jaz1-3* and *jaz3-4* alleles. I first measured the root length of *jaz1-3 jaz2-6*, *jaz2-6 jaz3-4*, and *jazT*. My data demonstrated that all tested multiple order mutants had significantly reduced root length when compared to the WT (Fig. 13A). Interestingly, the tested multiple order *jaz* mutants did not show any significant differences between each other.

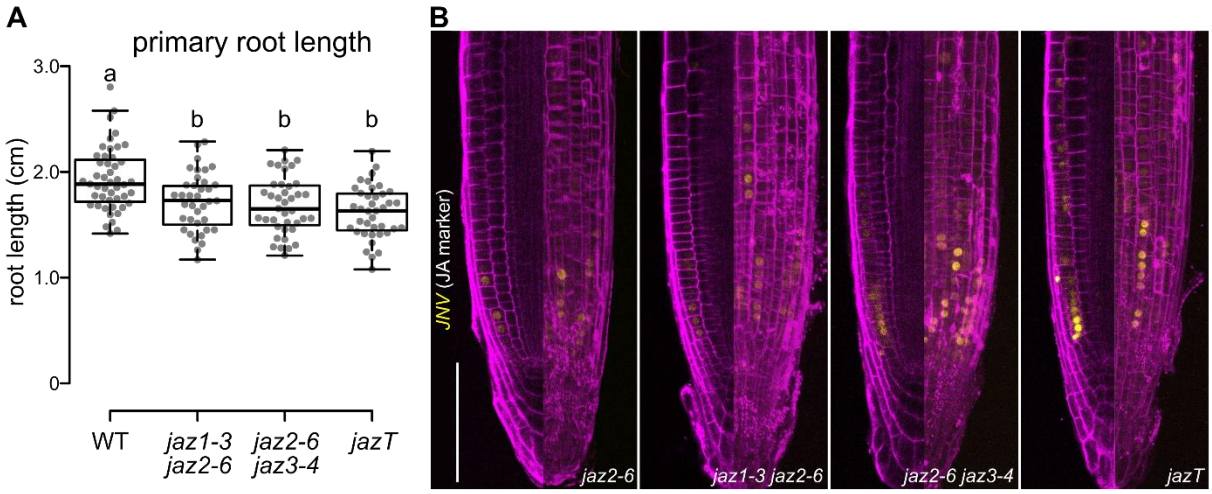

Figure 13: Constitutive JA signalling *jaz2* root tips can be further increased by additional *jaz1* and *jaz3* mutations. (**A**) Primary root length box plot summary of 7-do seedlings in indicated genotypes, with *jazT* referring to *jaz1-3 jaz2-6 jaz3-4*. Medians are represented inside the boxes by solid lines, circles depict individual measurements (n = 45-60). Letters denote statistically significant differences among samples as determined by One-Way ANOVA analysis followed by Tukey's HSD test ($p<0.05$). Described differences were observed in 2 independent experiments (**B**) *JNV* (yellow) activity in 5-do root tips of indicated genotypes. Images represent longitudinal optical sections (left side of each panel) and 3D Z-stack volume renderings (right side of each panel) (n = 10). Samples were counterstained with propidium iodide (magenta). Scale bar = 100 µm.

To verify the specificity of the *JNV* reporter, I also introduced it into the multiple order *jaz7-1 jaz8-v jaz10-1 jaz13-1* (*jazNon-basal* or *jazNB*) quadruple mutant as a negative control, which was published before (Thireault et al., 2015). I hypothesized that the loss-of-function of *JAZ7*, *JAZ8*, *JAZ10*, and *JAZ13* would have no effect on the basal *JNV* activity in the root of *jazNB*, as these genes display no basal expression in the root (Fig. 6B; Fig. S1A). Indeed, root length analysis of *jazNB* showed no effect on root growth compared to the WT, indicating no basal functionality of these genes (Fig. S3A). Consistent with this observation, *jazNB* displayed no *JNV* activity in the root, as expected (Fig. S3B).

I next analysed the roots of *JNV* marker lines by *in planta* live cell imaging of the root, as before for the single *jaz* mutants. In the case of *jaz1-3 jaz2-6*, the *JNV* reporter exhibited signal intensities comparable to those of the *jaz2-6* single mutant background (Fig. 13B). On the other hand, an increased *JNV* expression in *jaz2-6 jaz3-4* and *jazT* root tips was observed when compared to *jaz2-6* (Fig. 13B).

The root tip transcriptome of single and multiple order *jaz2* mutants

To gain an overview of the global transcriptional changes in the root tips of *jaz* mutants with constitutive JA signalling (elevated *JNV* activity), I conducted an RNA-seq analysis of WT and *jaz2-6*, *jaz2-6 jaz3-4*, and *jazT* root tips (Fig. 14; Fig. S4). The aim was to categorize differentially expressed genes (DEG) de-repressed in this zone by specific JAZ repressors. I excluded the *jaz1-3 jaz2-6* mutant from this experiment, as the

JNV reporter displayed a similar expression pattern as in the root tip of the single *jaz2-6* mutant. Additionally, due to the challenging nature of collecting root tips, I had to split the collection of my RNA-seq samples into two experimental days (Experiment 1 [Exp 1]: WT and *jaz2-6*; Experiment 2 [Exp 2]: WT, *jaz2-6 jaz3-4*, *jazT*). Therefore, the data included samples from both collection days.

To ensure that collecting root tips on two separate days did not influence the experiment, we performed a principal component analysis (PCA) to investigate how the genotypes of both collection days clustered (Fig. 14A; Fig. S4A). Ideally, WT samples from Exp 1 and Exp 2 should cluster together. As one WT biological replicate did not cluster with others (Fig. S4A), I excluded it from the analysis. Once this biological replicate was removed, all WT samples from the two collection dates clustered together (Fig. 14A), indicating that the root tip collection over two separate days could be analysed together. PCA plots indicated that all genotypes clustered separately, while *jaz2-6 jaz3-4* and *jazT* clustered together, indicating that their root tip transcriptomes share the highest similarities. To proceed in the analysis, each mutant was normalized to WT values.

To verify the results observed with the *JNV* reporter (Fig. 13B), I first analysed *JAZ10* expression in root tips in the RNA-seq data (Fig. 14B). Root tip *JAZ10* expression was significantly induced in *jazT*, consistent with my expectations. However, root tip *JAZ10* expression was not significantly upregulated in *jaz2-6* and *jaz2-6 jaz3-4,* as the *JNV* reporter indicated before. This could be due to a dilution effect in the collected material or a difference in promoter activity of the *JNV* reporter and the actual *JAZ10* transcript levels.

To gain an overview of global transcriptional changes, I normalized the transcriptome of each genotype to the values of the WT, using a cut-off of 2-fold change (FC, i.e. $\log_2 FC = \pm 1.0$). RNA sequencing (Fig. S4B) revealed 203 differently expressed genes (DEGs) in *jaz2-6* (63 upregulated, 140 downregulated), 447 genes in *jaz2-6 jaz3-4* (329 upregulated, 118 downregulated), and 740 genes in *jazT* (507 upregulated, 233 downregulated), when compared to the WT. Additionally, 66 genes were found to be mis-regulated in all tested genotypes. A total of 290 DEGs were found to be shared among *jaz2-6 jaz3-4* and *jazT*. A major portion of 352 genes were exclusively mis-regulated in *jazT*. Interestingly, 95 genes were mis-regulated in *jaz2-6*, but not in *jaz2-6 jaz3-4* and *jazT*. Moreover, the RNA-seq analysis revealed 10 DEGs which were mis-regulated in *jaz2-6* and *jaz2-6 jaz3-4*, but were not significantly altered in *jazT*. 32 genes were altered in *jaz2-6* and *jazT*, but not affected in *jaz2-6 jaz3-4*.

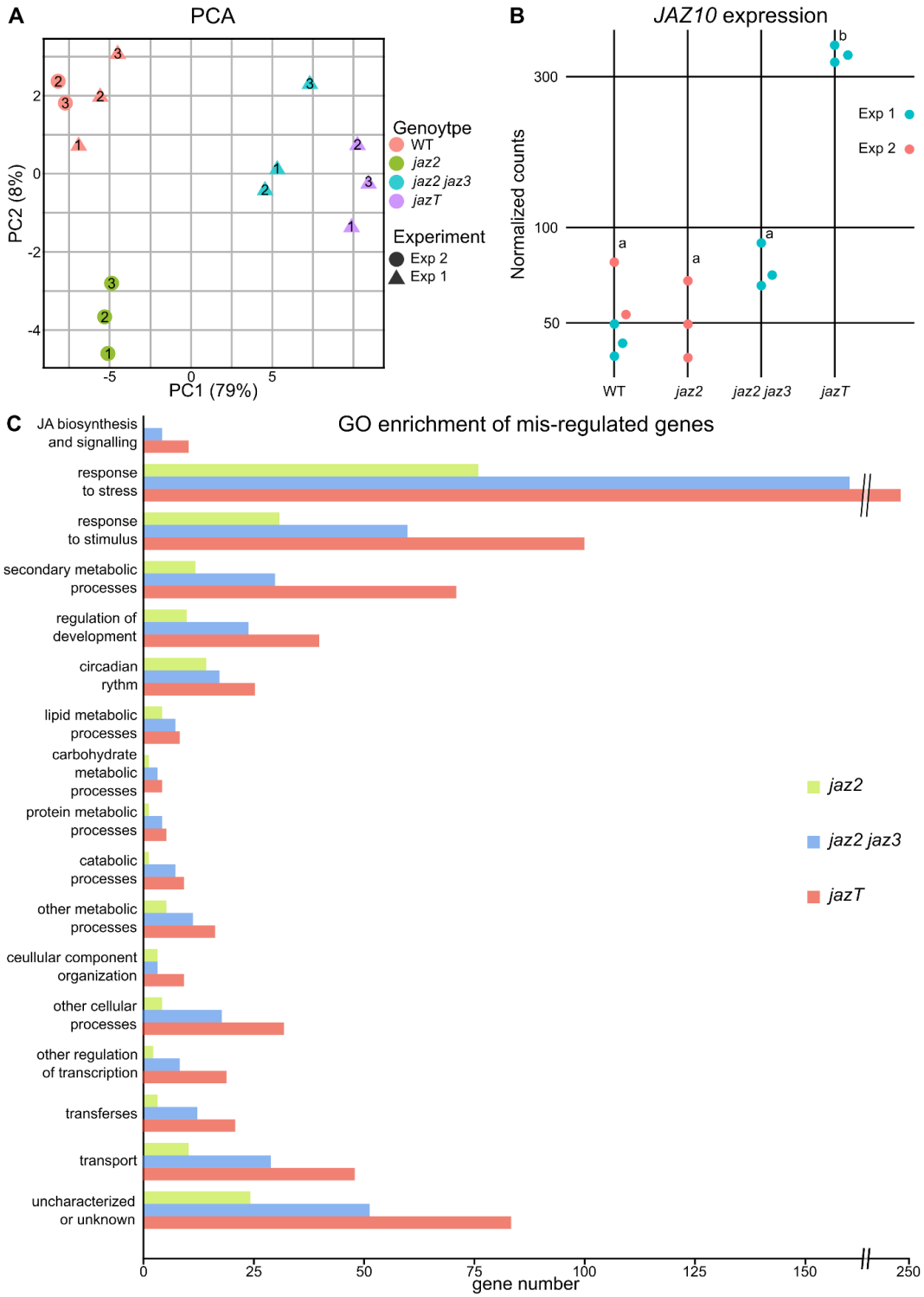

Figure 14: Root tip transcriptome analysis reveals differentially expressed genes (DEGs) in *jaz2-6* (*jaz2*), *jaz2-6 jaz3-4* (*jaz2 jaz3*), and *jaz1-3 jaz2-6 jaz3-4* (*jazT*). (**A**) Principal component analysis (PCA) of biological replicates from indicated genotypes collected on two separate days. One WT biological replicate was removed from the analysis Figure S4A (Exp1 = first sample collection day; Exp2 = second sample collection day). (**B**) Basal *JAZ10* transcript counts in *jaz2*, *jaz2 jaz3*, and *jazT* root tips relatively to the WT. Letters denote statistically significant differences among samples as determined by ANOVA followed by Tukey's HSD test ($P < 0.05$). (**C**) Gene ontology (GO) enriched terms of DEGs in *jaz2*, *jaz2 jaz3*, and *jazT*. The indicated genotypes were normalized to the WT (cutoff: log2FC = ±1; p-value: 0.01). (aspect "biological process"; false discovery rate < 0.05). Full dataset is available in Supplementary Tables S2. (n = 3, each biological replicate contains a pool of ~180 root tips of 5-do seedlings).

As can be expected from CRISPR/Cas mutants (Shalem et al., 2015), reads mapping to *JAZ1* and *JAZ3* were found upregulated in the double and triple mutants, as well as to *JAZ2* in the triple mutant (Tab. S2). However, the reads do not cover the full- length genes and cluster in externally flanking regions of the designed sgRNAs (Fig. S5), confirming that *jaz1-3* and *jaz2-6* are full KO alleles. Similarly, the previously characterized *jaz3-4* T-DNA insertion allele (Campos et al., 2016) also showed upregulation of the *JAZ3* reads only for the last 3 exons. Hence, the upregulation of *JAZ1*, *JAZ2*, and *JAZ3* in the double and triple *jaz* mutants does not cover the respective full-length genes but can be considered as evidence of activated JA signalling in these mutants.

To categorize DEGs in the three genotypes, I performed a Gene Ontology (GO) enrichment analysis for "biological processes" (Fig. 14C; Fig. S4C and D). The analysis revealed terms involved in stress response, stimulus response, secondary metabolites, and developmental regulation for all tested genotypes. Notably, a larger proportion of DEGs were classified as being involved in the circadian rhythm, which might be a result of the time-consuming sample collection which occurred over 6 h for each collection day.

The transcriptome analysis revealed the upregulation of genes involved in the JA pathway in *jaz2-6 jaz3-4* and *jazT* root tips, but not in the *jaz2-6* single mutant. Specifically, the upregulation of *LOX3*, *AOS*, *JAZ1*, and *JAZ3* was found in the double and triple mutant, and a broader upregulation of the JA pathway genes was found exclusively in the triple mutant including *JOX3*, *JAZ2*, *JAZ5*, *JAZ6*, *JAZ9*, and *JAZ10* (Tab. S2).

In planta localization of JAZ1, JAZ2, and JAZ3 proteins in the primary root

To date, JAZ proteins have only been visualized in plants through the overexpression of constitutive promoters (Chini et al., 2007; Shyu et al., 2012; Thines et al., 2007), which does not accurately represent their endogenous localization. To determine whether JAZ repressors can be visualized under the control of their native promoters, translational reporters expressing C-terminal-tagged JAZ proteins fused to a CITRINE (CIT) fluorophore (*JAZp:JAZ-CIT*) were generated for the basally active promoters. As negative controls, I also generated *JAZp:JAZ-CIT* reporters of non-basally active *JAZ* promoters (Fig. 6B; Fig. S1A), including *JAZ8p:JAZ8-CIT*, *JAZ10p:JAZ10-CIT*, and *JAZ11p:JAZ11-CIT*. These reporters were then transformed into the respective *jaz* mutant backgrounds. Eventually, I selected the lines and analysed their expression in T_3 roots (Fig. 15; Fig. S6).

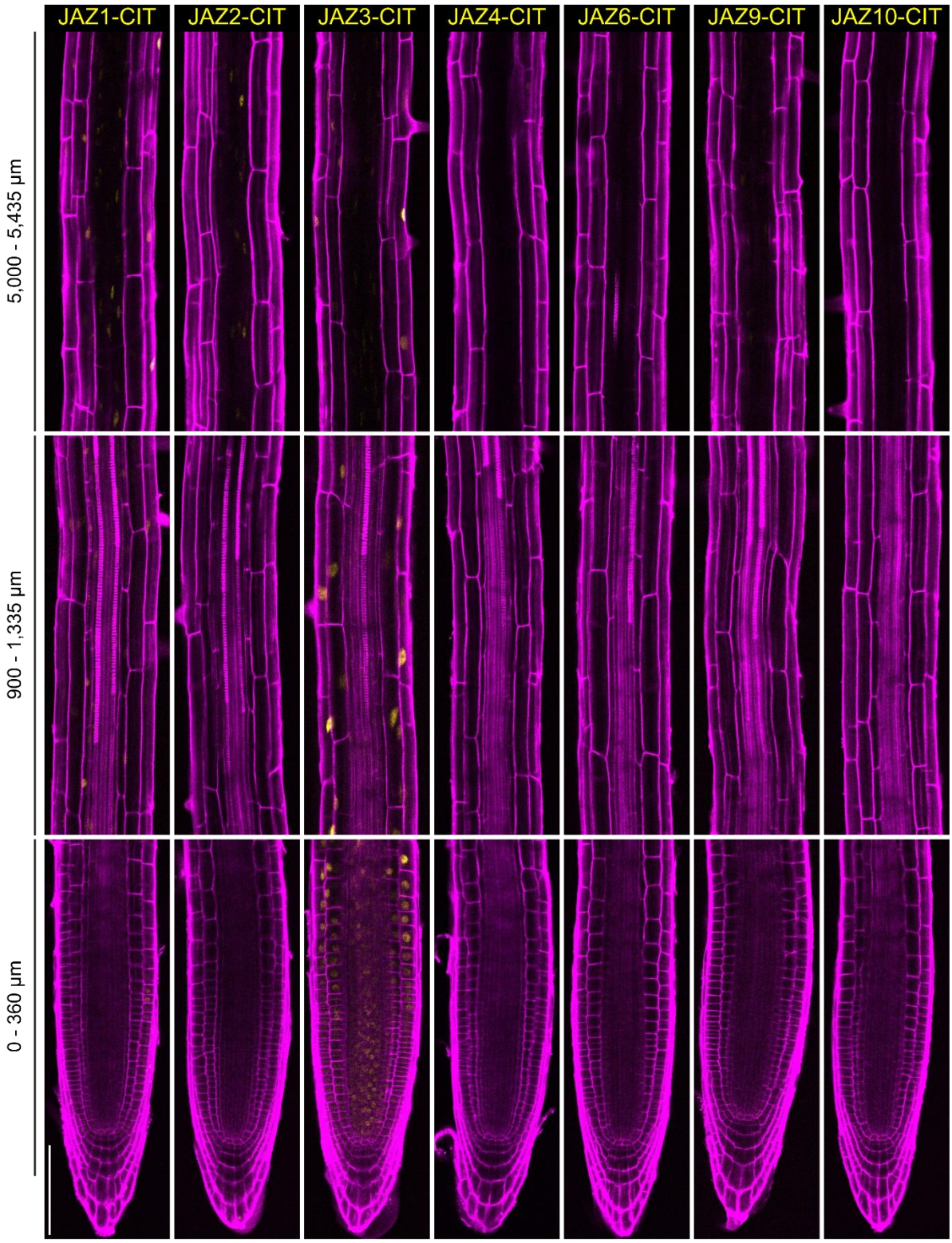

Figure 15: JAZ1-CIT, JAZ2-CIT, and JAZ3-CIT expressed under their native promoters can be visualized in primary root tips. Representative images of longitudinal optical sections of 5-do *JAZp:JAZ-CIT* reporter roots stained with PI (magenta), potentially displaying JAZ-CIT (yellow) expression, and imaged live (n=10, from two independent T_3 lines for each construct). Black bars indicate the distance from the QC towards the shoot (0-270 µm: division and elongation zone; 900-1,335 µm: EDZ; 5,000-5,425 µm: LDZ). Scale bar =100 µm.

JAZ1p:JAZ1-CIT, *JAZ2p:JAZ2-CIT*, and *JAZ3p:JAZ3-CIT* exhibited detectable protein expression, while *JAZ4p:JAZ4-CIT*, *JAZ6p:JAZ6-CIT*, and *JAZ9p:JAZ9-CIT* displayed almost no fluorescence signal in any of the tested root zones (Fig. 15). On average, the fluorescence signal from transcriptional reporters was weaker compared to that of the translational reporters (Fig. 7; Fig. 15). As expected, JAZ-CIT proteins localized to the nucleus (Fig. 15) (Chini et al., 2007; Shyu et al., 2012; Thines et al., 2007). Both JAZ1-CIT and JAZ3-CIT exhibited a pattern of localization consistent with their respective transcriptional reporters (Fig. 6A; Fig. 7; Fig. 8; Fig. 15). In agreement with the transcriptional map (Fig. 7; Fig. 8), the *JAZ1p:JAZ1-CIT* reporter was only sporadically active in the root tip and in EDZ (Fig. 15). In contrast, *JAZ2p:JAZ2-CIT* was present in the vascular system of the LDZ (Fig. 15). Notably, although transcriptional reporters of *JAZ2* exhibited promoter activity in the root tip (Fig. 7; Fig. 8), JAZ2-CIT was notably detectable in the root tip when examined using the corresponding translational reporter (Fig. 15). However, similar to the *JAZ2p:NLS-3xVEN* reporter (Fig. 7; Fig. 8), *JAZ2p:JAZ2-CIT* displayed a signal in the vasculature of older root zones (Fig. 15). Consistent with previous negative data (Fig. 6B; Fig. S1A), *JAZ8p:JAZ8-CIT*, *JAZ10p:JAZ10-CIT*, and *JAZ11p:JAZ11-CIT* displayed no reporter expression in the root (Fig. 15; Fig. S6).

Generation of ratiometric translational reporters for JAZ turnover measurements *in planta*

While the *in planta* localization of JAZ-CIT proteins expressed under their native promoters uncovered their cell type-specific expression under basal conditions (Fig. 15), evaluating their turnover rates in response to changing hormone levels can be hindered by their rapid degradation rates and lack of an internal normalizer (Larrieu et al., 2015). Specifically, the degradation of the Jas9 motif started within minutes of exogenous JA application (Larrieu et al., 2015). Furthermore, even minor unintentional sample mistreatments during mounting could lead to JAZ-CIT degradation and inaccurate interpretations. Therefore, while it was remarkable to observe JAZ-CIT signals in living roots mounted on microscopy slides (Fig. 15), I next designed new constructs by combining *JAZp:JAZ-CIT* reporters with a normalizer within the same transgene with the aim to perform ratiometric reporter analyses (Fig. 16).

The normalization construct contains a constitutively active *UBIQUITIN10* promoter (*UBQp*) driving the expression of a JA-Ile-insensitive Jas9 degron (Ijas9) fused to a nuclear tandem dimer TOMATO fluorophore (tdTOMATO, here referred as TOM) (Fig. 16A). I designed Ijas9 based on a strategy used by (Liao et al., 2015) to generate a ratiometric auxin reporter called R2D2, in which an auxin-insensitive degron of an AUX/IAA protein is expressed as the normalization protein. I hence mutated three amino acids (aa) within the Jas9 degron (R223A, K224A, F230A) that are essential for JAZ9-COI1 and JAZ9-MYC3

binding (Fig. 16B) (Larrieu et al., 2015; Melotto et al., 2008; F. Zhang et al., 2015). R223A, K224A, and F30A mutations eliminate the binding between JAZ9 and COI1, resulting in the insensitivity of Ijas9 to ligands (Larrieu et al., 2015; Melotto et al., 2008; F. Zhang et al., 2015). Additionally, the F30A mutation is expected to prevent the binding of JAZ9 to MYC2, MYC3, and MYC4 (F. Zhang et al., 2015), thereby avoiding a constitutive repression effect of Ijas9 on JA-responsive genes.

Previously, a ratiometric JA-Ile sensor named Jas9-VENUS (*rat.Jas9-VEN*) has been developed to sense hormone levels *in planta* (Larrieu et al., 2015). The sensor uses the overexpression of the JAZ9 degron (Jas9) fused to CIT as the hormone sensor on one transgene (*35Sp:Jas9-CIT*), and the overexpression of HISTONE 2B (H2B) fused to RED FLUORESCENT PROTEIN (RFP) as the normalizer (*35Sp:H2B-RFP*) on a second transgene. While the design procedures between the *rat.Jas9-VEN* sensor and my *rat.JAZp:JAZ-CIT* reporters may appear similar, it is important to note that my *rat.JAZp:JAZ-CIT* were developed to map JAZ cellular localizations and measure their turnover rates in planta, and not to sense the hormone generally. Furthermore, the *rat.Jas9-VEN* sensor expresses only the Jas9 degron motif, whereas my reporters express full-length JAZ proteins. An additional advantage of my *rat.JAZp:JAZ-CIT* is the expression of the sensing and normalization constructs from the same transgene easing selection after crossing, and a similar epigenetic regulation deriving from the integration at the same genomic position.

In total, I generated ratiometric (*rat.JAZp:JAZ-CIT*) reporters for all *JAZs* driven by basally active promoters (*JAZ1*, *JAZ2*, *JAZ3*, *JAZ4*, *JAZ6*, and *JAZ9*), as well as a *rat.JAZ10p:JAZ10-CIT* as a representative of a non-basally active promoter serving as negative control (Fig. 16C and D; Fig. S7). Similarly to the non-ratiometric *JAZp:JAZ-CIT* translational reporters (Fig. 15), I transformed the *rat.JAZp:JAZ-CIT* reporters in respective *jaz* single mutants and analysed the reporter activities in Arabidopsis roots by confocal microscopy, focussing on the root DZ and EDZ (Fig. 16C and D; Fig. S7).

The fluorescence of the normalization *UBQp:Ijas9-TOM* reporter was visible in the nuclei of all cell types tested (Fig. 16C and D; Fig. S7). Similarly to the non-ratiometric *JAZp:JAZ-CIT* reporters (Fig. 15), *rat.JAZ2p:JAZ2-CIT*, *rat.JAZ4p:JAZ4-CIT*, *rat.JAZ6p:JAZ6-CIT*, *rat.JAZ9p:JAZ9-CIT*, and *rat.JAZ10p:JAZ10-CIT* showed no or only weak JAZ-CIT expression in the respective root zones (Fig. S7). Importantly, *rat.JAZ1p:JAZ1-CIT* and *rat.JAZ3p:JAZ3-CIT* showed good fluorescence signal intensities (Fig. 16C and D) and with similar JAZ-CIT localization patterns as their non-ratiometric counterparts (Fig. 15). Therefore, I selected these two reporters for subsequent experiments.

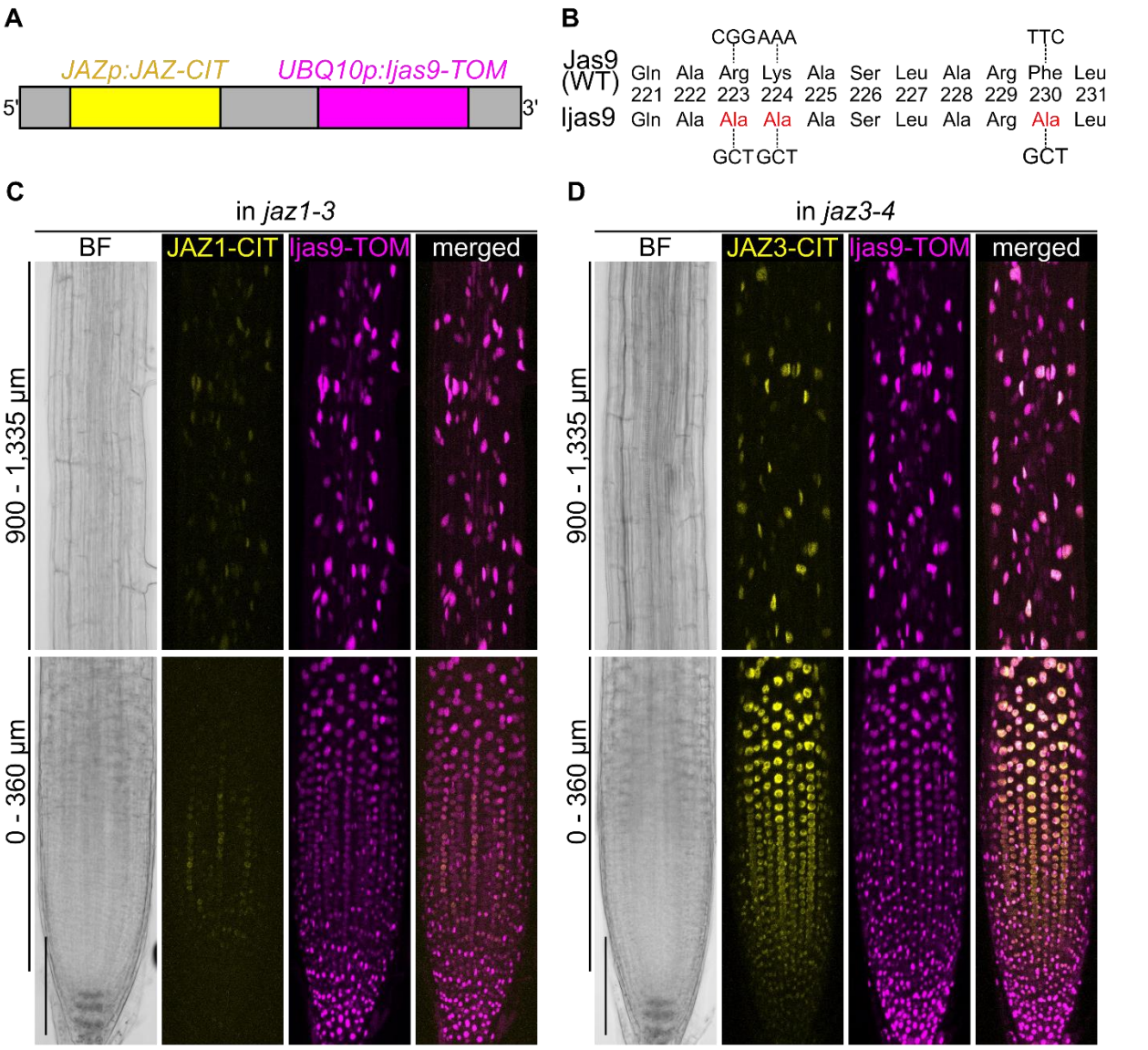

Figure 16: Root expression of ratiometric JAZ-CIT reporters in respective *jaz* mutants. (**A**) Scheme of ratiometric *rat.JAZp:JAZ-CIT* transgenes, in which *JAZp:JAZ-CIT* was cloned next to a JA-Ile insensitive *UBQp:Ijas9-CIT* normalizer in the same construct. *Ijas9* refers to a mutated Jas9 motif insensitive to JA-Ile (Ijas9). (**B**) Amino acid (aa) sequences of the WT Jas9 degron and the JA-Ile-insensitive Ijas9 used as a normalizer, including modified amino acids (in red) predicted to abolish COI1 and MYC3 interaction. (**C,D**) Representative root images of 3D Z-stack volume renderings of 5-do (**C**) *rat.JAZ1p:JAZ1-CIT* in *jaz1-3* and (**D**) *JAZ3p:JAZ3-CIT* in *jaz3-4* seedlings in bright filed (BF), JAZ-CIT (yellow), and Ijas9-TOM (magenta) channels (n=10 roots from two independent T_3 lines). Black bars indicate the distance from the QC towards the shoot (0-360 µm: division and elongation zone; 900-1,335: early differentiation zone). Scale bar = 100 µm.

To determine the basal steady state of *JAZp:JAZ-CIT* and *UBQp:Ijas9-TOM* reporters, I measured the signal intensity as Arbitrary Fluorescence Unit (AFU) in *rat.JAZ1p:JAZ1-CIT* and *rat.JAZ3p:JAZ3-CIT* roots over a 15-minute time period (Fig. 17, Fig. S8). To increase the measurement specificity, I detected fluorescence intensities over time from single nuclei in the outer cell layers of the EDZs, where both JAZ1-CIT and

JAZ3-CIT fluorescence signals were visible (Fig. 17A and B; Fig. S8). Each time point represents the average AFU from at least 10 roots, with 5-7 nuclear measurements per root as technical replicates (Fig. 17C and D). The same imaging setting were applied for both ratiometric reporters, and nuclei of non-transgenic Arabidopsis WT roots (n=10) in the same EDZ were imaged to obtain background AFU levels. These WT values were used as background thresholds and were subtracted from JAZ-CIT and Ijas9-TOM measurements, respectively.

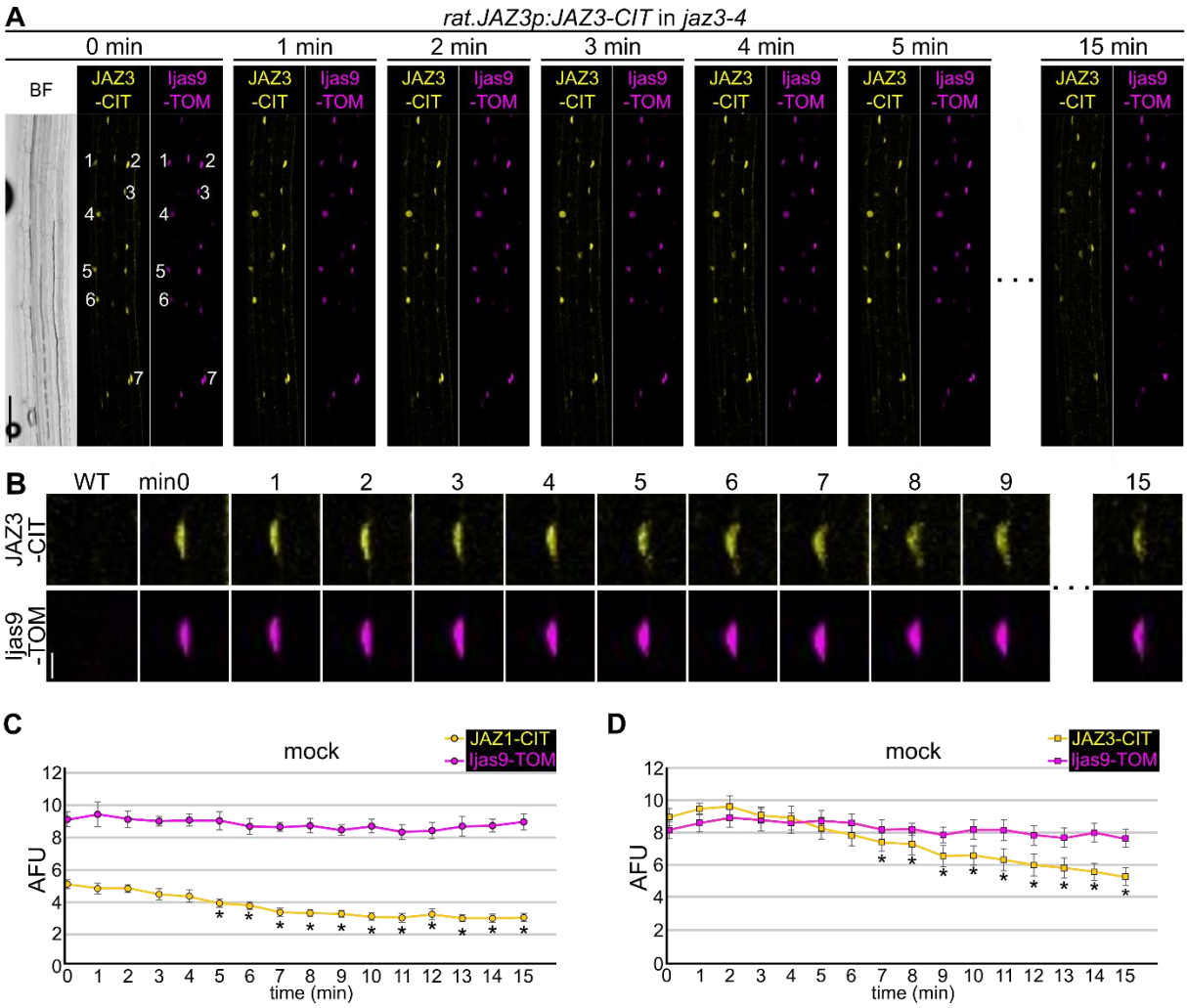

Figure 17: JAZ-CIT fluorescence signals are not stable under mock conditions in *jaz* mutants. (A) Representative images of *JAZ3p:JAZ3-CIT* (JAZ3-CIT, yellow) and *UBQ10p:Ijas9-TOM* (Ijas9-TOM, magenta) expression in the root EDZ of 5-do *jaz3-4* mutant seedlings over a 15min imaging time course under mock conditions. A bright field (BF) image is presented for reference. Numbers depict individual nuclei evaluated in the ratiometric (rat.) JAZ reporters. **(B)** Close-up view of JAZ3-CIT and Ijas9-TOM from individual nuclei during the mock time course. Untransformed WT plants were used to subtract background signals. (**C,D**) Arbitrary Fluorescence Unit (AFU) measurements from the rat.JAZ reporters in (**C**) *rat.JAZ1p:JAZ1-CIT* in *jaz1-3* and (**D**) *rat.JAZ3p:JAZ3-CIT* in *jaz3-4* mutants. Fluorescence signals were quantified from 5-7 nuclei in at least 10 roots per construct at a frequency of 1 image per minute. Asterisks denote statistically significant differences at each time point compared to initial AFU at t=0 as determined by One-Way ANOVA analysis followed by Tukey's HSD test ($p<0.05$). Error bars = SEM. Scale bars (A) = 100 µm, (B) = 10 µm.

With these parameters, the JAZ1-CIT signal intensity was consistently lower than JAZ3-CIT, while the normalization constructs were similar between the two lines (Fig. 17C and D). Interestingly, while the normalization Ijas9-TOM signal was stable over the 15 min imaging time course and had similar AFU intensities among the 2 transgenic lines, I observed a significant decrease in JAZ1-CIT and JAZ3-CIT signal over time under mock conditions (Fig. 17C and D). Possible reasons for the JAZ-CIT signal decreases could be unintentional wounding during seedling manipulation, which may have increased endogenous JA-Ile levels and triggered unintended JAZ-CIT degradation (Chini et al., 2007; Thines et al., 2007; Yan et al., 2007). Due to their unstable steady state, results indicate that JAZ-CIT stability cannot be assessed accurately in *jaz* mutant backgrounds. To address this issue and prevent unintended JAZ-CIT degradation caused by sample manipulation, I therefore transformed the reporters into a JA-Ile deficient *aos* KO mutant (Park et al., 2002).

Evaluating ratiometric JAZ-CIT reporters in a JA-Ile deficient mutant background

I first confirmed whether the expression patterns of the *rat.JAZp:JAZ-CIT* reporters in *aos* (Fig. 18A and B; Fig. S9) were in line with those in the *jaz* mutant backgrounds (Fig. 16C and D; Fig. S7). Consistent to my previous data (Fig. 16C and D), *JAZ1p:JAZ1-CIT* and *JAZ3p:JAZ3-CIT* displayed the same expression domains, independently from the mutant background (Fig. 18A and B). The *rat.JAZ1p:JAZ1-CIT* in *aos* showed weaker JAZ1-CIT expression in the epidermis and cortex cells within the apical root meristem and the EDZ, as well as in the endodermis of the EDZ (Fig. 18A). On the other hand, *rat.JAZ3p:JAZ3-CIT* in *aos* exhibited JAZ3-CIT localization in the root DZ and the EDZ (Fig. 18B). Consistent with previous observations (Fig. 15; Fig. 16C and D), the JAZ3-CIT signal was generally stronger compared to JAZ1-CIT (Fig. 18A and B). Similarly to the ratiometric and the non-ratiometric constructs in the *jaz* mutant backgrounds (Fig. 15; Fig. S7) *JAZ2p:JAZ2-CIT*, *JAZ4p:JAZ4-CIT*, *JAZ6p:JAZ6-CIT*, *JAZ9p:JAZ9-CIT*, and *JAZ10p:JAZ10-CIT* had no or only weak fluorescence signals in the *aos* mutant (Fig. S9), precluding their further analysis. In parallel, I probed the expression patterns of the JA-Ile insensitive *UBQp:Ijas9-TOM* normalizer. Similar to the *jaz* mutants (Fig. 16C and D), Ijas9-TOM was expressed across all root cells of *aos* and with similar AFUs in both ratiometric reporters (Fig. 18A and B).

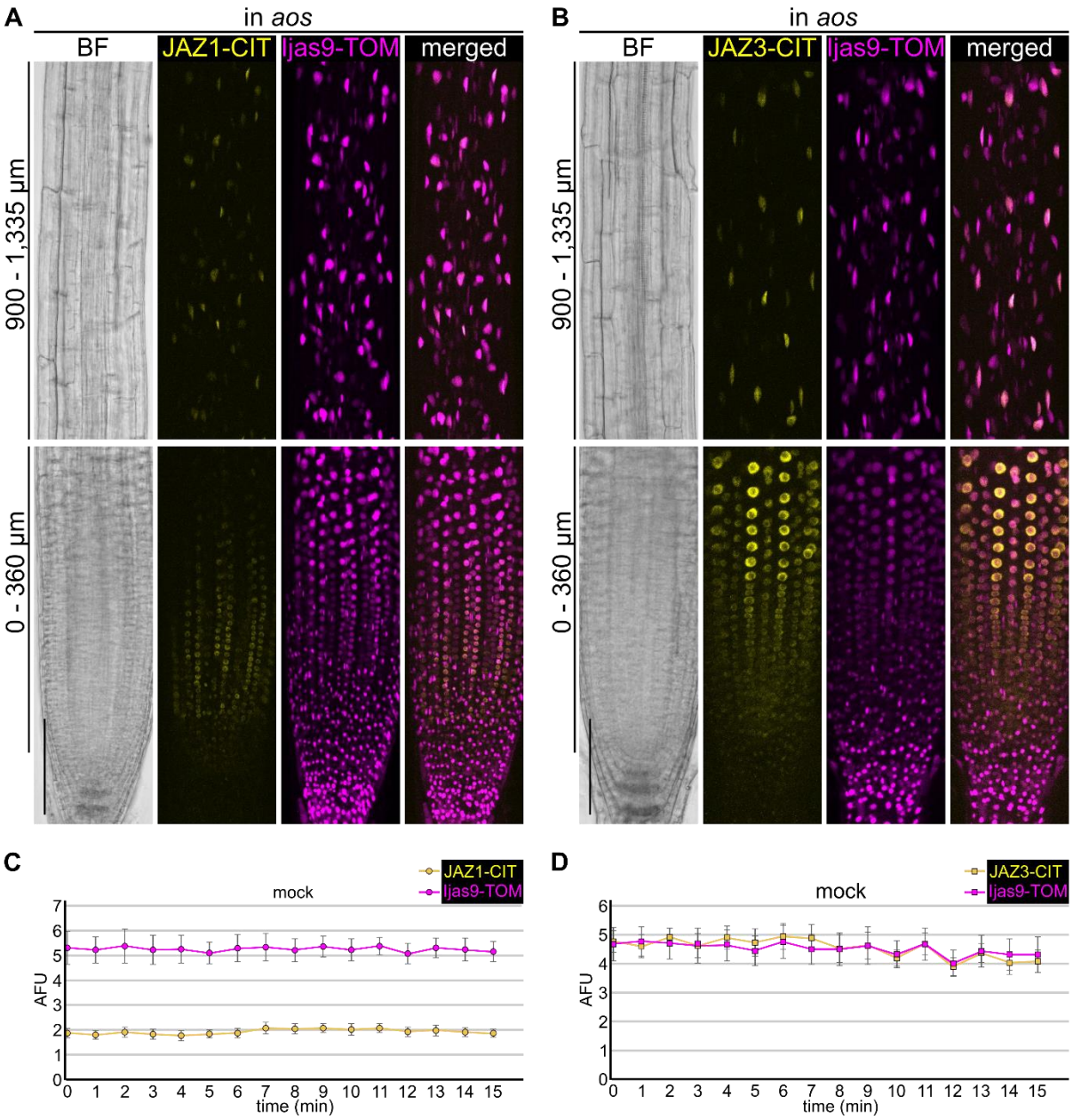

Figure 18: *rat.JAZ1p:JAZ1-CIT* and *rat.JAZ3p:JAZ3-CIT* steady states in the JA-Ile-deficient mutant *aos*. (**A,B**) Representative root images of 3D Z-stack volume renderings of 5-do (**A**) *rat.JAZ1p:JAZ1-CIT* and (**B**) *JAZ3p:JAZ3-CIT* in *aos* seedlings in bright filed (BF), JAZ-CIT (yellow), and Ijas9-TOM (magenta) channels (n=10 roots from two independent T_3 lines). Black bars indicate the distance from the QC towards the shoot (0-360 µm: division and elongation zone; 900-1,335: early differentiation zone). (**C,D**) Arbitrary Fluorescence Unit (AFU) measurements from the rat.JAZ reporters in (**C**) *rat.JAZ1p:JAZ1-CIT* and (**D**) *rat.JAZ3p:JAZ3-CIT* in the *aos* mutant under mock conditions. Fluorescence signals were quantified from 5-7 nuclei in at least 10 roots per construct at a frequency of 1 image per minute. Scale bars = 100 µm.

As expected, Ijas9-TOM in the *aos* background showed a stable fluorescence signal over the 15 minutes mock time course for both constructs (Fig. 18C and D). Furthermore, Ijas9-TOM intensities were similar across the two constructs (Fig. 18C and D). Contrary to what was observed in *jaz* mutant backgrounds,

JAZ1-CIT and JAZ3-CIT fluorescence signals in *aos* were also stable during the imaging time course (Fig. 18C and D), indicating that the decrease in fluorescence observed in *jaz* backgrounds was likely due to increases in endogenous hormone levels following sample manipulation. Interestingly, the basal total JAZ1-CIT AFU values were found to be around 3 times lower of those observed in JAZ3-CIT AFU (Fig. 18C and D). This observation aligns with the fact that the JAZ1-CIT signal appeared weaker compared to the JAZ3-CIT signal in all reporters and mutant backgrounds (Fig. 15; Fig. 16C and D). Since the ratiometric JAZ-CIT reporters exhibited a stable steady state fluorescence signal at basal conditions in the *aos* background (Fig. 18C and D), these lines were optimal for measuring JAZ-CIT turnover rates in planta following external hormone applications.

To this end, I first evaluated the sensitivity of the normalization Ijas9-TOM construct to the JA-Ile mimic COR (Feys et al., 1994; Fonseca, Chini, et al., 2009; Sheard et al., 2010; Staswick & Tiryaki, 2004). As expected, 1 µM COR treatment did not impact Ijas9-TOM AFU in both *rat.JAZ1p:JAZ1-CIT* and *rat.JAZ3p:JAZ3-CIT* reporters during a 15 min imaging time frame (Fig. 19). In contrast, COR treatments caused a rapid JAZ1-CIT and JAZ3-CIT signal decay, as can be observed by their respective AFU decreases (Fig. 19).

The COR-dependent JAZ1-CIT and JAZ3-CIT degradation indicated that the fusion proteins can bind to COI1 in the nucleus and undergo degradation, which is indicative of the constructs being functional. A further experiment to test the construct functionality was attempted by transforming the *rat.JAZ1p:JAZ1-CIT* and *rat.JAZ3p:JAZ3-CIT* constructs in *jaz1-3 jaz2-6* and *jaz2-6 jaz3-4* double mutant backgrounds displaying shorter roots with respect to the WT (Fig. 13). However, the transformed genotypes had poor germination rates, likely due to a pest contamination during seed development, which resulted in reduced seed quality. Therefore, I was unable to perform the complementation assay with these seed batches. Nevertheless, the induction of JAZ1-CIT and JAZ3-CIT degradation by COR (Fig. 19), along with their nuclear localization (Fig. 15; Fig. 16C and D; Fig. 18A and B), strongly support the functionality of JAZ1-CIT and JAZ3-CIT fusion proteins.

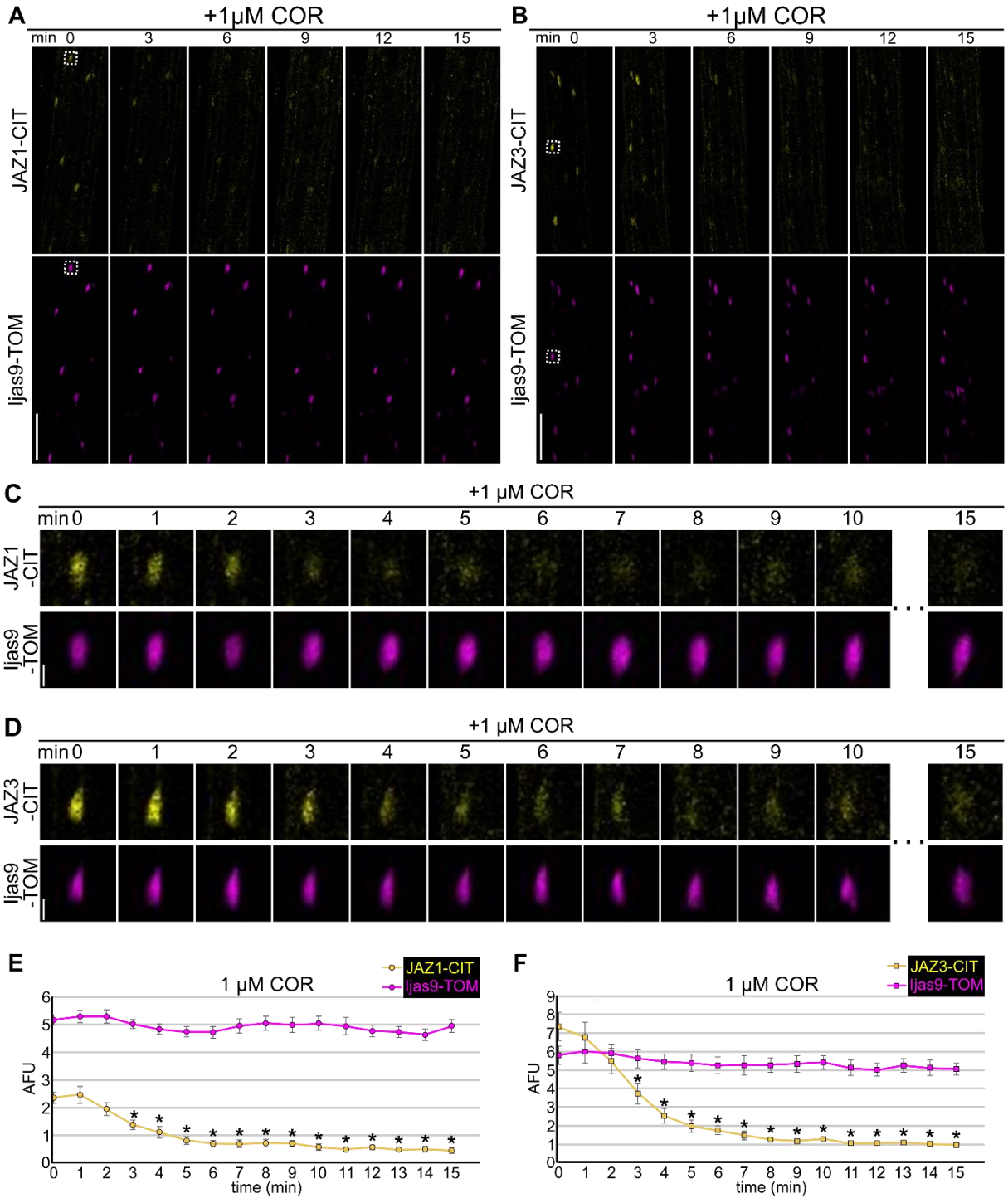

Figure 19: Ratiometric measurements of *rat.JAZ1p:JAZ1-CIT* and *rat.JAZ3p:JAZ3-CIT* reporters in *aos* after exogenous COR treatment. (**A,B**) Representative images of *JAZp:JAZ-CIT* (JAZ-CIT, yellow) and *UBQ10p:Ijas9-TOM* (Ijas9-TOM, magenta) expression in the root EDZ of 5-do *aos* mutant seedlings over a 15min imaging time course following 1 µM COR treatment. (**C,D**) Representative images of single nuclei (dotted squares) from (**A**) and (**B**), respectively. (**E,F**) Arbitrary Fluorescence Unit (AFU) measurements from the rat.JAZ reporters in (**E**) *rat.JAZ1p:JAZ1-CIT* and (**F**) *rat.JAZ3p:JAZ3-CIT* in *aos* mutants. Fluorescence signals were quantified from 5-7 nuclei in at least 10 roots per construct at a frequency of 1 image per minute. Asterisks denote statistically significant differences at each time point compared to initial AFU at t=0 as determined by One-Way ANOVA analysis followed by Tukey's HSD test ($p<0.05$). Error bars = SEM. Scale bars (A,B) = 100 µm, (C,D) = 10 µm.

COR promotes JAZ-CIT degradation in a dose-dependent manner

Having evaluated the suitability of the *rat.JAZ1p:JAZ1-CIT* and *rat.JAZ3p:JAZ3-CIT* reporter lines in the *aos* mutant background, I proceeded to perform relative JAZ-CIT turnover quantifications as defined by the combination of protein synthesis, life-time, and degradation (Toyama & Hetzer, 2013). Hence, I determined the nucleus-specific relative turnover rate of JAZ-CIT in the root EDZ by calculating the ratio of nucleus-specific AFU from JAZ-CIT to that of Ijas9-TOM. This calculation enabled the assessment of the JAZ-CIT turnover rate relative to the stable reference Ijas9-TOM signal (Fig. 20).

Previous studies have suggested that ligand-dependent JAZ degradation is dose-dependent (Larrieu et al., 2015). However, this has never been confirmed *in planta* for full-length JAZs expressed under the control of their endogenous promoters. Hence, I treated *rat.JAZ1p:JAZ1-CIT* and *rat.JAZ3p:JAZ3-CIT* reporters in the *aos* background with different COR concentrations (0 µM, 0.01 µM, 0.1 µM, 1 µM) and followed their relative AFU in single root nuclei immediately after treatment, following the same principles as described earlier. Then, I measured the dose-dependent JAZ1-CIT/Ijas9-TOM and JAZ3-CIT/Ijas9-TOM turnover rates in response to COR (Fig. 20A and B).

As expected from the individual assessment of JAZ-CIT and Ijas9-TOM channels (Fig. 18A and B), the JAZ-CIT/Ijas9-TOM ratiometric analysis indicated stable fluorescence levels for the mock treatment over 15min for both *rat.JAZ1p:JAZ1-CIT* and *rat.JAZ3p:JAZ3-CIT aos* lines, including stable Ijas9-TOM signals during all COR treatments (Fig. 20A and B; Fig. S10A; Fig. S11A). On the contrary, all COR treatments led to a decrease in JAZ-CIT AFU compared to the mock within the treatment time course (Fig. 20A and B). Higher COR doses exhibited more pronounced effects, with 0.1 µM and 1 µM COR treatments showing no significant differences in responsiveness between each other, as determined by two-way ANOVA analysis (Fig. 20A and B), suggesting COR saturation levels might be reached around 0.1 µM COR.

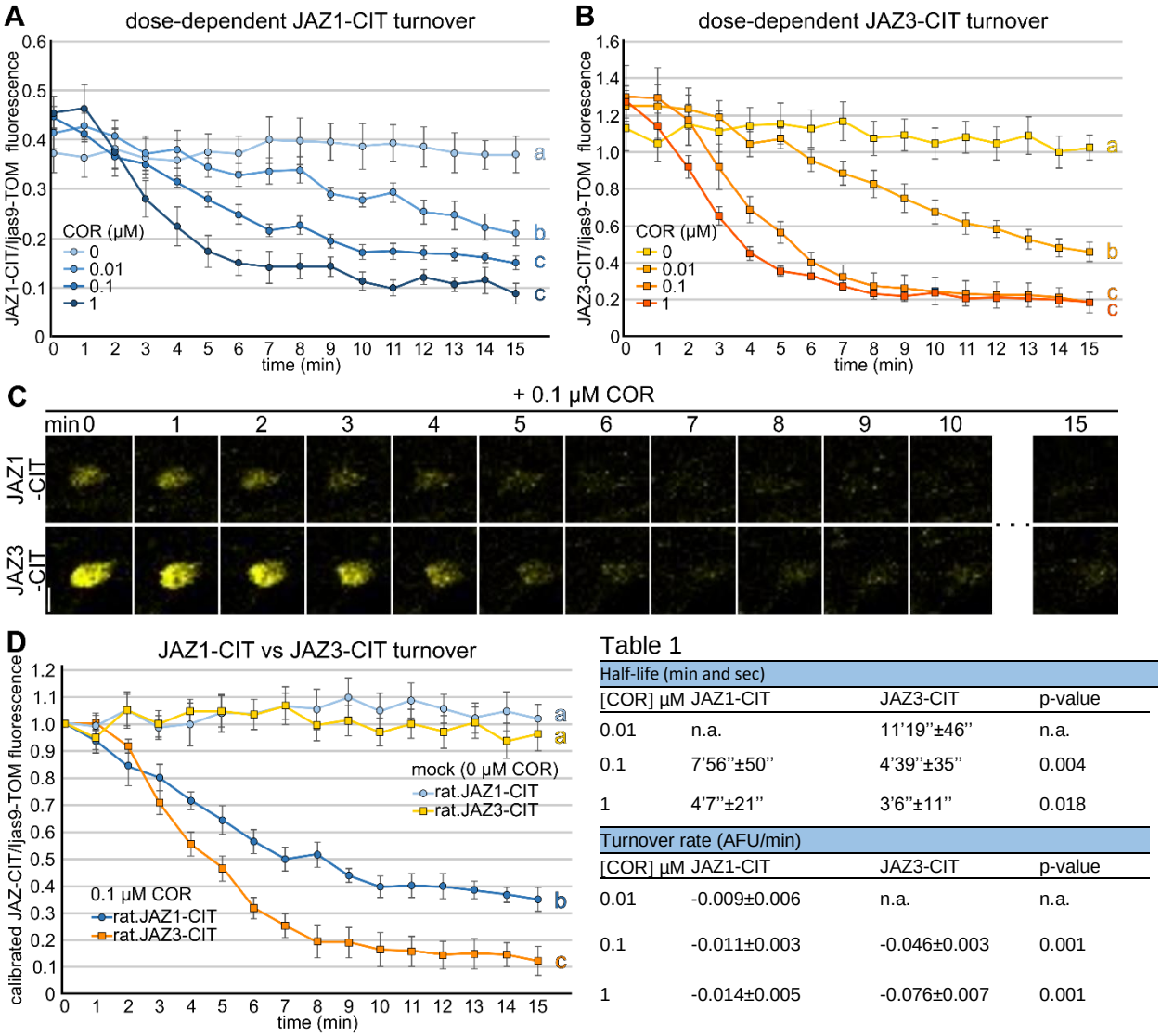

Table 1

Half-life (min and sec)			
[COR] µM	JAZ1-CIT	JAZ3-CIT	p-value
0.01	n.a.	11'19''±46''	n.a.
0.1	7'56''±50''	4'39''±35''	0.004
1	4'7''±21''	3'6''±11''	0.018

Turnover rate (AFU/min)			
[COR] µM	JAZ1-CIT	JAZ3-CIT	p-value
0.01	-0.009±0.006	n.a.	n.a.
0.1	-0.011±0.003	-0.046±0.003	0.001
1	-0.014±0.005	-0.076±0.007	0.001

Figure 20: JAZ-CIT/Ijas9-TOM turnover rates in response to COR. (**A,B**) Normalized JAZ-CIT/Ijas9-TOM fluorescence over time in (**A**) *rat.JAZ1p:JAZ1-CIT* and (**B**) *rat.JAZ3p:JAZ3-CIT* in *aos* root EDZs after treatment with different COR concentrations (0 µM [mock], 0.01 µM, 0.1 µM, 1µM). (**C**) Representative images of JAZ1-CIT and JAZ3-CIT nuclear expression in *aos*, after 0.1 µM COR treatment. (**D**) Direct comparison between normalized JAZ1-CIT/Ijas9-TOM fluorescence and JAZ3-CIT/Ijas9-TOM fluorescence following 0.1 µM COR treatment calibrated to respective initial percentage values. (**A,B,D**) Fluorescence signals were quantified from 5-7 nuclei in at least 10 roots per construct. Letters denote statistical differences among treatments determined by Two-Way ANOVA analysis followed by Tukey's HSD test ($p<0.05$). Error bars = SEM. Scale bars = 10 µm. **Table 1: Half-lives and turnover rates of JAZ1-CIT and JAZ3-CIT normalized to Ijas9-TOM at different COR concentrations.** Ratiometric measurements were quantified from 5-7 nuclei in at least 10 roots per construct. P-values were determined by One-Way ANOVA analysis followed by Tukey's HSD test ($p<0.05$). n.a.= not analysed.

JAZ1-CIT and JAZ3-CIT display differential *in vivo* COR-dependent half-lives and turnover rates

To determine if the COR-dependent decrease in relative JAZ-CIT AFU follows a linear or exponential decay enabling the computation of parameters such as half-life and turnover rate, the measured dose-response data was evaluated for its likelihood of fitting functions via regression analysis (Fig. S12; see "Material and

Methods" for regression analysis using GraphPad). The coefficient of determination (R^2) with the highest values (R^2>0.95) across all COR concentrations for both JAZ1-CIT and JAZ3-CIT was found to best fit a plateau followed by one phase exponential decay function for both reporters across all treatments (Fig. S13).

Having determined the type of COR-dependent JAZ1-CIT and JAZ3-CIT decay, I next calculated the relative JAZ-CIT half-lives described as the time point at which the initial amount (JAZ-CIT/Ijas9-TOM AFU) is halved (Tab. 1) (Hallare & Gerriets, 2023). The rapid decrease of JAZ3-CIT signal relative to JAZ1-CIT after the treatment with different COR concentrations already indicate a faster turnover of JAZ3-CIT compared to that of JAZ1-CIT (Fig. 20C). Moreover, I investigated potential differences in responsiveness between JAZ1-CIT and JAZ3-CIT at mock and 0.1 µM. Subsequently, I normalized the values to 100% and conducted a two-way ANOVA analysis. The findings reveal a significant difference in responsiveness between the JAZ-CIT constructs at 0.1 µM COR, suggesting differences in terms of JAZ-CIT turnover rates (Fig. 20D). Consistent with these observations, the half-life values indicate significantly shorter values for JAZ3-CIT with respect to JAZ1-CIT for 0.1 µM and 1 µM COR ($p<0.05$) (Tab. 1). Specifically, at 0.1 µM COR, the half-life of JAZ1-CIT was 7min and 56sec, significantly different from the half-life of JAZ3-CIT, which was 4min and 39sec (Fig. 20C and D; Tab. 1). At 1 µM COR, the half-life of JAZ1-CIT was 4min and 7sec, significantly different from the half-life of JAZ3-CIT, which was 3min and 6sec (Tab. 1). The statistical analysis for the half-life of JAZ1-CIT and JAZ3-CIT at 0.01 µM COR was not conducted, as the calculated half-life for JAZ1-CIT was computed to be beyond the 15min measurement window (16min and 20sec).

I therefore evaluated if there is a difference between the COR-dependent turnover rates between JAZ1-CIT and JAZ3-CIT. To do so, I first estimated the initial and ending plateau values for each curve. Upon COR treatment, JAZ1-CIT AFU decrease did not occur in the first 3min under any COR concentration, whereas JAZ3-CIT AFU signals were stable in the first 2min (Fig. S14; Fig. S15). This initial plateau suggests COR requires a brief period to initiate the degradation of JAZ proteins, possibly due to tissue penetration. While seedlings were mounted and imaged as consistently as possible, it is important to note the manual experimental setup precludes to determine if the initial plateaus (Fig. S12C) are significantly different between JAZ1-CIT and JAZ3-CIT. I next estimated when does the ending plateau start for each reporter at different COR concentrations based on stable JAZ-CIT/Ijas9-TOM AFU values at later time points during the time course (Fig. S10B, C, and D; Fig. S10B, C, and D). For JAZ1-CIT the ending plateau was estimated to start at 14min for 0.01 µM, at 13min for 0.1 µM and at 10min for 1 µM COR (Fig. S10B, C, and D),

whereas for JAZ3-CIT the ending plateau was not reached during the time course at 0.01 µM COR, started at 14min at 0.1 µM and at 8min at 1 µM COR (Fig. S11B, C, and D). The AFU measured during the ending plateau indicate that the COR treatment has reached its saturation effects, and that the remaining measured AFU are likely the result of JAZ-CIT protein de-novo translation and COR-mediated degradation.

I next estimated the turnover rate for each JAZ-CIT at all COR concentrations, indicated as the average JAZ-CIT/Ijas9-TOM AFU decrease per min within the decay phase. JAZ1-CIT had a similar range of turnover rates across COR treatments, ranging from 0.009 to 0.014 decay of AFU units per minute (Tab. 1). In contrast, JAZ3-CIT turnover was not measurable at low 0.01 µM COR as the end plateau was not reached within the time course, while the turnover rates were 4 to 7 times higher than JAZ1-CIT at higher COR concentrations, ranging from 0.046 to 0.076 AFU decay units per minute (Tab. 1). Results therefore show that the *in planta* turnover rates between JAZ1 and JAZ3, and possibly other JAZ repressors, is different.

To account for potential differences in JAZ-CIT turnover rates, I compared potential Ub sites occurring on Lys residues (Hershko & Ciechanover, 1998) and variations in the Jas degron motif (Fig. 21). Overall, there are 7 different residues of the 27 composing the degron between Jas1 and Jas3, with 3 conservative (Ile–Leu; Arg –Lys; Asp–Glu) and 4 non-conservative (Glu–Ala; His–Ala; Lys–Val; Ala–Ser) differences (Fig. 21A). In terms of putative Ub sites, JAZ1 contains 16 Lys residues and JAZ3 14 (Fig. 21B). While this sequence analysis is too preliminary to draw any conclusions about COI1 binding or ubiquitylation, it serves to highlight differences in the sequence that may lead to differences in turnover rates in vivo.

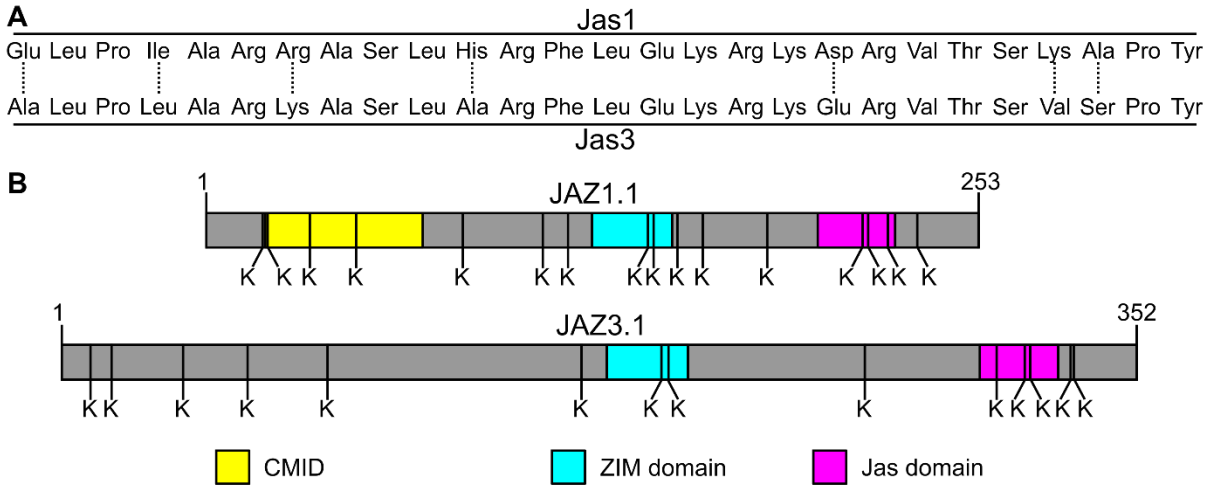

Figure 21: Amino acid sequence comparisons between JAZ1 and JAZ3: (**A**) The Jas degron sequences of JAZ1.1 (Jas1) and JAZ3.1 (Jas3) reveal seven distinct amino acids (aa) that may potentially impact the JA-Ile/COR-dependent binding to COI1. aa variations between Jas1 and Jas3 are denoted with dotted lines (**B**) Schematic representation illustrating lysines (K) as potential ubiquitylation sites within the aa sequences of JAZ1.1 and JAZ3.1.

Section III - Discussion and future perspectives

Roots growing in soil are exposed to various stimuli, which vary in intensity and depth within tissues (Motte et al., 2019; Rellan-Alvarez et al., 2016). These cellular responses need to be decoded and integrated at a whole tissue and plant scale. Arabidopsis has evolved 13 repressors of JA signalling, potentially accounting for 30 different proteins (Fig. 5), engaging in COI1 interactions to form the JA-Ile sensing complex (Chini et al., 2007; Howe et al., 2018; Thines et al., 2007; Thireault et al., 2015; Yan et al., 2007). Specifically focusing on JAZ repressors, the overarching aim of this project was to unveil the molecular mechanisms governing how individual cell types respond to increases in hormone levels.

Only half of the available Arabidopsis JAZs employ to the basal repression complex

The inhibition of JA signalling by the basal repression complex is crucial, given that the activation of JA signalling is energetically costly (Barto & Cipollini, 2005; Zavala & Baldwin, 2006). Due to the reported redundancy observed among the JAZs (Chini et al., 2007; Thines et al., 2007; Thireault et al., 2015), it is often assumed that a substantial portion, if not all, of the JAZs simultaneously contribute to the formation of the basal repression complex in all cells types. However, only a few studies have been conducted regarding the *JAZ* expression patterns (Acosta et al., 2013; Gimenez-Ibanez et al., 2017; Grunewald et al., 2009) providing potential insights into which JAZs contribute to the basal repression complex. In fact, the results of my study reveal that *JAZ1*, *JAZ2, JAZ3*, *JAZ4*, *JAZ6*, and *JAZ9*, exhibit constitutive promoter activity within the primary root (Fig. 6; Fig. 7; Fig. 8; Fig. S1). This observation strongly suggests that solely these genes contribute to the expression of JAZ repressors under basal condition. This observation is further supported by the fact that all *JAZs* exhibiting basal promoter activity also manifest basal gene transcription (Fig. 10 and Fig. 11). Translational reporters could only support basal JAZ localization for JAZ1, JAZ2, and JAZ3 (Fig. 15). However, even the translational reporters for JAZ1 and JAZ3 exhibit diminished strength compared to their respective transcriptional reporter counterparts (Fig. 7; Fig. 15). Thus, it can be anticipated that translational reporters for the remaining JAZs are undetectable, likely due to inherent limitations in the detection process. Reason for this could be different features between NLS-3xVEN and JAZ-CIT, such as brightness of the chimeric fluorophores, protein folding, or multiple labelling in case of 3xVEN under the tested conditions, respectively (Day & Davidson, 2009; Shaner et al., 2005; Toseland, 2013) (www.fpbase.org). In fact, CIT and VEN exhibit similar brightness (www.fpbase.org). However, the transcriptional reporters express three VEN fluorophores, which likely enhances the signal intensity compared to the translational reporters, with only one CIT tag. In conclusion, it can be assumed

that my transcriptional reporters are also reliable in indicating JAZ protein expression sites. In summary, it can be said that only a portion of Arabidopsis JAZs exhibits basal expression, likely contributing to the formation of the basal repression complex (Geerinck et al., 2010). Significantly, my transcriptional reporters revealed distinctive expression patterns, underscoring that JAZs possess cell type-specific repression sites (Fig. 7; Fig. 8). This characteristic facilitates the establishment of cell type-specific repression complexes (Geerinck et al., 2010), effectively repressing JA-responsive genes within a cellular context.

During the course of this project, studies were published that investigated the tissue-specific promoter activities of *JAZs* using the *JAZp:GUS* reporter, similar to our approach (DeMott et al., 2021; Liu et al., 2021). The findings presented in these studies exhibit some differences compared to our results (Fig. 6; Fig. S1). For instance, (DeMott et al., 2021) demonstrated promoter activity of *JAZ4* in the root tip of both primary and lateral roots. However, our reporter indicates that *JAZ4p* activity is primarily located in epidermal and cortical cells within the differentiation zone (Fig. 6; Fig. 7; Fig. 8). Moreover, *JAZ2p:GUS* reporters used in (Liu et al., 2021), indicate, in contrast to our results (Fig. 6; Fig. 7; Fig. 8), no promoter activity in the root tip, but weak activity in outer cell layers of the differentiation zone. The same study also highlights the lack of *JAZ1p:GUS* staining in the root meristem (Liu et al., 2021), a divergence to the observations made with our reporters (Fig. 6; Fig. 7; Fig. 8). Moreover, although our *JAZ6p:NLS-3xVEN* reporter did only demonstrate weak *JAZ6p* activity in the root meristem (Fig. 7; Fig. 8), *JAZ6p* activity was strongly activated in that region in the study of (Liu et al., 2021). Additionally, the reporters utilized in (Liu et al., 2021) did not observe *JAZ9p* activity in the root, in contrast to our results (Fig. 6; Fig. 7; Fig. 8). Conversely, the same study (Liu et al., 2021) demonstrated *JAZp:GUS* expression in the roots for *JAZ5*, *JAZ7*, *JAZ8*, *JAZ11*, *JAZ12*, and *JAZ13*, whereas our data classified these expressions as weak or non-basally active (Fig. S1B). However, it is to note that the experiments in these studies were conducted under different testing conditions compared to my research, such as the use of seedling samples at later developmental stages.

Certainly, *JAZs* are not the first genes encoding phytohormone response repressors that have been demonstrated to exhibit diverse expression patterns. In fact, multiple studies have shown that other genes encoding repressors engaged in the regulation of diverse phytohormone pathways, like the *AUX/IAAs*, display specific promoter activity patterns (Groover et al., 2003; Kim et al., 2020; Rusak et al., 2010; Tian et al., 2002; Windels et al., 2014). For instance, research has indicated that *IAA3p* is active in

cotyledons and hypocotyls, while *IAA7p* shows activity in both the shoot and root (Tian et al., 2002). Moreover, it has been discovered that *IAA2* exhibits weak promoter activity in lateral root tips and leaves (Rusak et al., 2010). In case of *IAA8* it was shown that the promoter is predominantly active in vascular tissues and apices (Groover et al., 2003). In recent studies, it has been observed that *IAA15p* is active in diverse plant tissues, including the shoot apical meristem, petioles, veins, cotyledon tips, primary root tips, lateral root primordia, and lateral root tips (Kim et al., 2020). Moreover, *IAA15p* activity remains consistent throughout every developmental stage of morphologically identifiable lateral root primordia and is notably elevated in the tips of mature primordia (Kim et al., 2020). Additionally, tissue-specific expression of different *AUX/IAAs* has also been observed at the transcript level (Abel et al., 1995; Klepikova et al., 2016). Significantly, research has also revealed that not all *AUX/IAAs*, exemplified by *IAA12*, exhibit basal promoter activities (Windels et al., 2014), mirroring what I observed for the non-basally active *JAZs* (Fig. 6B). Taken together, these results suggest that AUX/IAAs also exhibit different cellular localization patterns. In addition, transcript data (Klepikova et al., 2016) indicate distinct localization patterns also for further phytohormone response repressors, which adhere to the fundamental principle of "activation by degradation". Examples include the SL signalling repressors SMAX1-LIKEs (SMXLs) (Bennett et al., 2016; Liang et al., 2016; Soundappan et al., 2015; Wang et al., 2015), as well as the GA signalling repressors DELLAs (Harberd et al., 2009; Peng et al., 1997; Silverstone et al., 1998; Sun, 2010). In conclusion, the diversity in expression is not unique to *JAZs* but extends to other regulatory elements in the plant hormone signalling network.

What regulatory mechanisms control the expression of basally expressed JAZs?

To sustain the repressor complex under basal conditions, regulatory mechanisms are necessary to ensure the expression of its components. As demonstrated by my translational reporters, the basal expression of JAZs can also occur in the biosynthesis mutant *aos* (Fig. 18) (Park et al., 2002), indicating that the expression of basal JAZs is independent of JA-Ile. Therefore, it is anticipated that under basal conditions, basally active *JAZp* are maintained by regulatory mechanisms other than JA-Ile. In fact, JA signalling exhibits partially antagonistic crosstalk with Auxin signalling in several aspects (Jang et al., 2020; Yang et al., 2019). For example, it was shown that JA-mediated root growth inhibition is mediated by antagonistic JA/Auxin crosstalk (Chen et al., 2011). In this context, it has been demonstrated that JA-mediated root growth reduction is facilitated by MYC2, which negatively modulates the expression of PLETHORA 1 (PLT1) and PLT2, two auxin-responsive TFs positively regulating stem cell niche maintenance and cell proliferation (Chen et al., 2011; Mahonen et al., 2014). Therefore, it can be hypothesized that Auxin, often

associated with positively regulating plant development and growth (Mockaitis & Estelle, 2008), might upregulate the expression of basal JAZs to repress JA responses, such as reducing root growth. Certainly, several studies demonstrated that *JAZ1* expression is inducible by Auxin (Goda et al., 2008; Grunewald et al., 2009; Vanneste et al., 2005). In this context, it has been demonstrated that the Auxin-induced expression of *JAZ1* is mediated by AUXIN RESPONSE FACTOR 6 (ARF6) and ARF8 (Grunewald et al., 2009), members of TFs regulating Auxin signalling (Cance et al., 2022; Guilfoyle & Hagen, 2007). This suggests that Auxin plays a role in the regulation of JAZ1 expression in this case. However, JA signalling exhibits intensive, partially antagonistic crosstalk with other phytohormone pathways, including ABA, SA, GA, ET, and CK signalling, as reviewed in (Jang et al., 2020; Yang et al., 2019). This suggests that these phytohormones may also participate in the positive regulation of basal JAZ expression.

The exact regulatory mechanisms ensuring basal *JAZp* activity remain elusive. Future research could explore cis-elements upstream of basally expressed *JAZs*, for instance by utilizing online tools such as the "Arabidopsis Gene Regulatory Information Server" (AGRIS) (Davuluri et al., 2003; Palaniswamy et al., 2006; Yilmaz et al., 2011). Approaches like this, could help to identify potential TF binding sites, revealing which other signalling pathways might participate in the regulation of basally expressed *JAZs*.

How does the localization of basally expressed JAZs modulate cellular specificities?

As reviewed in (Wasternack & Strnad, 2018), JA-Ile regulates many different responses. These responses require precise regulation, particularly considering that JA signalling is linked to a "defense/growth trade-off" (Zavala & Baldwin, 2006). The diverse expression patterns of *JAZs* indicate cell type-specific repression complexes, potentially contributing to effective JA signalling modulation within a cellular context. Hence, the modulation of cellular specificities could be achieved among others by the different cell type-specific JAZ/MYC combinations. Research has revealed that MYCs exhibit variabilities in targeting different clusters of genes (Fernandez-Calvo et al., 2011; Godoy et al., 2011; Zander et al., 2020). Further investigations have demonstrated distinct binding capabilities of JAZs to MYCs (Tab. S1) (Cheng et al., 2011; Chini et al., 2009; Chini et al., 2007; Fernandez-Calvo et al., 2011; Niu et al., 2011; Qi et al., 2015; Thireault et al., 2015), potentially impacting the repression intensities exerted by JAZs on MYCs. Therefore, the specific cellular combinations of "strong" and "weak" JAZ repressors may be crucial for the cellular regulation of MYCs and their associated target genes. However, it is crucial to emphasize that the strength of the JAZ/MYC interaction alone likely does not exclusively dictate the repression intensity of JAZs on MYCs, given that other components of the repressor complex also contribute to the modulation

of JA signalling repression (Howe et al., 2018). Nevertheless, it is likely that the JAZ/MYC interaction serves as a guiding parameter for the repression intensity on JA-responsive genes.

Distinct interactions between MYCs and specific JAZs can arise from various features. When comparing the structures of JAZ1 and JAZ3, the designated representative JAZs in this project, I observed that they differ in the amino acid composition of their Jas degron domains (Fig. 21), potentially influencing their binding capabilities to MYCs (Cheng et al., 2011; Chini et al., 2009; Fernandez-Calvo et al., 2011; Goossens et al., 2015; Niu et al., 2011; Thireault et al., 2015; F. Zhang et al., 2015). Indeed, structure analyses revealed distinct conformations among various Jas degrons and MYC3, potentially influencing the binding capabilities between different JAZs to MYCs in general (Ona Chuquimarca et al., 2020; F. Zhang et al., 2015). Hence, it is reasonable to assume that variations in residues between the Jas degrons of JAZ1 and JAZ3 (as well as among other JAZs) play a pivotal role in determining their individual binding capacities to MYCs.

When comparing JAZ1 and JAZ3 structures further, an additional distinction arises: JAZ1 possesses a CMID, a feature that is absent in the JAZ3 protein (Fig. 5). The CMID is known to exclusively bind to MYCs, whereas, conversely, the Jas degron can bind to both COI1 and MYCs. (Cheng et al., 2011; Chini et al., 2009; Chini et al., 2007; Fernandez-Calvo et al., 2011; Goossens et al., 2015; Moreno et al., 2013; Niu et al., 2011; Thireault et al., 2015; Zhang et al., 2017). Given that the Jas degron and the CMID share the same binding site at the N-terminus of MYCs (Cheng et al., 2011; Fernandez-Calvo et al., 2011; Moreno et al., 2013; Niu et al., 2011), it is unlikely that JAZs possessing both, a Jas degron and a CMID, would enhance their binding capability with MYCs by simultaneously engaging with both domains (Moreno et al., 2013). Nevertheless, crystal structure analyses, using the Jas degron and CMID of JAZ10 as examples, suggest that the CMID forms a more intricate and potentially more compact interaction with MYC3 compared to the Jas motif (Zhang et al., 2017). In conclusion, the binding intensity of JAZ1 to MYCs is likely dependent on whether it binds with the Jas degron or the CMID. Therefore, the CMID of JAZ1 could be a further factor that distinguishes JAZ1 from JAZ3 in terms of binding intensity to MYCs, as JAZ3 lacks the CMID.

Similar to the *JAZs*, it has been demonstrated that *MYC2*, *MYC3*, and *MYC4* exhibit cell type-specific expression patterns (Gasperini et al., 2015). These findings, combined with my own research, contribute to our knowledge of JAZ/MYC combinations that are potentially involved in forming cell-specific repression complexes. For example, within the context of the EDZ, *MYC2* demonstrates exclusive

expression activity in the epidermis and endodermis (Gasperini et al., 2015). When considering the epidermis of the EDZ, it is likely that MYC2 interacts with JAZ1, JAZ3, and JAZ4, as these genes are specifically expressed here (Fig. 7; Fig. 8). However, within the context of epidermal cells in the EDZ, MYC2 could form complexes solely with JAZ1 and JAZ3 (Fig. 7; Fig. 8). In contrast, the promoter of *MYC3* exhibits additional activity in the cortex of the EDZ (Gasperini et al., 2015), suggesting that MYC3 has the potential to form complexes with JAZ1, JAZ3, JAZ4, and JAZ6 in that region (Fig. 7; Fig. 8). However, given the diverse binding capabilities of JAZs with MYCs, it is to recognize that JAZ/MYC combinations may not necessarily occur even when these proteins co-localize within the same cell type. For example, despite the overlapping expression sites of *JAZ4* (Fig. 7; Fig. 8) and *MYC3* (Gasperini et al., 2015), the interaction of their coding proteins could not be verified in previous studies (Cheng et al., 2011; Schweizer et al., 2013). On the contrary, certain JAZs demonstrated to interact with specific MYCs (Cheng et al., 2011; Chini et al., 2009; Chini et al., 2007; Fernandez-Calvo et al., 2011; Niu et al., 2011; Qi et al., 2015; Thireault et al., 2015) do not necessarily share overlapping expression sites with these specific MYCs (Fig. 7; Fig. 8) (Gasperini et al., 2015). In this context, it has been demonstrated that JAZ6 is capable to interact with MYC2 (Chini et al., 2009). However, in terms of the EDZ, *MYC2* expression is indicated in the epidermis and endodermis (Gasperini et al., 2015), while *JAZ6* expression is suggested to be predominantly in the cortex of the EDZ (Fig. 7; Fig. 8). In this specific case, the interaction between MYC2 and JAZ6 within the EDZ seems improbable.

In addition to the potential to modulate cell type-specific JA signalling through various JAZ/MYC complexes, the regulation of cell type-specific JA signalling could additionally be achieved through distinct cell-specific JAZ dimerization combinations (Chini et al., 2009; Chung & Howe, 2009). The variability of JAZs to form both hetero- and homodimers (Chini et al., 2009; Chung & Howe, 2009), coupled with my findings highlighting cell-specific JAZ localization patterns, strongly suggests the possibility of cell type-specific JAZ/JAZ dimers. Consequently, this could impact the regulatory capabilities of cell-specific repression complexes, thereby influencing the regulation of cell type-specific JA-responsive genes. Similar as for potential JAZ/MYC combinations, the generated *JAZ* expression maps of this project can provide insights into the potential formation of cell type-specific JAZ/JAZ dimers (Fig. 7; Fig. 8). For example, in the epidermis of the EDZ, *JAZ1* co-expresses with *JAZ3* and *JAZ4* (Fig. 7; Fig. 8), potentially leading to a specific dimer combination of their coding proteins in this cellular context.

Moreover, the regulation of cellular specificities of JA signalling could also be achieved by cell-specific combination of JAZs with non-canonical interaction partners (Tab. S1). A previous study has demonstrated that RHD6, which is specifically expressed in root hair cells to promote their development (Masucci & Schiefelbein, 1994), interacts with JAZ2, JAZ4, JAZ8, JAZ9, and JAZ10 to regulate root hair formation (Tab. S1) (Han et al., 2020). However, based on our transcriptional reporter analysis, I observed that only *JAZ4* display basal promoter activity in epidermal cells where root hair formation is possible (Fig. 7; Fig. 8). This suggests that JAZ4 may be the primary interactor of RHD6 in this context, implying that among all JAZs, JAZ4 predominantly contributes to the regulation of root hair formation.

In conclusion, cellular specificities are potentially regulated by the diverse cellular combinations of JAZs with direct components of the repressor complex, as well as their cell-specific interactions with other non-canonical interaction partners.

What is the role of non-basally expressed *JAZs*?

While *JAZs* with basally active promoters seem to code repressors that are crucial to form the primary repression complex, a question arises regarding the biological and molecular functions of *JAZs* with low or no basal promoter activity (Fig. S1). The lack of promoter activity in these genes suggests that they do not express JAZ repressors that participate in the formation of the basal repression complex. This observation could potentially explain why even the *jazNB* mutant with multiple gene KO mutations does not exhibit any basal phenotype (Fig. S3) (Thireault et al., 2015). It is well established that JA signalling exerts a negative regulation on vegetative growth (Howe et al., 2018; Huang et al., 2017). Consequently, to return to a resting state, JA signalling is repressed through a negative feedback loop (Chung et al., 2008; Thines et al., 2007; Yan et al., 2007). In this regard, it is probable that non-basally active *JAZs* primarily function as crucial components of the negative feedback loop. This hypothesis is reinforced by the observation that both the promoter activity and transcription of most *JAZs*, including the non-basally active *JAZs*, can be stimulated by wounding or MeJA treatment, respectively (Fig. 10; Fig. 11, Fig. S1). Among the *JAZs* with non-basal promoter activity, certain genes express JAZ repressors with unique Jas features, influencing JAZ/COI1 interaction and therefore JA-Ile dependent degradation (Fig. 5) (Bai et al., 2011; Chung & Howe, 2009; Shyu et al., 2012; Thireault et al., 2015). As mentioned before, it was shown that the JAZ10.3 and JAZ10.4 splicing variants are characterized by a truncated Jas degron and the absence of a Jas degron, respectively (Fig. 5) (Chung & Howe, 2009). Hence JAZ10.3 exhibits increased stability in the presence of JA-Ile compared to JAZs with full-length Jas degron (e.g. JAZ10.1), while JAZ10.4

demonstrates complete resistance to degradation in a JA-Ile-dependent manner (Chung & Howe, 2009). Furthermore, JAZ7, JAZ8, and JAZ13 feature a divergent Jas degron, leading to the absence of JA-Ile-dependent degradation (Fig. 5) (Bai et al., 2011; Shyu et al., 2012; Thireault et al., 2015). It is noteworthy that these particularly named JAZs may play a significant role in the negative feedback loop: Despite the continued presence of high JA-Ile levels, their expression alone could potentially exert an inhibitory effect on JA-responsive genes, as they might not undergo degradation. Eventually, this effect could counteract excessive JA responses and prevent overly pronounced reduction in growth. This hypothesis could explain why KO mutants of these genes exhibit hypersensitive JA responses, such as reduced root growth, without displaying any basal phenotypes (Fig. S3A) (Sehr et al., 2010; Thireault et al., 2015). Indeed, previous studies have demonstrated that the JA hypersensitivity observed in *jaz10-1* can be effectively complemented by the JAZ10.4 splicing variant (Moreno et al., 2013; Sehr et al., 2010). This finding strongly supports the specific function of *JAZ10* and its splicing variants in the negative feedback loop regulating JA signalling.

Future projects have the potential to explore the role of non-basally expressed JAZs in the negative feedback loop. For instance, by analysing *rat.JAZp:JAZ-CIT* reporters for these *JAZs* could help to reveal their expression dynamics, especially in the long term following JA treatment. In this context, exploring the dynamics of JAZs with divergent, truncated, or no Jas degron during sustained high levels of JA or COR would be particularly intriguing.

The role of JAZs in modulating cellular specificities in other plant species

As the diversity of JAZs and their distinct cellular localization appears to be a significant factor in regulating cellular specificity in the model plant Arabidopsis, it raises the question of whether the same holds true for other plant species. Similar to Arabidopsis, other vascular plant species also exhibit a variety of different *JAZs* (Chao et al., 2019; Chini et al., 2009; Ye et al., 2009; L. Zhang et al., 2015; Zhang et al., 2012; Z. Zhang et al., 2015). For instance, cultivated dicotyledonous plants, such as tomato (*Solanum lycopersicum*) and grapevine (*Vitis vinifera*), have been shown to encode 12 and 11 *JAZs*, respectively (Chini et al., 2017; Zhang et al., 2012). The rubber tree (*Hevea brasiliensis*), crucial for commercial natural rubber production (Chao et al., 2016), presents an extensive repertoire with 18 *JAZs* (Chao et al., 2019). Monocotyledonous crop plants, like rice (*Oryza sativa*), possess 15 *JAZs* (Ye et al., 2009), while maize (*Zea mays*) exhibits an even larger diversity with 26 different *JAZs* (Z. Zhang et al., 2015). Furthermore, transcriptomic data reveal distinct tissue-specific expression patterns for various *JAZ* genes in other plants

such as tomato and maize (www.bar.utoronto.ca). For example, *JAZ5* from *Solanum lycopersicum* (*SlJAZ5*) exhibits predominant expression in unopened flower buds and roots, whereas *SlJAZ10* expression is primarily restricted to unopened flower buds only (Tomato Genome, 2012). This observation suggests the possibility of different localization sites for JAZ proteins within these tissues. As vascular plants exhibit a high degree of cell type complexity (Agusti & Blazquez, 2020), it is plausible that they generally possess distinct cellular JAZ localization sites, influencing cell type-specific regulation of JA signalling. Future projects could address the question of JAZ localization in other vascular plants, shedding light on how cellular JA signalling specificities are modulated by their JAZ proteins.

Contrary to vascular plants (Chao et al., 2019; Chini et al., 2009; Chini et al., 2007; Thines et al., 2007; Thireault et al., 2015; Yan et al., 2007; Ye et al., 2009; L. Zhang et al., 2015; Zhang et al., 2012; Z. Zhang et al., 2015), the liverwort *Marchantia polymorpha* (Marchantia) is characterized by the presence of only one *JAZ*, encoding for two alternatively spliced transcripts (Monte et al., 2019). Therefore, it is likely that cellular specificity regulation by the sole *JAZ* in Marchantia plays a diminished role, which is plausible since Marchantia exhibits low cell-type complexity (Kohchi et al., 2021). Certainly, JA signalling in Marchantia effectively regulates defense responses, whereas other responses, such as fertility regulation in vascular plants, emerged later during evolution (Monte et al., 2018). Therefore, given the lower complexity of JA responses in Marchantia, it seems likely that JA responses require less fine-tuning by diverse JAZs compared to vascular plants.

The potentials of cell specific JA signalling activation

Cell-specific JA signalling activation holds significant potential, particularly in developing defense and other strategies for crops and other commercial plants, without adversely affecting growth and development. Certainly, earlier studies have addressed the challenges to overcome the "growth/defense trade-off" associated with JA signalling activation (Campos et al., 2016; Takaoka et al., 2018). While specific studies concentrated on developing selective ligands to activate certain JAZs and mitigate the "growth/defense trade-off", which is associated with the drawback of continuous treatment (Takaoka et al., 2018), alternative research delved into genetic approaches to overcome this challenge (Campos et al., 2016). As mentioned earlier, the *jazQ phyB* mutant consistently exhibits heightened defense responses without affecting growth (Campos et al., 2016). It is assumed that this phenomenon is attributed to the regulation of parallel defense and growth signalling pathways (Campos et al., 2016). On the one hand, the absence of specific JAZs (JAZ1, JAZ3, JAZ4, JAZ9, JAZ10) in *jazQ* triggers defense activation via the MYCs

(Schweizer et al., 2013). Concurrently, the absence of these JAZs releases the inhibition on DELLAs, leading to the repression of the GA signalling pathways and consequently culminating in impaired growth (Campos et al., 2016; Hou et al., 2010; Yang et al., 2012). However, in the *jazQ phyb* mutant, the simultaneous absence of phyB results in an increased promotion of growth via the GA pathway, ultimately establishing a balance between reduced growth due to the absence of JAZs and enhanced growth due to the absence of phyB (Campos et al., 2016; de Lucas et al., 2008). Significantly, the mutated *jaz* alleles chosen to create the *jazQ* mutant, were selected based on their phylogenetic relationship within the JAZ family (Campos et al., 2016), regardless of the potential cellular localization of their encoded proteins. The JAZ expression map created in this project (Fig. 7; Fig. 8) has the potential to activate cellular JA signalling in primary roots with minimal *JAZ* mutations. This provides an opportunity to achieve selective JA responses, such as heightened defense, without altering growth.

Indeed, my experiments with single and multiple orders of *jaz* mutants revealed that only a few strategically chosen *JAZ* mutations based on their expression sites are sufficient to elicit specific JA signalling responses (Fig. 7; Fig. 8; Fig. 12; Fig. 13, Fig. 14). For instance, molecular phenotype analysis indicates continuous JA signalling in the root tip of *jaz2* mutants without accompanying growth phenotypes (Fig. 12). In fact, the RNA-seq analysis of *jaz2-6* root tips elucidated DEGs related to stress response (Tab. S2). In the stress response cluster of *jaz2-6*, 24 DEGs were identified, which are associated with defense responses (Tab. S2; see red highlighted Arabidopsis Genome Initiative codes [AGIs]). Furthermore, the root tips of *jaz2-6* exhibit numerous DEGs linked to secondary metabolic processes (Tab. S2). Certainly, secondary metabolites have been suggested to play essential roles in defense, with various groups of these compounds demonstrated to be dependent on JA signalling, as reviewed in (Goossens et al., 2017; Reymond et al., 2004). Prominent secondary metabolites that have been identified to be involved in defense responses in Arabidopsis are glucosinolates (Mewis et al., 2006). However, only one mis-regulated gene (AGI code: AT5G26270), encoding an uncharacterized transmembrane protein, was associated with glucosinolate metabolism in *jaz2-6* root tips (Tab. S2). Nevertheless, the DEGs identified in the root tips of *jaz2-6*, particularly those associated with defense and secondary metabolic metabolism, suggest potential alterations in the defense responses of *jaz2-6*, despite showing no obvious growth phenotype. However, the RNA-seq data are currently too preliminary to draw final conclusions regarding potential defense alterations in *jaz2-6*. Future projects could delve deeper into understanding the impact of DEGs in the root tip of *jaz2-6* mutants on defense. This could be achieved, for instance, by conducting bioassays. This could potentially enhance our understanding of defense responses in the root tip and

unveil mechanisms for improving crop plants' defense without compromising their growth. While root defense response assays against pathogens such as *Pythium irregulare*, *Fusarium oxysporum*, or nematodes like *Heterodera schachtii* have been established (Bohlmann & Wieczorek, 2015; Kesten et al., 2019; Sohrabi et al., 2015), it would be particularly interesting to implement a system for evaluating defense responses specifically in the root tips of *jaz2-6* mutants. The question also arises, whether the upregulation of transcripts associated with defense responses in the tested genotypes results in increased proteins and/or metabolites serving as defense compounds. Performing proteomic and metabolomic profiling in this direction could offer valuable insights.

In addition to enhancing defense responses, the targeted activation of JA signalling in a cell type-specific manner could also contribute to the improvement of various other plant features without impacting growth. As freshwater increasingly becomes a limited resource, also impacting agricultural practices, the development of strategies to ensure water availability for plants becomes progressively more crucial (Ingrao et al., 2023). As reviewed in (Dietrich, 2018), the root tip plays a pivotal role in sensing water availability and bends towards water sources to ensure a steady water supply for the plant, a process termed hydrotropism. Recently, a noteworthy connection between JA signalling and hydrotropism was uncovered (Mielke et al., 2021). This relationship influences the bending of the root tip toward water availability in a cell wall mutant with a mutation in *KORRIGAN1* (*KOR1*), which exhibits increased JA production and heightened JA signalling (Lane et al., 2001; Lei et al., 2014; Lopez-Cruz et al., 2014; Mielke et al., 2021; Peng et al., 2002; Vain et al., 2014). Although the *kor1* mutant exhibited the ability to bend toward water availability similar as the WT, *kor1* mutants carrying an additional *aos* mutation, which hampers JA-Ile biosynthesis, showed impaired hydrotropism (Mielke et al., 2021). This suggests a regulatory role for JA signalling in hydrotropism (Mielke et al., 2021). In fact, among the genes mis-regulated in *jaz2-6* root tip, 12 genes were shown to be related to responses to water deprivation (Tab. S2; see turquoise highlighted AGIs). As mentioned before, the data is currently too preliminary to draw conclusions regarding alterations in the response to water deprivation. However, future experiments could involve measuring the root hydrotropic responses of *jaz2-6* to reveal putative changes in these responses, potentially aiding in the identification of strategies to enhance water availability for plants.

In summary, the targeted activation of JA signalling could enhance various features in plants, including heightened defense responses, improved performance under water deficiency, regulation of

development, and other processes. Importantly, these benefits could be realized in agricultural settings without adversely impacting overall plant growth.

The regulatory roles of JAZ1, JAZ2, and JAZ3 in the root tip

Given the limited comprehension of JA signalling modulation at the cellular level, especially within the root, I conducted an RNA-seq analysis on the root tips of single and multiple order *jaz* mutants (Fig. 14; Tab. S2), as elevated JA signalling was indicated in this region (Fig. 12B). This analysis aimed among others to unveil the molecular mechanisms behind JA signalling in the root tip and potentially uncover novel functions regulated by JA signalling there.

Among all tested *jaz* single alleles, only the *jaz2-5* and *jaz2-6* mutants exhibited the activation of the JA signalling reporter, albeit with relatively weak fluorescence signals (Fig. 12B). Nevertheless, the activation of JA signalling reporter in the root tip supports that JAZ2 functions as a repressor of JA responsive genes particularly in this region. However, the RNA-seq analysis did not show significant upregulation of *JAZ10* transcription in *jaz2-6* root tips (Fig. 14B). One possible explanation for this discrepancy is that during sample collection, more material above the root tip was inadvertently included, as indicated before. This could potentially lead to a dilution effect on *JAZ10* expression specifically in the root tips. Alternative approaches, such as Laser Capture Microdissection (LCM), offer a solution to mitigate the dilution effect encountered in conventional methods, as reviewed in (Jensen, 2013). LCM is a technique that enables the precise isolation of specific cell types from a designated region of interest (Jensen, 2013). This method ensures the purity of the targeted cells, thereby effectively reducing the dilution effect typically associated with the inadvertent inclusion of unwanted cells during collection (Jensen, 2013).

Notably, *jaz2-6* root tips did not show gene transcription alterations specifically involved in JA-Ile biosynthesis or perception (Fig. 14C; Tab. S2). However, as indicated before, significant alterations were observed in other clusters of JA signalling-related genes, including those related to response to stimulus and stress, developmental regulation, and secondary metabolic processes (Fig. 14C; Tab. S2) (Dennis & Norris, 2015; Wasternack & Feussner, 2018). This suggests that JAZ2 alone does not primarily regulate JA-Ile biosynthesis or perception genes; but it participates in the regulation of other genes linked to JA signalling.

JAZs are known to repress several positive TFs, such as the MYCs (Goossens et al., 2017). However, *jaz2-6* root tips exhibited a higher number of down regulated genes compared to upregulated genes which was first unexpected (Fig. S4C and D; Tab. S2). Earlier research has uncovered that JAZs play a role in suppressing a subset of bHLH TFs referred to as JA-ASSOCIATED MYC2-LIKEs (JAMs), which in turn, are characterized as negative regulators of JA responses (Fonseca et al., 2014; Goossens et al., 2017; Nakata et al., 2013; Qi et al., 2015; Sasaki-Sekimoto et al., 2013; Song et al., 2013). The absence of JAZ2 in *jaz2-6* could lead to the release of negative JA response regulators, like JAMs, potentially providing an explanation for the increased number of down regulated genes in the *jaz2-6* background. The observed downregulation of genes in *jaz2-6* could also be attributed to the disrupted inhibitory function of JAZ2 on other intermediates of other hormone pathways. For instance, previous studies have shown that JAZs inhibit the repressive function of DELLAs on PIFs through competitive binding (Tab. S1) (Hou et al., 2010). In this context, the abolishment of JAZ2 in *jaz2-6* could potentially release other repressor proteins, such as DELLAs, to repress their target genes, eventually leading to elevated amounts of down regulated genes. Furthermore, the increased number of downregulated genes in *jaz2-6* may also stem from the expression of genes encoding other negative regulators. Typically repressed by JAZ2, the absence of JAZ2 in *jaz2-6* could lead to elevated expression of these genes, resulting in a higher abundance of negative regulators. Consequently, this excess of negative regulators may repress several other target genes in *jaz2-6*. However, considering the preliminary nature of the RNA-seq data (Tab. S2), it is too early to conclusively establish the presence of potential negative regulators of TFs among the upregulated genes in the *jaz2-6* mutant root tip.

Furthermore, based on my generated expression maps, it is suggested that JAZ1 and JAZ3 also localize in the root tip and play a role in repressing JA-responsive genes (Fig. 7; Fig. 8). This hypothesis is supported by the phenotype findings from the *jaz2-6 jaz3-4* and *jaz1-3 jaz2-6 jaz3-4* (*jazT*) mutants (Fig. 13; Fig. 14; Fig. S4), which not only lack *JAZ2* functionality but also have disrupted *JAZ3* or *JAZ1* and *JAZ3* functionality, respectively. These multiple order mutants showed a strong increase in the number of DEGs compared to the *jaz2-6* single allele (Fig. 14C; Fig. S4C and D; Tab. S2). Additionally, the *jazT* mutant exhibited an even higher number of DEGs compared to the *jaz2-6 jaz3-4* mutant (Fig. 14C; Fig. S4C and D; Tab. S2). These results indicate that the combined loss of *JAZ2* with *JAZ3* or both *JAZ1* and *JAZ3* leads to a more pronounced effect on gene expression, suggesting a cooperative role of these JAZ proteins in repressing JA-responsive genes in the root tip (Fig. 14C; Fig. S4C and D; Tab. S2). Moreover, both *jaz2-6 jaz3-4* and *jazT* mutants exhibit biological clusters related to stress and stimulus response, development, and

secondary metabolites, similar as *jaz2-6* (Fig. 14C; Fig. S4C and D; Tab. S2). However, these mutant combinations also show upregulated genes involved in JA-Ile biosynthesis and perception, which also involves other *JAZs* (Fig. 14C; Fig. S4C and D; Tab. S2). In case of *jazT*, this includes an almost 9-fold upregulation of *JAZ10*, which correlates with the elevated *JNV* expression in *jazT* root tips (Fig. 13B; Fig. 14B; Tab. S2). In summary, my data suggests that the dysfunction of JAZ2, combined with the loss of JAZ3 or both JAZ1 and JAZ3, leads to an even more pronounced mis-regulation in target genes. This encompasses genes associated with JA responses, including those involved in JA-Ile biosynthesis and JA signalling.

Both *jaz2-6 jaz3-4* and *jazT* mutants exhibited a small but significant reduction in root length, while the roots of *jaz2* mutants did not show significant alterations (Fig. 12A, Fig. 13A). Moreover, the DEGs related to development regulation in *jaz2-6 jaz3-4* and *jazT* root tips were around 2-fold and 4-fold higher, respectively, in comparison to *jaz2-6* (Fig. 14C). This included among other genes involved in root development (e.g., ARABINOGALACTAN PROTEIN 30 [AGP30]) (Tab. S2). These findings suggest that the mis-regulation of these genes may contribute to the reduced root growth observed in *jaz2-6 jaz3-4* and *jazT* mutants. It is well established that JA signalling negatively regulates both cell proliferation and cell elongation (Chen et al., 2011). However, the *JNV* reporter predominantly expresses in the meristem of *jaz2-6 jaz3-4* and *jazT* mutants (Fig. 13B), indicating that reduced root growth might be attributed to a decrease in cell proliferation there. Future projects could determine whether cell proliferation is diminished in the root meristem of *jaz2-6 jaz3-4* and *jazT*. This could be accomplished by quantifying the cortical cells within the region from the QC to the first elongated cell (Casamitjana-Martinez et al., 2003; Dello Ioio et al., 2007). Furthermore, a marker that drives the expression of GUS by the *CYCLIN-DEPENDENT PROTEIN KINASE* (*CYCB1;1*) promoter has been established to indicate the G2/M-phase of the cell cycle (Colon-Carmona et al., 1999). In this context, reduced *CYCB1;1p:GUS* expression indicates reduced cell division activity (Colon-Carmona et al., 1999). By determining the *CYCB1;1p:GUS* marker in *jaz2-6 jaz3-4* and *jazT*, it could be confirmed whether potentially reduced cell number is due to a reduced cell division.

Among the DEGs falling into the development cluster, several genes have been identified that are not immediately associated with root development. These include genes involved in pollen tube growth, flowering regulation, and leaf development (Tab. S2). Indeed, instances in which single genes function in various tissues have been documented before. A prominent example is *WUSCHEL* (*WUS*), which

orchestrates various cellular processes, as reviewed in (Jha et al., 2020). *WUS* is expressed in both the shoot and root, where it plays among others a crucial role in maintaining the stem cell niche in both contexts (Jha et al., 2020). Another example is *ARF8*, which has entirely different functions depending on the context of the tissue (Goetz et al., 2006; Tian et al., 2004). In this context, *ARF8* functions as a negative regulator of fruit development in floral tissues (Goetz et al., 2006), while it plays a role in promoting growth in the hypocotyl and root (Tian et al., 2004). Therefore, the JA-dependent regulation of genes associated with pollen tube growth, flowering regulation, and leaf development raises intriguing questions regarding their functional relevance in the root tip. Future research could potentially elucidate their function in the root tip through phenotype analyses, focusing specifically on the root tip of the KO mutants of mentioned genes.

All tested genotypes showed a cluster of DEGs related to circadian rhythm in their root tips (Fig. 14C; Fig. S4C and D, Tab. S2). These findings are likely a result of the time-consuming process of collecting root tip samples throughout the day during the experiment that took place over 6h. However, it is crucial to acknowledge that some of these genes can also be linked to other biological processes, such as stress response genes (e.g., PATHOGEN AND CIRCADIAN CONTROLLED 1 [PCC1] or GLYCINE RICH PROTEIN 2 [GRP2]) (Tab. S2). This could suggest that the mis-regulation of these genes is indeed a consequence of the absence of specific JAZs that typically repress them. On the other hand, crosstalk between JA signalling and circadian rhythm has been reported before (Thines et al., 2019). For example, it has been shown that the accumulation of MYC2 is negatively regulated through its interaction with TIME FOR COFFEE (TIC) in a circadian rhythm-dependent manner (Shin et al., 2012). Therefore, given the preliminary status of the RNA-seq data, conclusions cannot be drawn regarding whether DEGs related to the circadian rhythm are a result of the time-consuming root tip collection or indeed a consequence of dysregulated processes due to the absence of JAZs in the tested mutants.

The RNA-seq analysis also revealed interesting DEG patterns between the tested genotypes (Fig. S4B). Among the total DEGs, 66 genes were consistently mis-regulated in all tested genotypes, suggesting that the *jaz2-6* mutation alone was sufficient to induce mis-regulation in these genes. 290 genes were found to be shared between *jaz2-6 jaz3-4* and *jazT*, indicating that these genes are regulated by *JAZ3* alone or in combination with *JAZ2*. Notably, a significant portion of 352 genes were exclusively mis-regulated in *jazT* (Fig. S4B), suggesting that these genes might be regulated by *JAZ1* alone, *JAZ1* in combination with *JAZ2* or *JAZ3,* or *JAZ1* together with both genes.

In contrast, 95 genes were found to be mis-regulated in *jaz2-6*, but not in *jaz2-6 jaz3-4* and *jazT* mutants (Fig. S4B). These results suggest that *jaz2-6 jaz3-4* and *jazT* mutants activate transcriptional regulatory genes, such as other *JAZs*, which are not affected in the *jaz2-6* mutant. As a result, *jaz2-6 jaz3-4* and *jazT* mutants accumulate JAZ repressors, which may counteract the mis-regulation of some genes caused by the *jaz2-6* allele. Indeed, the RNA-seq revealed upregulated *JAZs* in *jaz2-6 jaz3-4* and *jazT*, supporting this hypothesis (Tab. S2). Moreover, the RNA-seq revealed 10 DEGs that were solely shared by *jaz2-6* and *jaz2-6 3-4*, as well as and 81 genes that were exclusively mis-regulated in *jaz2-6 3-4*. It is likely that the DEGs exclusively shared in *jaz2-6* and *jaz2-6 jaz3-4* are mis-regulated due to the absence of JAZ2, while DEGs present only in *jaz2-6 jaz3-4* are probably influenced by the lack of JAZ3. However, with the absence of JAZ1 in *jazT*, the triple mutants might accumulate other exclusive JAZ repressors usually inhibited by JAZ1, which then re-modulate DEGs shared in *jaz2-6* and *jaz2-6 jaz3-4*, as well as those solely mis-regulated in *jaz2-6 jaz3-4*. Supporting this hypothesis, the RNA-seq data revealed an upregulation of *JAZs*, solely observed in *jazT* (Tab. S2).

Surprisingly, 32 genes were found to be altered in both, *jaz2-6* and *jazT* mutants, but not affected in *jaz2-6 jaz3-4* (Fig. S4B). These findings indicate a compensatory effect of the *JAZ1* gene, suggesting that *JAZ1* expression might be upregulated in the *jaz2-6 jaz3-4* and *jazT* mutants. This upregulation of *JAZ1* in *jaz2-6 jaz3-4* may then re-control certain DEGs. However, since *jazT* lacks *JAZ1* functionality (Fig. S5A), there is no such compensatory effect on these mis-regulated genes affected in *jazT* mutant. Indeed, the RNA-seq analysis revealed an upregulation of *JAZ1* expression in both the *jaz2-6 jaz3-4* mutants and the *jazT* mutant, although the *JAZ1* transcript in *jazT* mutants is dysfunctional (Tab. S2).

In conclusion, my RNA-seq results illustrate the complex regulatory interplay among JAZ1, JAZ2, and JAZ3 in the modulation of JA signalling in the context of the root tip. Furthermore, the RNA-seq reveals additional novel genes that are regulated by JA signalling in the root tip. Exploring these genes within the context of the root tip has the potential to enhance our understanding of additional functions governed by JA signalling in this specific root region.

Potentials of *rat.JAZp:JAZ-CIT* reporters generated in this work

Previous studies showed ligand- and proteasome-dependent degradation of chimeric JAZs *in vivo* (Chini et al., 2007; Shyu et al., 2012; Thines et al., 2007). Nevertheless, prior studies that explored the stabilities

of full-length chimeric JAZ proteins *in planta* relied on overexpression lines, lacking the precision of ratiometric quantification (Chini et al., 2007; Shyu et al., 2012; Thines et al., 2007). I designed and utilized ratiometric translational reporters, allowing for both the localization of JAZ-CIT when expressed under their endogenous promoter and the quantitative measurement of relative JAZ-CIT levels *in planta*. (Fig. 16A and B). The JAZ-CIT expression driven by their endogenous promoters facilitates nuclear JAZ-CIT turnover measurements, encompassing processes such as *de-novo* synthesis, protein life-time, and degradation (Toyama & Hetzer, 2013), aiming to accurately represent the *in planta* scenario. To refine my nuclear turnover measurements, I specifically focused on the nucleus since JA-Ile perception occurs there, minimizing background signal interference.

Features potentially influencing JAZ-CIT turnover variations

The ratiometric reporters indicate that nuclear turnover differs between JAZ1-CIT and JAZ3-CIT following COR treatment (Fig. 20). These differences could be attributed to inherent biochemical features affecting ligand-mediated degradation, as well as differences in interaction partners.

When comparing the aa sequences of the Jas degron between JAZ1 and JAZ3, seven different residues were identified, four of which exhibited non-conservative differences (Fig. 21A). As the variability in the sequence of Jas degrons has been shown to influence JAZ/ligands/COI1 interaction (Melotto et al., 2008; Sheard et al., 2010; F. Zhang et al., 2015), these differences may also have an impact on the ligand-dependent COI1 interaction of JAZ1-CIT and JAZ3-CIT in my reporter construct and subsequently influence their degradation. Additionally, recent studies on Auxin signalling pathway repressors AUX/IAAs, have demonstrated that structural elements outside the degron region influence the interaction intensity between AUX/IAAs and the F-Box protein TRANSPORT INHIBITOR RESPONSE 1 (TIR1) (Mockaitis & Estelle, 2008; Niemeyer et al., 2020). Therefore, potential variability in COI1 interaction between JAZ1 and JAZ3 could hypothetically be influenced by structural elements outside the Jas degron. To determine if binding affinities between COI1 and full-length JAZ1 or JAZ3 differ, future saturation binding assay experiments could be performed. In fact, *in vitro* COI1/JAZ saturation binding assays have never been conducted with full-length JAZ proteins; instead, they have been solely performed with Jas degrons, as demonstrated for Jas1 and Jas6 (Sheard et al., 2010). Although the K_D values measured in these experiments indicate varying binding capabilities between different Jas degrons and COI1 (Sheard et al., 2010), they might not be representative for full-length JAZs. Also the *rat.Jas9-VEN* construct, incorporating the Jas9 degron targeted to VEN as a JA-Ile sensor (Larrieu et al., 2015), does not fully represent the turnover of full-length

JAZ9, limiting the ability to draw conclusions about full-length JAZ9/COI1 interaction *in planta*. Taken together, it would be intriguing to investigate in *vitro* COI1/JAZ interactions with full-length JAZs to assess the full structural impact on JAZ/COI1 binding and see if the results correlate with the *in planta* measurements provided by my *rat.JAZp:JAZ-CIT* reporter.

Previous studies have also indicated correlations between the ubiquitination rate of proteins targeted by the proteasome and the dynamics of proteasome-dependent degradation (Winkler et al., 2017). As discussed in the review by (Hershko & Ciechanover, 1998), Ub is typically conjugated to lysine residues during the E1/E2/E3-driven ubiquitylation process. Interestingly, when directly comparing lysines as potential ubiquitylation sites between JAZ1 and JAZ3, only marginal differences are observable (Fig. 21B). Specifically, JAZ1 exhibits 16 lysines; two more than JAZ3 (Fig. 21B). Nevertheless, studies have shown that non-canonical residues, including serine, tyrosine, and threonine, can also function as ubiquitylation sites, marking proteins for proteasome-dependent degradation (Gilkerson et al., 2015). This suggests that the ubiquitylation rate of a specific JAZ is not solely determined by the quantity of lysines alone. Furthermore, it has been shown that not all lysine residues act as ubiquitination sites (Niemeyer et al., 2020; Winkler et al., 2017). Building on research involving AUX/IAAs, it is suggested that ubiquitylation preferentially takes place in exposed intrinsically disordered regions of AUX/IAAs when they are recruited to the co-receptor TIR1 (Niemeyer et al., 2020). This underscores the significance of the position of lysine residues in the ubiquitylation process (Niemeyer et al., 2020). Importantly, this aspect could also impact the ubiquitylation of distinct JAZs. Indeed, it has been demonstrated that JAZs are highly intrinsically disordered proteins (Fig. 22) (Pazos et al., 2013). Hence, it could be that the intrinsically disordered regions of JAZs engage with other partners during the ubiquitylation process, potentially masking ubiquitination sites of JAZs. In conclusion, the amount of potential Ub sites do not necessarily correlate with their ubiquitylation levels. Therefore, it is challenging to draw definitive conclusions regarding the actual ubiquitination of JAZ1 and JAZ3.

Recently, *in vitro* ubiquitylation (IVU) assays of AUX/IAAs has been developed to identify substrate Ub sited following TIR1-SCF complex (SCF^{TIR1}) binding (Winkler et al., 2017). This innovative assay has already effectively been utilized to investigate the ubiquitylation of the entire JAZ9 protein in rice (OsJAZ9), providing insights into how the enhanced ubiquitylation of OsJAZ9 induced by the pathogen *Xanthomonas oryzae* influences JA signalling and, consequently, the susceptibility of rice to the pathogen (S. Wang et al., 2021). Therefore, it would be valuable to conduct IVU assays on full-length Arabidopsis JAZ1 and JAZ3,

selected as representatives in this project, to investigate whether their ubiquitylation rates align with the observations derived from the *rat.JAZp:JAZ CIT* experiments.

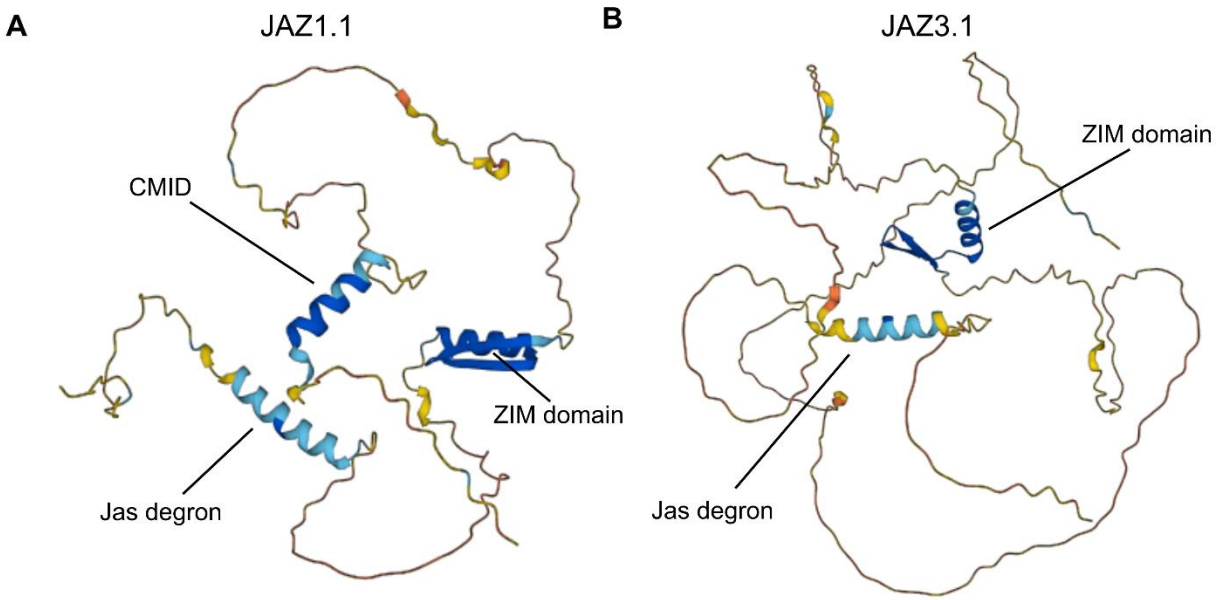

Figure 22: JAZ proteins exhibit highly intrinsically disordered regions. (**A,B**) Structure prediction, exemplified with (**A**) JAZ1.1 and (**B**) JAZ3.1, demonstrates the significant intrinsic disorder characteristic of JAZ proteins (www.alphafold.ebi.ac.uk.). Colours denote the model confidence as per-residue model confidence score (pLDDT): Dark blue = Very high (pLDDT > 90); light blue = high (90 > pLDDT > 70); yellow = (70 > pLDDT > 50); orange = very low (pLDDT < 50).

Significantly, the ligand-dependent degradation of JAZs *in planta* can potentially vary in the context of respective JAZ localization sites. Studies have demonstrated that leaf wounding leads to distinct spatial and temporal variations in JA-Ile levels, depending on the specific leaf tissues examined (Glauser et al., 2008; Grebner et al., 2013). Additionally, it was shown that after wounding, distal tissues display different spatial and temporal JA-Ile concentration dynamics as local wounded tissues (Glauser et al., 2009; Koo et al., 2009; Schulze et al., 2019). Therefore, *in planta* JAZ degradation is likely to differ among different tissues and cell types due to variations in JA-Ile levels across these regions. This assumes that ligand-mediated JAZ degradation is dose-dependent. In fact, my data demonstrates that ligand-mediated turnover of full-length JAZ-CIT is concentration-dependent (Fig. 20A and B), likely attributable to dose-dependent degradation.

Furthermore, it has been shown that JAZ degradation can also be modulated by distinct interaction partners (Pauwels et al., 2015). In this context, it was demonstrated, that the E3 RING ligase KEEP ON GOING (KEG), a negative regulator of ABA signalling (Liu & Stone, 2010, 2013), particularly interacts with

JAZ12, partially counteracting COI1-dependent degradation of JAZ12 (Pauwels et al., 2015). Therefore, *in planta* JAZ degradation is likely influenced by the cellular co-localization of specific JAZs and certain interaction partners.

To investigate whether different turnover rates of rat.JAZ-CIT result from varying degradation rates *in planta*, the *rat.JAZp:JAZ-CIT* reporters could be subjected to Cycloheximide (CHX) treatment, an inhibitor of *de novo* synthesis (Obrig et al., 1971).

The role of differential JAZ turnover rates in modulating cell-specific JA signalling

The cell type-specific expression of JAZs and the specific activation of a JA signalling marker in specific *jaz* mutants in a cell type-specific manner strongly indicate the crucial role of JAZs in modulating JA signalling in these locations (Fig. 7; Fig. 8; Fig. 15; Fig. 16C and D; Fig. 18A and B). Furthermore, specific attributes of JAZs, such as their repressive capacity on TFs, the target genes under their regulation, and their ligand-dependent turnover, might impact the precise control of JA responses.

Indeed, the data I collected from my ratiometric reporters strongly suggests that JAZs expressed under their endogenous promoters exhibit ligand dose-dependent turnover, and distinct variations in turnover dynamics among different JAZs (Fig. 20). Consequently, cellular specificities in JA signalling could be achieved through a combination of different cell type-specific JAZ expression and ligand-dependent turnover dynamics. Various cell types showcase distinct combinations of JAZs with diverse ratios of relatively low and high JA-Ile/COR-dependent turnover rates. As a result, the turnover dynamics of cell type-specific JAZ compositions are likely to be unique. Consequently, a specific JA-Ile or COR level might elicit differential responses from JA response genes in a cell-specific context.

The specific combination of JAZs tailored to each cell type, featuring varying ratios of relatively low and high ligand-dependent turnover rates, potentially facilitate precise fine-tuning of JA responses. For instance, in response to a relatively weak stimulus, like minor wounding, a specific cell type may receive relatively low levels of JA-Ile (Zhang & Turner, 2008), leading primarily to the degradation of less stable JAZs. As a result, more stable JAZs would remain as repressors, resulting in a relatively low JA response. Conversely, a stronger stimulus such as major wounding could induce higher levels of JA-Ile, leading to the degradation of both, stable and unstable JAZs, resulting in a higher JA response. Certainly, the RNA-seq analysis demonstrates that the response increases with the removal of each additional JAZ, as

indicated by the increasing number of DEGs with each successive *JAZ* mutation (Fig. 14C). This suggests that indeed different strong stimuli resulting in different remaining JAZs also influence the intensity of the response. Different cell types are exposed to different stimuli and express distinct sets of JAZs with individual protein features to finely tune JA signalling according to their specific environment, consequently allowing cellular specificities.

The cell-specific localization and the diverse turnover rates of JAZs may also play pivotal roles in regulating regional and distal responses, particularly in the event of injury. As mentioned earlier, after wounding, temporal, as well as spatial JA-Ile levels vary between regional and distal sites (Glauser et al., 2009; Koo et al., 2009; Schulze et al., 2019). Consequently, the turnover of JAZs potentially differs between regional and distal wounding sites, leading to distinct regulation of regional and distal responses.

It is important to note that other factors, including expression levels, life-time, and degradation (Toyama & Hetzer, 2013), can influence the overall protein amounts of different JAZs, subsequently impacting JA responses. For example, a relatively weak stimulus promotes the decrease of JAZs with higher degradation rates over JAZs with lower degradation rates. However, if the basal amount of JAZ proteins is initially low in this scenario, the resulting JA response could be high despite the relatively low degradation rate. Conversely, the initial JA response triggered by the degradation of a JAZ with a relatively high ligand-dependent degradation rate might be subdued when the initial amount of the corresponding JAZ is substantial.

It is to acknowledge that factors beyond JAZ turnover rates, such as the repression intensity of JAZs on MYCs, likely play significant roles in modulating JA signalling (Boter et al., 2004; Chini et al., 2007; Fernandez-Calvo et al., 2011; Lorenzo et al., 2004; Ona Chuquimarca et al., 2020; F. Zhang et al., 2015). In this context, even at low abundance levels, JAZs may exhibit strong repression on TFs, resulting in a dampened JA response. On the other hand, high levels of weak repressors may have minimal impact on inhibiting JA responses. The fact that JAZs demonstrate different binding capabilities with canonical components of the repressor complex (Tab. S1) (Ona Chuquimarca et al., 2020; F. Zhang et al., 2015), suggests that the repression strength exerted by JAZs plays an essential role in modulating JA signalling specificities. Hence, it would be exciting to investigate the repression capabilities of JAZs in the context of JA signalling modulation in future projects.

In addition to their potential to regulate cellular specificities and fine-tune JA responses, JAZs potentially modulate the temporal dynamics of JA signalling via these differing turnover rates. As mentioned earlier, JA-responsive genes exhibit distinct temporal patterns, categorizable into short-term genes (e.g., *JAZs* and *MYC2*), reaching peak expression 1h after stimulus initiation, mid-term genes (e.g., *AOS*, *LOX3*, and *LOX4*), peaking expression between 2 to 4h after stimulus initiation, and long-term genes (e.g., *VSP1*, *VSP2*, and *PDF1.2*), reaching peak expression more than 4h after stimulus initiation (Chung et al., 2008). In this context, varying JAZ turnover rates at a specific JA-Ile or COR concentration could lead to the de-repression of target genes at distinct time points, thereby contributing to their differential expression patterns of JA responsive genes over time. In conclusion, the turnover rates of individual JAZs, serve as potential regulatory mechanisms to respond to varying concentrations of bioactive ligands resulting from different external stimuli.

It is worth noting that both tested reporters exhibited a rapid decrease in turnover within minutes (Fig. 20). In fact, the fast degradation of repressors to rapidly respond to hormonal signals has been previously observed (Abel et al., 1995; Abel et al., 1994). Auxin, for instance, is known for inducing rapid transcriptional and physiological alterations (Guilfoyle, 1986; Theologis, 1986). This is ensured among others by the fast degradation of the Auxin signalling repressors AUX/IAAs (Abel et al., 1995; Abel et al., 1994). One illustrative example showcases the Auxin-dependent degradation of Arabidopsis IAA1 - IAA14 occurring within a timeframe of 4 to 30min (Abel et al., 1995). These studies, combined with my results of rat.JAZ turnover measurements underscore the remarkable speed at which plants can acclimate to their environment (Abel et al., 1995; Abel et al., 1994; Chung et al., 2008; Guilfoyle, 1986; Theologis, 1986)

Future prospects for *rat.JAZp:JAZ-CIT* reporters

Given that JA signalling is prominently known to be initiated by wounding to activate defense responses (Wasternack & Feussner, 2018), it would be intriguing to explore the dynamics of my reporters post-wounding. As I could not stabilize JAZ-CIT in my reporters without abolishing JA-Ile biosynthesis in the plants using the *aos* background (Park et al., 2002), it becomes crucial to explore alternative systems that facilitate ratiometric JAZ-CIT (rat.JAZ-CIT) turnover measurements following wounding. Indeed, (Grossmann et al., 2011) developed a microfluidic chip platform called "RootChip," enabling live-cell imaging with minimal interference. Utilizing systems like this could facilitate the measurement of rat.JAZ-CIT turnover dynamics in my reporters after intentional wounding.

It is worth noting that all my turnover measurement experiments were conducted using COR as the bioactive ligand. Nevertheless, it would be highly intriguing to investigate the dynamics of JAZ-CIT proteins using JA-Ile, as this is the bioactive endogenous ligand *in planta* (Fonseca, Chini, et al., 2009). Earlier reports suggested that COR is approximately 1,000 times more potent than JA-Ile (Katsir et al., 2008), implying that higher levels of JA-Ile might be necessary to achieve comparable turnover decays observed with COR.

Since the expression of *JAZ* genes increases as part of a negative feedback loop following initiated JA signalling (Chung et al., 2008; Thines et al., 2007; Yan et al., 2007), it would be intriguing to explore the dynamics of my ratiometric reporters in long-term experiments exceeding the 15min duration used in my experiments. This extended timeframe would enable the investigation of the dynamics associated with the re-expression of JAZ-CIT following their degradation.

Furthermore, the JA-Ile/COR-independent normalization principle demonstrated by the *UBQp:Ijas9*-TOM normalizer could be extended to investigate additional aspects. Additional ratiometric reporters could be designed to quantify the dynamics of nucleus-localizing proteins encoded by genes regulated through JA signalling, such as the MYCs (Chung et al., 2008; Yan et al., 2007).

Conclusion

In conclusion, my data suggest that the distinct cellular localization of constitutively expressed JAZs, along with their varying ligand-dependent turnover rates, are essential factors in modulating cellular JA signalling specificities and fine-tuning JA responses (Fig. 23).

These insights not only enhance our understanding of how cellular specificities are regulated in the context of JA signalling but also propose similar regulatory mechanisms for other signalling pathways within a cell-specific context. *AUX/IAAs*, serving as an example, exhibit diverse expression patterns (Abel et al., 1995; Groover et al., 2003; Kim et al., 2020; Klepikova et al., 2016; Rusak et al., 2010; Tian et al., 2002; Windels et al., 2014), while AUX/IAA proteins have been demonstrated to undergo varying Auxin-dependent degradation velocities (Abel et al., 1995; Abel et al., 1994). This observation suggests that the cellular modulation of Auxin signalling may be governed by regulatory mechanisms similar as those observed in JA signalling. The findings from this study contribute to our understanding of how plants, as sessile organisms, rapidly and precisely acclimate to their changing environment. The knowledge gained

from this work may also pave the way for the development of new strategies to enhance agricultural plants, such as devising novel defense strategies for crop plants.

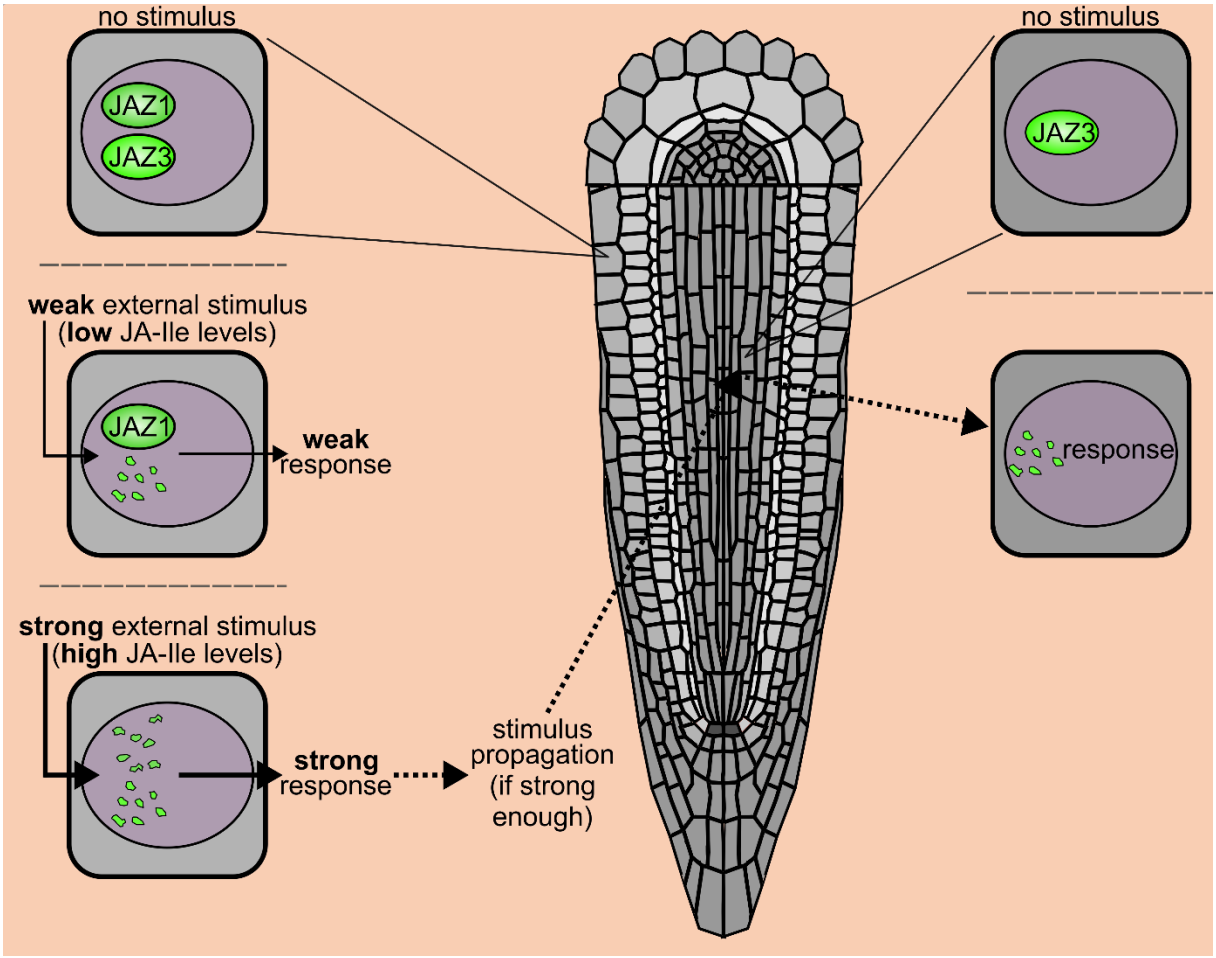

Figure 23: Model illustrating the potential regulation of cellular specificities by JAZs based on the data from this thesis. Exemplifying JAZ1 and JAZ3 as representative JAZs, the model illustrates the potential modulation of cellular specificities, highlighting specific localizations such as the epidermis and stele in the root meristem. Under basal conditions (no stimulus), basal JAZs exhibit a cell-specific localization pattern and repress JA responses. A relatively weak stimulus (e.g., minor wounding of the epidermis), triggers relatively low JA-Ile levels. Consequently, this leads to the ligand-dependent turnover of relatively unstable JAZs (e.g., JAZ3 within the epidermal cells), resulting in correspondingly modest cellular responses. Conversely, when exposed to a stronger stimulus (e.g., major epidermal wounding), JA-Ile levels are higher. This heightened concentration triggers the ligand-dependent turnover of both relatively unstable and stable JAZs (e.g., JAZ1 and JAZ3 within the epidermis). Consequently, the cell-type specific responses become more pronounced and robust under these conditions. When the stimulus is sufficiently strong, it reaches other cell types (e.g., stele) where JAZs, explicitly localized in those regions, undergo ligand-dependent turnover, thereby triggering cell-specific responses in those areas.

Section IV - Material and methods

Key resources

Table 2: Key resources table

REAGENT or RESOURCE	SOURCE	IDENTIFIER
Bacterial strains		
Escherica coli DH5α	Thermo Fisher	18265017
Agrobacterium tumefaciens GV3101	GoldBio	CC-207-A
Chemicals, Peptides, and Recombinant Proteins/Enzymes		
Murashige & Skoog (MS) basal salt mix	Duchefa	M0221.0025
2-(N-morpholino)ethanesulfonic acid (MES)	Sigma	M8250
Plant agar	Applichem	A2111
Propidium Iodide (PI)	Sigma	P4864
Aceton	VWR Chemicals	20165.323
Sodium phosphate	Sigma	RDD007-1KG
Triton X-100	Roth	9009-93-1
Potassium ferricyanide (II)	Roth	7971.1
Potassium ferricyanide (III)	Roth	7971.4
X-Gluc	Biomol	AG-CN2-0023-M001
Ethanol	Brüggemann Alkohol	06041056
Chloral hydrate	Sigma	15307-500G-R
Glycerol	Roth	3908.2
Methly Jasmonate (MeJA)	Sigma	392707
Coronatine (COR)	Sigma	C8115-1MG
Carbenicillin	Roth	6344.2
Gentamycin	Duchefa	G0124
Kanamycin	Roth	T832
Spectinomycin	Serva	3529401
LB broth high salt	Duchefa	L1704.0500
Bacto peptone	Duchefa	P1328
Bacto yeast extract	Duchefa	Y1333
Bacto agar	Roth	1347.3
Bacto tryptone	Thermo Fisher	216699
Sodium chloride	Roth	3957.1
Potassium chloride	Sigma	P-9333
Sucrose	Sigma	16104-1KG
Silwet L-77	Biotrend	30630216-4

Hydrochloric acid fuming, 37%	Roth	4625.1
Hydrochloric acid standard 2N	Sigma	653799-500ML
Tris base	Roth	5429.3
Boric acid	Merck	1001651000
Lithium Chloride	Roth	3739.1
Ethylenediamine tetraacetic acid (EDTA) disodiumsalt dihydrate	Roth	8043.2
Sodium lauryl sulfate (SDS)	Roth	5136.1
Rotophorese 10xTBE	Roth	3061.1
Agarose Standard	Roth	3810.4
Biozym Phor Agarose	Biozym	850180
Serva DNA Stain G	Serva	39803.02
Brom phenol blue	Roth	A512.3
Xylene cyanole FF	Simga	X-4126
Magnesiumchlorid-hexahydrat	Sigma	M0250-500G
Deoxynucleotide Triphosphate (dNTP)	Promega	U1240
Thermosensitive Alkaline Phosphatase (TSAP)	Promega	M9910
5xHF buffer	Thermo Fisher	00966015
10x CutSmart	Biolabs	372045
LigaFast Rapid DNA Ligation System	Promega	M8221
T4 DNA Ligase	Promega	M1804
Diethyl pyrocarbonate (DEPC)	Applichem	A0881.0020
AflII	Biolabs	R0520S
KpnI	Biolabs	R0142S
XmaI	Biolabs	R0180S
BP clonase	Thermo Fisher	11789-100
LR clonase	Thermo Fisher	11791-100
LR Plus clonase	Thermo Fisher	12176590
Phusion High-Fidelity DNA Polymerase	Thermo Fisher	10342020
Taq DNA Polymerase	Life Technologies	F530
RT M-MLV	Promega	M3683
M-MLV RT 5X Buffer	Promega	M531A
SYBR Green	Invitrogen	S7563
6-carboxy-X-rhodamine	Invitrogen	12223-012
Go Taq Polymerase	Promega	M7848
Kits		
DNeasy Plant Mini Kit	Qiagen	69106
RNeasy Plant Mini Kit	Qiagen	74904
NuleoSpin Gel and PCR CleanUp	Marchery & Nagel	740609.25

QIAprep Spin MiniPrep Kit	Qiagen	27106
Experimental models		
Arabidopsis thaliana: *aos*	(Park et al., 2002)	T-DNA (N/A)
Arabidopsis thaliana: *jaz1-1*	NASC; (Demianski et al., 2012)	T-DNA (SALK_011957)
Arabidopsis thaliana: *jaz1-2*	(Campos et al., 2016)	T-DNA (JIC-SM.22668)
Arabidopsis thaliana: *jaz1-3*	This study	CRISPR/Cas9 (886 bp deletion)
Arabidopsis thaliana: *jaz2-1*	NASC; (Thines et al., 2007)	T-DNA (SALK_122858)
Arabidopsis thaliana: *jaz2-2*	NASC; (Thatcher et al., 2016)	T-DNA (SALK_025279)
Arabidopsis thaliana: *jaz2-5*	This study	CRISPR/Cas9 (Thymine deletion)
Arabidopsis thaliana: *jaz2-6*	This study	CRISPR/Cas9 (Adenine insertion)
Arabidopsis thaliana: *jaz3-1*	NASC; (Thatcher et al., 2016) 2016	T-DNA (SALK_139337)
Arabidopsis thaliana: *jaz3-4*	(Campos et al., 2016)	T-DNA (GABI_097F09)
Arabidopsis thaliana: *jaz4-1*	NASC; (Jiang et al., 2014)	T-DNA (SALK_141628)
Arabidopsis thaliana: *jaz5-1*	NASC; (Demianski et al., 2012)	SALK_053775
Arabidopsis thaliana: *jaz6-1*	NASC; (Thatcher et al., 2016)	SAIL_1156_C06
Arabidopsis thaliana: *jaz6-2*	NASC	SALK_017531
Arabidopsis thaliana: *jaz6-3*	NASC; (de Torres Zabala et al., 2016)	GABI_102A03
Arabidopsis thaliana: *jaz6-5*	This study	CRISPR/Cas9 (Adenine insertion)
Arabidopsis thaliana: *jaz6-6*	This study	CRISPR/Cas9 (1684 bp deletion)
Arabidopsis thaliana: *jaz7-1*	NASC; (Sehr et al., 2010)	WiscDsLox7H11
Arabidopsis thaliana: *jaz8-v*	(Cao et al., 2011; Thireault et al., 2015)	*jaz8-vash* (bp substitution Cytosine to Adenine)
Arabidopsis thaliana: *jaz9-1*	NASC; (Yang et al., 2012)	T-DNA (SALK_004872)
Arabidopsis thaliana: *jaz9-4*	NASC; (Campos et al., 2016)	T-DNA (GABI_265H05)
Arabidopsis thaliana: *jaz10-1*	(Sehr et al., 2010)	T-DNA (SAIL_92_D08)
Arabidopsis thaliana: *jaz11-2*	This study	CRISPR/Cas9 (Adenine insertion)
Arabidopsis thaliana: *jaz11-3*	This study	CRISPR/Cas9 (Thymine deletion)
Arabidopsis thaliana: *jaz12-1*	NASC; (Pauwels et al., 2015)	T-DNA (SALK_055032)
Arabidopsis thaliana: *jaz12-2*	NASC; (Thatcher et al., 2016)	T-DNA (SALK_044058)
Arabidopsis thaliana: *jaz13-1*	NASC; (Thireault et al., 2015)	T-DNA (GABI_193G07)
Arabidopsis thaliana: *jaz1-3*x*jaz2-6*	This study	See single mutants
Arabidopsis thaliana:	This study	See single mutants

*jaz1-3*x*jaz3-4*		
Arabidopsis thaliana: *jaz2-6*x*jaz3-4*	This study	See single mutants
Arabidopsis thaliana: *jaz1-3*x*jaz2-6*x*jaz3-4* (*jazT*)	This study	See single mutants
Arabidopsis thaliana: *jaz7-1*x*jaz8-v*x *jaz10-1*x*jaz13-1* (j*azNB*)	(Thireault et al., 2015)	See single mutants
Transgenic lines		
Arabidopsis thaliana: JAZ1p:GUSns in Col-0	This study	N/A
Arabidopsis thaliana: JAZ2p:GUSns in Col-0	This study	N/A
Arabidopsis thaliana: JAZ3p:GUSns in Col-0	This study	N/A
Arabidopsis thaliana: JAZ4p:GUSns in Col-0	This study	N/A
Arabidopsis thaliana: JAZ5p:GUSns in Col-0	This study	N/A
Arabidopsis thaliana: JAZ6p:GUSns in Col-0	This study	N/A
Arabidopsis thaliana: JAZ7p:GUSns in Col-0	This study	N/A
Arabidopsis thaliana: JAZ8p:GUSns in Col-0	This study	N/A
Arabidopsis thaliana: JAZ9p:GUSns in Col-0	This study	N/A
Arabidopsis thaliana: JAZ10p:GUSns (JGPns) in Col-0	(Gasperini et al., 2015)	N/A
Arabidopsis thaliana: JAZ11p:GUSns in Col-0	This study	N/A
Arabidopsis thaliana: JAZ12p:GUSns in Col-0	This study	N/A
Arabidopsis thaliana: JAZ13p:GUSns in Col-0	This study	N/A
Arabidopsis thaliana: JAZ1p:NLS-3xVEN in Col-0	This study	N/A
Arabidopsis thaliana: JAZ2p:NLS-3xVEN in Col-0	This study	N/A
Arabidopsis thaliana: JAZ3p:NLS-3xVEN in Col-0	This study	N/A
Arabidopsis thaliana: JAZ4p:NLS-3xVEN in Col-0	This study	N/A
Arabidopsis thaliana: JAZ6p:NLS-3xVEN in Col-0	This study	N/A

Arabidopsis thaliana: JAZ9p:NLS-3xVEN in Col-0	This study	N/A
Arabidopsis thaliana: JAZ10p:NLS-3xVEN (JNV) in Col-0	(Mielke et al., 2021)	N/A
Arabidopsis thaliana: JNV in *jaz1-3*	This study	N/A
Arabidopsis thaliana: JNV in *jaz2-5*	This study	N/A
Arabidopsis thaliana: JNV in *jaz2-6*	This study	N/A
Arabidopsis thaliana: JNV in *jaz3-4*	This study	N/A
Arabidopsis thaliana: JNV in *jaz4-1*	This study	N/A
Arabidopsis thaliana: JNV in *jaz6-6*	This study	N/A
Arabidopsis thaliana: JNV in *jaz9-1*	This study	N/A
Arabidopsis thaliana: JNV in *jaz1-3 jaz2-6*	This study	N/A
Arabidopsis thaliana: JNV in *jaz2-6 jaz3-4*	This study	N/A
Arabidopsis thaliana: JNV in *jazT*	This study	N/A
Arabidopsis thaliana: JNV in *jazNB*	This study	N/A
Arabidopsis thaliana: JAZ1p:JAZ1.1-CIT in *jaz1-3*	This study	N/A
Arabidopsis thaliana: JAZ2p:JAZ2.1-CIT in *jaz2-6*	This study	N/A
Arabidopsis thaliana: JAZ3p:JAZ3.1-CIT in *jaz3-4*	This study	N/A
Arabidopsis thaliana: JAZ4p:JAZ4.1-CIT in *jaz4-1*	This study	N/A
Arabidopsis thaliana: JAZ6p:JAZ6.1-CIT in *jaz6-6*	This study	N/A
Arabidopsis thaliana: JAZ9p:JAZ9.1-CIT in *jaz9-4*	This study	N/A
Arabidopsis thaliana: JAZ10p:JAZ10.1-CIT in *jaz0-1*	This study	N/A
Arabidopsis thaliana: JAZ1p:JAZ1.1-CIT + UBQ10p:Ijas9-TOM in *aos*	This study	N/A
Arabidopsis thaliana: JAZ1p:JAZ1.1-CIT + UBQ10p:Ijas9-TOM in *jaz1-3*	This study	N/A
Arabidopsis thaliana: JAZ1p:JAZ1.1-CIT + UBQ10p:Ijas9-TOM in *jaz1-3 jaz2-6*	This study	N/A
Arabidopsis thaliana: JAZ1p:JAZ1.1-CIT + UBQ10p:Ijas9-TOM in *jaz1-3 jaz3-4*	This study	N/A

Arabidopsis thaliana: JAZ1p:JAZ1.1-CIT + UBQ10p:Ijas9-TOM in *jazT*	This study	N/A
Arabidopsis thaliana: JAZ2p:JAZ2.1-CIT + UBQ10p:Ijas9-TOM in *aos*	This study	N/A
Arabidopsis thaliana: JAZ2p:JAZ2.1-CIT + UBQ10p:Ijas9-TOM in *jaz2-6*	This study	N/A
Arabidopsis thaliana: JAZ2p:JAZ2.1-CIT + UBQ10p:Ijas9-TOM in *jaz1-3 jaz2-6*	This study	N/A
Arabidopsis thaliana: JAZ2p:JAZ2.1-CIT + UBQ10p:Ijas9-TOM in *jaz2-6 jaz3-4*	This study	N/A
Arabidopsis thaliana: JAZ2p:JAZ2.1-CIT + UBQ10p:Ijas9-TOM in *jazT*	This study	N/A
Arabidopsis thaliana: JAZ3p:JAZ3.1-CIT + UBQ10p:Ijas9-TOM in *aos*	This study	N/A
Arabidopsis thaliana: JAZ3p:JAZ3.1-CIT + UBQ10p:Ijas9-TOM in *jaz3-4*	This study	N/A
Arabidopsis thaliana: JAZ3p:JAZ3.1-CIT + UBQ10p:Ijas9-TOM in *jaz1-3 jaz3-4*	This study	N/A
Arabidopsis thaliana: JAZ3p:JAZ3.1-CIT + UBQ10p:Ijas9-TOM in *jaz2-6 jaz3-4*	This study	N/A
Arabidopsis thaliana: JAZ3p:JAZ3.1-CIT + UBQ10p:Ijas9-TOM in *jazT*	This study	N/A
Arabidopsis thaliana: JAZ4p:JAZ4.1-CIT + UBQ10p:Ijas9-TOM in *aos*	This study	N/A
Arabidopsis thaliana: JAZ4p:JAZ4.1-CIT + UBQ10p:Ijas9-TOM in *jaz4-1*	This study	N/A
Arabidopsis thaliana: JAZ6p:JAZ6.1-CIT + UBQ10p:Ijas9-TOM in *aos*	This study	N/A

Arabidopsis thaliana: JAZ6p:JAZ6.1-CIT + UBQ10p:Ijas9-TOM in *jaz6-6*	This study	N/A
Arabidopsis thaliana: JAZ9p:JAZ9.1-CIT + UBQ10p:Ijas9-TOM in *aos*	This study	N/A
Arabidopsis thaliana: JAZ9p:JAZ9.1-CIT + UBQ10p:Ijas9-TOM in *jaz9-1*	This study	N/A
Arabidopsis thaliana: JAZ10p:JAZ10.1-CIT UBQ10p:Ijas9-TOM in *aos*	This study	N/A
Arabidopsis thaliana: JAZ10p:JAZ10.1-CIT + UBQ10p:Ijas9-TOM in *jaz10-1*	This study	N/A

N/A = Not available
NASC = Nottingham Arabidopsis Stock Centre
* = Stop codon

Table 3: Cloning and genotyping

TARGET GENE	PRIMER NAMEs	SEQUENCE	DESCRIPTION
Promoter cloning			
JAZ1 (AT1G19180)	JAZ1p.F JAZ1p.R	CGGGGTACCcatcgcggatctgtattcct TTCCCCCCCGGGctttaacaattaaaactttcaaac	promoter flanked by *XmaI* and *KpnI* (2162 bp)
JAZ2 (AT1G74950)	JAZ2p.F JAZ2p.R	CGGGGTACCggctgagatggatcattg TTCCCCCCCGGGcgttgaaaccgaaattgaaatc	promoter flanked by *XmaI* and *KpnI* (2179 bp)
JAZ3 (AT3G17860)	JAZ3p.F JAZ3pR	CGGGGTACCtcaagagcccacgaaagact TTCCCCCCCGGGctataataaagacacagcccgc	promoter flanked by *XmaI* and *KpnI* (2177 bp)
JAZ4 (AT1G48500)	JAZ4p.F JAZ4pR	CGGGGTACCcttttcaacactgctggaatttg TTCCCCCCCGGGcaagactgagtttgagagctttctt	promoter flanked by *XmaI* and *KpnI* (2209 bp)
JAZ5 (AT1G17380)	JAZ5p.F JAZ5p.R	CGGGGTACCcgtggtaacccgagactagc TTCCCCCCCGGGgttgttgtttattgagaagaaag	promoter flanked by *XmaI* and *KpnI* (2110 bp)
JAZ6 (AT1G72450)	JAZ6p.F JAZ6p.R	CGGGGTACCtgtcggtgtcaaagaaccaa TTCCCCCCCGGGactagtgtgatgaagattac	promoter flanked by

			XmaI and *KpnI* (2213 bp)
JAZ7 (AT2G34600)	JAZ7p.F JAZ7p.R	CGGGGTACCgatcaagagcccaaaactgc TTCCCCCCCGGGgattgtatgtgtcagtcagttg	promoter flanked by *XmaI* and *KpnI* (2069 bp)
JAZ8 (AT1G30135)	JAZ8p.1F JAZ8p.1R	CGGGGTACCgggattcgttggaaaattagc TTCCCCCCCGGGgttgtaagaataagaattgatg	promoter flanked by *XmaI* and *KpnI* (2137 bp)
JAZ9 (AT1G70700)	MST_015 MST_016	CGGGGTACCgcgtttcagtgttggtggta TTCCCCCCCGGGtgcaaaccaaatattcaatgac	promoter flanked by *XmaI* and *KpnI* (2184 bp)
JAZ11 (AT3G43440)	JAZ11p.F JAZ11p.R	CGGGGTACCggcagttccttcgttctctg TTCCCCCCCGGGgagcctctctgtgaataatatc	promoter flanked by *XmaI* and *KpnI* (2339 bp)
JAZ12 (AT5G20900)	JAZ12p.F JAZ12p.R	CGGGGTACCaacagtgtgatttccgttctg TTCCCCCCCGGGggcttgtctctcaaaatttgtag	promoter flanked by *XmaI* and *KpnI* (2047 bp)
JAZ13 (AT3G22275)	JAZ13p.F JAZ13p.R	CGGGGTACCcgtacacgaattcgaaggtg TTCCCCCCCGGGgatcctctctaggtaaatattc	promoter flanked by *XmaI* and *KpnI* (2022 bp)
CDS cloning			
JAZ1.1 (AT1G19180.1)	PDG027 PDG028	TGTACAAAAAAGCAGGCTGCatgtcgagttctatggaatg TTTGTACAAGAAAGCTGGGTTtatttcagctgctaaaccg	CDS* flanked by attB1 and attB2 (800 bp)
JAZ2.1 (AT1G74950.1)	ADS_001 ADS_002	TGTACAAAAAAGCAGGCTGCatgtcgagtttttctgccgag TTTGTACAAGAAAGCTGGGTTccgtgaactgagccaagctgg	CDS* flanked by attB1 and attB2 (788 bp)
JAZ3.1 (AT3G17860.1)	PDG029 PDG030	TGTACAAAAAAGCAGGCTGCatggagagagattttctcg TTTGTACAAGAAAGCTGGGTTggttgcagagctgagagaag	CDS* flanked by attB1 and attB2 (1097 bp)
JAZ4.1 (AT1G48500.1)	ADS_005 ADS_006	TGTACAAAAAAGCAGGCTGCatggagagagattttctcgg TTTGTACAAGAAAGCTGGGTTgtgcagatgatgagctggag	CDS* flanked by attB1 and attB2 (971 bp)
JAZ6.1 (AT1G72450.1)	ADS_009 ADS_010	TGTACAAAAAAGCAGGCTGCatgtcaacgggacaagcgccg TTTGTACAAGAAAGCTGGGTTaagcttgagttcaaggttttg	CDS* flanked by attB1 and attB2 (848 bp)
JAZ8.1 (AT1G30135.1)	ASC_004 ASC_005	TGTACAAAAAAGCAGGCTGCatgaagctacagcaaaattgtg TTTGTACAAGAAAGCTGGGTTtcgtcgtgaatggtacggtg	CDS* flanked by attB1 and attB2 (434 bp)

JAZ9.1 (AT1G70700.1)	ADS_013 ADS_014	TGTACAAAAAAGCAGGCTGCatggaaagagattttctggg TTTGTACAAGAAAGCTGGGTTtgtaggagaagtagaagag	CDS* flanked by attB1 and attB2 (842 bp)
JAZ10.1 (AT5G13220.1)	ASC_002 ASC_003	TGTACAAAAAAGCAGGCTGCatgtcgaaagctaccatag TTTGTACAAGAAAGCTGGGTTggccgatgtcggatagtaag g	CDS* flanked by attB1 and attB2 (632 bp)
JAZ11.1 (AT3G43440.1)	ASC_006 ASC_007	TGTACAAAAAAGCAGGCTGCatggctgaggtaaacggag TTTGTACAAGAAAGCTGGGTTtgtcacaatggggctggtttc	CDS* flanked by attB1 and attB2 (775 bp)
Genotyping			
aos	aos.F aos.R	gggagcgattgagaaaatgg cgacgagaaattaacggagc	amplifies 449 bp in WT and ca. 200 bp in *aos*
jaz1-1 (SALK_011957)	MST_041 MST_042	aggtaaatgcggagagagagg aggcaccgctaatagcttagc	genotyping T-DNA insertion
jaz1-2 (JIC-SM.22668)	MST_083 MST_084	accgagacacattcccgatt catcaggcttgcatgccatt	genotyping T-DNA insertion
jaz1-3 (CRISPR/Cas9*)*	MZ_150 MST_029	ccaaaccaaccaaccccaaa gcaaggggatttagacaggc	amplifies 1371 bp in WT and 485 bp in *jaz1-3*
jaz2-1 (SALK_122858)	MST_077 MST_078	aattctctcaaatgtgggcag tcgtaattcgcaacaggaaac	genotyping T-DNA insertion
jaz2-2 (SALK_025279)	MST_001 MST_002	agcctggtctgatctactccac tctacggtggtcgagttatgg	genotyping T-DNA insertion
jaz2-5 + *jaz2-6* (CRISPR/Cas9)	MZ_151 MST_070	ttcaacaactcaggaaggaaga catcttctttggtcccagagg	amplifies 693 bp in WT, 692 bp in *jaz2-5*, and 694 bp in *jaz2-6* (indel analysis by sequencing)
jaz3-1 (SALK_139337)	MST_003 MST_004	atgggctacaacacaaaatgg gtgcctctgtcgattcttcag	genotyping T-DNA insertion
jaz3-4 (GABI_097F09)	MST_086 MST_087	tcattatgcaccaggaggaag ctgagacattgaaaagaccgc	genotyping T-DNA insertion
jaz4-1 (SALK_141628)	MST_005 MST_006	taatgaccctgcaagaaaacg tttcttctgctgcaatggatc	genotyping T-DNA insertion

jaz5-1 (SALK_053775)	MST_024 MST_025	acgttccacgatctgattttg gtactcttccattttacgcgc	genotyping T-DNA insertion
jaz6-1 (SAIL_1156_C06)	MST_049 MST_050	tttggtactctttggcattgc ctgtggcttttaacctctccc	genotyping T-DNA insertion
jaz6-2 (SALK_017531)	MST_051 MST_052	tttgcaaatgccctcatttac tgctaataatcaacgaagcagg	genotyping T-DNA insertion
jaz6-3 (GABI_102A03)	MST_053 MST_054	tttgcaaatgccctcatttac ttagaacagaaattgcaaaccg	genotyping T-DNA insertion
jaz6-5 + *jaz6-6* (CRISPR/Cas9)	ASC_001 MST_064	aacgtgccggaacttgtaac acgtgaactcgatcgtgcat	amplifies 2384 bp in WT, 2385 bp in *jaz6-5* (indel analysis by sequencing), and 736 bp in *jaz6-6*
jaz7-1 (WiscDsLox7H11)	MST_020 MST_021	catcatcaaaaactgcgacaagcc ggtaacggtggtaaggggaagt	genotyping T-DNA insertion
jaz8-v	MST_075 MST_076	tgtcctaagagtccgccgttgt tttggaggatccgacccgtttg	amplicons of 588 bp, digested with *AflII* results in WT (588 bp) and *jaz8-v* (407 bp + 18 bp)
jaz9-1 (SALK_004872)	MST_055 MST_056	aaacctctctttgcgcttctc gttaagagctggtagggtcgg	genotyping T-DNA insertion
jaz9-4 (GABI_265H05)	MST_043 MST_044	tcatgctcattgcattagtcg agggttaagtacgaaggcagc	genotyping T-DNA insertion
jaz10-1 (SAIL_92_D08)	MST_022 MST_023	cttctcgagaaaacgttgcag tcacatgagaaatcagaatccg	genotyping T-DNA insertion
jaz11-2 + *jaz11-3* (CRISPR/Cas9)	MZ_153 MZ_154	cgttgcgtagagaagagaacc actgtgatactgagttgcttcg	amplifies 2231 bp in WT, 2232 bp in *jaz11-2*, and 2230 bp in *jaz11-3* (indel analysis by sequencing)

jaz12-1 (SALK_055032)	MST_057 MST_058	agttatggcacactcccattg agcatcagtcctgtctcatcg	genotyping T-DNA insertion
jaz12-2 (SALK_044058)	MST_059 MST_060	gagccaaaacccagatctttc aagaatccaattgttccagcc	genotyping T-DNA insertion
jaz13-1 (GABI_193G07	MST_013 MST_014	gtggatccagcgagttaaatg ttgaaacatgaagcacgtgac	genotyping T-DNA insertion
-	GABI.LB	atattgaccatcatactcattgc	all GK T-DNA insertion lines
-	JIC_ Ds3-1	acccgaccggatcgtatcggt	all JIC.SM T-DNA insertion lines
-	SAIL.LB3	tagcatctgaatttcataaccaatctcgatacac	all SAIL T-DNA insertion lines
-	SALK. LBb1.3	attttgccgatttcggaac	all SALK T-DNA insertion lines
-	WiscDsLox.LB	aacgtccgcaatgtgttattaagttgtc	all WiscDsLox T-DNA insertion lines
RT-PCR primer			
JAZ1 (AT1G19180)	MST_028 MST_068	atattctacgccgggcaagtg catatttcagctgctaaaccgag	fragment of 377 bp
JAZ2 (AT1G74950)	MST_030 MST_069	tgttgggacttctctggtcg tgatgtgatcctatccttcctct	fragment of 651 bp
JAZ3 (AT3G17860)	MST_032 MST116	ccttcaggccaactcaagaag tacgctcgtgacccttttctttg	fragment of 818 bp
JAZ4 (AT1G48500)	MST_035 MST_115	gccatagagaaggcagcagt cagctcactacaggaagacag	fragment of 522 bp
JAZ5 (AT1G17380)	MST_024 MST_071	acgttccacgatctgattttg accagggaaacaaaatgcga	fragment of 370 bp
JAZ6 (AT1G72450)	MST_063 MST_072	gtatgtcaacgggacaagcg cagccctgtcttttcgtttag	fragment of 612 bp
JAZ7 (AT2G34600)	ASC_092 ASC_093	catcaaaaactgcgacaagcc atcggtaacggtggtaaggg	fragment of 434 bp
JAZ8 (AT1G30135)	ASC_090 ASC_091	acttggaacttcgtctttttccc cgtcgtgaatggtacggtga	fragment of 370 bp
JAZ9 (AT1G70700)	MST_037 MST_114	ccgccataaaagattgtgagc gtcgaagaacgagggttaagta	fragment of 299 bp
JAZ10 (AT5G13220)	ASC_086 ASC_087	gagagacgcgtggaccg actcgatttcctcggacttga	fragment of 253 bp
JAZ11 (AT3G43440)	ASC_107 ASC_108	tgaggtaaacggagatttcc tttgtgcagggacaccattg	fragment of 185 bp
JAZ12 (AT5G20900)	ASC_100 ASC_101	aggtgaaagatgagccacgc gcagttggaaattcctccttga	fragment of 553 bp

JAZ13 (AT3G22275)	ASC_094 ASC_095	gggttgcagcttagatcttcac tgaagagaggaggatgatgagga	fragment of 363 bp
UBC21 (AT5G25760)	ASC_113 ASC_114	agagcgcgactgtttaaaga acttgaggaggttgcaaagg	fragment of 200 bp
Primer for qRT-PCR			
JAZ10 (AT5G13220)	JAZ10.qF JAZ10.qR	atcccgatttctccggtcca actttctccttgcgatgggaaga	fragment of 222 bp
UBC21 (AT5G25760)	UBQ.qF UBQ.qR	cagtctgtgtgtagagctatcatagcat agaagattccctgagtcgcagtt	fragment of 83 bp
sgRNAs for CRISPR/Cas9			
JAZ1 (AT1G19180)	SMI001 SMI002	ATTgttctgagttcgtcggtagc AAACgctaccgacgaactcagaac	for targeting first exon
JAZ1 (AT1G19180)	SMI003 SMI004	ATTgagccacgacatgttgcctg AAACcaggcaacatgtcgtggctc	for targeting last exon
JAZ2 (AT1G74950)	SMI005 SMI006	ATTgccgagtgttgggacttctc AAACgagaagtcccaacactcggc	for targeting first exon
JAZ2 (AT1G74950)	SMI007 SMI008	ATTgctgaaccgtctatttggta AAACtaccaaatagacggttcagc	for targeting last exon
JAZ5 (AT1G17380)	SMI009 SMI010	ATTGcggagaaatctgactttacc AAACggtaaagtcagatttctccg	for targeting first exon
JAZ5 (AT1G17380)	SMI011 SMI012	ATTGaccggtcaaccactagaggc AAACgcctctagtggttgaccggt	for targeting last exon
JAZ6 (AT1G72450)	SMI013 SMI014	ATTGagagatgtagtctgctcagc AAACgctgagcagactacatctct	for targeting first exon
JAZ6 (AT1G72450)	SMI015 SMI016	ATTggcccataaccatatgccga AAACtcggcatatggttatgggcc	for targeting last exon
JAZ11 (AT3G43440)	SMI017 SMI018	ATTGcgtcggcgaaactaggaacg AAACcgttcctagtttcgccgacg	for targeting first exon
JAZ11 (AT3G43440)	SMI019 SMI020	ATTgccttactctgctacgactt AAACaagtcgtagcagagtaaggc	for targeting last exon
JAZ12 (AT5G20900)	SMI021 SMI022	ATTGccacgcgcttccgttgaagg AAACccttcaacggaagcgcgtgg	for targeting first exon in
JAZ12 (AT5G20900)	SMI023 SMI024	ATTGaaaaagacagatgtcccaac AAACgttgggacatctgtcttttt	For targeting last exon

Plant material and growth conditions

The genetic background for all transgenic and mutant plant lines in this study was the *Arabidopsis thaliana* Columbia-0 (Col-0) accession. A comprehensive list of the genetic materials used can be found in Tab. 2. To perform assays on solid plant growth media, seeds were sterilized, plated on a 0.5x solid Murashige and Skoog (MS) media supplemented with 0.5 g/L 2-(N-Morpholino)ethanesulfonic acid (MES) hydrate, and subjected to a 2-day stratification period at 4 °C in the dark, following the protocol described by (Acosta et al., 2013). For horizontal growth, 0.7% plant agar was added to the media, while for vertical growth, 0.85% plant agar was used. For Kanamycin selection of transgenic lines transformed with CRISPR/Cas9 constructs, plants were grown on 0.5x solid MS + 50 µg/ml Kanamycin, following the protocol as described by (Pauwels et al., 2018). In the case of horizontally grown seedlings, a nylon mesh with a pore size of 200 µm (Lanz-Anliker AG, Rohrbach, Switzerland) was placed on top of the MS media as described by (Acosta et al., 2013). Seedlings intended for root tip RNA-seq were grown vertically on autoclaved Whatman® paper, positioned on top on 0.5x solid MS + 0.85% plant agar. This setup was chosen to enhance the precision of root tip excision during the cutting process. Controlled growth conditions were maintained at a temperature of 21°C under a light intensity of 100 µE m-2 s-1, with a 14-hour light and 10-hour dark photoperiod. For propagation, transformation, and crossing purposes, plants were grown in soil under the same conditions, but with continuous light.

Genotyping

Genomic DNA was extracted and purified using the DNeasy Plant Mini Kit (Qiagen) following the manufacturer's protocol. Genotyping of T-DNA insertion lines was conducted in 20 µL PCR reactions. The reaction mixture contained 20 ng of genomic DNA, 500 nM each of specific forward and reverse primers, 500 nM of the general T-DNA left border primer, 200 µM Deoxynucleotide Triphosphates, 1x PCR buffer (Invitrogen), and 0.1 U of Taq DNA polymerase (Invitrogen). The PCR amplification was performed on a Thermocycler (Eppendorf™ Mastercycler™ PRO) with an initial denaturation step at 95°C for 5 minutes, followed by 35 amplification cycles consisting of denaturation at 95°C for 30 seconds, annealing at 58°C for 30 seconds, and extension at 72°C for 60 seconds. For genotyping purposes of all other genotypes, the same PCR conditions were used, but without the general T-DNA primer. PCR products with single base pair indels were sent for sequencing analysis. Genotyping of the *jaz8-v* PCR products was performed by restriction enzyme cleavage. Specific restriction enzymes and primer used are listed in Tab. 2 and Tab. 3, respectively. PCR products larger than 300 bp were separated by electrophoresis on 0.9% agarose gels,

while products smaller than 300 bp were separated on 2% agarose gels in 0.5x Tris-Borate-EDTA (TBE) buffer.

Histochemical detection of GUS activity

GUS staining was conducted as described in (Gasperini et al., 2015). After staining, seedlings were mounted in a solution of chloral hydrate, glycerol, and water (8:2:1). Images were captured using a Leica M165 FC stereomicroscope equipped with a Leica MC170 HD camera.

Plant treatments

Seedling cotyledon wounds and MeJA treatments were conducted as described (Acosta et al., 2013). To assess the localization of fluorophore-fusion proteins of transcriptional and translational reporter plants, primary roots of 5-do vertically grown seedlings were mounted in 0.5x MS solution with 30 µg/ml propidium iodide (PI), and immediately imaged on a Zeiss confocal laser scanning microscope LSM780 (n=10). JAZ-CIT and Ijas9-TOM localization analysis of *rat.JAZp:JAZ-CIT* plants were taken under similar conditions, but without PI staining. To determine nuclei specific JAZ-CIT/Ijas9-TOM turnover rates of *rat.JAZp:JAZ-CIT* plants, seedlings were mounted as above in either mock, 0.01, 0.1, or 1 µM COR 0.5x MS (without PI staining) and observed using a Zeiss confocal laser scanning microscope LSM900 (n=10, 5-7 nuclei per biological replicate).

Root growth

Primary root length was assessed in 7-do seedlings as described (Acosta et al., 2013). The seedlings were grown as previously mentioned ("plant material and growth conditions") for a period of 7 days and subsequently scanned. The measurement of root length was conducted using the image processing software Fiji.

Gene expression analysis

RNA extraction and qRT-PCR procedures were performed as described (Gasperini et al., 2015; Schulze et al., 2019). The transcripts were amplified using primers listed in Tab. 3, and primer efficiency was optimized for each pair to achieve a range of 1.9-2.1. For RNAseq analysis, aseptic conditions were maintained for the growth of WT, *jaz2-6*, *jaz2-6 jaz3-4*, and *jazT*, as previously described ("Plant material

and growth conditions"). Total RNA was extracted from 5-do root tips using a RNeasy Plant Mini Kit (Qiagen). Each genotype and experimental collection day included three biological replicates, with each replicate consisting of 180 roots. A total of 3 µg of RNA was precipitated with 0.1 volumes of Sodium acetat (NaOAc) and 2 volumes of EtOH (50 µL sample + 5 µL NaOAc + 110 µL EtOH). RNA quality was verified using an Agilent 2100 Bioanalyzer (Agilent) and samples were sent to GENEWIZ/Azenta (www.genewiz.com) for Illumina RNA sequencing of strand-specific mRNA libraries, and 150 bp paired-end (PE) reads. The RNAseq bioinformatics analysis was performed in R by René Dreos (University of Lausanne, Switzerland). The reads were quality-filtered using PrinSeq (v. 0.20.4) and mapped to the *A. thaliana* genome (TAIR10, www.arabidopsis.org) using Tophat (v. 2.1.1) (Schmieder & Edwards, 2011; Trapnell et al., 2009). Gene locus quantification was performed using htseq-count (v. 0.12.4) (Anders et al., 2015). Differential gene expression analysis was done using the DESeq2 package (Love et al., 2014). GO analysis was performed using GO term enrichment from TAIR (www.arabidopsis.org).

Development of novel *jaz* alleles with CRISPR/Cas9

A CRISPR/Cas9 double guide approach (Pauwels et al., 2018) was used to generate loss-of-function *jaz1-3*, *jaz2-5*, *jaz2-6*, *jaz6-5*, *jaz6-6*, *jaz11-2*, and *jaz11-3* alleles. Briefly, sgRNA1 and sgRNA2 were designed using the online tool (www.crispor.tefor.net/) to target the first (sgRNA1) and last (sgRNA2) exon of each target gene, and thus excise almost a complete *JAZ* genomic sequence. Each sgRNA consisted of overlapping oligos listed in Tab. 3, that were annealed and cloned by restriction into *pMR217_pDONR_P1P* and *pMR218_pDONR_P5P* vectors as described (Pauwels et al., 2018). Resulting in pEN-L1-*sgRNA1*-L5 and pEN-L1-*sgRNA2*-L5 were then recombined into *pMR278_pDE_Cas9_Kan* by Multisite Gateway (Thermo Fisher) (Pauwels et al., 2018). Plasmids were generated *in silico* and evaluated by Sanger sequencing with the SeqBuilder and SeqManUltra (DNASTAR Lasergene). Verified plasmids were transformed in Col-0 plants via *Agrobacterium tumefaciens* transformation (strain GV3101) of floral buds (Clough & Bent, 1998). For each construct, approximately 1500 to 2000 T_1 seeds were sown on 0.5x soild MS + 50 µg/ml Kanamycin media to identify transformed plants. Selected T_1 seedlings were transferred to soil and genotyped with primers external to the sgRNA1 and sgRNA2 targets to identify large deletions (genotyping primers are listed in Tab. 3). Transgenic T_1 plants with no obvious deletion were sequenced around the target sgRNA1 region to identify potential smaller indels or frameshifts. Resulting T_2 and/or T_3 plants were then genotyped to confirm the presence of the homozygous *jaz* mutations and selected against the Cas9 transgene cassette.

Generation of transgenic reporter lines

All transcriptional and translation reporter constructs were generated using double or triple Multisite Gateway Technology (Thermo Fisher). The ENTRY plasmids (pEN) containing the *JAZ10* promoter (pEN-L4-*JAZ10p*-R1) and pEN-L1-*NLS-3xVEN*-L2, pEN-L1-*GUS*-L2, and pEN-R2-*CIT*-L3 were as described in previous studies (Acosta et al., 2013; Gasperini et al., 2015; Mielke et al., 2021). The remaining *JAZ* promoters (2kb upstream of the ATG) were amplified from WT genomic DNA using Phusion High-Fidelity DNA Polymerase (Thermo Fisher) and oligonucleotides containing appropriate restriction sites for cloning the promoter amplicons into pUC57, resulting in the creation of pEN-L4-*JAZp*-R1 clones, following the protocol as described in (Gasperini et al., 2015). Primers are listed in Tab. 3. For transcriptional reporters, the pEN-L4-*JAZp*-R1 plasmids were recombined with pEN-L1-*NLS-3xVEN**-L2 (* = stop codon) or pEN-L1-*GUS**-L2 into *pEDO097*, as described in (Gasperini et al., 2015).

For non-ratiometric translational reporters, *JAZs* inserts lacking stop codons were amplified from wounded WT cDNA using oligonucleotides listed in Tab. 3 containing appropriate *att* sites and recombined into *pDONR221* to obtain pEN-L1-*JAZ*-L2. Finally, pEN-L4-*JAZp*-R1, pEN-L1-*JAZ*-L2, and pEN-R2-*CIT**-L3 were recombined into *pFR7m34gw* to generate *JAZp:JAZ-CIT** constructs, as described (Mielke et al., 2021).

For ratiometric translational reporters, pEN plasmids with L1-*JAZ-CIT**-L2 and R2-*UBQ10p:Ijas9-TOM**-L3 inserts were generated via Gene Synthesis at Eurofins Genomics (sequences available in appendix data "FASTA sequences for gene synthesis") and recombined with pEN-L4-*JAZp*-R1 and *pFR7m34gw* to obtain ratiometric *JAZp:JAZ-CIT*/UBQ10p:Ijas9-TOM** (*rat. JAZp:JAZ-CIT*) constructs. The degron sequence of JAZ9 (Jas9) was modified to result in R223A, K224A, and F30A substitutions (Fig. 16B), resulting in JA-Ile insensitivity (IJas9). The linker sequences connecting *JAZ* and *CIT*, as well as *Ijas9* and *TOM*, were adopted from (Liao et al., 2015).

Transcriptional reporters were transformed into Col-0, and translational reporters were transformed into *aos* or respective *jaz* mutants as described above. Transgenic plants were selected by identifying seeds expressing RED FLUORESCENT PROTEIN (RFP) in T_1, T_2, and T_3 generations, and by selecting T_2 families with Mendelian segregation. For each construct, a minimum of two independent T_2 or T_3 transgenic lines were used to ensure experimental reproducibility and perform experiments.

Confocal laser scanning microscopy

The localization of NLS-3xVEN, JAZ-CIT, and Ijas9-TOM proteins in living 5-do Arabidospsis roots was performed on a Zeiss LSM780 instrument, whereas ratiometric JAZ-CIT/Ijas9-TOM turnover measurements were performed on a Zeiss LSM900 instrument. Detection settings were as follows:

	LSM780	LSM900
Fluorophore	**Detection λ (nm)**	**Detection λ (nm)**
VEN	517-544	-
CIT	517-544	508-574
PI	588-718	-
TOM	588-718	574-700

Table 4: Fluorophores and their corresponding detection ranges. This table provides an overview of the fluorophores utilized in this study, along with their respective detection ranges λ (nm), integrated with the specific LSM employed.

To avoid cross-excitation, fluorescent signals were excited and detected separately throughout experiments. All images within each experiment were captured with identical settings and analysed on a minimum of 10 individual plants from at least 2 independent transgenic lines. Image processing was performed in Fiji, with Z-Stacks presented as texture-based volume renderings using the 3D viewer plugin.

***In planta* turnover measurements**

Individual seedlings were carefully transferred from vertically grown media plates to microscopy slides containing mock or coronatine (COR)- containing solutions (0.01 µM, 0.1 µM, 1 µM COR; see "Plant treatments") and imaged immediately (t=0). This mounting procedure enabled the submergence of roots only, while green tissues remained free and not in contact with a coverslip. Images were captured every min for a total duration of 15min. The early elongation zone was chosen as the imaging area as most of the JAZ1-CIT and JAZ3-CIT nuclei were clearly visible, and the focus was adjusted based on the stable Ijas9-TOM signal during the time course. Arbitrary Fluorescence Intensities (AFUs) for CIT and TOM were extracted from a total of 5-7 nuclei per root on a minimum of 10 roots with Fiji. To minimize the influence of background signals, average thresholds levels were subtracted from each channel by imaging untransformed Col-0 roots with the same JAZ-CIT and Ijas9-TOM settings (n=10). Normalized turnover rates were computed by calculating the ratio of JAZ-CIT AFU values relative to those of Ijas9-TOM at each time point.

Regression, half-life, and turnover rate analysis

Linear and exponential regression analyses for JAZ-CIT/Ijas9-TOM turnover data curves were performed with GraphPad PRISM10. After establishing that the empirical curves best fitted a "plateau followed by one phase decay" model, JAZ-CIT half-lives were calculated by solving for X (time on the X axis) the following equation Y=Plateau+(Y0−Plateau)*e^(−K*(X−X0)), where Y = normalized JAZ-CIT/Ijas9-TOM AFU, X0 = time following the initial plateau at which the decay starts, Y0 = average Y value up to time X0 (expressed in the same units as Y), Plateau = Y value at infinite times (expressed in the same units as Y), K is the rate constant (expressed in the reciprocal of the time units on the X axis). Next, the equation was rearranged with respect to "X" to determine the time:

$$X=X0+(-1/K)\cdot \ln(Y0-Plateau/Y-Plateau)$$

Using this equation, the average half-lives was calculated by identifying the time at which the initial normalized JAZ-CIT/Ijas9-TOM AFU at time point 0 was reduced by half (Hallare & Gerriets, 2023), based on 10 biological replicates (5-7 nuclei as technical replicates).

The relative JAZ-CIT turnover rates were calculated as the average JAZ-CIT/Ijas9-TOM AFU decrease per min within the decay phase, based on measuring 5-7 nuclei from at least 10 roots. The decay phase was defined as the timeframe extending from the end of the initial plateau to the start of the ending plateau.

Other statistical analyses

Box plot and multiple comparison analyses of variance (one-way and two-way ANOVA) followed by Tukey's honest significant difference (HSD) were performed in R (One-Way ANOVA: www.astatsa.com/OneWay_Anova_with_TukeyHSD/; www.statskingdom.com/180Anova1way.html; Two-Way ANOVA: www.wessa.net/rwasp_Two Factor ANOVA.wasp). Scatter plot graphs were generated using Microsoft Excel.

References

Abe, H., Yamaguchi-Shinozaki, K., Urao, T., Iwasaki, T., Hosokawa, D., & Shinozaki, K. (1997). Role of arabidopsis MYC and MYB homologs in drought- and abscisic acid-regulated gene expression. *Plant Cell*, *9*(10), 1859-1868. https://doi.org/10.1105/tpc.9.10.1859

Abel, S., Nguyen, M. D., & Theologis, A. (1995). The PS-IAA4/5-like family of early auxin-inducible mRNAs in Arabidopsis thaliana. *J Mol Biol*, *251*(4), 533-549. https://doi.org/10.1006/jmbi.1995.0454

Abel, S., Oeller, P. W., & Theologis, A. (1994). Early auxin-induced genes encode short-lived nuclear proteins. *Proc Natl Acad Sci U S A*, *91*(1), 326-330. https://doi.org/10.1073/pnas.91.1.326

Acosta, I. F., Gasperini, D., Chetelat, A., Stolz, S., Santuari, L., & Farmer, E. E. (2013). Role of NINJA in root jasmonate signaling. *Proc Natl Acad Sci U S A*, *110*(38), 15473-15478. https://doi.org/10.1073/pnas.1307910110

Agusti, J., & Blazquez, M. A. (2020). Plant vascular development: mechanisms and environmental regulation. *Cell Mol Life Sci*, *77*(19), 3711-3728. https://doi.org/10.1007/s00018-020-03496-w

Amoutzias, G. D., Robertson, D. L., Van de Peer, Y., & Oliver, S. G. (2008). Choose your partners: dimerization in eukaryotic transcription factors. *Trends Biochem Sci*, *33*(5), 220-229. https://doi.org/10.1016/j.tibs.2008.02.002

An, C., Li, L., Zhai, Q., You, Y., Deng, L., Wu, F., Chen, R., Jiang, H., Wang, H., Chen, Q., & Li, C. (2017). Mediator subunit MED25 links the jasmonate receptor to transcriptionally active chromatin. *Proc Natl Acad Sci U S A*, *114*(42), E8930-E8939. https://doi.org/10.1073/pnas.1710885114

Anders, S., Pyl, P. T., & Huber, W. (2015). HTSeq--a Python framework to work with high-throughput sequencing data. *Bioinformatics*, *31*(2), 166-169. https://doi.org/10.1093/bioinformatics/btu638

Aziz, U., Rehmani, M. S., Wang, L., Xian, B., Luo, X., & Shu, K. (2022). Repressors: the gatekeepers of phytohormone signaling cascades. *Plant Cell Rep*, *41*(6), 1333-1341. https://doi.org/10.1007/s00299-022-02853-2

Bai, C., Sen, P., Hofmann, K., Ma, L., Goebl, M., Harper, J. W., & Elledge, S. J. (1996). SKP1 connects cell cycle regulators to the ubiquitin proteolysis machinery through a novel motif, the F-box. *Cell*, *86*(2), 263-274. https://doi.org/10.1016/s0092-8674(00)80098-7

Bai, Y., Meng, Y., Huang, D., Qi, Y., & Chen, M. (2011). Origin and evolutionary analysis of the plant-specific TIFY transcription factor family. *Genomics*, *98*(2), 128-136. https://doi.org/10.1016/j.ygeno.2011.05.002

Bannenberg, G., Martinez, M., Hamberg, M., & Castresana, C. (2009). Diversity of the enzymatic activity in the lipoxygenase gene family of Arabidopsis thaliana. *Lipids*, *44*(2), 85-95. https://doi.org/10.1007/s11745-008-3245-7

Barto, E. K., & Cipollini, D. (2005). Testing the optimal defense theory and the growth-differentiation balance hypothesis in Arabidopsis thaliana. *Oecologia*, *146*(2), 169-178. https://doi.org/10.1007/s00442-005-0207-0

Bashirullah, A., Cooperstock, R. L., & Lipshitz, H. D. (2001). Spatial and temporal control of RNA stability. *Proc Natl Acad Sci U S A*, *98*(13), 7025-7028. https://doi.org/10.1073/pnas.111145698

Bennett, T., Liang, Y., Seale, M., Ward, S., Muller, D., & Leyser, O. (2016). Strigolactone regulates shoot development through a core signalling pathway. *Biol Open*, *5*(12), 1806-1820. https://doi.org/10.1242/bio.021402

Blazquez, M. A., Nelson, D. C., & Weijers, D. (2020). Evolution of Plant Hormone Response Pathways. *Annu Rev Plant Biol*, *71*, 327-353. https://doi.org/10.1146/annurev-arplant-050718-100309

Bodenhausen, N., & Reymond, P. (2007). Signaling pathways controlling induced resistance to insect herbivores in Arabidopsis. *Mol Plant Microbe Interact*, *20*(11), 1406-1420. https://doi.org/10.1094/MPMI-20-11-1406

Bohlmann, H., & Wieczorek, K. (2015). Infection Assay of Cyst Nematodes on Arabidopsis Roots. *Bio Protoc*, *5*(18). https://doi.org/10.21769/BioProtoc.1596

Boter, M., Ruiz-Rivero, O., Abdeen, A., & Prat, S. (2004). Conserved MYC transcription factors play a key role in jasmonate signaling both in tomato and Arabidopsis. *Genes Dev*, *18*(13), 1577-1591. https://doi.org/10.1101/gad.297704

Breithaupt, C., Kurzbauer, R., Lilie, H., Schaller, A., Strassner, J., Huber, R., Macheroux, P., & Clausen, T. (2006). Crystal structure of 12-oxophytodienoate reductase 3 from tomato: self-inhibition by dimerization. *Proc Natl Acad Sci U S A*, *103*(39), 14337-14342. https://doi.org/10.1073/pnas.0606603103

Browse, J., & Wallis, J. G. (2019). Arabidopsis Flowers Unlocked the Mechanism of Jasmonate Signaling. *Plants (Basel)*, *8*(8). https://doi.org/10.3390/plants8080285

Caarls, L., Elberse, J., Awwanah, M., Ludwig, N. R., de Vries, M., Zeilmaker, T., Van Wees, S. C. M., Schuurink, R. C., & Van den Ackerveken, G. (2017). Arabidopsis JASMONATE-INDUCED OXYGENASES down-regulate plant immunity by hydroxylation and inactivation of the hormone jasmonic acid. *Proc Natl Acad Sci U S A*, *114*(24), 6388-6393. https://doi.org/10.1073/pnas.1701101114

Campos, M. L., Kang, J. H., & Howe, G. A. (2014). Jasmonate-triggered plant immunity. *J Chem Ecol*, *40*(7), 657-675. https://doi.org/10.1007/s10886-014-0468-3

Campos, M. L., Yoshida, Y., Major, I. T., de Oliveira Ferreira, D., Weraduwage, S. M., Froehlich, J. E., Johnson, B. F., Kramer, D. M., Jander, G., Sharkey, T. D., & Howe, G. A. (2016). Rewiring of jasmonate and phytochrome B signalling uncouples plant growth-defense tradeoffs. *Nat Commun*, *7*, 12570. https://doi.org/10.1038/ncomms12570

Cance, C., Martin-Arevalillo, R., Boubekeur, K., & Dumas, R. (2022). Auxin response factors are keys to the many auxin doors. *New Phytol*, *235*(2), 402-419. https://doi.org/10.1111/nph.18159

Cao, J., Schneeberger, K., Ossowski, S., Gunther, T., Bender, S., Fitz, J., Koenig, D., Lanz, C., Stegle, O., Lippert, C., Wang, X., Ott, F., Muller, J., Alonso-Blanco, C., Borgwardt, K., Schmid, K. J., & Weigel, D. (2011). Whole-genome sequencing of multiple Arabidopsis thaliana populations. *Nat Genet*, *43*(10), 956-963. https://doi.org/10.1038/ng.911

Carretero-Paulet, L., Galstyan, A., Roig-Villanova, I., Martinez-Garcia, J. F., Bilbao-Castro, J. R., & Robertson, D. L. (2010). Genome-wide classification and evolutionary analysis of the bHLH family of transcription factors in Arabidopsis, poplar, rice, moss, and algae. *Plant Physiol*, *153*(3), 1398-1412. https://doi.org/10.1104/pp.110.153593

Casamitjana-Martinez, E., Hofhuis, H. F., Xu, J., Liu, C. M., Heidstra, R., & Scheres, B. (2003). Root-specific CLE19 overexpression and the sol1/2 suppressors implicate a CLV-like pathway in the control of Arabidopsis root meristem maintenance. *Curr Biol*, *13*(16), 1435-1441. https://doi.org/10.1016/s0960-9822(03)00533-5

Causier, B., Ashworth, M., Guo, W., & Davies, B. (2012). The TOPLESS interactome: a framework for gene repression in Arabidopsis. *Plant Physiol*, *158*(1), 423-438. https://doi.org/10.1104/pp.111.186999

Cevik, V., Kidd, B. N., Zhang, P., Hill, C., Kiddle, S., Denby, K. J., Holub, E. B., Cahill, D. M., Manners, J. M., Schenk, P. M., Beynon, J., & Kazan, K. (2012). MEDIATOR25 acts as an integrative hub for the regulation of jasmonate-responsive gene expression in Arabidopsis. *Plant Physiol*, *160*(1), 541-555. https://doi.org/10.1104/pp.112.202697

Chao, J., Yang, S., Chen, Y., & Tian, W. M. (2016). Evaluation of Reference Genes for Quantitative Real-Time PCR Analysis of the Gene Expression in Laticifers on the Basis of Latex Flow in Rubber Tree (Hevea brasiliensis Muell. Arg.). *Front Plant Sci*, *7*, 1149. https://doi.org/10.3389/fpls.2016.01149

Chao, J., Zhao, Y., Jin, J., Wu, S., Deng, X., Chen, Y., & Tian, W. M. (2019). Genome-Wide Identification and Characterization of the JAZ Gene Family in Rubber Tree (Hevea brasiliensis). *Front Genet*, *10*, 372. https://doi.org/10.3389/fgene.2019.00372

Chen, Q., Sun, J., Zhai, Q., Zhou, W., Qi, L., Xu, L., Wang, B., Chen, R., Jiang, H., Qi, J., Li, X., Palme, K., & Li, C. (2011). The basic helix-loop-helix transcription factor MYC2 directly represses PLETHORA expression during jasmonate-mediated modulation of the root stem cell niche in Arabidopsis. *Plant Cell*, *23*(9), 3335-3352. https://doi.org/10.1105/tpc.111.089870

Chen, R., Jiang, H., Li, L., Zhai, Q., Qi, L., Zhou, W., Liu, X., Li, H., Zheng, W., Sun, J., & Li, C. (2012). The Arabidopsis mediator subunit MED25 differentially regulates jasmonate and abscisic acid signaling through interacting with the MYC2 and ABI5 transcription factors. *Plant Cell*, *24*(7), 2898-2916. https://doi.org/10.1105/tpc.112.098277

Cheng, H., Song, S., Xiao, L., Soo, H. M., Cheng, Z., Xie, D., & Peng, J. (2009). Gibberellin acts through jasmonate to control the expression of MYB21, MYB24, and MYB57 to promote stamen filament growth in Arabidopsis. *PLoS Genet*, *5*(3), e1000440. https://doi.org/10.1371/journal.pgen.1000440

Cheng, Z., Sun, L., Qi, T., Zhang, B., Peng, W., Liu, Y., & Xie, D. (2011). The bHLH transcription factor MYC3 interacts with the Jasmonate ZIM-domain proteins to mediate jasmonate response in Arabidopsis. *Mol Plant*, *4*(2), 279-288. https://doi.org/10.1093/mp/ssq073

Chico, J. M., Fernandez-Barbero, G., Chini, A., Fernandez-Calvo, P., Diez-Diaz, M., & Solano, R. (2014). Repression of Jasmonate-Dependent Defenses by Shade Involves Differential Regulation of Protein Stability of MYC Transcription Factors and Their JAZ Repressors in Arabidopsis. *Plant Cell*, *26*(5), 1967-1980. https://doi.org/10.1105/tpc.114.125047

Chini, A., Ben-Romdhane, W., Hassairi, A., & Aboul-Soud, M. A. M. (2017). Identification of TIFY/JAZ family genes in Solanum lycopersicum and their regulation in response to abiotic stresses. *PLoS One*, *12*(6), e0177381. https://doi.org/10.1371/journal.pone.0177381

Chini, A., Fonseca, S., Chico, J. M., Fernandez-Calvo, P., & Solano, R. (2009). The ZIM domain mediates homo- and heteromeric interactions between Arabidopsis JAZ proteins. *Plant J*, *59*(1), 77-87. https://doi.org/10.1111/j.1365-313X.2009.03852.x

Chini, A., Fonseca, S., Fernandez, G., Adie, B., Chico, J. M., Lorenzo, O., Garcia-Casado, G., Lopez-Vidriero, I., Lozano, F. M., Ponce, M. R., Micol, J. L., & Solano, R. (2007). The JAZ family of repressors is the missing link in jasmonate signalling. *Nature*, *448*(7154), 666-671. https://doi.org/10.1038/nature06006

Chini, A., Gimenez-Ibanez, S., Goossens, A., & Solano, R. (2016). Redundancy and specificity in jasmonate signalling. *Curr Opin Plant Biol*, *33*, 147-156. https://doi.org/10.1016/j.pbi.2016.07.005

Chung, H. S., Cooke, T. F., Depew, C. L., Patel, L. C., Ogawa, N., Kobayashi, Y., & Howe, G. A. (2010). Alternative splicing expands the repertoire of dominant JAZ repressors of jasmonate signaling. *Plant J*, *63*(4), 613-622. https://doi.org/10.1111/j.1365-313X.2010.04265.x

Chung, H. S., & Howe, G. A. (2009). A critical role for the TIFY motif in repression of jasmonate signaling by a stabilized splice variant of the JASMONATE ZIM-domain protein JAZ10 in Arabidopsis. *Plant Cell*, *21*(1), 131-145. https://doi.org/10.1105/tpc.108.064097

Chung, H. S., Koo, A. J., Gao, X., Jayanty, S., Thines, B., Jones, A. D., & Howe, G. A. (2008). Regulation and function of Arabidopsis JASMONATE ZIM-domain genes in response to wounding and herbivory. *Plant Physiol*, *146*(3), 952-964. https://doi.org/10.1104/pp.107.115691

Clough, S. J., & Bent, A. F. (1998). Floral dip: a simplified method for Agrobacterium-mediated transformation of Arabidopsis thaliana. *Plant J*, *16*(6), 735-743. https://doi.org/10.1046/j.1365-313x.1998.00343.x

Colon-Carmona, A., You, R., Haimovitch-Gal, T., & Doerner, P. (1999). Technical advance: spatio-temporal analysis of mitotic activity with a labile cyclin-GUS fusion protein. *Plant J*, *20*(4), 503-508. https://doi.org/10.1046/j.1365-313x.1999.00620.x

Cong, L., Ran, F. A., Cox, D., Lin, S., Barretto, R., Habib, N., Hsu, P. D., Wu, X., Jiang, W., Marraffini, L. A., & Zhang, F. (2013). Multiplex genome engineering using CRISPR/Cas systems. *Science*, *339*(6121), 819-823. https://doi.org/10.1126/science.1231143

Couvreur, V., Faget, M., Lobet, G., Javaux, M., Chaumont, F., & Draye, X. (2018). Going with the Flow: Multiscale Insights into the Composite Nature of Water Transport in Roots. *Plant Physiol*, *178*(4), 1689-1703. https://doi.org/10.1104/pp.18.01006

Cui, M., Du, J., & Yao, X. (2018). The Binding Mechanism Between Inositol Phosphate (InsP) and the Jasmonate Receptor Complex: A Computational Study. *Front Plant Sci*, *9*, 963. https://doi.org/10.3389/fpls.2018.00963

Davuluri, R. V., Sun, H., Palaniswamy, S. K., Matthews, N., Molina, C., Kurtz, M., & Grotewold, E. (2003). AGRIS: Arabidopsis gene regulatory information server, an information resource of Arabidopsis cis-regulatory elements and transcription factors. *BMC Bioinformatics*, *4*, 25. https://doi.org/10.1186/1471-2105-4-25

Day, R. N., & Davidson, M. W. (2009). The fluorescent protein palette: tools for cellular imaging. *Chem Soc Rev*, *38*(10), 2887-2921. https://doi.org/10.1039/b901966a

de Lucas, M., Daviere, J. M., Rodriguez-Falcon, M., Pontin, M., Iglesias-Pedraz, J. M., Lorrain, S., Fankhauser, C., Blazquez, M. A., Titarenko, E., & Prat, S. (2008). A molecular framework for light and gibberellin control of cell elongation. *Nature*, *451*(7177), 480-484. https://doi.org/10.1038/nature06520

De Smet, I. (2012). Lateral root initiation: one step at a time. *New Phytol*, *193*(4), 867-873. https://doi.org/10.1111/j.1469-8137.2011.03996.x

de Torres Zabala, M., Zhai, B., Jayaraman, S., Eleftheriadou, G., Winsbury, R., Yang, R., Truman, W., Tang, S., Smirnoff, N., & Grant, M. (2016). Novel JAZ co-operativity and unexpected JA dynamics underpin Arabidopsis defence responses to Pseudomonas syringae infection. *New Phytol*, *209*(3), 1120-1134. https://doi.org/10.1111/nph.13683

Delker, C., Zolman, B. K., Miersch, O., & Wasternack, C. (2007). Jasmonate biosynthesis in Arabidopsis thaliana requires peroxisomal beta-oxidation enzymes--additional proof by properties of pex6 and aim1. *Phytochemistry*, *68*(12), 1642-1650. https://doi.org/10.1016/j.phytochem.2007.04.024

Dello Ioio, R., Linhares, F. S., Scacchi, E., Casamitjana-Martinez, E., Heidstra, R., Costantino, P., & Sabatini, S. (2007). Cytokinins determine Arabidopsis root-meristem size by controlling cell differentiation. *Curr Biol*, *17*(8), 678-682. https://doi.org/10.1016/j.cub.2007.02.047

Demianski, A. J., Chung, K. M., & Kunkel, B. N. (2012). Analysis of Arabidopsis JAZ gene expression during Pseudomonas syringae pathogenesis. *Mol Plant Pathol*, *13*(1), 46-57. https://doi.org/10.1111/j.1364-3703.2011.00727.x

DeMott, L., Oblessuc, P. R., Pierce, A., Student, J., & Melotto, M. (2021). Spatiotemporal regulation of JAZ4 expression and splicing contribute to ethylene- and auxin-mediated responses in Arabidopsis roots. *Plant J*, *108*(5), 1266-1282. https://doi.org/10.1111/tpj.15508

Dempsey, D. A., Vlot, A. C., Wildermuth, M. C., & Klessig, D. F. (2011). Salicylic Acid biosynthesis and metabolism. *Arabidopsis Book*, *9*, e0156. https://doi.org/10.1199/tab.0156

Dennis, E. A., & Norris, P. C. (2015). Eicosanoid storm in infection and inflammation. *Nat Rev Immunol*, *15*(8), 511-523. https://doi.org/10.1038/nri3859

Devoto, A., Nieto-Rostro, M., Xie, D., Ellis, C., Harmston, R., Patrick, E., Davis, J., Sherratt, L., Coleman, M., & Turner, J. G. (2002). COI1 links jasmonate signalling and fertility to the SCF ubiquitin-ligase

complex in Arabidopsis. *Plant J*, *32*(4), 457-466. https://doi.org/10.1046/j.1365-313x.2002.01432.x

Dharmasiri, S. J., T.; Dharmasiri, N.;. (2013). Plant Hormone Signalling: Current Perspectives on Perception and Mechanisms of Action. *Ceylon Journal of Science (Biological Sciences)*, *42*.

Dietrich, D. (2018). Hydrotropism: how roots search for water. *J Exp Bot*, *69*(11), 2759-2771. https://doi.org/10.1093/jxb/ery034

Dobritzsch, S., Weyhe, M., Schubert, R., Dindas, J., Hause, G., Kopka, J., & Hause, B. (2015). Dissection of jasmonate functions in tomato stamen development by transcriptome and metabolome analyses. *BMC Biol*, *13*, 28. https://doi.org/10.1186/s12915-015-0135-3

Doench, J. G., Hartenian, E., Graham, D. B., Tothova, Z., Hegde, M., Smith, I., Sullender, M., Ebert, B. L., Xavier, R. J., & Root, D. E. (2014). Rational design of highly active sgRNAs for CRISPR-Cas9-mediated gene inactivation. *Nat Biotechnol*, *32*(12), 1262-1267. https://doi.org/10.1038/nbt.3026

Dolan, L., Duckett, C. M., Grierson, C., Linstead, P., Schneider, K., Lawson, E., Dean, C., Poethig, S., & Roberts, K. (1994). Clonal Relationships and Cell Patterning in the Root Epidermis of Arabidopsis. *Development*, *120*(9), 2465-2474. <Go to ISI>://WOS:A1994PF17600010

Ellinger, D., Stingl, N., Kubigsteltig, II, Bals, T., Juenger, M., Pollmann, S., Berger, S., Schuenemann, D., & Mueller, M. J. (2010). DONGLE and DEFECTIVE IN ANTHER DEHISCENCE1 lipases are not essential for wound- and pathogen-induced jasmonate biosynthesis: redundant lipases contribute to jasmonate formation. *Plant Physiol*, *153*(1), 114-127. https://doi.org/10.1104/pp.110.155093

Fernandez-Calvo, P., Chini, A., Fernandez-Barbero, G., Chico, J. M., Gimenez-Ibanez, S., Geerinck, J., Eeckhout, D., Schweizer, F., Godoy, M., Franco-Zorrilla, J. M., Pauwels, L., Witters, E., Puga, M. I., Paz-Ares, J., Goossens, A., Reymond, P., De Jaeger, G., & Solano, R. (2011). The Arabidopsis bHLH transcription factors MYC3 and MYC4 are targets of JAZ repressors and act additively with MYC2 in the activation of jasmonate responses. *Plant Cell*, *23*(2), 701-715. https://doi.org/10.1105/tpc.110.080788

Feys, B., Benedetti, C. E., Penfold, C. N., & Turner, J. G. (1994). Arabidopsis Mutants Selected for Resistance to the Phytotoxin Coronatine Are Male Sterile, Insensitive to Methyl Jasmonate, and Resistant to a Bacterial Pathogen. *Plant Cell*, *6*(5), 751-759. https://doi.org/10.1105/tpc.6.5.751

Figueroa, P., & Browse, J. (2015). Male sterility in Arabidopsis induced by overexpression of a MYC5-SRDX chimeric repressor. *Plant J*, *81*(6), 849-860. https://doi.org/10.1111/tpj.12776

Flanagan, P. M., Kelleher, R. J., 3rd, Sayre, M. H., Tschochner, H., & Kornberg, R. D. (1991). A mediator required for activation of RNA polymerase II transcription in vitro. *Nature*, *350*(6317), 436-438. https://doi.org/10.1038/350436a0

Fonseca, S., Chico, J. M., & Solano, R. (2009). The jasmonate pathway: the ligand, the receptor and the core signalling module. *Curr Opin Plant Biol*, *12*(5), 539-547. https://doi.org/10.1016/j.pbi.2009.07.013

Fonseca, S., Chini, A., Hamberg, M., Adie, B., Porzel, A., Kramell, R., Miersch, O., Wasternack, C., & Solano, R. (2009). (+)-7-iso-Jasmonoyl-L-isoleucine is the endogenous bioactive jasmonate. *Nat Chem Biol*, *5*(5), 344-350. https://doi.org/10.1038/nchembio.161

Fonseca, S., Fernandez-Calvo, P., Fernandez, G. M., Diez-Diaz, M., Gimenez-Ibanez, S., Lopez-Vidriero, I., Godoy, M., Fernandez-Barbero, G., Van Leene, J., De Jaeger, G., Franco-Zorrilla, J. M., & Solano, R. (2014). bHLH003, bHLH013 and bHLH017 are new targets of JAZ repressors negatively regulating JA responses. *PLoS One*, *9*(1), e86182. https://doi.org/10.1371/journal.pone.0086182

Galway, M. E., Masucci, J. D., Lloyd, A. M., Walbot, V., Davis, R. W., & Schiefelbein, J. W. (1994). The TTG gene is required to specify epidermal cell fate and cell patterning in the Arabidopsis root. *Dev Biol*, *166*(2), 740-754. https://doi.org/10.1006/dbio.1994.1352

Gasperini, D., Chetelat, A., Acosta, I. F., Goossens, J., Pauwels, L., Goossens, A., Dreos, R., Alfonso, E., & Farmer, E. E. (2015). Multilayered Organization of Jasmonate Signalling in the Regulation of Root Growth. *PLoS Genet*, *11*(6), e1005300. https://doi.org/10.1371/journal.pgen.1005300

Geerinck, J., Pauwels, L., De Jaeger, G., & Goossens, A. (2010). Dissection of the one-MegaDalton JAZ1 protein complex. *Plant Signal Behav*, *5*(8), 1039-1041. https://doi.org/10.4161/psb.5.8.12338

Gidda, S. K., Miersch, O., Levitin, A., Schmidt, J., Wasternack, C., & Varin, L. (2003). Biochemical and molecular characterization of a hydroxyjasmonate sulfotransferase from Arabidopsis thaliana. *J Biol Chem*, *278*(20), 17895-17900. https://doi.org/10.1074/jbc.M211943200

Gilkerson, J., Kelley, D. R., Tam, R., Estelle, M., & Callis, J. (2015). Lysine Residues Are Not Required for Proteasome-Mediated Proteolysis of the Auxin/Indole Acidic Acid Protein IAA1. *Plant Physiol*, *168*(2), 708-720. https://doi.org/10.1104/pp.15.00402

Gilroy, E., & Breen, S. (2022). Interplay between phytohormone signalling pathways in plant defence - other than salicylic acid and jasmonic acid. *Essays Biochem*, *66*(5), 657-671. https://doi.org/10.1042/EBC20210089

Gimenez-Ibanez, S., Boter, M., Ortigosa, A., Garcia-Casado, G., Chini, A., Lewsey, M. G., Ecker, J. R., Ntoukakis, V., & Solano, R. (2017). JAZ2 controls stomata dynamics during bacterial invasion. *New Phytol*, *213*(3), 1378-1392. https://doi.org/10.1111/nph.14354

Glauser, G., Dubugnon, L., Mousavi, S. A., Rudaz, S., Wolfender, J. L., & Farmer, E. E. (2009). Velocity estimates for signal propagation leading to systemic jasmonic acid accumulation in wounded Arabidopsis. *J Biol Chem*, *284*(50), 34506-34513. https://doi.org/10.1074/jbc.M109.061432

Glauser, G., Grata, E., Dubugnon, L., Rudaz, S., Farmer, E. E., & Wolfender, J. L. (2008). Spatial and temporal dynamics of jasmonate synthesis and accumulation in Arabidopsis in response to wounding. *J Biol Chem*, *283*(24), 16400-16407. https://doi.org/10.1074/jbc.M801760200

Goda, H., Sasaki, E., Akiyama, K., Maruyama-Nakashita, A., Nakabayashi, K., Li, W., Ogawa, M., Yamauchi, Y., Preston, J., Aoki, K., Kiba, T., Takatsuto, S., Fujioka, S., Asami, T., Nakano, T., Kato, H., Mizuno, T., Sakakibara, H., Yamaguchi, S., Nambara, E., Kamiya, Y., Takahashi, H., Hirai, M. Y., Sakurai, T., Shinozaki, K., Saito, K., Yoshida, S., & Shimada, Y. (2008). The AtGenExpress hormone and chemical treatment data set: experimental design, data evaluation, model data analysis and data access. *Plant J*, *55*(3), 526-542. https://doi.org/10.1111/j.0960-7412.2008.03510.x

Godoy, M., Franco-Zorrilla, J. M., Perez-Perez, J., Oliveros, J. C., Lorenzo, O., & Solano, R. (2011). Improved protein-binding microarrays for the identification of DNA-binding specificities of transcription factors. *Plant J*, *66*(4), 700-711. https://doi.org/10.1111/j.1365-313X.2011.04519.x

Goetz, M., Vivian-Smith, A., Johnson, S. D., & Koltunow, A. M. (2006). AUXIN RESPONSE FACTOR8 is a negative regulator of fruit initiation in Arabidopsis. *Plant Cell*, *18*(8), 1873-1886. https://doi.org/10.1105/tpc.105.037192

Gomez-Roldan, V., Fermas, S., Brewer, P. B., Puech-Pages, V., Dun, E. A., Pillot, J. P., Letisse, F., Matusova, R., Danoun, S., Portais, J. C., Bouwmeester, H., Becard, G., Beveridge, C. A., Rameau, C., & Rochange, S. F. (2008). Strigolactone inhibition of shoot branching. *Nature*, *455*(7210), 189-194. https://doi.org/10.1038/nature07271

Goossens, J., Mertens, J., & Goossens, A. (2017). Role and functioning of bHLH transcription factors in jasmonate signalling. *J Exp Bot*, *68*(6), 1333-1347. https://doi.org/10.1093/jxb/erw440

Goossens, J., Swinnen, G., Vanden Bossche, R., Pauwels, L., & Goossens, A. (2015). Change of a conserved amino acid in the MYC2 and MYC3 transcription factors leads to release of JAZ repression and increased activity. *New Phytol*, *206*(4), 1229-1237. https://doi.org/10.1111/nph.13398

Grebner, W., Stingl, N. E., Oenel, A., Mueller, M. J., & Berger, S. (2013). Lipoxygenase6-dependent oxylipin synthesis in roots is required for abiotic and biotic stress resistance of Arabidopsis. *Plant Physiol*, *161*(4), 2159-2170. https://doi.org/10.1104/pp.113.214544

Groover, A. T., Pattishall, A., & Jones, A. M. (2003). IAA8 expression during vascular cell differentiation. *Plant Mol Biol*, *51*(3), 427-435. https://doi.org/10.1023/a:1022039815537

Grossmann, G., Guo, W. J., Ehrhardt, D. W., Frommer, W. B., Sit, R. V., Quake, S. R., & Meier, M. (2011). The RootChip: an integrated microfluidic chip for plant science. *Plant Cell*, *23*(12), 4234-4240. https://doi.org/10.1105/tpc.111.092577

Grunewald, W., Vanholme, B., Pauwels, L., Plovie, E., Inze, D., Gheysen, G., & Goossens, A. (2009). Expression of the Arabidopsis jasmonate signalling repressor JAZ1/TIFY10A is stimulated by auxin. *EMBO Rep*, *10*(8), 923-928. https://doi.org/10.1038/embor.2009.103

Guan, L., Denkert, N., Eisa, A., Lehmann, M., Sjuts, I., Weiberg, A., Soll, J., Meinecke, M., & Schwenkert, S. (2019). JASSY, a chloroplast outer membrane protein required for jasmonate biosynthesis. *Proc Natl Acad Sci U S A*, *116*(21), 10568-10575. https://doi.org/10.1073/pnas.1900482116

Guilfoyle, T. J. (1986). Auxin-Regulated Gene-Expression in Higher-Plants. *Crc Critical Reviews in Plant Sciences*, *4*(3), 247-276. https://doi.org/Doi 10.1080/07352688609382226

Guilfoyle, T. J., & Hagen, G. (2007). Auxin response factors. *Curr Opin Plant Biol*, *10*(5), 453-460. https://doi.org/10.1016/j.pbi.2007.08.014

Guo, Q., Yoshida, Y., Major, I. T., Wang, K., Sugimoto, K., Kapali, G., Havko, N. E., Benning, C., & Howe, G. A. (2018). JAZ repressors of metabolic defense promote growth and reproductive fitness in Arabidopsis. *Proc Natl Acad Sci U S A*, *115*(45), E10768-E10777. https://doi.org/10.1073/pnas.1811828115

Gupta, R., & Chakrabarty, S. K. (2013). Gibberellic acid in plant: still a mystery unresolved. *Plant Signal Behav*, *8*(9). https://doi.org/10.4161/psb.25504

Halitschke, R., & Baldwin, I. T. (2003). Antisense LOX expression increases herbivore performance by decreasing defense responses and inhibiting growth-related transcriptional reorganization in Nicotiana attenuata. *Plant J*, *36*(6), 794-807. https://doi.org/10.1046/j.1365-313x.2003.01921.x

Hallare, J., & Gerriets, V. (2023). Half Life. In *StatPearls*. https://www.ncbi.nlm.nih.gov/pubmed/32119385

Han, X., Kui, M., He, K., Yang, M., Du, J., Jiang, Y., & Hu, Y. (2023). Jasmonate-regulated root growth inhibition and root hair elongation. *J Exp Bot*, *74*(4), 1176-1185. https://doi.org/10.1093/jxb/erac441

Han, X., Zhang, M., Yang, M., & Hu, Y. (2020). Arabidopsis JAZ Proteins Interact with and Suppress RHD6 Transcription Factor to Regulate Jasmonate-Stimulated Root Hair Development. *Plant Cell*, *32*(4), 1049-1062. https://doi.org/10.1105/tpc.19.00617

Harberd, N. P., Belfield, E., & Yasumura, Y. (2009). The angiosperm gibberellin-GID1-DELLA growth regulatory mechanism: how an "inhibitor of an inhibitor" enables flexible response to fluctuating environments. *Plant Cell*, *21*(5), 1328-1339. https://doi.org/10.1105/tpc.109.066969

Heitz, T., Smirnova, E., Marquis, V., & Poirier, L. (2019). Metabolic Control within the Jasmonate Biochemical Pathway. *Plant Cell Physiol*, *60*(12), 2621-2628. https://doi.org/10.1093/pcp/pcz172

Heitz, T., Widemann, E., Lugan, R., Miesch, L., Ullmann, P., Desaubry, L., Holder, E., Grausem, B., Kandel, S., Miesch, M., Werck-Reichhart, D., & Pinot, F. (2012). Cytochromes P450 CYP94C1 and CYP94B3 catalyze two successive oxidation steps of plant hormone Jasmonoyl-isoleucine for catabolic turnover. *J Biol Chem*, *287*(9), 6296-6306. https://doi.org/10.1074/jbc.M111.316364

Hershko, A., & Ciechanover, A. (1998). The ubiquitin system. *Annu Rev Biochem*, *67*, 425-479. https://doi.org/10.1146/annurev.biochem.67.1.425

Hickman, R., Van Verk, M. C., Van Dijken, A. J. H., Mendes, M. P., Vroegop-Vos, I. A., Caarls, L., Steenbergen, M., Van der Nagel, I., Wesselink, G. J., Jironkin, A., Talbot, A., Rhodes, J., De Vries, M., Schuurink, R. C., Denby, K., Pieterse, C. M. J., & Van Wees, S. C. M. (2017). Architecture and Dynamics of the Jasmonic Acid Gene Regulatory Network. *Plant Cell*, *29*(9), 2086-2105. https://doi.org/10.1105/tpc.16.00958

Hirose, N., Takei, K., Kuroha, T., Kamada-Nobusada, T., Hayashi, H., & Sakakibara, H. (2008). Regulation of cytokinin biosynthesis, compartmentalization and translocation. *J Exp Bot*, *59*(1), 75-83. https://doi.org/10.1093/jxb/erm157

Hong, G. J., Xue, X. Y., Mao, Y. B., Wang, L. J., & Chen, X. Y. (2012). Arabidopsis MYC2 interacts with DELLA proteins in regulating sesquiterpene synthase gene expression. *Plant Cell*, *24*(6), 2635-2648. https://doi.org/10.1105/tpc.112.098749

Hou, X., Lee, L. Y., Xia, K., Yan, Y., & Yu, H. (2010). DELLAs modulate jasmonate signaling via competitive binding to JAZs. *Dev Cell*, *19*(6), 884-894. https://doi.org/10.1016/j.devcel.2010.10.024

Howe, G. A., Lightner, J., Browse, J., & Ryan, C. A. (1996). An octadecanoid pathway mutant (JL5) of tomato is compromised in signaling for defense against insect attack. *Plant Cell*, *8*(11), 2067-2077. https://doi.org/10.1105/tpc.8.11.2067

Howe, G. A., Major, I. T., & Koo, A. J. (2018). Modularity in Jasmonate Signaling for Multistress Resilience. *Annu Rev Plant Biol*, *69*, 387-415. https://doi.org/10.1146/annurev-arplant-042817-040047

Hu, Y., Jiang, L., Wang, F., & Yu, D. (2013). Jasmonate regulates the inducer of cbf expression-C-repeat binding factor/DRE binding factor1 cascade and freezing tolerance in Arabidopsis. *Plant Cell*, *25*(8), 2907-2924. https://doi.org/10.1105/tpc.113.112631

Huang, H., Liu, B., Liu, L., & Song, S. (2017). Jasmonate action in plant growth and development. *J Exp Bot*, *68*(6), 1349-1359. https://doi.org/10.1093/jxb/erw495

Ingrao, C., Strippoli, R., Lagioia, G., & Huisingh, D. (2023). Water scarcity in agriculture: An overview of causes, impacts and approaches for reducing the risks. *Heliyon*, *9*(8), e18507. https://doi.org/10.1016/j.heliyon.2023.e18507

Ishida, T., Kurata, T., Okada, K., & Wada, T. (2008). A genetic regulatory network in the development of trichomes and root hairs. *Annu Rev Plant Biol*, *59*, 365-386. https://doi.org/10.1146/annurev.arplant.59.032607.092949

Ishiguro, S., Kawai-Oda, A., Ueda, J., Nishida, I., & Okada, K. (2001). The DEFECTIVE IN ANTHER DEHISCIENCE gene encodes a novel phospholipase A1 catalyzing the initial step of jasmonic acid biosynthesis, which synchronizes pollen maturation, anther dehiscence, and flower opening in Arabidopsis. *Plant Cell*, *13*(10), 2191-2209. https://doi.org/10.1105/tpc.010192

Jander, G., Cui, J., Nhan, B., Pierce, N. E., & Ausubel, F. M. (2001). The TASTY locus on chromosome 1 of Arabidopsis affects feeding of the insect herbivore Trichoplusia ni. *Plant Physiol*, *126*(2), 890-898. https://doi.org/10.1104/pp.126.2.890

Jang, G., Yoon, Y., & Choi, Y. D. (2020). Crosstalk with Jasmonic Acid Integrates Multiple Responses in Plant Development. *Int J Mol Sci*, *21*(1). https://doi.org/10.3390/ijms21010305

Jansen, R. P. (2001). mRNA localization: message on the move. *Nat Rev Mol Cell Biol*, *2*(4), 247-256. https://doi.org/10.1038/35067016

Jensen, E. (2013). Laser-capture microdissection. *Anat Rec (Hoboken)*, *296*(11), 1683-1687. https://doi.org/10.1002/ar.22791

Jha, P., Ochatt, S. J., & Kumar, V. (2020). WUSCHEL: a master regulator in plant growth signaling. *Plant Cell Rep*, *39*(4), 431-444. https://doi.org/10.1007/s00299-020-02511-5

Jiang, Y., Liang, G., Yang, S., & Yu, D. (2014). Arabidopsis WRKY57 functions as a node of convergence for jasmonic acid- and auxin-mediated signaling in jasmonic acid-induced leaf senescence. *Plant Cell*, *26*(1), 230-245. https://doi.org/10.1105/tpc.113.117838

Johnson, L. Y. D., Major, I. T., Chen, Y., Yang, C., Vanegas-Cano, L. J., & Howe, G. A. (2023). Diversification of JAZ-MYC signaling function in immune metabolism. *New Phytol*, *239*(6), 2277-2291. https://doi.org/10.1111/nph.19114

Ju, L., Jing, Y., Shi, P., Liu, J., Chen, J., Yan, J., Chu, J., Chen, K. M., & Sun, J. (2019). JAZ proteins modulate seed germination through interaction with ABI5 in bread wheat and Arabidopsis. *New Phytol*, *223*(1), 246-260. https://doi.org/10.1111/nph.15757

Kachroo, A., & Kachroo, P. (2009). Fatty Acid-derived signals in plant defense. *Annu Rev Phytopathol*, *47*, 153-176. https://doi.org/10.1146/annurev-phyto-080508-081820

Kagale, S., Links, M. G., & Rozwadowski, K. (2010). Genome-wide analysis of ethylene-responsive element binding factor-associated amphiphilic repression motif-containing transcriptional regulators in Arabidopsis. *Plant Physiol*, *152*(3), 1109-1134. https://doi.org/10.1104/pp.109.151704

Katsir, L., Schilmiller, A. L., Staswick, P. E., He, S. Y., & Howe, G. A. (2008). COI1 is a critical component of a receptor for jasmonate and the bacterial virulence factor coronatine. *Proc Natl Acad Sci U S A*, *105*(19), 7100-7105. https://doi.org/10.1073/pnas.0802332105

Kazan, K. (2015). Diverse roles of jasmonates and ethylene in abiotic stress tolerance. *Trends Plant Sci*, *20*(4), 219-229. https://doi.org/10.1016/j.tplants.2015.02.001

Kazan, K., & Manners, J. M. (2012). JAZ repressors and the orchestration of phytohormone crosstalk. *Trends Plant Sci*, *17*(1), 22-31. https://doi.org/10.1016/j.tplants.2011.10.006

Kazan, K., & Manners, J. M. (2013). MYC2: the master in action. *Mol Plant*, *6*(3), 686-703. https://doi.org/10.1093/mp/sss128

Kelleher, R. J., 3rd, Flanagan, P. M., & Kornberg, R. D. (1990). A novel mediator between activator proteins and the RNA polymerase II transcription apparatus. *Cell*, *61*(7), 1209-1215. https://doi.org/10.1016/0092-8674(90)90685-8

Kelley, D. R., & Estelle, M. (2012). Ubiquitin-mediated control of plant hormone signaling. *Plant Physiol*, *160*(1), 47-55. https://doi.org/10.1104/pp.112.200527

Kesten, C., Gamez-Arjona, F. M., Menna, A., Scholl, S., Dora, S., Huerta, A. I., Huang, H. Y., Tintor, N., Kinoshita, T., Rep, M., Krebs, M., Schumacher, K., & Sanchez-Rodriguez, C. (2019). Pathogen-induced pH changes regulate the growth-defense balance in plants. *EMBO J*, *38*(24), e101822. https://doi.org/10.15252/embj.2019101822

Kiba, T., & Krapp, A. (2016). Plant Nitrogen Acquisition Under Low Availability: Regulation of Uptake and Root Architecture. *Plant Cell Physiol*, *57*(4), 707-714. https://doi.org/10.1093/pcp/pcw052

Kilian, J., Whitehead, D., Horak, J., Wanke, D., Weinl, S., Batistic, O., D'Angelo, C., Bornberg-Bauer, E., Kudla, J., & Harter, K. (2007). The AtGenExpress global stress expression data set: protocols, evaluation and model data analysis of UV-B light, drought and cold stress responses. *Plant J*, *50*(2), 347-363. https://doi.org/10.1111/j.1365-313X.2007.03052.x

Kim, J. M., To, T. K., Matsui, A., Tanoi, K., Kobayashi, N. I., Matsuda, F., Habu, Y., Ogawa, D., Sakamoto, T., Matsunaga, S., Bashir, K., Rasheed, S., Ando, M., Takeda, H., Kawaura, K., Kusano, M., Fukushima, A., Endo, T. A., Kuromori, T., Ishida, J., Morosawa, T., Tanaka, M., Torii, C., Takebayashi, Y., Sakakibara, H., Ogihara, Y., Saito, K., Shinozaki, K., Devoto, A., & Seki, M. (2017). Acetate-mediated novel survival strategy against drought in plants. *Nat Plants*, *3*, 17097. https://doi.org/10.1038/nplants.2017.97

Kim, S. H., Bahk, S., An, J., Hussain, S., Nguyen, N. T., Do, H. L., Kim, J. Y., Hong, J. C., & Chung, W. S. (2020). A Gain-of-Function Mutant of IAA15 Inhibits Lateral Root Development by Transcriptional Repression of LBD Genes in Arabidopsis. *Front Plant Sci*, *11*, 1239. https://doi.org/10.3389/fpls.2020.01239

Kimberlin, A. N., Holtsclaw, R. E., Zhang, T., Mulaudzi, T., & Koo, A. J. (2022). On the initiation of jasmonate biosynthesis in wounded leaves. *Plant Physiol*, *189*(4), 1925-1942. https://doi.org/10.1093/plphys/kiac163

Kitaoka, N., Matsubara, T., Sato, M., Takahashi, K., Wakuta, S., Kawaide, H., Matsui, H., Nabeta, K., & Matsuura, H. (2011). Arabidopsis CYP94B3 encodes jasmonyl-L-isoleucine 12-hydroxylase, a key

enzyme in the oxidative catabolism of jasmonate. *Plant Cell Physiol*, *52*(10), 1757-1765. https://doi.org/10.1093/pcp/pcr110

Klepikova, A. V., Kasianov, A. S., Gerasimov, E. S., Logacheva, M. D., & Penin, A. A. (2016). A high resolution map of the Arabidopsis thaliana developmental transcriptome based on RNA-seq profiling. *Plant J*, *88*(6), 1058-1070. https://doi.org/10.1111/tpj.13312

Kloek, A. P., Verbsky, M. L., Sharma, S. B., Schoelz, J. E., Vogel, J., Klessig, D. F., & Kunkel, B. N. (2001). Resistance to Pseudomonas syringae conferred by an Arabidopsis thaliana coronatine-insensitive (coi1) mutation occurs through two distinct mechanisms. *Plant J*, *26*(5), 509-522. https://doi.org/10.1046/j.1365-313x.2001.01050.x

Kohchi, T., Yamato, K. T., Ishizaki, K., Yamaoka, S., & Nishihama, R. (2021). Development and Molecular Genetics of Marchantia polymorpha. *Annu Rev Plant Biol*, *72*, 677-702. https://doi.org/10.1146/annurev-arplant-082520-094256

Koo, A. J. (2018). Metabolism of the plant hormone jasmonate: a sentinel for tissue damage and master regulator of stress response. *Phytochem Rev*, *17*, 51-80.

Koo, A. J., Cooke, T. F., & Howe, G. A. (2011). Cytochrome P450 CYP94B3 mediates catabolism and inactivation of the plant hormone jasmonoyl-L-isoleucine. *Proc Natl Acad Sci U S A*, *108*(22), 9298-9303. https://doi.org/10.1073/pnas.1103542108

Koo, A. J., Gao, X., Jones, A. D., & Howe, G. A. (2009). A rapid wound signal activates the systemic synthesis of bioactive jasmonates in Arabidopsis. *Plant J*, *59*(6), 974-986. https://doi.org/10.1111/j.1365-313X.2009.03924.x

Laha, D., Johnen, P., Azevedo, C., Dynowski, M., Weiss, M., Capolicchio, S., Mao, H., Iven, T., Steenbergen, M., Freyer, M., Gaugler, P., de Campos, M. K., Zheng, N., Feussner, I., Jessen, H. J., Van Wees, S. C., Saiardi, A., & Schaaf, G. (2015). VIH2 Regulates the Synthesis of Inositol Pyrophosphate InsP8 and Jasmonate-Dependent Defenses in Arabidopsis. *Plant Cell*, *27*(4), 1082-1097. https://doi.org/10.1105/tpc.114.135160

Laha, D., Parvin, N., Dynowski, M., Johnen, P., Mao, H., Bitters, S. T., Zheng, N., & Schaaf, G. (2016). Inositol Polyphosphate Binding Specificity of the Jasmonate Receptor Complex. *Plant Physiol*, *171*(4), 2364-2370. https://doi.org/10.1104/pp.16.00694

Lambrix, V., Reichelt, M., Mitchell-Olds, T., Kliebenstein, D. J., & Gershenzon, J. (2001). The Arabidopsis epithiospecifier protein promotes the hydrolysis of glucosinolates to nitriles and influences Trichoplusia ni herbivory. *Plant Cell*, *13*(12), 2793-2807. https://doi.org/10.1105/tpc.010261

Lane, D. R., Wiedemeier, A., Peng, L., Hofte, H., Vernhettes, S., Desprez, T., Hocart, C. H., Birch, R. J., Baskin, T. I., Burn, J. E., Arioli, T., Betzner, A. S., & Williamson, R. E. (2001). Temperature-sensitive alleles of RSW2 link the KORRIGAN endo-1,4-beta-glucanase to cellulose synthesis and cytokinesis in Arabidopsis. *Plant Physiol*, *126*(1), 278-288. https://doi.org/10.1104/pp.126.1.278

Larrieu, A., Champion, A., Legrand, J., Lavenus, J., Mast, D., Brunoud, G., Oh, J., Guyomarc'h, S., Pizot, M., Farmer, E. E., Turnbull, C., Vernoux, T., Bennett, M. J., & Laplaze, L. (2015). A fluorescent hormone biosensor reveals the dynamics of jasmonate signalling in plants. *Nat Commun*, *6*, 6043. https://doi.org/10.1038/ncomms7043

Laudert, D., Pfannschmidt, U., Lottspeich, F., Hollander-Czytko, H., & Weiler, E. W. (1996). Cloning, molecular and functional characterization of Arabidopsis thaliana allene oxide synthase (CYP 74), the first enzyme of the octadecanoid pathway to jasmonates. *Plant Mol Biol*, *31*(2), 323-335. https://doi.org/10.1007/BF00021793

Lei, L., Zhang, T., Strasser, R., Lee, C. M., Gonneau, M., Mach, L., Vernhettes, S., Kim, S. H., D, J. C., Li, S., & Gu, Y. (2014). The jiaoyao1 Mutant Is an Allele of korrigan1 That Abolishes Endoglucanase Activity and Affects the Organization of Both Cellulose Microfibrils and Microtubules in Arabidopsis. *Plant Cell*, *26*(6), 2601-2616. https://doi.org/10.1105/tpc.114.126193

Leone, M., Keller, M. M., Cerrudo, I., & Ballare, C. L. (2014). To grow or defend? Low red : far-red ratios reduce jasmonate sensitivity in Arabidopsis seedlings by promoting DELLA degradation and increasing JAZ10 stability. *New Phytol*, *204*(2), 355-367. https://doi.org/10.1111/nph.12971

Li, C., Schilmiller, A. L., Liu, G., Lee, G. I., Jayanty, S., Sageman, C., Vrebalov, J., Giovannoni, J. J., Yagi, K., Kobayashi, Y., & Howe, G. A. (2005). Role of beta-oxidation in jasmonate biosynthesis and systemic wound signaling in tomato. *Plant Cell*, *17*(3), 971-986. https://doi.org/10.1105/tpc.104.029108

Li, H. M., & Yu, C. W. (2018). Chloroplast Galactolipids: The Link Between Photosynthesis, Chloroplast Shape, Jasmonates, Phosphate Starvation and Freezing Tolerance. *Plant Cell Physiol*, *59*(6), 1128-1134. https://doi.org/10.1093/pcp/pcy088

Li, L., Zhao, Y., McCaig, B. C., Wingerd, B. A., Wang, J., Whalon, M. E., Pichersky, E., & Howe, G. A. (2004). The tomato homolog of CORONATINE-INSENSITIVE1 is required for the maternal control of seed maturation, jasmonate-signaled defense responses, and glandular trichome development. *Plant Cell*, *16*(1), 126-143. https://doi.org/10.1105/tpc.017954

Li, Q., Zheng, J., Li, S., Huang, G., Skilling, S. J., Wang, L., Li, L., Li, M., Yuan, L., & Liu, P. (2017). Transporter-Mediated Nuclear Entry of Jasmonoyl-Isoleucine Is Essential for Jasmonate Signaling. *Mol Plant*, *10*(5), 695-708. https://doi.org/10.1016/j.molp.2017.01.010

Liang, Y., Ward, S., Li, P., Bennett, T., & Leyser, O. (2016). SMAX1-LIKE7 Signals from the Nucleus to Regulate Shoot Development in Arabidopsis via Partially EAR Motif-Independent Mechanisms. *Plant Cell*, *28*(7), 1581-1601. https://doi.org/10.1105/tpc.16.00286

Liao, C. Y., Smet, W., Brunoud, G., Yoshida, S., Vernoux, T., & Weijers, D. (2015). Reporters for sensitive and quantitative measurement of auxin response. *Nat Methods*, *12*(3), 207-210, 202 p following 210. https://doi.org/10.1038/nmeth.3279

Lin, Y. T., Chen, L. J., Herrfurth, C., Feussner, I., & Li, H. M. (2016). Reduced Biosynthesis of Digalactosyldiacylglycerol, a Major Chloroplast Membrane Lipid, Leads to Oxylipin Overproduction and Phloem Cap Lignification in Arabidopsis. *Plant Cell*, *28*(1), 219-232. https://doi.org/10.1105/tpc.15.01002

Liu, B., Seong, K., Pang, S., Song, J., Gao, H., Wang, C., Zhai, J., Zhang, Y., Gao, S., Li, X., Qi, T., & Song, S. (2021). Functional specificity, diversity, and redundancy of Arabidopsis JAZ family repressors in jasmonate and COI1-regulated growth, development, and defense. *New Phytol*, *231*(4), 1525-1545. https://doi.org/10.1111/nph.17477

Liu, H., & Stone, S. L. (2010). Abscisic acid increases Arabidopsis ABI5 transcription factor levels by promoting KEG E3 ligase self-ubiquitination and proteasomal degradation. *Plant Cell*, *22*(8), 2630-2641. https://doi.org/10.1105/tpc.110.076075

Liu, H., & Stone, S. L. (2013). Cytoplasmic degradation of the Arabidopsis transcription factor abscisic acid insensitive 5 is mediated by the RING-type E3 ligase KEEP ON GOING. *J Biol Chem*, *288*(28), 20267-20279. https://doi.org/10.1074/jbc.M113.465369

Liu, Y., Wei, H., Ma, M., Li, Q., Kong, D., Sun, J., Ma, X., Wang, B., Chen, C., Xie, Y., & Wang, H. (2019). Arabidopsis FHY3 and FAR1 Regulate the Balance between Growth and Defense Responses under Shade Conditions. *Plant Cell*, *31*(9), 2089-2106. https://doi.org/10.1105/tpc.18.00991

Lopez-Cruz, J., Finiti, I., Fernandez-Crespo, E., Crespo-Salvador, O., Garcia-Agustin, P., & Gonzalez-Bosch, C. (2014). Absence of endo-1,4-beta-glucanase KOR1 alters the jasmonate-dependent defence response to Pseudomonas syringae in Arabidopsis. *J Plant Physiol*, *171*(16), 1524-1532. https://doi.org/10.1016/j.jplph.2014.07.006

Lorenzo, O., Chico, J. M., Sanchez-Serrano, J. J., & Solano, R. (2004). JASMONATE-INSENSITIVE1 encodes a MYC transcription factor essential to discriminate between different jasmonate-regulated defense responses in Arabidopsis. *Plant Cell*, *16*(7), 1938-1950. https://doi.org/10.1105/tpc.022319

Love, M. I., Huber, W., & Anders, S. (2014). Moderated estimation of fold change and dispersion for RNA-seq data with DESeq2. *Genome Biol*, *15*(12), 550. https://doi.org/10.1186/s13059-014-0550-8

Lozano-Duran, R., Rosas-Diaz, T., Gusmaroli, G., Luna, A. P., Taconnat, L., Deng, X. W., & Bejarano, E. R. (2011). Geminiviruses subvert ubiquitination by altering CSN-mediated derubylation of SCF E3 ligase complexes and inhibit jasmonate signaling in Arabidopsis thaliana. *Plant Cell*, *23*(3), 1014-1032. https://doi.org/10.1105/tpc.110.080267

Mahonen, A. P., Ten Tusscher, K., Siligato, R., Smetana, O., Diaz-Trivino, S., Salojarvi, J., Wachsman, G., Prasad, K., Heidstra, R., & Scheres, B. (2014). PLETHORA gradient formation mechanism separates auxin responses. *Nature*, *515*(7525), 125-129. https://doi.org/10.1038/nature13663

Major, I. T., Yoshida, Y., Campos, M. L., Kapali, G., Xin, X. F., Sugimoto, K., de Oliveira Ferreira, D., He, S. Y., & Howe, G. A. (2017). Regulation of growth-defense balance by the JASMONATE ZIM-DOMAIN (JAZ)-MYC transcriptional module. *New Phytol*, *215*(4), 1533-1547. https://doi.org/10.1111/nph.14638

Manners, J. M., Penninckx, I. A., Vermaere, K., Kazan, K., Brown, R. L., Morgan, A., Maclean, D. J., Curtis, M. D., Cammue, B. P., & Broekaert, W. F. (1998). The promoter of the plant defensin gene PDF1.2 from Arabidopsis is systemically activated by fungal pathogens and responds to methyl jasmonate but not to salicylic acid. *Plant Mol Biol*, *38*(6), 1071-1080. https://doi.org/10.1023/a:1006070413843

Marasco, L. E., & Kornblihtt, A. R. (2023). The physiology of alternative splicing. *Nat Rev Mol Cell Biol*, *24*(4), 242-254. https://doi.org/10.1038/s41580-022-00545-z

Mashiguchi, K., Seto, Y., & Yamaguchi, S. (2021). Strigolactone biosynthesis, transport and perception. *Plant J*, *105*(2), 335-350. https://doi.org/10.1111/tpj.15059

Masucci, J. D., & Schiefelbein, J. W. (1994). The Rhd6 Mutation of Arabidopsis-Thaliana Alters Root-Hair Initiation through an Auxin-Associated and Ethylene-Associated Process. *Plant Physiology*, *106*(4), 1335-1346. https://doi.org/DOI 10.1104/pp.106.4.1335

McConn, M., & Browse, J. (1996). The Critical Requirement for Linolenic Acid Is Pollen Development, Not Photosynthesis, in an Arabidopsis Mutant. *Plant Cell*, *8*(3), 403-416. https://doi.org/10.1105/tpc.8.3.403

McConn, M., Creelman, R. A., Bell, E., Mullet, J. E., & Browse, J. (1997). Jasmonate is essential for insect defense in Arabidopsis. *Proc Natl Acad Sci U S A*, *94*(10), 5473-5477. https://doi.org/10.1073/pnas.94.10.5473

Mei, S., Zhang, M., Ye, J., Du, J., Jiang, Y., & Hu, Y. (2023). Auxin contributes to jasmonate-mediated regulation of abscisic acid signaling during seed germination in Arabidopsis. *Plant Cell*, *35*(3), 1110-1133. https://doi.org/10.1093/plcell/koac362

Melotto, M., Mecey, C., Niu, Y., Chung, H. S., Katsir, L., Yao, J., Zeng, W., Thines, B., Staswick, P., Browse, J., Howe, G. A., & He, S. Y. (2008). A critical role of two positively charged amino acids in the Jas motif of Arabidopsis JAZ proteins in mediating coronatine- and jasmonoyl isoleucine-dependent interactions with the COI1 F-box protein. *Plant J*, *55*(6), 979-988. https://doi.org/10.1111/j.1365-313X.2008.03566.x

Mewis, I., Tokuhisa, J. G., Schultz, J. C., Appel, H. M., Ulrichs, C., & Gershenzon, J. (2006). Gene expression and glucosinolate accumulation in Arabidopsis thaliana in response to generalist and specialist herbivores of different feeding guilds and the role of defense signaling pathways. *Phytochemistry*, *67*(22), 2450-2462. https://doi.org/10.1016/j.phytochem.2006.09.004

Mielke, S., & Gasperini, D. (2019). Interplay between Plant Cell Walls and Jasmonate Production. *Plant Cell Physiol*, *60*(12), 2629-2637. https://doi.org/10.1093/pcp/pcz119

Mielke, S., Zimmer, M., Meena, M. K., Dreos, R., Stellmach, H., Hause, B., Voiniciuc, C., & Gasperini, D. (2021). Jasmonate biosynthesis arising from altered cell walls is prompted by turgor-driven mechanical compression. *Sci Adv*, *7*(7). https://doi.org/10.1126/sciadv.abf0356

Mignone, F., Gissi, C., Liuni, S., & Pesole, G. (2002). Untranslated regions of mRNAs. *Genome Biol*, *3*(3), REVIEWS0004. https://doi.org/10.1186/gb-2002-3-3-reviews0004

Mockaitis, K., & Estelle, M. (2008). Auxin receptors and plant development: a new signaling paradigm. *Annu Rev Cell Dev Biol*, *24*, 55-80. https://doi.org/10.1146/annurev.cellbio.23.090506.123214

Monte, I., Franco-Zorrilla, J. M., Garcia-Casado, G., Zamarreno, A. M., Garcia-Mina, J. M., Nishihama, R., Kohchi, T., & Solano, R. (2019). A Single JAZ Repressor Controls the Jasmonate Pathway in Marchantia polymorpha. *Mol Plant*, *12*(2), 185-198. https://doi.org/10.1016/j.molp.2018.12.017

Monte, I., Ishida, S., Zamarreno, A. M., Hamberg, M., Franco-Zorrilla, J. M., Garcia-Casado, G., Gouhier-Darimont, C., Reymond, P., Takahashi, K., Garcia-Mina, J. M., Nishihama, R., Kohchi, T., & Solano, R. (2018). Ligand-receptor co-evolution shaped the jasmonate pathway in land plants. *Nat Chem Biol*, *14*(5), 480-488. https://doi.org/10.1038/s41589-018-0033-4

Moreno, J. E., Shyu, C., Campos, M. L., Patel, L. C., Chung, H. S., Yao, J., He, S. Y., & Howe, G. A. (2013). Negative feedback control of jasmonate signaling by an alternative splice variant of JAZ10. *Plant Physiol*, *162*(2), 1006-1017. https://doi.org/10.1104/pp.113.218164

Morin, H., Chetelat, A., Stolz, S., Marcourt, L., Glauser, G., Wolfender, J. L., & Farmer, E. E. (2023). Wound-response jasmonate dynamics in the primary vasculature. *New Phytol*. https://doi.org/10.1111/nph.19207

Mosblech, A., Thurow, C., Gatz, C., Feussner, I., & Heilmann, I. (2011). Jasmonic acid perception by COI1 involves inositol polyphosphates in Arabidopsis thaliana. *Plant J*, *65*(6), 949-957. https://doi.org/10.1111/j.1365-313X.2011.04480.x

Motte, H., Vanneste, S., & Beeckman, T. (2019). Molecular and Environmental Regulation of Root Development. *Annu Rev Plant Biol*, *70*, 465-488. https://doi.org/10.1146/annurev-arplant-050718-100423

Nakata, M., Mitsuda, N., Herde, M., Koo, A. J., Moreno, J. E., Suzuki, K., Howe, G. A., & Ohme-Takagi, M. (2013). A bHLH-type transcription factor, ABA-INDUCIBLE BHLH-TYPE TRANSCRIPTION FACTOR/JA-ASSOCIATED MYC2-LIKE1, acts as a repressor to negatively regulate jasmonate signaling in arabidopsis. *Plant Cell*, *25*(5), 1641-1656. https://doi.org/10.1105/tpc.113.111112

Niemeyer, M., Moreno Castillo, E., Ihling, C. H., Iacobucci, C., Wilde, V., Hellmuth, A., Hoehenwarter, W., Samodelov, S. L., Zurbriggen, M. D., Kastritis, P. L., Sinz, A., & Calderon Villalobos, L. I. A. (2020). Flexibility of intrinsically disordered degrons in AUX/IAA proteins reinforces auxin co-receptor assemblies. *Nat Commun*, *11*(1), 2277. https://doi.org/10.1038/s41467-020-16147-2

Niu, Y., Figueroa, P., & Browse, J. (2011). Characterization of JAZ-interacting bHLH transcription factors that regulate jasmonate responses in Arabidopsis. *J Exp Bot*, *62*(6), 2143-2154. https://doi.org/10.1093/jxb/erq408

Noir, S., Bomer, M., Takahashi, N., Ishida, T., Tsui, T. L., Balbi, V., Shanahan, H., Sugimoto, K., & Devoto, A. (2013). Jasmonate controls leaf growth by repressing cell proliferation and the onset of endoreduplication while maintaining a potential stand-by mode. *Plant Physiol*, *161*(4), 1930-1951. https://doi.org/10.1104/pp.113.214908

Oblessuc, P. R., Obulareddy, N., DeMott, L., Matiolli, C. C., Thompson, B. K., & Melotto, M. (2020). JAZ4 is involved in plant defense, growth, and development in Arabidopsis. *Plant J*, *101*(2), 371-383. https://doi.org/10.1111/tpj.14548

Obrig, T. G., Culp, W. J., McKeehan, W. L., & Hardesty, B. (1971). The mechanism by which cycloheximide and related glutarimide antibiotics inhibit peptide synthesis on reticulocyte ribosomes. *J Biol Chem*, *246*(1), 174-181. https://www.ncbi.nlm.nih.gov/pubmed/5541758

Oka, K., Kobayashi, M., Mitsuhara, I., & Seo, S. (2013). Jasmonic acid negatively regulates resistance to Tobacco mosaic virus in tobacco. *Plant Cell Physiol*, *54*(12), 1999-2010. https://doi.org/10.1093/pcp/pct137

Ona Chuquimarca, S., Ayala-Ruano, S., Goossens, J., Pauwels, L., Goossens, A., Leon-Reyes, A., & Angel Mendez, M. (2020). The Molecular Basis of JAZ-MYC Coupling, a Protein-Protein Interface Essential for Plant Response to Stressors. *Front Plant Sci*, *11*, 1139. https://doi.org/10.3389/fpls.2020.01139

Ortigosa, A., Fonseca, S., Franco-Zorrilla, J. M., Fernandez-Calvo, P., Zander, M., Lewsey, M. G., Garcia-Casado, G., Fernandez-Barbero, G., Ecker, J. R., & Solano, R. (2020). The JA-pathway MYC transcription factors regulate photomorphogenic responses by targeting HY5 gene expression. *Plant J*, *102*(1), 138-152. https://doi.org/10.1111/tpj.14618

Pacifici, E., Polverari, L., & Sabatini, S. (2015). Plant hormone cross-talk: the pivot of root growth. *J Exp Bot*, *66*(4), 1113-1121. https://doi.org/10.1093/jxb/eru534

Palaniswamy, S. K., James, S., Sun, H., Lamb, R. S., Davuluri, R. V., & Grotewold, E. (2006). AGRIS and AtRegNet. a platform to link cis-regulatory elements and transcription factors into regulatory networks. *Plant Physiol*, *140*(3), 818-829. https://doi.org/10.1104/pp.105.072280

Park, J. H., Halitschke, R., Kim, H. B., Baldwin, I. T., Feldmann, K. A., & Feyereisen, R. (2002). A knock-out mutation in allene oxide synthase results in male sterility and defective wound signal transduction in Arabidopsis due to a block in jasmonic acid biosynthesis. *Plant J*, *31*(1), 1-12. https://doi.org/10.1046/j.1365-313x.2002.01328.x

Pauwels, L., Barbero, G. F., Geerinck, J., Tilleman, S., Grunewald, W., Perez, A. C., Chico, J. M., Bossche, R. V., Sewell, J., Gil, E., Garcia-Casado, G., Witters, E., Inze, D., Long, J. A., De Jaeger, G., Solano, R., & Goossens, A. (2010). NINJA connects the co-repressor TOPLESS to jasmonate signalling. *Nature*, *464*(7289), 788-791. https://doi.org/10.1038/nature08854

Pauwels, L., De Clercq, R., Goossens, J., Inigo, S., Williams, C., Ron, M., Britt, A., & Goossens, A. (2018). A Dual sgRNA Approach for Functional Genomics in Arabidopsis thaliana. *G3 (Bethesda)*, *8*(8), 2603-2615. https://doi.org/10.1534/g3.118.200046

Pauwels, L., Ritter, A., Goossens, J., Durand, A. N., Liu, H., Gu, Y., Geerinck, J., Boter, M., Vanden Bossche, R., De Clercq, R., Van Leene, J., Gevaert, K., De Jaeger, G., Solano, R., Stone, S., Innes, R. W., Callis, J., & Goossens, A. (2015). The RING E3 Ligase KEEP ON GOING Modulates JASMONATE ZIM-DOMAIN12 Stability. *Plant Physiol*, *169*(2), 1405-1417. https://doi.org/10.1104/pp.15.00479

Pazos, F., Pietrosemoli, N., Garcia-Martin, J. A., & Solano, R. (2013). Protein intrinsic disorder in plants. *Front Plant Sci*, *4*, 363. https://doi.org/10.3389/fpls.2013.00363

Peng, J., Carol, P., Richards, D. E., King, K. E., Cowling, R. J., Murphy, G. P., & Harberd, N. P. (1997). The Arabidopsis GAI gene defines a signaling pathway that negatively regulates gibberellin responses. *Genes Dev*, *11*(23), 3194-3205. https://doi.org/10.1101/gad.11.23.3194

Peng, L., Kawagoe, Y., Hogan, P., & Delmer, D. (2002). Sitosterol-beta-glucoside as primer for cellulose synthesis in plants. *Science*, *295*(5552), 147-150. https://doi.org/10.1126/science.1064281

Penninckx, I. A., Eggermont, K., Terras, F. R., Thomma, B. P., De Samblanx, G. W., Buchala, A., Metraux, J. P., Manners, J. M., & Broekaert, W. F. (1996). Pathogen-induced systemic activation of a plant defensin gene in Arabidopsis follows a salicylic acid-independent pathway. *Plant Cell*, *8*(12), 2309-2323. https://doi.org/10.1105/tpc.8.12.2309

Perez, A. C., & Goossens, A. (2013). Jasmonate signalling: a copycat of auxin signalling? *Plant Cell Environ*, *36*(12), 2071-2084. https://doi.org/10.1111/pce.12121

Peumans, W. J., & Van Damme, E. J. (1995). Lectins as plant defense proteins. *Plant Physiol*, *109*(2), 347-352. https://doi.org/10.1104/pp.109.2.347

Qi, T., Huang, H., Song, S., & Xie, D. (2015). Regulation of Jasmonate-Mediated Stamen Development and Seed Production by a bHLH-MYB Complex in Arabidopsis. *Plant Cell*, *27*(6), 1620-1633. https://doi.org/10.1105/tpc.15.00116

Qi, T., Huang, H., Wu, D., Yan, J., Qi, Y., Song, S., & Xie, D. (2014). Arabidopsis DELLA and JAZ proteins bind the WD-repeat/bHLH/MYB complex to modulate gibberellin and jasmonate signaling synergy. *Plant Cell*, *26*(3), 1118-1133. https://doi.org/10.1105/tpc.113.121731

Qi, T., Song, S., Ren, Q., Wu, D., Huang, H., Chen, Y., Fan, M., Peng, W., Ren, C., & Xie, D. (2011). The Jasmonate-ZIM-domain proteins interact with the WD-Repeat/bHLH/MYB complexes to regulate Jasmonate-mediated anthocyanin accumulation and trichome initiation in Arabidopsis thaliana. *Plant Cell*, *23*(5), 1795-1814. https://doi.org/10.1105/tpc.111.083261

Qin, H., He, L., & Huang, R. (2019). The Coordination of Ethylene and Other Hormones in Primary Root Development. *Front Plant Sci*, *10*, 874. https://doi.org/10.3389/fpls.2019.00874

Rask, L., Andreasson, E., Ekbom, B., Eriksson, S., Pontoppidan, B., & Meijer, J. (2000). Myrosinase: gene family evolution and herbivore defense in Brassicaceae. *Plant Mol Biol*, *42*(1), 93-113. https://www.ncbi.nlm.nih.gov/pubmed/10688132

Rellan-Alvarez, R., Lobet, G., & Dinneny, J. R. (2016). Environmental Control of Root System Biology. *Annu Rev Plant Biol*, *67*, 619-642. https://doi.org/10.1146/annurev-arplant-043015-111848

Reymond, P., Bodenhausen, N., Van Poecke, R. M., Krishnamurthy, V., Dicke, M., & Farmer, E. E. (2004). A conserved transcript pattern in response to a specialist and a generalist herbivore. *Plant Cell*, *16*(11), 3132-3147. https://doi.org/10.1105/tpc.104.026120

Reymond, P., Weber, H., Damond, M., & Farmer, E. E. (2000). Differential gene expression in response to mechanical wounding and insect feeding in Arabidopsis. *Plant Cell*, *12*(5), 707-720. https://doi.org/10.1105/tpc.12.5.707

Rudus, I., Terai, H., Shimizu, T., Kojima, H., Hattori, K., Nishimori, Y., Tsukagoshi, H., Kamiya, Y., Seo, M., Nakamura, K., Kepczynski, J., & Ishiguro, S. (2014). Wound-induced expression of DEFECTIVE IN ANTHER DEHISCENCE1 and DAD1-like lipase genes is mediated by both CORONATINE INSENSITIVE1-dependent and independent pathways in Arabidopsis thaliana. *Plant Cell Rep*, *33*(6), 849-860. https://doi.org/10.1007/s00299-013-1561-8

Rusak, G., Cerni, S., Polancec, D. S., & Ludwig-Müller, J. (2010). The responsiveness of the IAA2 promoter to IAA and IBA is differentially affected in Arabidopsis roots and shoots by flavonoids. *Biologia Plantarum*, *54*(3), 403-414. https://doi.org/10.1007/s10535-010-0075-2

Ryu, S. B. (2004). Phospholipid-derived signaling mediated by phospholipase A in plants. *Trends Plant Sci*, *9*(5), 229-235. https://doi.org/10.1016/j.tplants.2004.03.004

Santner, A., & Estelle, M. (2009). Recent advances and emerging trends in plant hormone signalling. *Nature*, *459*(7250), 1071-1078. https://doi.org/10.1038/nature08122

Santner, A., & Estelle, M. (2010). The ubiquitin-proteasome system regulates plant hormone signaling. *Plant J*, *61*(6), 1029-1040. https://doi.org/10.1111/j.1365-313X.2010.04112.x

Sasaki-Sekimoto, Y., Jikumaru, Y., Obayashi, T., Saito, H., Masuda, S., Kamiya, Y., Ohta, H., & Shirasu, K. (2013). Basic helix-loop-helix transcription factors JASMONATE-ASSOCIATED MYC2-LIKE1 (JAM1), JAM2, and JAM3 are negative regulators of jasmonate responses in Arabidopsis. *Plant Physiol*, *163*(1), 291-304. https://doi.org/10.1104/pp.113.220129

Schiefelbein, J., Kwak, S. H., Wieckowski, Y., Barron, C., & Bruex, A. (2009). The gene regulatory network for root epidermal cell-type pattern formation in Arabidopsis. *J Exp Bot*, *60*(5), 1515-1521. https://doi.org/10.1093/jxb/ern339

Schmieder, R., & Edwards, R. (2011). Quality control and preprocessing of metagenomic datasets. *Bioinformatics*, *27*(6), 863-864. https://doi.org/10.1093/bioinformatics/btr026

Schmitz, R. J., Grotewold, E., & Stam, M. (2022). Cis-regulatory sequences in plants: Their importance, discovery, and future challenges. *Plant Cell*, *34*(2), 718-741. https://doi.org/10.1093/plcell/koab281

Schubert, R., Dobritzsch, S., Gruber, C., Hause, G., Athmer, B., Schreiber, T., Marillonnet, S., Okabe, Y., Ezura, H., Acosta, I. F., Tarkowska, D., & Hause, B. (2019). Tomato MYB21 Acts in Ovules to Mediate Jasmonate-Regulated Fertility. *Plant Cell*, *31*(5), 1043-1062. https://doi.org/10.1105/tpc.18.00978

Schubert, R., Grunewald, S., von Sivers, L., & Hause, B. (2019). Effects of Jasmonate on Ethylene Function during the Development of Tomato Stamens. *Plants (Basel)*, *8*(8). https://doi.org/10.3390/plants8080277

Schulze, A., Zimmer, M., Mielke, S., Stellmach, H., Melnyk, C. W., Hause, B., & Gasperini, D. (2019). Wound-Induced Shoot-to-Root Relocation of JA-Ile Precursors Coordinates Arabidopsis Growth. *Mol Plant*, *12*(10), 1383-1394. https://doi.org/10.1016/j.molp.2019.05.013

Schweizer, F., Fernandez-Calvo, P., Zander, M., Diez-Diaz, M., Fonseca, S., Glauser, G., Lewsey, M. G., Ecker, J. R., Solano, R., & Reymond, P. (2013). Arabidopsis basic helix-loop-helix transcription factors MYC2, MYC3, and MYC4 regulate glucosinolate biosynthesis, insect performance, and feeding behavior. *Plant Cell*, *25*(8), 3117-3132. https://doi.org/10.1105/tpc.113.115139

Sehr, E. M., Agusti, J., Lehner, R., Farmer, E. E., Schwarz, M., & Greb, T. (2010). Analysis of secondary growth in the Arabidopsis shoot reveals a positive role of jasmonate signalling in cambium formation. *Plant J*, *63*(5), 811-822. https://doi.org/10.1111/j.1365-313X.2010.04283.x

Seo, H. S., Song, J. T., Cheong, J. J., Lee, Y. H., Lee, Y. W., Hwang, I., Lee, J. S., & Choi, Y. D. (2001). Jasmonic acid carboxyl methyltransferase: a key enzyme for jasmonate-regulated plant responses. *Proc Natl Acad Sci U S A*, *98*(8), 4788-4793. https://doi.org/10.1073/pnas.081557298

Seo, Y. S., Kim, E. Y., Kim, J. H., & Kim, W. T. (2009). Enzymatic characterization of class I DAD1-like acylhydrolase members targeted to chloroplast in Arabidopsis. *FEBS Lett*, *583*(13), 2301-2307. https://doi.org/10.1016/j.febslet.2009.06.021

Shalem, O., Sanjana, N. E., & Zhang, F. (2015). High-throughput functional genomics using CRISPR-Cas9. *Nat Rev Genet*, *16*(5), 299-311. https://doi.org/10.1038/nrg3899

Shaner, N. C., Steinbach, P. A., & Tsien, R. Y. (2005). A guide to choosing fluorescent proteins. *Nat Methods*, *2*(12), 905-909. https://doi.org/10.1038/nmeth819

Sheard, L. B., Tan, X., Mao, H., Withers, J., Ben-Nissan, G., Hinds, T. R., Kobayashi, Y., Hsu, F. F., Sharon, M., Browse, J., He, S. Y., Rizo, J., Howe, G. A., & Zheng, N. (2010). Jasmonate perception by inositol-phosphate-potentiated COI1-JAZ co-receptor. *Nature*, *468*(7322), 400-405. https://doi.org/10.1038/nature09430

Shin, J., Heidrich, K., Sanchez-Villarreal, A., Parker, J. E., & Davis, S. J. (2012). TIME FOR COFFEE represses accumulation of the MYC2 transcription factor to provide time-of-day regulation of jasmonate signaling in Arabidopsis. *Plant Cell*, *24*(6), 2470-2482. https://doi.org/10.1105/tpc.111.095430

Shyu, C., Figueroa, P., Depew, C. L., Cooke, T. F., Sheard, L. B., Moreno, J. E., Katsir, L., Zheng, N., Browse, J., & Howe, G. A. (2012). JAZ8 lacks a canonical degron and has an EAR motif that mediates transcriptional repression of jasmonate responses in Arabidopsis. *Plant Cell*, *24*(2), 536-550. https://doi.org/10.1105/tpc.111.093005

Silverstone, A. L., Ciampaglio, C. N., & Sun, T. (1998). The Arabidopsis RGA gene encodes a transcriptional regulator repressing the gibberellin signal transduction pathway. *Plant Cell*, *10*(2), 155-169. https://doi.org/10.1105/tpc.10.2.155

Skowyra, D., Craig, K. L., Tyers, M., Elledge, S. J., & Harper, J. W. (1997). F-box proteins are receptors that recruit phosphorylated substrates to the SCF ubiquitin-ligase complex. *Cell*, *91*(2), 209-219. https://doi.org/10.1016/s0092-8674(00)80403-1

Smalle, J., & Vierstra, R. D. (2004). The ubiquitin 26S proteasome proteolytic pathway. *Annu Rev Plant Biol*, *55*, 555-590. https://doi.org/10.1146/annurev.arplant.55.031903.141801

Smirnova, E., Marquis, V., Poirier, L., Aubert, Y., Zumsteg, J., Menard, R., Miesch, L., & Heitz, T. (2017). Jasmonic Acid Oxidase 2 Hydroxylates Jasmonic Acid and Represses Basal Defense and Resistance Responses against Botrytis cinerea Infection. *Mol Plant*, *10*(9), 1159-1173. https://doi.org/10.1016/j.molp.2017.07.010

Sohrabi, R., Huh, J. H., Badieyan, S., Rakotondraibe, L. H., Kliebenstein, D. J., Sobrado, P., & Tholl, D. (2015). In planta variation of volatile biosynthesis: an alternative biosynthetic route to the formation of the pathogen-induced volatile homoterpene DMNT via triterpene degradation in Arabidopsis roots. *Plant Cell*, *27*(3), 874-890. https://doi.org/10.1105/tpc.114.132209

Song, S., Huang, H., Wang, J., Liu, B., Qi, T., & Xie, D. (2017). MYC5 is Involved in Jasmonate-Regulated Plant Growth, Leaf Senescence and Defense Responses. *Plant Cell Physiol*, *58*(10), 1752-1763. https://doi.org/10.1093/pcp/pcx112

Song, S., Qi, T., Fan, M., Zhang, X., Gao, H., Huang, H., Wu, D., Guo, H., & Xie, D. (2013). The bHLH subgroup IIId factors negatively regulate jasmonate-mediated plant defense and development. *PLoS Genet*, *9*(7), e1003653. https://doi.org/10.1371/journal.pgen.1003653

Song, S., Qi, T., Huang, H., Ren, Q., Wu, D., Chang, C., Peng, W., Liu, Y., Peng, J., & Xie, D. (2011). The Jasmonate-ZIM domain proteins interact with the R2R3-MYB transcription factors MYB21 and MYB24 to affect Jasmonate-regulated stamen development in Arabidopsis. *Plant Cell*, *23*(3), 1000-1013. https://doi.org/10.1105/tpc.111.083089

Soundappan, I., Bennett, T., Morffy, N., Liang, Y., Stanga, J. P., Abbas, A., Leyser, O., & Nelson, D. C. (2015). SMAX1-LIKE/D53 Family Members Enable Distinct MAX2-Dependent Responses to Strigolactones and Karrikins in Arabidopsis. *Plant Cell*, *27*(11), 3143-3159. https://doi.org/10.1105/tpc.15.00562

Srivastava, A. K., Lu, Y., Zinta, G., Lang, Z., & Zhu, J. K. (2018). UTR-Dependent Control of Gene Expression in Plants. *Trends Plant Sci*, *23*(3), 248-259. https://doi.org/10.1016/j.tplants.2017.11.003

Staswick, P. E., Su, W., & Howell, S. H. (1992). Methyl jasmonate inhibition of root growth and induction of a leaf protein are decreased in an Arabidopsis thaliana mutant. *Proc Natl Acad Sci U S A*, *89*(15), 6837-6840.

Staswick, P. E., & Tiryaki, I. (2004). The oxylipin signal jasmonic acid is activated by an enzyme that conjugates it to isoleucine in Arabidopsis. *Plant Cell*, *16*(8), 2117-2127. https://doi.org/10.1105/tpc.104.023549

Stenzel, I., Hause, B., Maucher, H., Pitzschke, A., Miersch, O., Ziegler, J., Ryan, C. A., & Wasternack, C. (2003). Allene oxide cyclase dependence of the wound response and vascular bundle-specific generation of jasmonates in tomato - amplification in wound signalling. *Plant J*, *33*(3), 577-589. https://doi.org/10.1046/j.1365-313x.2003.01647.x

Stitz, M., Gase, K., Baldwin, I. T., & Gaquerel, E. (2011). Ectopic expression of AtJMT in Nicotiana attenuata: creating a metabolic sink has tissue-specific consequences for the jasmonate metabolic network and silences downstream gene expression. *Plant Physiol*, *157*(1), 341-354. https://doi.org/10.1104/pp.111.178582

Strauss, S. Y., & Agrawal, A. A. (1999). The ecology and evolution of plant tolerance to herbivory. *Trends Ecol Evol*, *14*(5), 179-185. https://doi.org/10.1016/s0169-5347(98)01576-6

Stuhlfelder, C., Mueller, M. J., & Warzecha, H. (2004). Cloning and expression of a tomato cDNA encoding a methyl jasmonate cleaving esterase. *Eur J Biochem*, *271*(14), 2976-2983. https://doi.org/10.1111/j.1432-1033.2004.04227.x

Su, S. H., Gibbs, N. M., Jancewicz, A. L., & Masson, P. H. (2017). Molecular Mechanisms of Root Gravitropism. *Curr Biol*, *27*(17), R964-R972. https://doi.org/10.1016/j.cub.2017.07.015

Sun, T. P. (2010). Gibberellin-GID1-DELLA: a pivotal regulatory module for plant growth and development. *Plant Physiol*, *154*(2), 567-570. https://doi.org/10.1104/pp.110.161554
Suzuki, K., Takaoka, Y., & Ueda, M. (2021). Rational design of a stapled JAZ9 peptide inhibiting protein-protein interaction of a plant transcription factor. *RSC Chem Biol*, *2*(2), 499-502. https://doi.org/10.1039/d0cb00204f
Symons, G. M., Ross, J. J., Jager, C. E., & Reid, J. B. (2008). Brassinosteroid transport. *J Exp Bot*, *59*(1), 17-24. https://doi.org/10.1093/jxb/erm098
Takaoka, Y., Iwahashi, M., Chini, A., Saito, H., Ishimaru, Y., Egoshi, S., Kato, N., Tanaka, M., Bashir, K., Seki, M., Solano, R., & Ueda, M. (2018). A rationally designed JAZ subtype-selective agonist of jasmonate perception. *Nat Commun*, *9*(1), 3654. https://doi.org/10.1038/s41467-018-06135-y
Takaoka, Y., Suzuki, K., Nozawa, A., Takahashi, H., Sawasaki, T., & Ueda, M. (2022). Protein-protein interactions between jasmonate-related master regulator MYC and transcriptional mediator MED25 depend on a short binding domain. *J Biol Chem*, *298*(1), 101504. https://doi.org/10.1016/j.jbc.2021.101504
Tamogami, S., Rakwal, R., & Agrawal, G. K. (2008). Interplant communication: airborne methyl jasmonate is essentially converted into JA and JA-Ile activating jasmonate signaling pathway and VOCs emission. *Biochem Biophys Res Commun*, *376*(4), 723-727. https://doi.org/10.1016/j.bbrc.2008.09.069
Thatcher, L. F., Cevik, V., Grant, M., Zhai, B., Jones, J. D., Manners, J. M., & Kazan, K. (2016). Characterization of a JAZ7 activation-tagged Arabidopsis mutant with increased susceptibility to the fungal pathogen Fusarium oxysporum. *J Exp Bot*, *67*(8), 2367-2386. https://doi.org/10.1093/jxb/erw040
Theodoulou, F. L., Job, K., Slocombe, S. P., Footitt, S., Holdsworth, M., Baker, A., Larson, T. R., & Graham, I. A. (2005). Jasmonic acid levels are reduced in COMATOSE ATP-binding cassette transporter mutants. Implications for transport of jasmonate precursors into peroxisomes. *Plant Physiol*, *137*(3), 835-840. https://doi.org/10.1104/pp.105.059352
Theologis, A. (1986). Rapid Gene-Regulation by Auxin. *Annual Review of Plant Physiology and Plant Molecular Biology*, *37*, 407-438. https://doi.org/DOI 10.1146/annurev.arplant.37.1.407
Thines, B., Katsir, L., Melotto, M., Niu, Y., Mandaokar, A., Liu, G., Nomura, K., He, S. Y., Howe, G. A., & Browse, J. (2007). JAZ repressor proteins are targets of the SCF(COI1) complex during jasmonate signalling. *Nature*, *448*(7154), 661-665. https://doi.org/10.1038/nature05960
Thines, B., Mandaokar, A., & Browse, J. (2013). Characterizing jasmonate regulation of male fertility in Arabidopsis. *Methods Mol Biol*, *1011*, 13-23. https://doi.org/10.1007/978-1-62703-414-2_2
Thines, B., Parlan, E. V., & Fulton, E. C. (2019). Circadian Network Interactions with Jasmonate Signaling and Defense. *Plants (Basel)*, *8*(8). https://doi.org/10.3390/plants8080252
Thireault, C., Shyu, C., Yoshida, Y., St Aubin, B., Campos, M. L., & Howe, G. A. (2015). Repression of jasmonate signaling by a non-TIFY JAZ protein in Arabidopsis. *Plant J*, *82*(4), 669-679. https://doi.org/10.1111/tpj.12841
Tian, C. E., Muto, H., Higuchi, K., Matamura, T., Tatematsu, K., Koshiba, T., & Yamamoto, K. T. (2004). Disruption and overexpression of auxin response factor 8 gene of Arabidopsis affect hypocotyl elongation and root growth habit, indicating its possible involvement in auxin homeostasis in light condition. *Plant J*, *40*(3), 333-343. https://doi.org/10.1111/j.1365-313X.2004.02220.x
Tian, Q., Uhlir, N. J., & Reed, J. W. (2002). Arabidopsis SHY2/IAA3 inhibits auxin-regulated gene expression. *Plant Cell*, *14*(2), 301-319. https://doi.org/10.1105/tpc.010283
Toda, Y., Tanaka, M., Ogawa, D., Kurata, K., Kurotani, K., Habu, Y., Ando, T., Sugimoto, K., Mitsuda, N., Katoh, E., Abe, K., Miyao, A., Hirochika, H., Hattori, T., & Takeda, S. (2013). RICE SALT SENSITIVE3 forms a ternary complex with JAZ and class-C bHLH factors and regulates jasmonate-induced

gene expression and root cell elongation. *Plant Cell*, *25*(5), 1709-1725. https://doi.org/10.1105/tpc.113.112052

Toledo-Ortiz, G., Huq, E., & Quail, P. H. (2003). The Arabidopsis basic/helix-loop-helix transcription factor family. *Plant Cell*, *15*(8), 1749-1770. https://doi.org/10.1105/tpc.013839

Tomato Genome, C. (2012). The tomato genome sequence provides insights into fleshy fruit evolution. *Nature*, *485*(7400), 635-641. https://doi.org/10.1038/nature11119

Toseland, C. P. (2013). Fluorescent labeling and modification of proteins. *J Chem Biol*, *6*(3), 85-95. https://doi.org/10.1007/s12154-013-0094-5

Toyama, B. H., & Hetzer, M. W. (2013). Protein homeostasis: live long, won't prosper. *Nat Rev Mol Cell Biol*, *14*(1), 55-61. https://doi.org/10.1038/nrm3496

Trapnell, C., Pachter, L., & Salzberg, S. L. (2009). TopHat: discovering splice junctions with RNA-Seq. *Bioinformatics*, *25*(9), 1105-1111. https://doi.org/10.1093/bioinformatics/btp120

Umehara, M., Hanada, A., Yoshida, S., Akiyama, K., Arite, T., Takeda-Kamiya, N., Magome, H., Kamiya, Y., Shirasu, K., Yoneyama, K., Kyozuka, J., & Yamaguchi, S. (2008). Inhibition of shoot branching by new terpenoid plant hormones. *Nature*, *455*(7210), 195-200. https://doi.org/10.1038/nature07272

Vain, T., Crowell, E. F., Timpano, H., Biot, E., Desprez, T., Mansoori, N., Trindade, L. M., Pagant, S., Robert, S., Hofte, H., Gonneau, M., & Vernhettes, S. (2014). The Cellulase KORRIGAN Is Part of the Cellulose Synthase Complex. *Plant Physiol*, *165*(4), 1521-1532. https://doi.org/10.1104/pp.114.241216

van der Velden, A. W., & Thomas, A. A. (1999). The role of the 5' untranslated region of an mRNA in translation regulation during development. *Int J Biochem Cell Biol*, *31*(1), 87-106. https://doi.org/10.1016/s1357-2725(98)00134-4

Vanneste, S., De Rybel, B., Beemster, G. T., Ljung, K., De Smet, I., Van Isterdael, G., Naudts, M., Iida, R., Gruissem, W., Tasaka, M., Inze, D., Fukaki, H., & Beeckman, T. (2005). Cell cycle progression in the pericycle is not sufficient for SOLITARY ROOT/IAA14-mediated lateral root initiation in Arabidopsis thaliana. *Plant Cell*, *17*(11), 3035-3050. https://doi.org/10.1105/tpc.105.035493

Vierstra, R. D. (2009). The ubiquitin-26S proteasome system at the nexus of plant biology. *Nat Rev Mol Cell Biol*, *10*(6), 385-397. https://doi.org/10.1038/nrm2688

Vijayan, P., Shockey, J., Levesque, C. A., Cook, R. J., & Browse, J. (1998). A role for jasmonate in pathogen defense of Arabidopsis. *Proc Natl Acad Sci U S A*, *95*(12), 7209-7214. https://doi.org/10.1073/pnas.95.12.7209

Voges, D., Zwickl, P., & Baumeister, W. (1999). The 26S proteasome: a molecular machine designed for controlled proteolysis. *Annu Rev Biochem*, *68*, 1015-1068. https://doi.org/10.1146/annurev.biochem.68.1.1015

Wang, D. D., Li, P., Chen, Q. Y., Chen, X. Y., Yan, Z. W., Wang, M. Y., & Mao, Y. B. (2021). Differential Contributions of MYCs to Insect Defense Reveals Flavonoids Alleviating Growth Inhibition Caused by Wounding in Arabidopsis. *Front Plant Sci*, *12*, 700555. https://doi.org/10.3389/fpls.2021.700555

Wang, K., Guo, Q., Froehlich, J. E., Hersh, H. L., Zienkiewicz, A., Howe, G. A., & Benning, C. (2018). Two Abscisic Acid-Responsive Plastid Lipase Genes Involved in Jasmonic Acid Biosynthesis in Arabidopsis thaliana. *Plant Cell*, *30*(5), 1006-1022. https://doi.org/10.1105/tpc.18.00250

Wang, L., Wang, B., Jiang, L., Liu, X., Li, X., Lu, Z., Meng, X., Wang, Y., Smith, S. M., & Li, J. (2015). Strigolactone Signaling in Arabidopsis Regulates Shoot Development by Targeting D53-Like SMXL Repressor Proteins for Ubiquitination and Degradation. *Plant Cell*, *27*(11), 3128-3142. https://doi.org/10.1105/tpc.15.00605

Wang, S., Li, S., Wang, J., Li, Q., Xin, X. F., Zhou, S., Wang, Y., Li, D., Xu, J., Luo, Z. Q., He, S. Y., & Sun, W. (2021). A bacterial kinase phosphorylates OSK1 to suppress stomatal immunity in rice. *Nat Commun*, *12*(1), 5479. https://doi.org/10.1038/s41467-021-25748-4

Wasternack, C., & Feussner, I. (2018). The Oxylipin Pathways: Biochemistry and Function. *Annu Rev Plant Biol*, *69*, 363-386. https://doi.org/10.1146/annurev-arplant-042817-040440

Wasternack, C., & Hause, B. (2013). Jasmonates: biosynthesis, perception, signal transduction and action in plant stress response, growth and development. An update to the 2007 review in Annals of Botany. *Ann Bot*, *111*(6), 1021-1058. https://doi.org/10.1093/aob/mct067

Wasternack, C., & Strnad, M. (2018). Jasmonates: News on Occurrence, Biosynthesis, Metabolism and Action of an Ancient Group of Signaling Compounds. *Int J Mol Sci*, *19*(9). https://doi.org/10.3390/ijms19092539

Westfall, C. S., Zubieta, C., Herrmann, J., Kapp, U., Nanao, M. H., & Jez, J. M. (2012). Structural basis for prereceptor modulation of plant hormones by GH3 proteins. *Science*, *336*(6089), 1708-1711. https://doi.org/10.1126/science.1221863

Widemann, E., Miesch, L., Lugan, R., Holder, E., Heinrich, C., Aubert, Y., Miesch, M., Pinot, F., & Heitz, T. (2013). The amidohydrolases IAR3 and ILL6 contribute to jasmonoyl-isoleucine hormone turnover and generate 12-hydroxyjasmonic acid upon wounding in Arabidopsis leaves. *J Biol Chem*, *288*(44), 31701-31714. https://doi.org/10.1074/jbc.M113.499228

Windels, D., Bielewicz, D., Ebneter, M., Jarmolowski, A., Szweykowska-Kulinska, Z., & Vazquez, F. (2014). miR393 is required for production of proper auxin signalling outputs. *PLoS One*, *9*(4), e95972. https://doi.org/10.1371/journal.pone.0095972

Winkler, M., Niemeyer, M., Hellmuth, A., Janitza, P., Christ, G., Samodelov, S. L., Wilde, V., Majovsky, P., Trujillo, M., Zurbriggen, M. D., Hoehenwarter, W., Quint, M., & Calderon Villalobos, L. I. A. (2017). Variation in auxin sensing guides AUX/IAA transcriptional repressor ubiquitylation and destruction. *Nat Commun*, *8*, 15706. https://doi.org/10.1038/ncomms15706

Withers, J., Yao, J., Mecey, C., Howe, G. A., Melotto, M., & He, S. Y. (2012). Transcription factor-dependent nuclear localization of a transcriptional repressor in jasmonate hormone signaling. *Proc Natl Acad Sci U S A*, *109*(49), 20148-20153. https://doi.org/10.1073/pnas.1210054109

Wu, D., Qi, T., Li, W. X., Tian, H., Gao, H., Wang, J., Ge, J., Yao, R., Ren, C., Wang, X. B., Liu, Y., Kang, L., Ding, S. W., & Xie, D. (2017). Viral effector protein manipulates host hormone signaling to attract insect vectors. *Cell Res*, *27*(3), 402-415. https://doi.org/10.1038/cr.2017.2

Wu, J., Wang, L., & Baldwin, I. T. (2008). Methyl jasmonate-elicited herbivore resistance: does MeJA function as a signal without being hydrolyzed to JA? *Planta*, *227*(5), 1161-1168. https://doi.org/10.1007/s00425-008-0690-8

Wu, K., Zhang, L., Zhou, C., Yu, C. W., & Chaikam, V. (2008). HDA6 is required for jasmonate response, senescence and flowering in Arabidopsis. *J Exp Bot*, *59*(2), 225-234. https://doi.org/10.1093/jxb/erm300

Xie, D. X., Feys, B. F., James, S., Nieto-Rostro, M., & Turner, J. G. (1998). COI1: an Arabidopsis gene required for jasmonate-regulated defense and fertility. *Science*, *280*(5366), 1091-1094. https://doi.org/10.1126/science.280.5366.1091

Yamaguchi, S. (2008). Gibberellin metabolism and its regulation. *Annu Rev Plant Biol*, *59*, 225-251. https://doi.org/10.1146/annurev.arplant.59.032607.092804

Yan, C., & Xie, D. (2015). Jasmonate in plant defence: sentinel or double agent? *Plant Biotechnol J*, *13*(9), 1233-1240. https://doi.org/10.1111/pbi.12417

Yan, J., Li, H., Li, S., Yao, R., Deng, H., Xie, Q., & Xie, D. (2013). The Arabidopsis F-box protein CORONATINE INSENSITIVE1 is stabilized by SCFCOI1 and degraded via the 26S proteasome pathway. *Plant Cell*, *25*(2), 486-498. https://doi.org/10.1105/tpc.112.105486

Yan, Y., Stolz, S., Chetelat, A., Reymond, P., Pagni, M., Dubugnon, L., & Farmer, E. E. (2007). A downstream mediator in the growth repression limb of the jasmonate pathway. *Plant Cell*, *19*(8), 2470-2483. https://doi.org/10.1105/tpc.107.050708

Yang, D. L., Yao, J., Mei, C. S., Tong, X. H., Zeng, L. J., Li, Q., Xiao, L. T., Sun, T. P., Li, J., Deng, X. W., Lee, C. M., Thomashow, M. F., Yang, Y., He, Z., & He, S. Y. (2012). Plant hormone jasmonate prioritizes defense over growth by interfering with gibberellin signaling cascade. *Proc Natl Acad Sci U S A*, *109*(19), E1192-1200. https://doi.org/10.1073/pnas.1201616109

Yang, J., Duan, G., Li, C., Liu, L., Han, G., Zhang, Y., & Wang, C. (2019). The Crosstalks Between Jasmonic Acid and Other Plant Hormone Signaling Highlight the Involvement of Jasmonic Acid as a Core Component in Plant Response to Biotic and Abiotic Stresses. *Front Plant Sci*, *10*, 1349. https://doi.org/10.3389/fpls.2019.01349

Yang, J. Y., Iwasaki, M., Machida, C., Machida, Y., Zhou, X., & Chua, N. H. (2008). betaC1, the pathogenicity factor of TYLCCNV, interacts with AS1 to alter leaf development and suppress selective jasmonic acid responses. *Genes Dev*, *22*(18), 2564-2577. https://doi.org/10.1101/gad.1682208

Yang, M., Hu, Y., Lodhi, M., McCombie, W. R., & Ma, H. (1999). The Arabidopsis SKP1-LIKE1 gene is essential for male meiosis and may control homologue separation. *Proc Natl Acad Sci U S A*, *96*(20), 11416-11421. https://doi.org/10.1073/pnas.96.20.11416

Yang, W., Devaiah, S. P., Pan, X., Isaac, G., Welti, R., & Wang, X. (2007). AtPLAI is an acyl hydrolase involved in basal jasmonic acid production and Arabidopsis resistance to Botrytis cinerea. *J Biol Chem*, *282*(25), 18116-18128. https://doi.org/10.1074/jbc.M700405200

Yang, Z., Huang, Y., Yang, J., Yao, S., Zhao, K., Wang, D., Qin, Q., Bian, Z., Li, Y., Lan, Y., Zhou, T., Wang, H., Liu, C., Wang, W., Qi, Y., Xu, Z., & Li, Y. (2020). Jasmonate Signaling Enhances RNA Silencing and Antiviral Defense in Rice. *Cell Host Microbe*, *28*(1), 89-103 e108. https://doi.org/10.1016/j.chom.2020.05.001

Ye, H., Du, H., Tang, N., Li, X., & Xiong, L. (2009). Identification and expression profiling analysis of TIFY family genes involved in stress and phytohormone responses in rice. *Plant Mol Biol*, *71*(3), 291-305. https://doi.org/10.1007/s11103-009-9524-8

Yilmaz, A., Mejia-Guerra, M. K., Kurz, K., Liang, X., Welch, L., & Grotewold, E. (2011). AGRIS: the Arabidopsis Gene Regulatory Information Server, an update. *Nucleic Acids Res*, *39*(Database issue), D1118-1122. https://doi.org/10.1093/nar/gkq1120

Yoshida, Y., Sano, R., Wada, T., Takabayashi, J., & Okada, K. (2009). Jasmonic acid control of GLABRA3 links inducible defense and trichome patterning in Arabidopsis. *Development*, *136*(6), 1039-1048. https://doi.org/10.1242/dev.030585

Zander, M., Lewsey, M. G., Clark, N. M., Yin, L., Bartlett, A., Saldierna Guzman, J. P., Hann, E., Langford, A. E., Jow, B., Wise, A., Nery, J. R., Chen, H., Bar-Joseph, Z., Walley, J. W., Solano, R., & Ecker, J. R. (2020). Integrated multi-omics framework of the plant response to jasmonic acid. *Nat Plants*, *6*(3), 290-302. https://doi.org/10.1038/s41477-020-0605-7

Zavala, J. A., & Baldwin, I. T. (2006). Jasmonic acid signalling and herbivore resistance traits constrain regrowth after herbivore attack in Nicotiana attenuata. *Plant Cell Environ*, *29*(9), 1751-1760. https://doi.org/10.1111/j.1365-3040.2006.01551.x

Zhai, Q., Zhang, X., Wu, F., Feng, H., Deng, L., Xu, L., Zhang, M., Wang, Q., & Li, C. (2015). Transcriptional Mechanism of Jasmonate Receptor COI1-Mediated Delay of Flowering Time in Arabidopsis. *Plant Cell*, *27*(10), 2814-2828. https://doi.org/10.1105/tpc.15.00619

Zhang, C., Ding, Z., Wu, K., Yang, L., Li, Y., Yang, Z., Shi, S., Liu, X., Zhao, S., Yang, Z., Wang, Y., Zheng, L., Wei, J., Du, Z., Zhang, A., Miao, H., Li, Y., Wu, Z., & Wu, J. (2016). Suppression of Jasmonic Acid-Mediated Defense by Viral-Inducible MicroRNA319 Facilitates Virus Infection in Rice. *Mol Plant*, *9*(9), 1302-1314. https://doi.org/10.1016/j.molp.2016.06.014

Zhang, F., Ke, J., Zhang, L., Chen, R., Sugimoto, K., Howe, G. A., Xu, H. E., Zhou, M., He, S. Y., & Melcher, K. (2017). Structural insights into alternative splicing-mediated desensitization of jasmonate signaling. *Proc Natl Acad Sci U S A*, *114*(7), 1720-1725. https://doi.org/10.1073/pnas.1616938114

Zhang, F., Yao, J., Ke, J., Zhang, L., Lam, V. Q., Xin, X. F., Zhou, X. E., Chen, J., Brunzelle, J., Griffin, P. R., Zhou, M., Xu, H. E., Melcher, K., & He, S. Y. (2015). Structural basis of JAZ repression of MYC transcription factors in jasmonate signalling. *Nature*, *525*(7568), 269-273. https://doi.org/10.1038/nature14661

Zhang, L., You, J., & Chan, Z. (2015). Identification and characterization of TIFY family genes in Brachypodium distachyon. *J Plant Res*, *128*(6), 995-1005. https://doi.org/10.1007/s10265-015-0755-2

Zhang, Y., Gao, M., Singer, S. D., Fei, Z., Wang, H., & Wang, X. (2012). Genome-wide identification and analysis of the TIFY gene family in grape. *PLoS One*, *7*(9), e44465. https://doi.org/10.1371/journal.pone.0044465

Zhang, Y., & Turner, J. G. (2008). Wound-induced endogenous jasmonates stunt plant growth by inhibiting mitosis. *PLoS One*, *3*(11), e3699. https://doi.org/10.1371/journal.pone.0003699

Zhang, Z., Li, X., Yu, R., Han, M., & Wu, Z. (2015). Isolation, structural analysis, and expression characteristics of the maize TIFY gene family. *Mol Genet Genomics*, *290*(5), 1849-1858. https://doi.org/10.1007/s00438-015-1042-6

Zhao, Y. (2008). The role of local biosynthesis of auxin and cytokinin in plant development. *Curr Opin Plant Biol*, *11*(1), 16-22. https://doi.org/10.1016/j.pbi.2007.10.008

Zheng, X. Y., Spivey, N. W., Zeng, W., Liu, P. P., Fu, Z. Q., Klessig, D. F., He, S. Y., & Dong, X. (2012). Coronatine promotes Pseudomonas syringae virulence in plants by activating a signaling cascade that inhibits salicylic acid accumulation. *Cell Host Microbe*, *11*(6), 587-596. https://doi.org/10.1016/j.chom.2012.04.014

Zhou, C., Zhang, L., Duan, J., Miki, B., & Wu, K. (2005). HISTONE DEACETYLASE19 is involved in jasmonic acid and ethylene signaling of pathogen response in Arabidopsis. *Plant Cell*, *17*(4), 1196-1204. https://doi.org/10.1105/tpc.104.028514

Zhou, W., Yao, R., Li, H., Li, S., & Yan, J. (2013). New perspective on the stabilization and degradation of the F-box protein COI1 in Arabidopsis. *Plant Signal Behav*, *8*(8). https://doi.org/10.4161/psb.24973

Zhu, C., Gan, L., Shen, Z., & Xia, K. (2006). Interactions between jasmonates and ethylene in the regulation of root hair development in Arabidopsis. *J Exp Bot*, *57*(6), 1299-1308. https://doi.org/10.1093/jxb/erj103

Zhu, Z., An, F., Feng, Y., Li, P., Xue, L., A, M., Jiang, Z., Kim, J. M., To, T. K., Li, W., Zhang, X., Yu, Q., Dong, Z., Chen, W. Q., Seki, M., Zhou, J. M., & Guo, H. (2011). Derepression of ethylene-stabilized transcription factors (EIN3/EIL1) mediates jasmonate and ethylene signaling synergy in Arabidopsis. *Proc Natl Acad Sci U S A*, *108*(30), 12539-12544. https://doi.org/10.1073/pnas.1103959108

Appendix

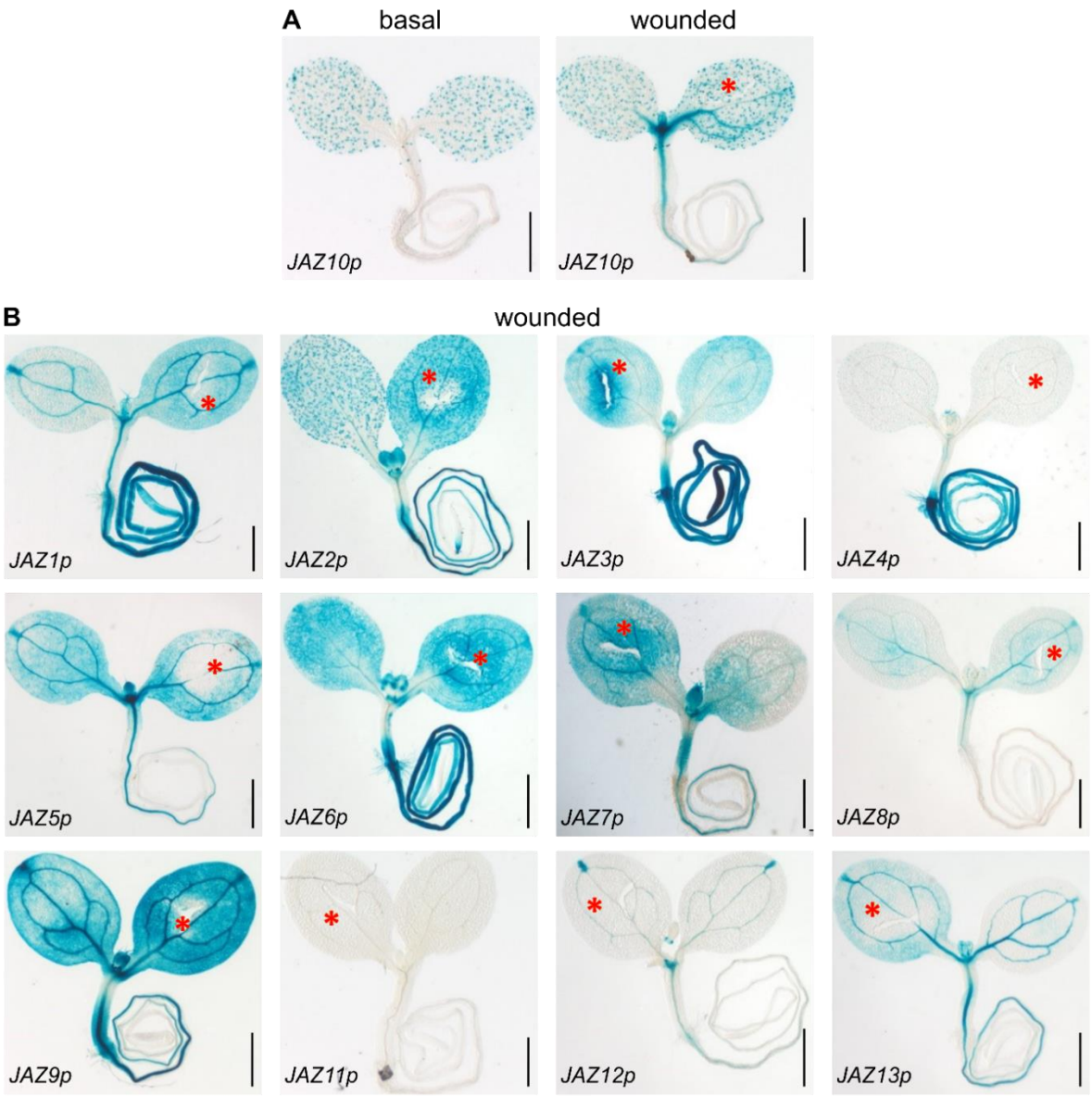

Figure S1: Shoot wounding elevates promoter activity for most of the *JAZs*. (**A,B**) Representative image of 5-do GUS stained *JAZp:GUS* seedlings 2h after shoot wounding. (**A**) The principle of shoot wounding demonstrated on *JAZ10p:GUS*. left: unwounded seedling; right: wounded seedling. (**B**) *JAZp:GUS* activity of remaining *JAZ* promoters (*JAZ1-JAZ9* and *JAZ11-JAZ13*) after shoot wounding. Asterisks indicate wounding sites. Scale bar = 0.5 mm.

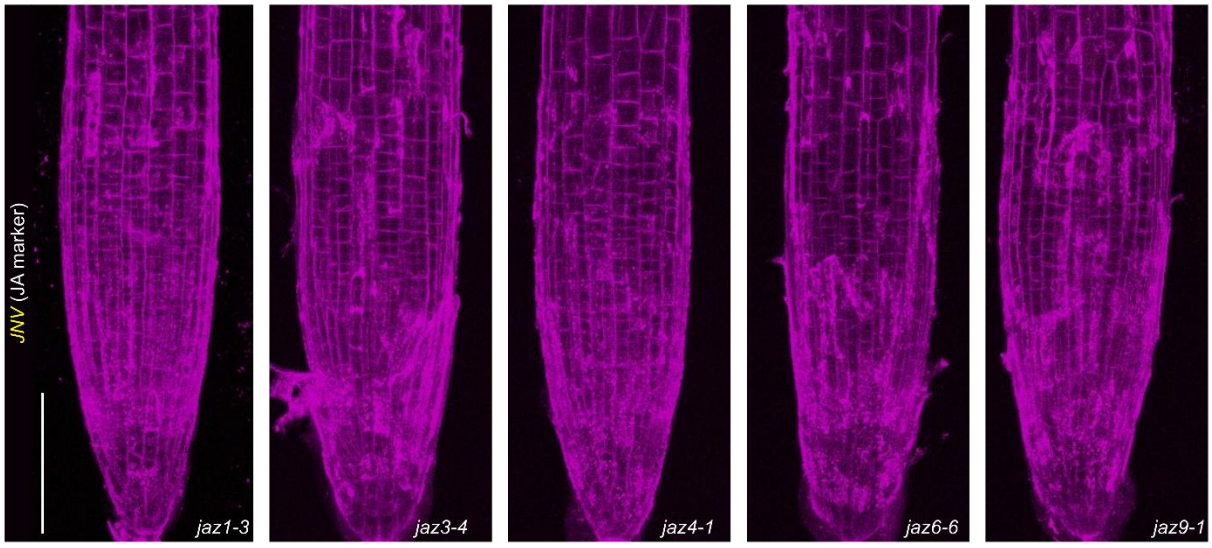

Figure S2: Most of the single order *jaz* mutants tested display no *JNV* activation in the root tip. *JAZ10p:NLS-3xVEN* (*JNV*; yellow) activity in *jaz-1-3*, *jaz3-4,jaz6-6,* and *jaz9-1* 5-do root tips. Images represent 3D Z-stack volume renderings (n = 10). Samples were counterstained with propidium iodide (magenta). Scale bar = 100 µm.

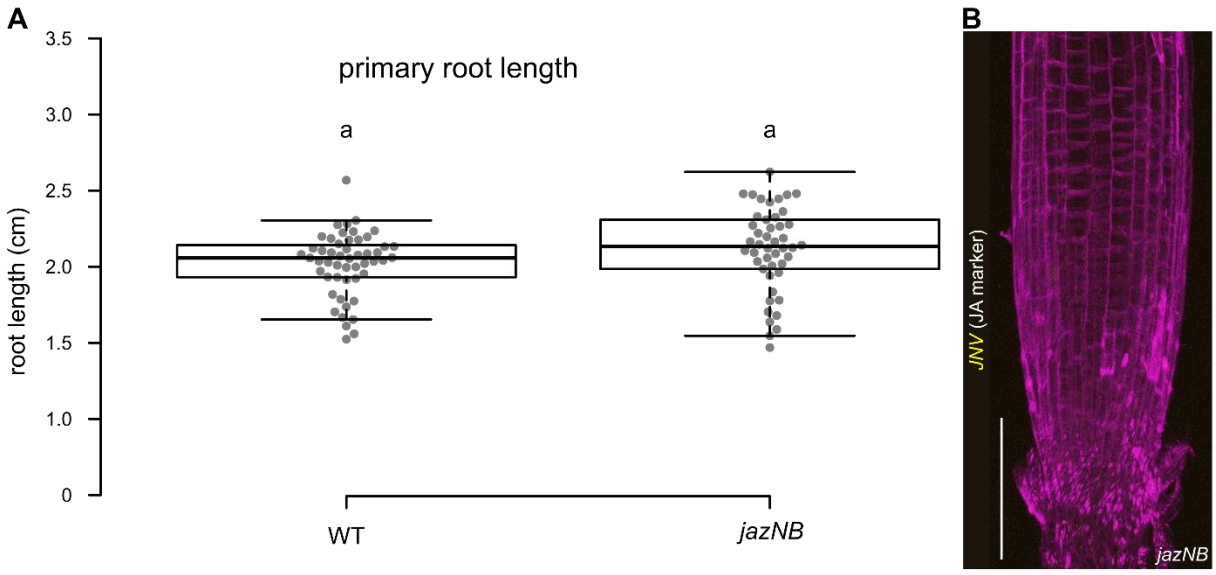

Figure S3: The multiple order mutant *jaz7-1 jaz8-v jaz10-1 jaz13-1* (*jazNB*) mutant exhibits no obvious phenotype. (**A**) Box plot summary of primary root length of 7-do seedlings in indicated genotypes. Medians are represented inside the boxes by solid lines, circles depict individual measurements (n = 45-60). Letters denote statistically significant differences among samples as determined by One-Way ANOVA analysis followed by Tukey's HSD test ($p<0.05$). Results presented were similar across 3 independent experiments). (**B**) *JNV* (yellow) expression in *jazNB* 5-do root tips. Images represent 3D Z-stack volume renderings (n = 10). Samples were counterstained with propidium iodide (magenta). Scale bar = 100 µm.

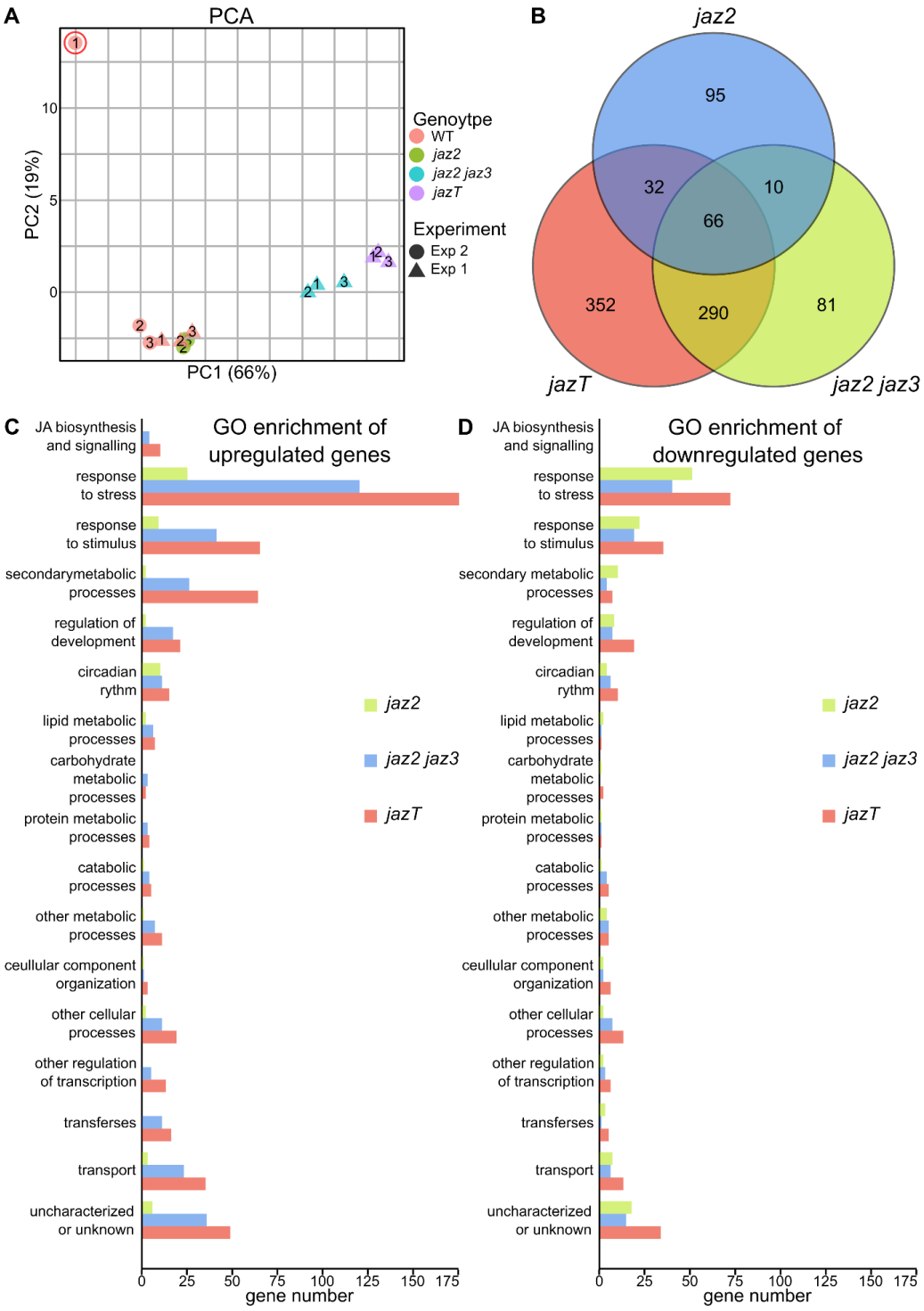

Figure S4: (extended information) Root tip transcriptome analysis reveals differentially expressed genes (DEGs) in *jaz2-6* (*jaz2*), *jaz2-6 jaz3-4* (*jaz2 jaz3*), and *jaz1-3 jaz2-6 jaz3-4* (*jazT*). (**A**) Principal component analysis (PCA) of biological replicates from indicated genotypes collected on two separate days. One WT biological replicate which was removed in Figure 14 is circled in red (Exp1 = first sample collection day; Exp2 = second sample collection day). (**B**) Schematic representation of overlapping different expressed genes (DEGs) between *jaz2*, *jaz2 jaz3*, and *jazT*. (**C,D**) Gene ontology (GO) enriched terms of DEGs in *jaz2*, *jaz2 jaz3*, and *jazT*. The indicated genotypes were normalized to the WT (cutoff: log2FC = ±1; p-value: 0.01). (aspect "biological process"; false discovery rate < 0.05). Full dataset is available in Supplementary Tables S2. (n = 3, each biological replicate contains a pool of ~180 root tips of 5-do seedlings). (**C**) GO enrichment of upregulated genes. (**D**) GO enrichment of downregulated genes.

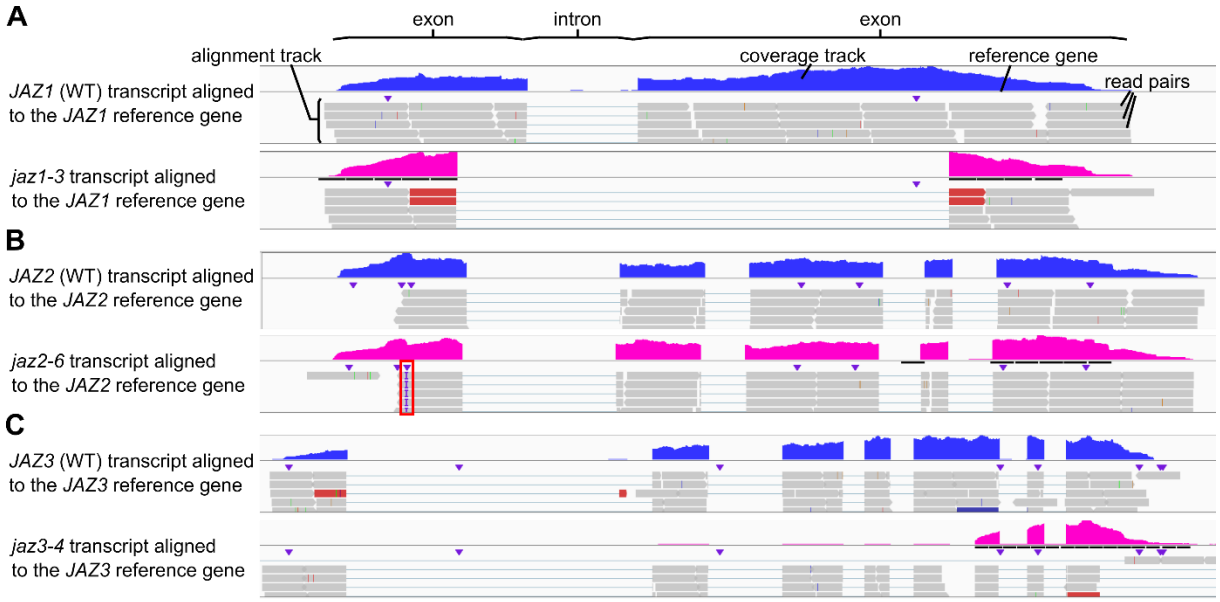

Figure S5: RNA-seq analysis confirms mutations in the transcripts of *jaz1-3*, *jaz2-6*, and *jaz3-4* alleles. (**A-C**) Alignment reads of *JAZ1*, *JAZ2*, and *JAZ3* transcripts in WT and *jazT* root tips from Figure 14 to the associated reference gene (n=180). Grey arrows denote read pairs counts within the alignment track. Coverage tracks denote the depth of the reads displayed at each locus (blue read coverage track = WT; magenta read coverage track = mutant). (**A**) Alignment results of *jaz1-3* and WT *JAZ1* transcripts. *jaz1-3* transcripts exhibit a major sequence deletion in the centre of the transcript. (**B**) Alignment results of *jaz2-6* and WT *JAZ2* transcripts. *jaz2-6* transcripts exhibit one bp insertion (red frame) in the first exon. (**C**) Alignment results of *jaz3-4* and WT *JAZ3* transcripts. *jaz3-4* transcripts exhibit only WT alignment to the last 3 exons.

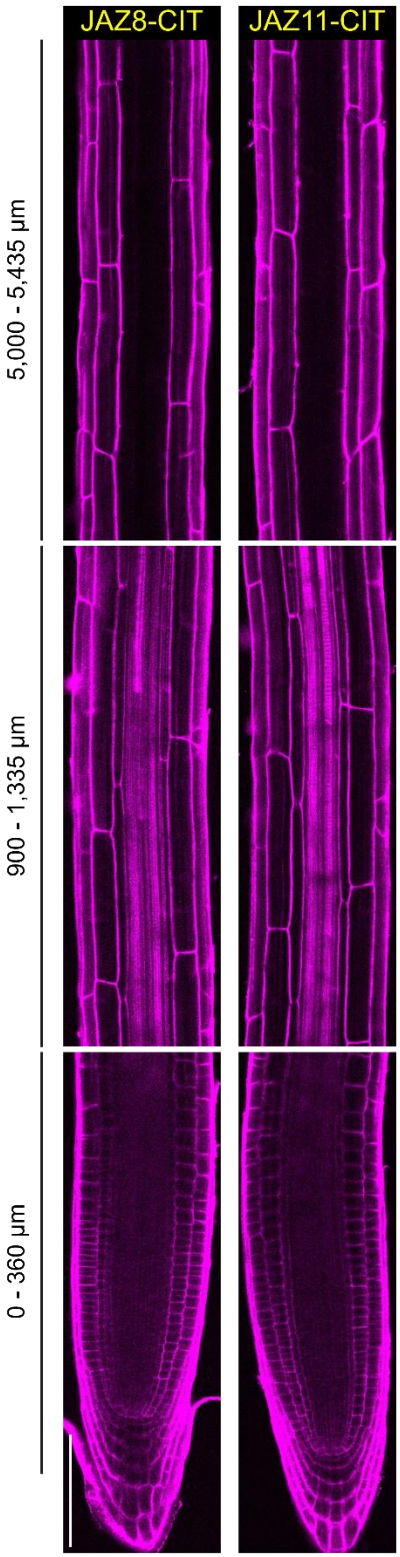

Figure S6: *JAZp8:JAZ8-CIT* and *JAZ11p:JAZ11-CIT* negative controls display no protein localization in the root. Representative images of longitudinal optical sections of 5-do *JAZp:JAZ-CIT* reporter roots stained with PI (magenta), potentially displaying JAZ-CIT (yellow) expression, and imaged live (n=10, from two independent T_3 lines for each construct). Black bars indicate the distance from the quiescent centre (QC) towards the shoot (0-270 µm: division and elongation zone; 900-1,335 µm: EDZ; 5,000-5,425 µm: LDZ). Scale bar =100 µm.

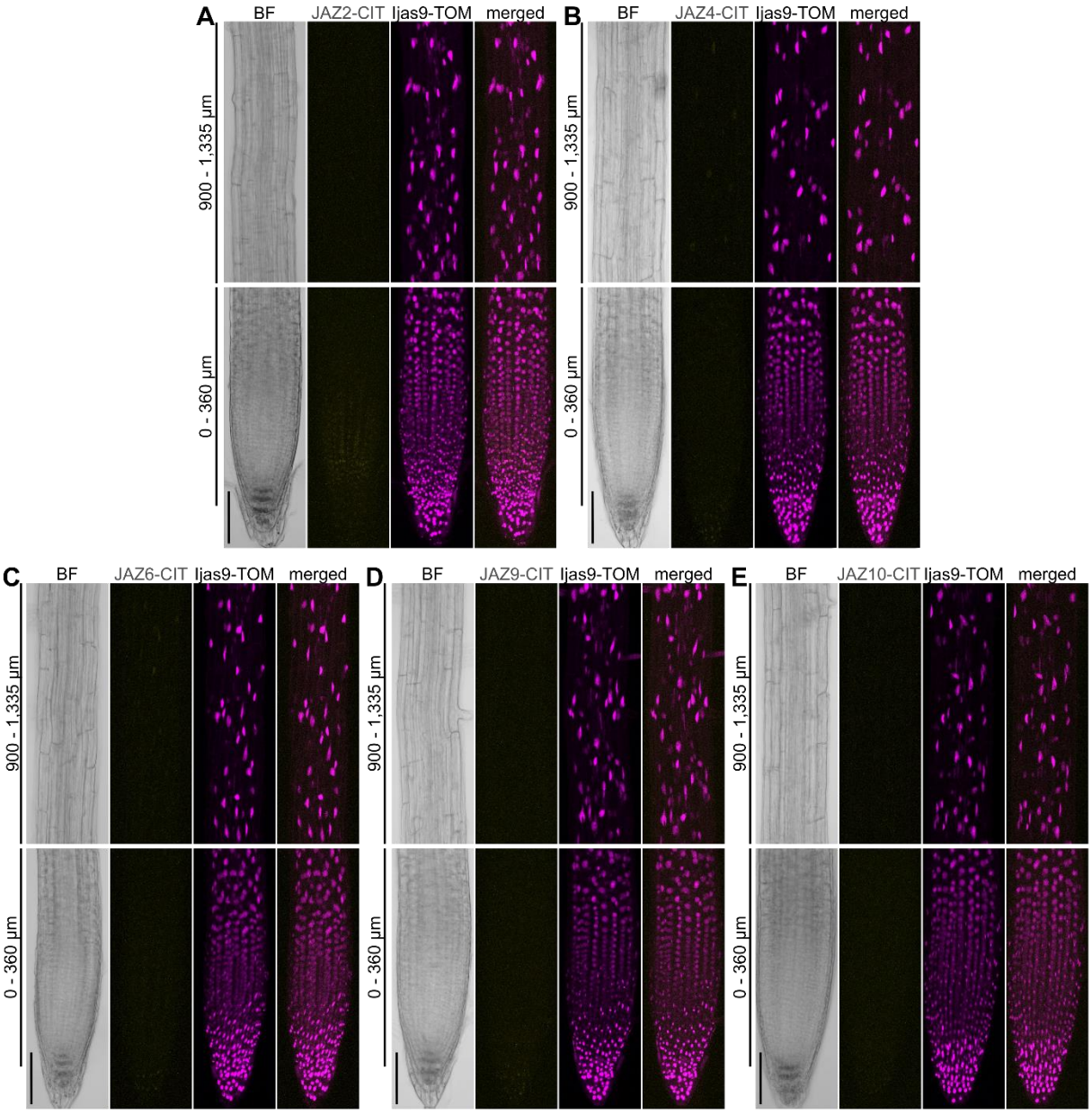

Figure S7: The majority of *rat.JAZp:JAZ-CIT* reporter display no or only weak JAZ-CIT signal in *jaz* mutant backgrounds. (**A-E**) Representative root images of 3D Z-stack volume renderings of 5-do (**A**) *rat.JAZ2p:JAZ2-CIT jaz2-6,* (**B**) *rat.JAZ4p:JAZ4-CIT jaz4-1,* (**C**) *rat.JAZ6p:JAZ6-CIT jaz6-6,* (**D**) *rat.JAZ9p:JAZ9-CIT jaz9-1* and (**E**) *JAZ10p:JAZ10-CIT jaz10-1* seedlings in bright filed (BF), JAZ-CIT (yellow), and Ijas9-TOM (magenta) channels (n=10 roots from two independent T_3 lines). Black bars indicate the distance from the QC towards the shoot (0-360 µm: division and elongation zone; 900-1,335: early differentiation zone). Scale bar = 100 µm.

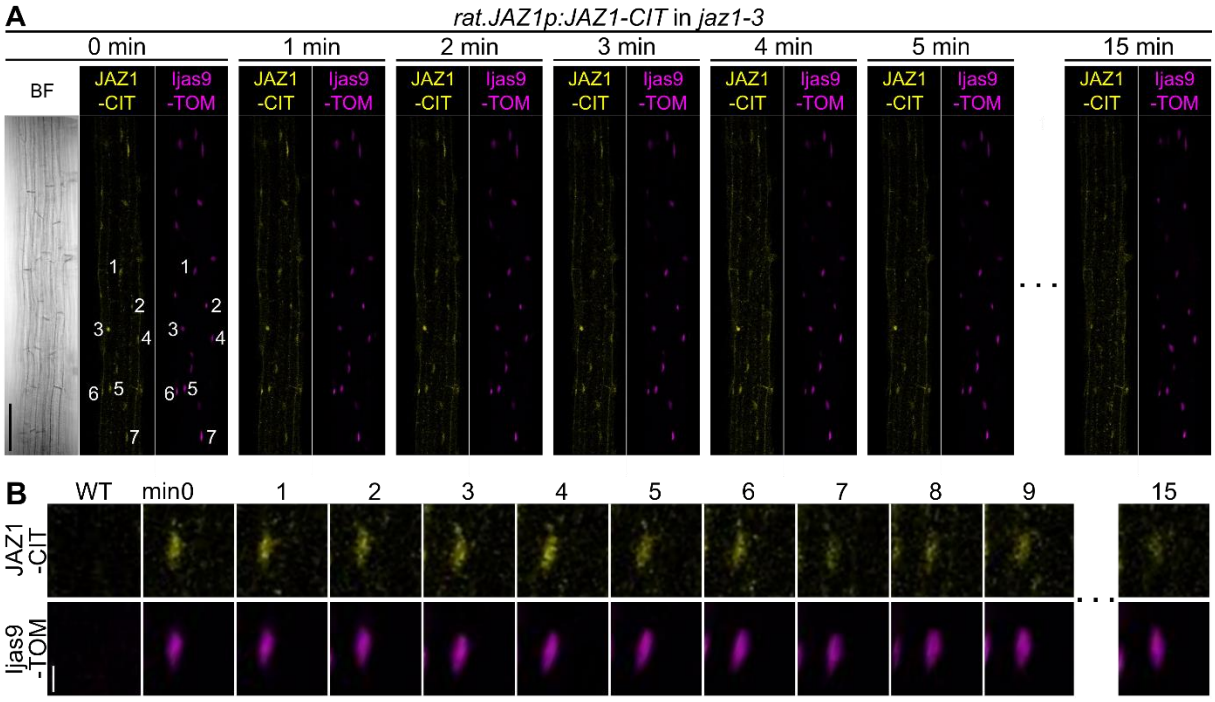

Figure S8: (extended information) JAZ-CIT fluorescence signals are not stable under mock conditions in *jaz* mutants. (**A**) Representative images of *JAZ1p:JAZ1-CIT* (JAZ1-CIT, yellow) and *UBQ10p:Ijas9-TOM* (Ijas9-TOM, magenta) expression in the root EDZ of 5-do *jaz1-3* mutant seedlings over a 15min imaging time course under mock conditions. A bright field (BF) image is presented for reference. Numbers depict individual nuclei evaluated in the ratiometric (rat.) JAZ reporters. (**B**) Close-up view of JAZ1-CIT and Ijas9-TOM from individual nuclei during the mock time course. Untransformed WT plants were used to subtract background signals. Scale bars (A) = 100 µm, (B) = 10 µm.

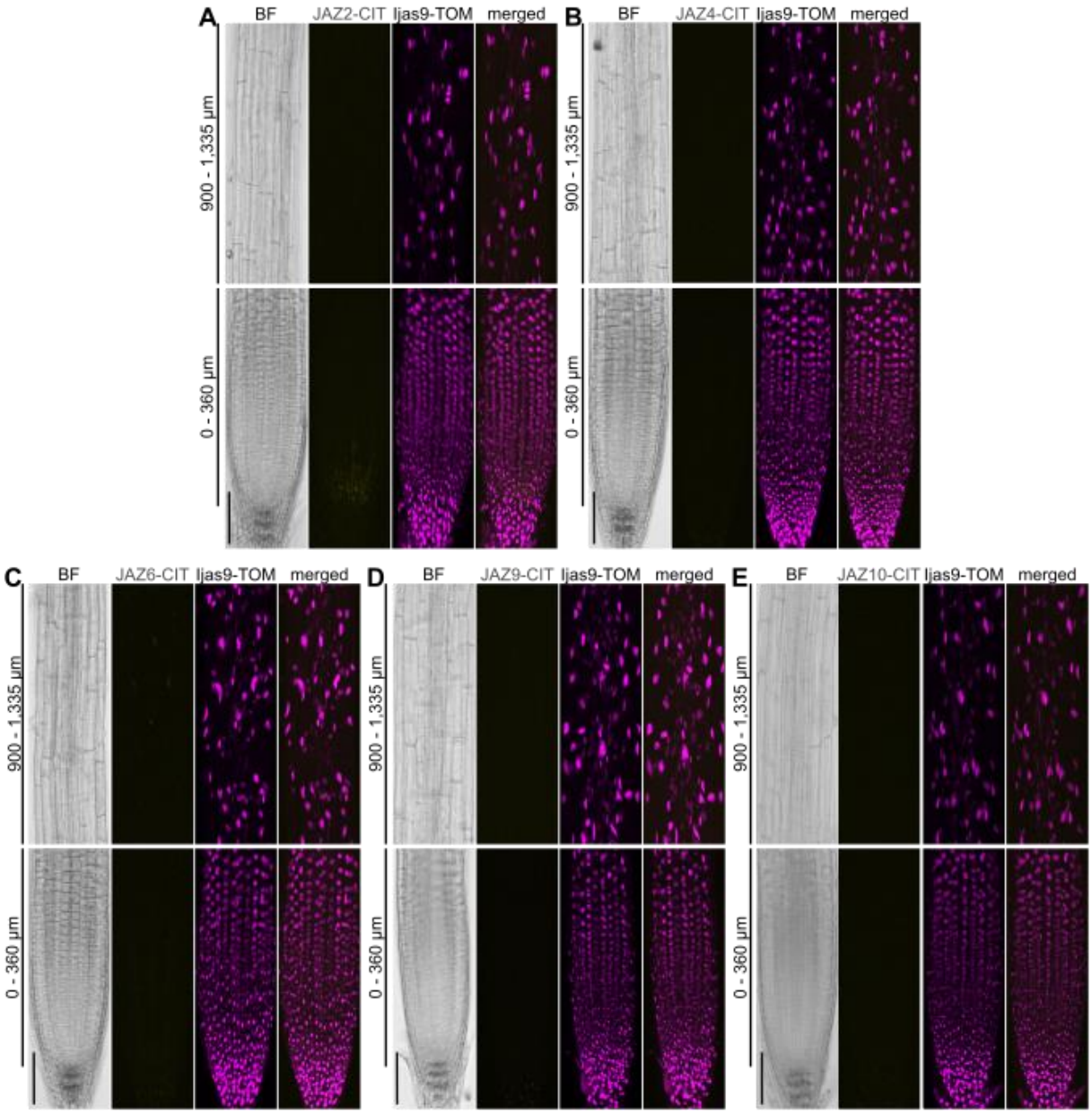

Figure S9: The majority of the *rat.JAZp:JAZ-CIT* reporter display no or only weak JAZ-CIT signal in the *aos* background. (**A-E**) Representative root images of 3D Z-stack volume renderings of 5-do (**A**) *rat.JAZ2p:JAZ2-CIT aos,* (**B**) *rat.JAZ4p:JAZ4-CIT aos,* (**C**) *rat.JAZ6p:JAZ6-CIT aos,* (**D**) *rat.JAZ9p:JAZ9-CIT aos* and (**E**) *JAZ10p:JAZ10-CIT aos* seedlings in bright filed (BF), JAZ-CIT (yellow), and Ijas9-TOM (magenta) channels (n=10 roots from two independent T_3 lines). Black bars indicate the distance from the QC towards the shoot (0-360 µm: division and elongation zone; 900-1,335: early differentiation zone). Scale bar = 100 µm.

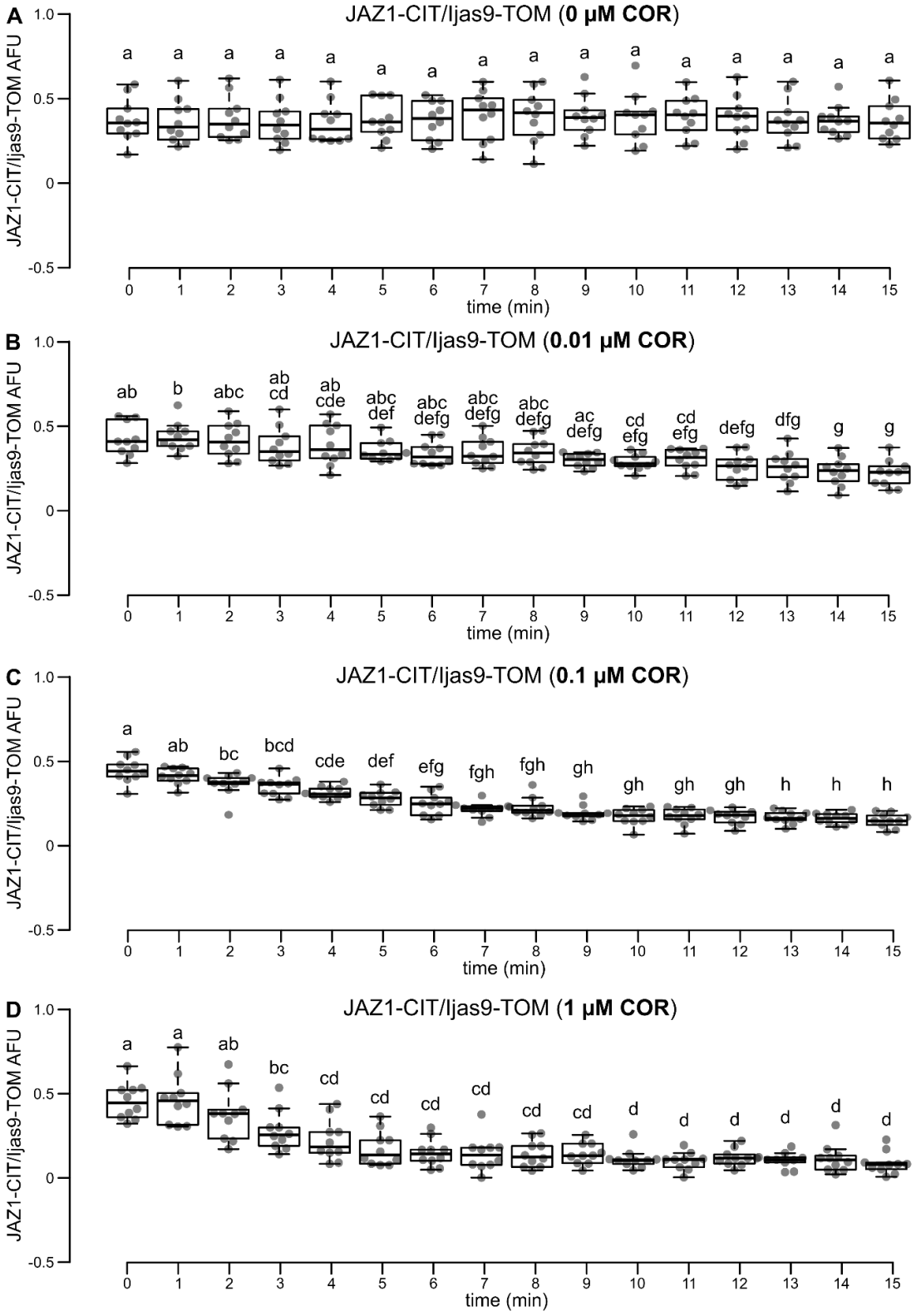

Figure S10: COR treatment leads to JAZ1-CIT/Ijas9-TOM AFU decrease over time. (**A-D**) Box plots of nucleus specific JAZ1-CIT/Ijas9-TOM AFUs in *rat.JAZ1p:JAZ1-CIT aos* EDZs over time after the treatment with (**A**) 0 µM [mock], (**B**) 0.01 µM, (**C**) 0.1 µM, and (**D**) 1 µM COR, respectively. Letters indicate statistically significant differences between COR concentrations at various time points as determined by One-Way-ANOVA followed by Tukey's HSD test ($P < 0.05$).

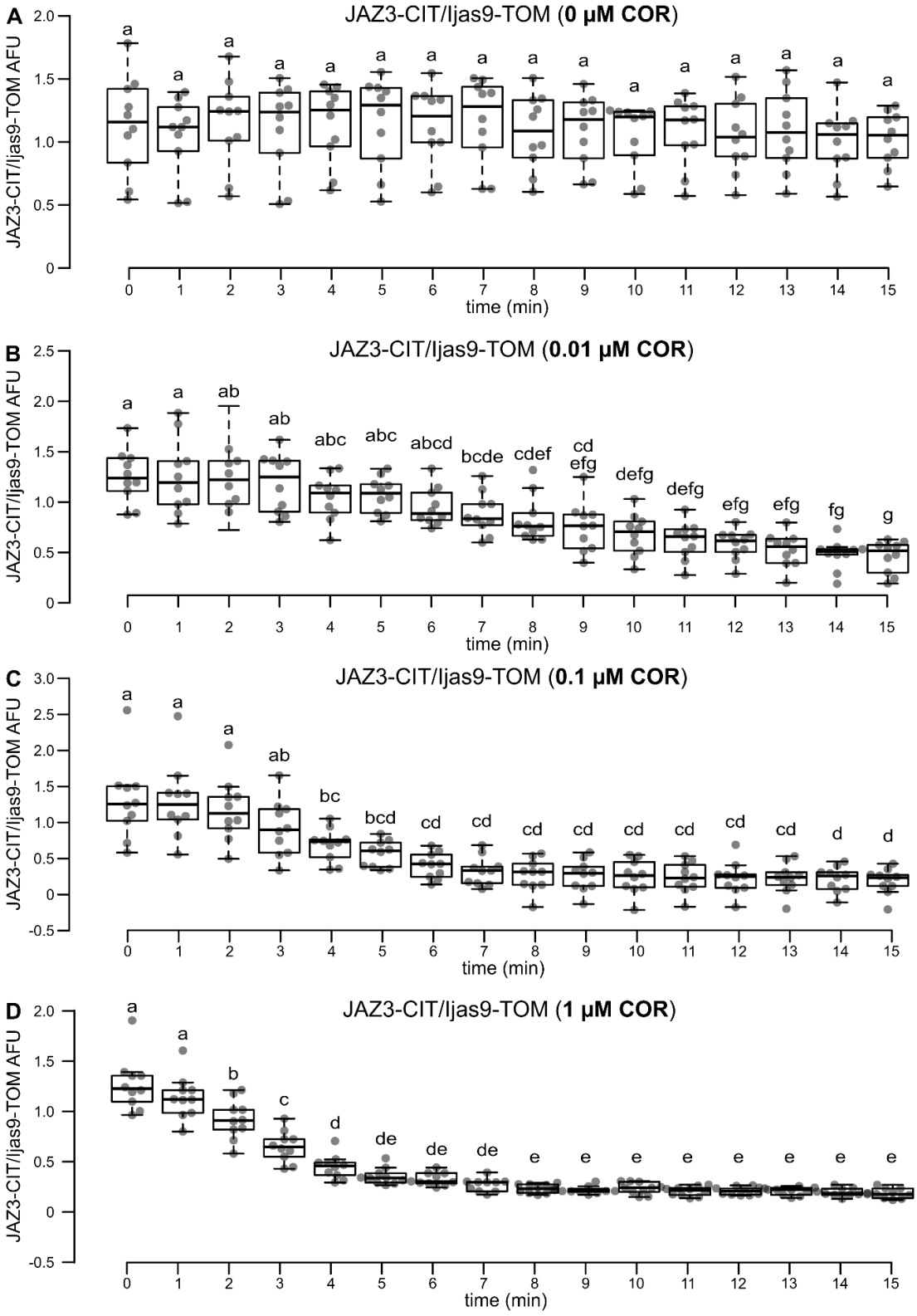

Figure S11: COR treatment leads to JAZ3-CIT/Ijas9-TOM AFU decrease over time. (**A-D**) Box plots of nucleus specific JAZ3-CIT/Ijas9-TOM AFUs in *rat.JAZ3p:JAZ3-CIT aos* EDZs over time after the treatment with (**A**) 0 µM [mock], (**B**) 0.01 µM, (**C**) 0.1 µM, and (**D**) 1 µM COR, respectively. Letters indicate statistically significant differences between COR concentrations at various time points as determined by One-Way-ANOVA followed by Tukey's HSD test ($P < 0.05$).

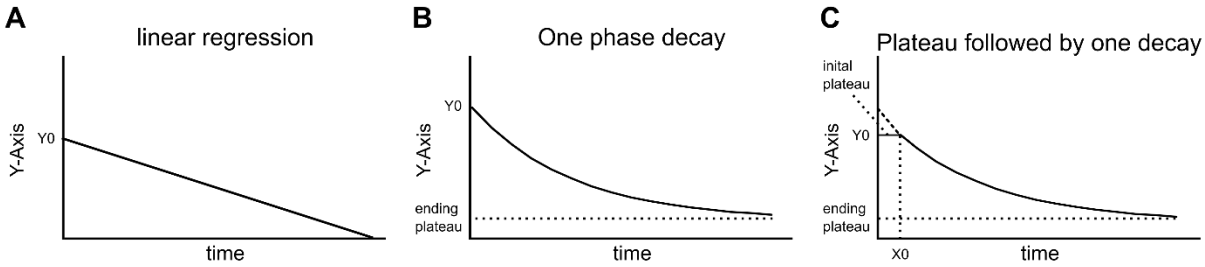

Figure S12: Linear and non-linear regressions models. (**A-C**) Schematic representations of various decrease scenarios, each best fitted by different regression models, including (**A**) the "linear regression" model, (**B**) the "One phase decay" model, and (**C**) the "Plateau followed by one phase decay" model. Y0 = value of Y when X (time) is 0, X0 = time X when the decrease begins, initial plateau = measured base-line before decay starts, end-plateau = measured base-line at the end of the decay phase.

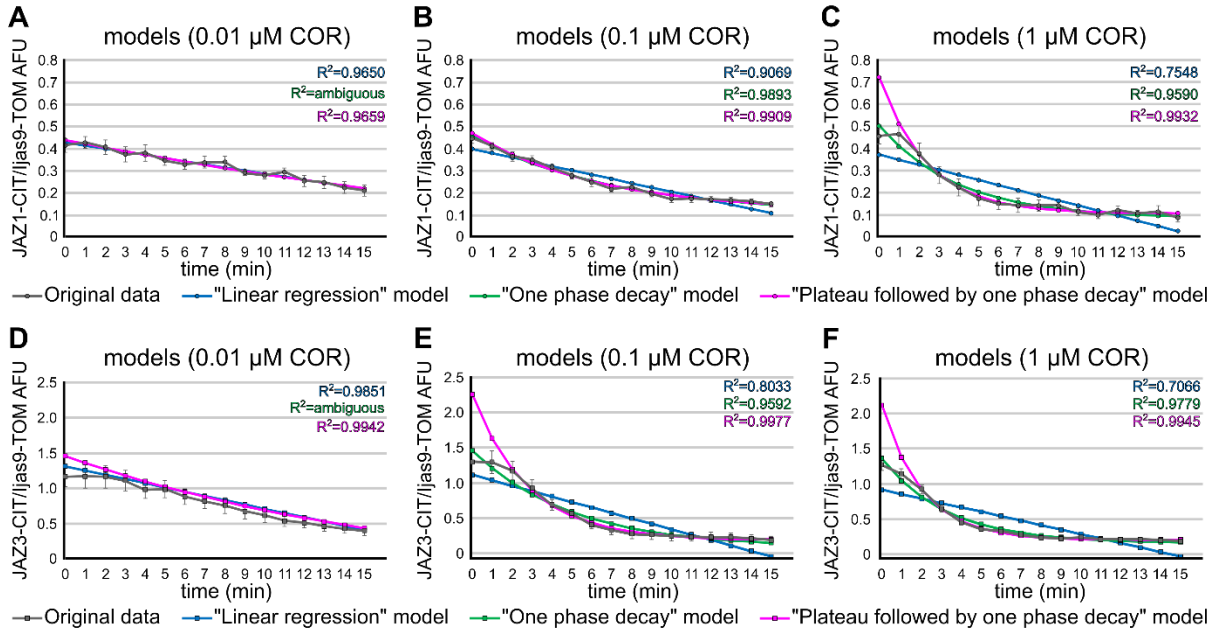

Figure S13: Regression analysis identified the "Plateau followed by one phase decay" model as the most suitable for characterizing the turnover of JAZ-CIT/Ijas9-TOM following COR treatment: (**A-F**) Graphical representation models were generated using various regression models, including "linear regression" (blue), "one phase decay" (green), and "plateau followed by one decay" (magenta). Regression analyses were performed for (**A-C**) JAZ1-CIT/Ijas9-TOM and (**D-F**) JAZ3-CIT/Ijas9-TOM at different COR concentrations. The models are presented alongside the original JAZ-CIT/Ijas9-TOM data (grey) for direct comparison. R^2 = coefficient of determination (R^2>0.95). Error bars = SEM.

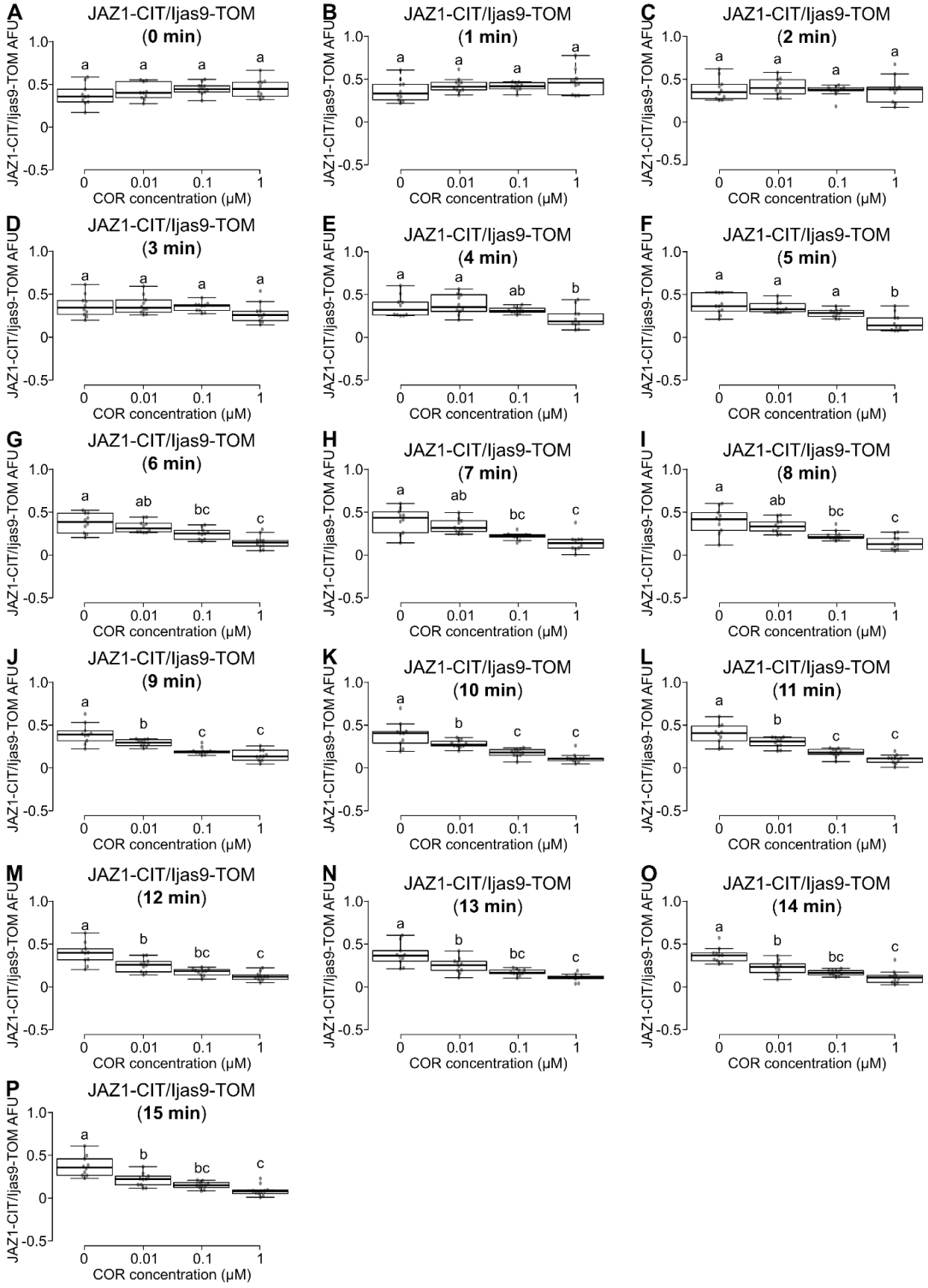

Figure S14 The treatment with COR results in a significant decrease in JAZ1-CIT/Ijas9-TOM levels within the 15-minute measurement window compared to the mock treatment. (**A-P**) Box plots of nucleus specific JAZ-CIT/Ijas9-TOM AFUs in *rat.JAZ1p:JAZ1-CIT aos* EDZs treated with 0 µM, 0.01 µM, 0.1 µM, and 1 µM COR at specific time points post-treatment. Letters indicate statistically significant differences between COR concentrations at various time points as determined by One-Way-ANOVA followed by Tukey's HSD test ($P < 0.05$).

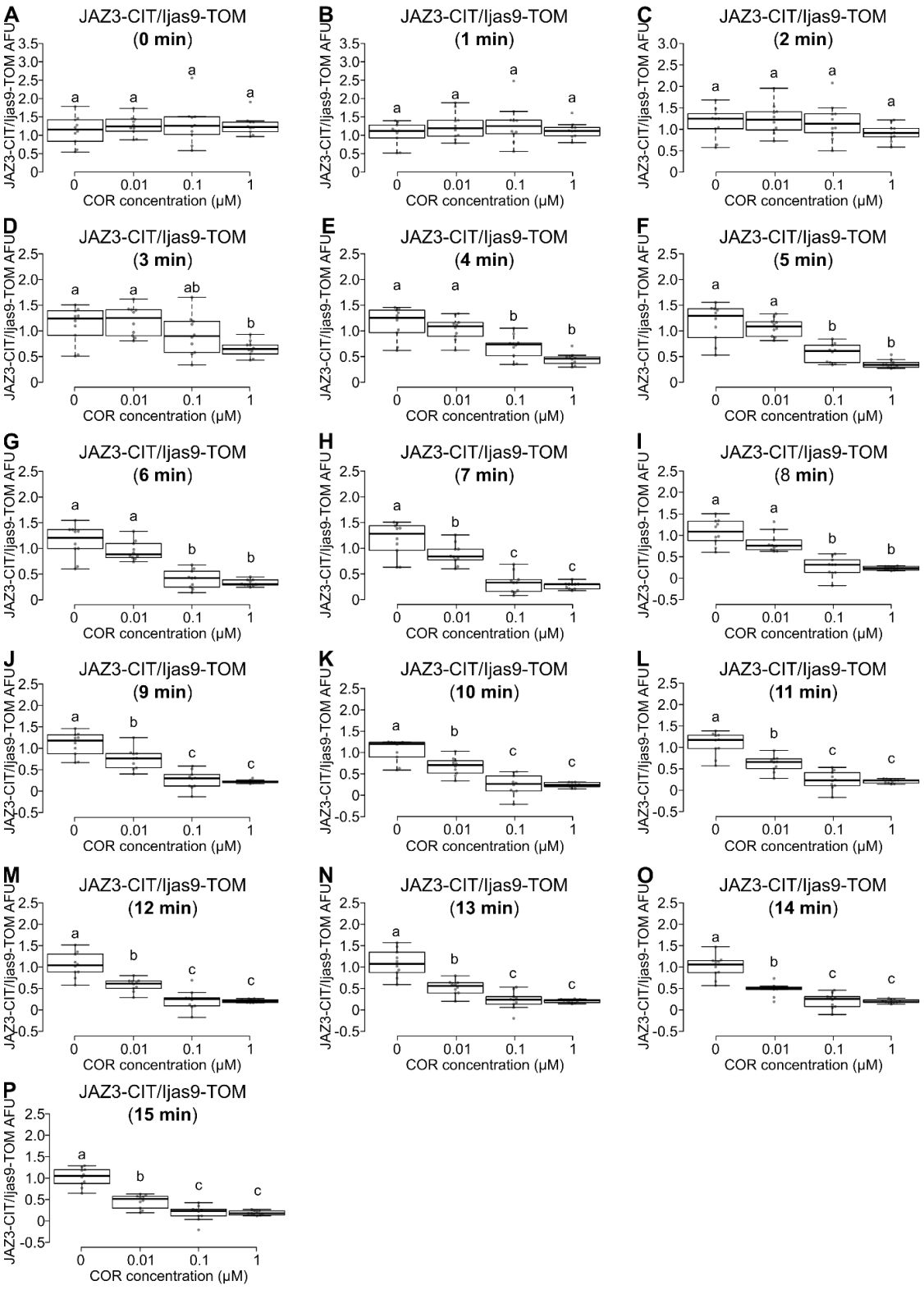

Figure S15. The treatment with COR results in a significant decrease in JAZ3-CIT/ljas9-TOM levels within the 15-minute measurement window compared to the mock treatment. (**A-P**) Box plots of nucleus specific JAZ-CIT/ljas9-TOM AFUs in *rat.JAZ3p:JAZ3-CIT aos* EDZs treated with 0 µM, 0.01 µM, 0.1 µM, and 1 µM COR at specific time points post-treatment. Letters indicate statistically significant differences between COR concentrations at various time points as determined by One-Way-ANOVA followed by Tukey's HSD test ($P < 0.05$).

Table S1: JAZ interactors

JAZ interactions with components of the Jasmonate perception & repression complex (for JAZ1 - JAZ7)							
	JAZ1	**JAZ2**	**JAZ3**	**JAZ4**	**JAZ5**	**JAZ6**	**JAZ7**
JAZ1	✓ Y2H[4]	X Y2H[4] ✓ Y2H[5]	X Y2H[4] ✓ Y2H[5]	✓ Y2H[4]	X Y2H[4] ✓ Y2H[5]	X Y2H[4] ✓ Y2H[5]	X Y2H[4]
JAZ2	X Y2H[4] ✓ Y2H[5]	X Y2H[4] ✓ Y2H[5]	X Y2H[4] ✓ Y2H[5]	X Y2H[4]	X Y2H[4] ✓ Y2H[5]	X Y2H[4] ✓ Y2H[5]	X Y2H[4]
JAZ3	X Y2H[4] ✓ Y2H[5]	X Y2H[4] ✓ Y2H[5]	✓ Y2H[4] ✓ BiFC[5]	✓ Y2H[4]	X Y2H[4]	X Y2H[4]	X Y2H[4]
JAZ4	X Y2H[4] ✓ Y2H[5]	X Y2H[4]	✓ Y2H[4]	✓ Y2H[4]	X Y2H[4]	X Y2H[4]	X Y2H[4]
JAZ5	X Y2H[4] ✓ Y2H[5]	X Y2H[4] ✓ Y2H[5]	X Y2H[4]	X Y2H[4]	X Y2H[4] ✓ Y2H[5]	X Y2H[4] ✓ Y2H[5]	X Y2H[4]
JAZ6	X Y2H[4] ✓ Y2H[5]	X Y2H[4] ✓ Y2H[5]	X Y2H[4]	X Y2H[4]	X Y2H[4] ✓ Y2H[5]	X Y2H[4] ✓ Y2H[5]	X Y2H[4]
JAZ7	X Y2H[4]	X Y2H[4]	X Y2H[4]	X Y2H[4]	X Y2H[4]	X Y2H[4]	X Y2H[4]
JAZ8	✓ Y2H[4] ✓ PD[16]	X Y2H[4] ✓ Y2H[5]	X Y2H[4] ✓ Y2H[5]	X Y2H[4] ✓ Y2H[5]	X Y2H[4] ✓ Y2H[5]	X Y2H[4] ✓ Y2H[5]	X Y2H[4]
JAZ9	X Y2H[4] ✓ Y2H[5]	X Y2H[4] ✓ Y2H[5]	✓ Y2H[4]	✓ Y2H[4] X Y2H[5]	X Y2H[4]	X Y2H[4]	X Y2H[4]
JAZ10	X Y2H[4] ✓ Y2H[5] ✓ PD[16]	X Y2H[4] ✓ Y2H[5]	X Y2H[4] ✓ Y2H[5]	X Y2H[4] ✓ Y2H[5]	X Y2H[4]	X Y2H[4] ✓ Y2H[5]	X Y2H[4]
JAZ11	X Y2H[4] ✓ Y2H[5]	X Y2H[4] ✓ Y2H[5]	X Y2H[4] ✓ Y2H[5]	X Y2H[4] ✓ Y2H[5]	X Y2H[4]	X Y2H[4]	X Y2H[4]
JAZ12	X Y2H[4] ✓ Y2H[5] ✓ PD[7]	X Y2H[4] ✓ Y2H[5] ✓ PD[19]	X Y2H[4]	X Y2H[4]	X Y2H[4] ✓ Y2H[5]	X Y2H[4] ✓ Y2H[5] ✓ PD[19]	X Y2H[4]
JAZ13	X Y2H[21]	X Y2H[21]	✓ Y2H[21]	X Y2H[21]	X Y2H[21]	X Y2H[21]	X Y2H[2]
MYC2	✓ Y2H[3] ✓ PD[4] ✓ LCI[9]	✓ Y2H[4] ✓ PD[4]	✓ Y2H[1] ✓ PD[1]	X Y2H[4] ✓ Y2H[9] ✓ PD[4]	✓ Y2H[4] ✓ PD[4]	✓ Y2H[4] ✓ PD[4]	X Y2H[4] ✓ Y2H[9] X PD[4]
MYC3	✓ Y2H[9,10] ✓ LCI[9] ✓ PD[7]	✓ Y2H[9,10] ✓ PD[10]	X Y2H[9] ✓ Y2H[10] ✓ PD[10]	X Y2H[9,10] X PD[10]	✓ Y2H[9,10] ✓ PD[10]	✓ Y2H[9,10] X PD[10]	X Y2H[9] ✓ Y2H[10] ✓ PD[10]
MYC4	✓ Y2H[10] ✓ PD[10]	✓ Y2H[10] ✓ PD[10]	✓ Y2H[10] ✓ PD[10]	✓ Y2H[10] ✓ PD[10]	✓ Y2H[10] ✓ PD[10]	✓ Y2H[10] ✓ PD[10]	✓ Y2H[10] ✓ PD[10]
MYC5	X Y2H[11] ✓ Y2H[20] ✓ BiFC[20]	✓ Y2H[20]	X Y2H[11]	X Y2H[20]	✓ Y2H[20]	✓ Y2H[20]	X Y2H[20]
COI1	✓ PD[2] ✓ Y2H[2] ✓ SAT[8]	X PD[19] ✓ PD[16]	✓ PD[1] ✓ Y2H[3]	n.d.	n.d.	X PD[19] ✓ PD[16] ✓ SAT[8]	n.d.
NINJA	✓ PD[7] ✓ Y2H[7]	✓ Y2H[7]	✓ Y2H[7]	✓ Y2H[7]	✓ Y2H[7]	✓ Y2H[7]	X Y2H[7]
TPL	n.d.	n.d.	n.d.	n.d.	✓ Y2H[15] ✓ PD[23]	✓ Y2H[15]	✓ Y2H[23] ✓ PD[23]

JAZ interactions with components of the Jasmonate perception & repression complex (for JAZ8 - JAZ13)						
	JAZ8	**JAZ9**	**JAZ10**	**JAZ11**	**JAZ12**	**JAZ13**
JAZ1	✓ Y2H[4] ✓ PD[16]	✓ Y2H[4]	X Y2H[4] ✓ Y2H[5] ✓ PD[16]	X Y2H[4] ✓ Y2H[5]	X Y2H[4] ✓ Y2H[5] ✓ PD[7]	X Y2H[21]

JAZ2	X Y2H[4] ✓ Y2H[5]	X Y2H[4] ✓ Y2H[5]	X Y2H[4] ✓ Y2H[5]	X Y2H[4] ✓ Y2H[5]	X Y2H[4] ✓ Y2H[5] ✓ PD[19]	X Y2H[21]
JAZ3	X Y2H[4] ✓ Y2H[5]	✓ Y2H[4]	X Y2H[4] ✓ Y2H[5]	X Y2H[4] ✓ Y2H[5]	X Y2H[4]	✓ Y2H[21]
JAZ4	X Y2H[4] ✓ Y2H[5]	✓ Y2H[4] X Y2H[5]	X Y2H[4] ✓ Y2H[5]	X Y2H[4] ✓ Y2H[5]	X Y2H[4]	X Y2H[21]
JAZ5	X Y2H[4] ✓ Y2H[5]	X Y2H[4]	X Y2H[4]	X Y2H[4]	X Y2H[4] ✓ Y2H[5]	X Y2H[21]
JAZ6	X Y2H[4] ✓ Y2H[5]	X Y2H[4]	X Y2H[4] ✓ Y2H[5]	X Y2H[4]	X Y2H[4] ✓ Y2H[5]	X Y2H[21]
JAZ7	X Y2H[4]	X Y2H[4]	X Y2H[4]	X Y2H[4]	X Y2H[4]	X Y2H[21]
JAZ8	X Y2H[4]	X Y2H[4] ✓ Y2H[5]	X Y2H[4] ✓ Y2H[5]	X Y2H[4]	X Y2H[4] ✓ Y2H[5]	X Y2H[21]
JAZ9	X Y2H[4] ✓ Y2H[5]	X Y2H[4]	X Y2H[4] ✓ Y2H[5]	X Y2H[4] ✓ Y2H[5]	X Y2H[4]	X Y2H[21]
JAZ10	X Y2H[4] ✓ Y2H[5]	X Y2H[4] ✓ Y2H[5]	X 2H[4] ✓ Y2H[5]	X Y2H[4] ✓ Y2H[5]	X Y2H[4] ✓ Y2H[5]	X Y2H[21]
JAZ11	X Y2H[4]	X Y2H[4] ✓ Y2H[5]	X Y2H[4] ✓ Y2H[5]	X Y2H[4]	X Y2H[4]	X Y2H[21]
JAZ12	X Y2H[4] ✓ Y2H[5]	X Y2H[4]	X Y2H[4] ✓ Y2H[5] ✓ PD[19]	X Y2H[4]	X Y2H[4] ✓ PD[19]	X Y2H[21]
JAZ13	X Y2H[21]	X Y2H[21]	X Y2H[21]	X Y2H[21]	X Y2H[21]	X Y2H[21]
MYC2	✓ Y2H[4] ✓ PD[4]	✓ Y2H[3] ✓ PD[4]	✓ Y2H[4] ✓ PD[4]	✓ Y2H[4] ✓ PD[4]	✓ Y2H[4] ✓ PD[4] ✓ LCI[19]	✓ Y2H[21]
MYC3	✓ Y2H[9,10] ✓ PD[10]	✓ Y2H[9,10] ✓ PD[10]	✓ Y2H[9,10] ✓ PD[10]	✓ Y2H[9,10] ✓ PD[10]	X Y2H[9] ✓ Y2H[10] ✓ PD[10]	n.d.
MYC4	✓ Y2H[10] ✓ PD[10]	✓ Y2H[10] ✓ PD[10]	✓ Y2H[10] ✓ PD[10]	✓ Y2H[10] ✓ PD[10]	✓ Y2H[10] ✓ PD[10]	n.d.
MYC5	✓ Y2H[20]	X Y2H[11]	✓ Y2H[20] ✓ BiFC[20]	X Y2H[20]	X Y2H[20]	n.d.
COI1	X PD[16] X SAT[16]	✓ PD[3] X PD[19] ✓ Y2H[3]	✓ PD[16] ✓ SAT[16]	n.d.	✓ PD[19]	n.d.
NINJA	X Y2H[7] ✓ PD[16]	✓ Y2H[7]	✓ Y2H[7] ✓ PD[16]	✓ Y2H[7]	✓ Y2H[7] ✓ PD[19]	X Y2H[21]
TPL	✓ Y2H[16] ✓ PD[23]	n.d.	X Y2H[21]	n.d.	n.d.	✓ Y2H[21]

JAZ interactions with other partners (for JAZ1 - JAZ7)

	JAZ1	JAZ2	JAZ3	JAZ4	JAZ5	JAZ6	JAZ7
RGA	✓ Y2H[6] ✓ BiFC[6] ✓ PD[6]	n.d.	✓ Y2H[6]	n.d.	n.d.	n.d.	n.d.
RGL1/ GAI	✓ Y2H[6]	n.d.	n.d.	n.d.	n.d.	n.d.	n.d.
EGL3/ GL3/ TT8	✓ Y2H[12]	✓ Y2H[12]	X Y2H[12]	X Y2H[12]	✓ Y2H[12]	✓ Y2H[12]	X Y2H[12]
MYB75	✓ Y2H[12]	X Y2H[12]	X Y2H[12]	X Y2H[12]	X Y2H[12]	X Y2H[12]	X Y2H[12]
GL1	✓ Y2H[12]	X Y2H[12]	X Y2H[12]	X Y2H[12]	X Y2H[12]	X Y2H[12]	X Y2H[12]

MYB21/ MYB24	✓ Y2H[13]	X Y2H[13]	X Y2H[13]	X Y2H[13]	X Y2H[13]	X Y2H[13]	X Y2H[13]
EIN3	✓ BiFC[14] ✓ PD[14] ✓ Y2H[14]	n.d.	✓ Y2H[14]	n.d.	n.d.	n.d.	n.d.
EIL1	✓ Y2H[14]	n.d.	✓ Y2H[14]	n.d.	n.d.	n.d.	n.d.
HDA6	✓ BiFC[14] ✓ PD[14] ✓ Y2H[14]	n.d.	✓ Y2H[14]	n.d.	n.d.	n.d.	n.d.
ICE1/ ICE2	✓ BiFC[17] ✓ PD[17] ✓ Y2H[17]	X Y2H[17]	✓ Y2H[17]	✓ BiFC[17] ✓ PD[17] ✓ Y2H[17]	X Y2H[17]	X Y2H[17]	X Y2H[17]
WRKY57	n.d.	n.d.	n.d.	✓ Y2H[18] ✓ BiFC[18] ✓ PD[18]	n.d.	n.d.	n.d.
KEG	X PD[19]	X PD[19]	X PD[19]	X PD[19]	X PD[19]	X PD[19]	X PD[19]
TOE1/ TOE2	✓ BiFC[22] ✓ PD[22] ✓ Y2H[22]	X Y2H[22]	✓ Y2H[22]	✓ Y2H[22]	X Y2H[22]	X Y2H[22]	X Y2H[22]
ABI5	X LCI[24]	✓ LCI[24]	✓ BiF[24] ✓ LCI[24] ✓ PD[24]	X LCI[24]	✓ LCI[24]	✓ LCI[24]	X LCI[24]
FHY3	✓ BiFC[25] ✓ PD[25] ✓ Y2H[25]	X Y2H[25]	X Y2H[25]	X Y2H[25]	X Y2H[25]	✓ BiFC[25] ✓ PD[25] ✓ Y2H[25]	X Y2H[25]
FAR1	✓ Y2H[25]	X Y2H[25]	X Y2H[25]	X Y2H[25]	X Y2H[25]	✓ Y2H[25]	X Y2H[25]
RHD6/ RSL1	X BiFC[26] X Y2H[26]	✓ BiFC[26] ✓ Y2H[26]	X Y2H[26]	X BiFC[26] X PD[26] X Y2H[26]	X Y2H[26]	X Y2H[26]	X Y2H[26]
ARF10	✓ BiFC[27] ✓ PD[27] ✓ Y2H[27]	X Y2H[27]	✓ Y2H[27]	✓ Y2H[27]	X Y2H[27]	X Y2H[27]	✓ Y2H[27]
ARF16	✓ BiFC[27] ✓ PD[27] ✓ Y2H[27]	X Y2H[27]	X Y2H[27]	✓ Y2H[27]	X Y2H[27]	X Y2H[27]	✓ Y2H[27]

JAZ interactions with other partners (for JAZ8 - JAZ13)

	JAZ8	JAZ9	JAZ10	JAZ11	JAZ12	JAZ13
RGA	n.d.	✓ Y2H[6]	n.d.	n.d.	n.d.	n.d.
RGL1/ GAI	n.d.	n.d.	n.d.	n.d.	n.d.	n.d.
EGL3/ GL3/ TT8	✓ Y2H[12]	✓ Y2H[12]	✓ Y2H[12]	✓ Y2H[12]	X Y2H[12]	n.d.
MYB75	✓ Y2H[12]	X Y2H[12]	X Y2H[12]	✓ Y2H[12]	X Y2H[12]	n.d.
GL1	✓ Y2H[12]	X Y2H[12]	✓ Y2H[12]	✓ Y2H[12]	X Y2H[12]	n.d.
MYB21/ MYB24	✓ Y2H[13] ✓ LCI[13]	X Y2H[13]	✓ Y2H[13]	✓ Y2H[13] ✓ LCI[13]	X Y2H[13]	n.d.
EIN3	n.d.	✓ Y2H[14]	n.d.	n.d.	n.d.	n.d.
EIL1	n.d.	✓ Y2H[14]	n.d.	n.d.	n.d.	n.d.
HDA6	n.d.	✓ Y2H[14]	n.d.	n.d.	n.d.	n.d.
ICE1/ ICE2	X Y2H[17]	✓ Y2H[17]	X Y2H[17]	✓ Y2H[17]	X Y2H[17]	n.d.

WRKY57	✓ Y2H[18] ✓ BiFC[18] ✓ PD[18]	n.d.	n.d.	n.d.	n.d.	n.d.
KEG	X PD[19]	X PD[19]	X PD[19]	X PD[19]	✓ BiFC[19] ✓ PD[19] ✓ Y2H[19]	X PD[19]
TOE1/ TOE2	X Y2H[22]	✓ Y2H[22]	X Y2H[22]	X Y2H[22]	X Y2H[22]	n.d.
ABI5	✓ LCI[24]	✓ LCI[24]	✓ LCI[24]	✓ LCI[24]	✓ LCI[24]	X LCI[24]
FHY3	✓ BiFC[25] ✓ PD[25] ✓ Y2H[25]	✓ BiFC[25] ✓ PD[25] ✓ Y2H[25]	✓ BiFC[25] ✓ PD[25] ✓ Y2H[25]	✓ BiFC[25] ✓ PD[25] ✓ Y2H[25]	X Y2H[25]	n.d.
FAR1	✓ Y2H[25]	✓ Y2H[25]	✓ Y2H[25]	✓ Y2H[25]	X Y2H[25]	n.d.
RHD6/ RSL1	✓ BiFC[26] ✓ PD[26] ✓ Y2H[26]	✓ BiFC[26] ✓ Y2H[26]	✓ BiFC[26] ✓ Y2H[26]	X BiFC[26]	X BiFC[26]	n.d.
ARF10	X BiFC[27] X Y2H[27]	✓ BiFC[27] ✓ PD[27] ✓ Y2H[27]	X Y2H[27]	✓ Y2H[27]	X Y2H[27]	n.d.
ARF16	X BiFC[27] X Y2H[27]	✓ BiFC[27] ✓ PD[27] ✓ Y2H[27]	X Y2H[27]	X Y2H[27]	X Y2H[27]	n.d.

List of Arabidopsis JAZ interactions with different proteins. ✓, positive interaction; X, negative interaction; n.d., no data available. Abbreviations next to the indicated positive/negative interactions denote the method through which a particular interaction outcome was tested: BiFC, bimolecular fluorescence complementation; LCI, luciferase complementation imaging; PD, Pull-down; SAT, saturation binding assay; Y2H, Yeast-two-hybrid. Numbers depicted as superscripts denote the publication in which the interaction was first tested using the indicated method (see references below). This list does not provide quantitative information about the strength of reported interactions. Note that certain tests can display varying interaction outcomes across different publications using the same method. This list displays a selection of studied JAZ interactions and does not claim to be complete (e.g., further JAZ interactors were found in (Pauwels et al., 2015), but were not further investigated in more detail).

Abbreviations of proteins: JAZ, ZIM-DOMAIN PROTEIN; MYC2, bHLH-transcription factor of the MYC-family; COI1, CORONATINE INSENSITIVE 1; NINJA, NOVEL INTERACTOR OF JAZ; TPL, TOPLESS; RGA, REPRESSOR OF GA; RGL1, RGA-LIKE1; GAI, GIBBERELLIC ACID INSENSITIVE; EGL3, ENHANCER OF GLABRA; GL, GLABRA; TT8, TRANSPARENT TESTA 8; MYB, MYB DOMAIN PROTEIN; EIN3, ETHYLENE INSENSITIVE 3; EIL1, EIN3-LIKE 1; HDA6, HISTONE DEACETYLASE; ICE, INDUCER OF CBF EXPRESSION; WRKY57, WRKY DNA-BINDING PROTEIN 57; KEG, KEEP ON GOING; TOE, TARGET OF EAT; ABI5, ABA INSENSETIVE 5; FHY3, FAR-RED ELONGATED HYPOCOTYLS 3; FAR1, FAR-RED IMPAIRED RESPONSE 1; RDH6, ROOT HAIR DEFECTIVE 6; RSL1, RDH6-LIKE1; ARF, AUXIN RESPONSE FACTOR.

The information regarding JAZ interactors were gathered from following publications:

1 = (Chini et al., 2007)
2 = (Thines et al., 2007)
3 = (Melotto et al., 2008)
4 = (Chini et al., 2009)
5 = (Chung & Howe, 2009)
6 = (Hou et al., 2010)
7 = (Pauwels et al., 2010)
8 = (Sheard et al., 2010)
9 = (Cheng et al., 2011)
10 = (Fernandez-Calvo et al., 2011)
11 = (Niu et al., 2011)

12 = (Qi et al., 2011)
13 = (Song et al., 2011)
14 = (Zhu et al., 2011) --14
15 = (Causier et al., 2012)
16 = (Shyu et al., 2012)
17 = (Hu et al., 2013)
18 = (Jiang et al., 2014)
19 = (Pauwels et al., 2015)
20 = (Qi et al., 2015)
21 = (Thireault et al., 2015)
22 = (Zhai et al., 2015)
23 = (Thatcher et al., 2016)
24 = (Ju et al., 2019)
25 = (Liu et al., 2019)
26 = (Han et al., 2020)
27 = (Mei et al., 2023)

Table S2: Differentially expressed genes in *jaz2*, *jaz2xjaz3*, and *jazT* root tips

	log2FC[B]			p-value[C]			
AGI code[A]	*jaz2*	*jaz2xjaz3*	*jazT*	*jaz2*	*jaz2xjaz3*	*jazT*	Description
JA biosynthesis and signalling							
AT1G17380	/	/	2,3022	/	/	0,002501441	jasmonate-zim-domain protein 5 (JAZ5)
AT1G17420	/	5,3135	4,679	/	0,00326085	0,010116191	lipoxygenase 3 (LOX3)
AT1G19180	/	1,3427	1,1352	/	1,54E-69	6,01E-50	jasmonate-zim-domain protein 1 (JAZ1)
AT1G70700	/	/	1,6847	/	/	3,87E-07	jasmonate-zim-domain proteinn (JAZ9)
AT1G72450	/	/	1,5509	/	/	1,43E-13	jasmonate-zim-domain protein 6 (JAZ6)
AT1G74950	/	/	1,6415	/	/	3,19E-68	jasmonate-zim-domain proteinn (JAZ2)
AT3G17860	/	4,0263	3,6703	/	0	0	jasmonate-zim-domain protein 3 (JAZ3)
AT3G55970	/	/	4,4596	/	/	2,29E-06	jasmonate-regulated 21 (JOX3)
AT5G13220	/	/	3,0177	/	/	1,53E-35	jasmonate-zim-domain protein 10 (JAZ10)
AT5G42650	/	1,1776	1,4549	/	1,91E-20	1,35E-30	allene oxide synthase (AOS)
response to stress							
AT1G01140	/	/	-1,3252	/	/	9,21E-06	CBL-interacting protein kinase 9 (CIPK9)
AT1G02205	/	/	-1,5581	/	/	4,81E-16	Fatty acid hydroxylase superfamily (CER1)
AT1G02220	/	-1,0614	/	/	3,31E-10	/	NAC domain containing protein 3 (NAC3)
AT1G02310	1,0395	/	/	0,000267555	/	/	Glycosyl hydrolase superfamily protein (MAN1)
AT1G02930	/	2,3281	2,2491	/	1,63E-49	2,65E-46	glutathione S-transferase 6 (GSTF6)
AT1G05880	-2,2955	3,2641	2,8875	0,001509076	5,47E-10	4,64E-08	RING/U-box superfamily protein (ARI12)
AT1G06160	/	/	-3,8804	/	/	0,008274483	octadecanoid-responsive AP2/ERF 59 (ORA59)
AT1G06460	-1,4493	/	-1,4148	0,001688218	/	0,000820424	alpha-crystallin domain 32.1 (ACD32.1)
AT1G06830	/	1,6709	/	/	0,004378067	/	Glutaredoxin family protein
AT1G07985	/	-1,251	/	/	2,41E-06	/	Expressed protein

AT1G08810	/	/	5,1428	/	/	0,002349096	myb domain protein 60 (MYB60)
AT1G09750	/	/	-1,5301	/	/	2,54E-20	Eukaryotic aspartyl protease family protein
AT1G11210	-1,9841	-1,8503	-4,0015	8,12E-12	2,58E-12	6,71E-36	cotton fiber protein, putative (DUF761)
AT1G13310	/	2,4742	/	/	0,00336464	/	Endosomal targeting BRO1-like domain-containing protein
AT1G14960	/	/	1,0472	/	/	2,51E-15	Polyketide cyclase/dehydrase and lipid transport superfamily protein
AT1G15610	/	2,6033	/	/	0,004597885	/	transmembrane protein
AT1G16370	/	1,257	1,8108	/	6,78E-32	2,17E-65	organic cation/carnitine transporter 6 (OCT6)
AT1G17615	/	/	3,4619	/	/	0,002858536	Disease resistance protein (TIR-NBS class)
AT1G18300	/	1,3967	/	/	6,51E-10	/	nudix hydrolase homolog 4 (NUDT4)
AT1G19190	/	/	1,381	/	/	2,43E-18	alpha/beta-Hydrolases superfamily protein
AT1G20020	/	-1,5336	-1,3207	/	6,63E-09	3,79E-07	ferredoxin-NADP[+]-oxidoreductase 2 (FNR2)
AT1G20030	/	/	-1,2176	/	/	9,29E-09	Pathosis-related thaumatin superfamily protein
AT1G20823	/	/	1,1134	/	/	9,34E-12	RING/U-box superfamily protein
AT1G22110	/	-1,3267	-1,7025	/	0,003470176	0,000232734	structural constituent of ribosome
AT1G22150	/	1,1441	1,1139	/	3,56E-06	6,39E-06	sulfate transporter (SULTR1:3)
AT1G22480	/	/	-1,4833	/	/	0,002196419	Cupredoxin superfamily protein
AT1G23740	1,6336	/	/	0,00039214	/	/	Oxidoreductase, zinc-binding dehydrogenase family protein (AOR)
AT1G23850	/	/	1,1946	/	/	4,62E-14	transmembrane protein
AT1G26250	-2,5173	/	/	0,001723092	/	/	Proline-rich extensin-like family protein
AT1G26380	-5,6085	/	/	1,46E-05	/	/	FAD-binding Berberine family protein
AT1G26420	/	/	-1,5718	/	/	0,00243786	FAD-binding Berberine family protein
AT1G26730	/	1,2296	1,389	/	3,66E-06	1,48E-07	EXS (ERD1/XPR1/SYG1) family protein
AT1G26800	-1,3422	/	/	0,000268302	/	/	RING/U-box superfamily protein
AT1G27730	/	1,625	1,6868	/	4,40E-13	4,97E-14	salt tolerance zinc finger (STZ)
AT1G27950	/	/	-1,1901	/	/	5,03E-17	glycosylphosphatidylinositol-anchored lipid protein transfer 1 (LTPG1)
AT1G28570	/	/	2,0686	/	/	8,46E-06	SGNH hydrolase-type esterase superfamily protein
AT1G31710	/	1,0139	1,4505	/	4,64E-10	4,29E-19	Copper amine oxidase family protein
AT1G31750	/	1,7696	1,356	/	2,03E-05	0,001219233	proline-rich family protein
AT1G32970	/	/	4,2191	/	/	0,007560379	Subtilisin-like serine endopeptidase family protein (SBT3.2)
AT1G33700	/	1,0266	/	/	1,74E-06	/	Beta-glucosidase, GBA2 type family protein
AT1G34510	/	2,2894	3,0535	/	7,01E-30	5,90E-52	Peroxidase superfamily protein
AT1G34640	/	/	-3,406	/	/	0,001207671	peptidase
AT1G35140	1,5349	/	/	0,000286503	/	/	Phosphate-responsive 1 family protein (PH-1)
AT1G36622	/	1,8773	1,6963	/	3,76E-12	3,82E-10	transmembrane protein
AT1G44020	/	/	1,0058	/	/	8,98E-12	Cysteine/Histidine-rich C1 domain family protein
AT1G49220	/	/	-5,5725	/	/	0,001744645	RING/U-box superfamily protein
AT1G49230	/	/	-1,4495	/	/	2,68E-06	RING/U-box superfamily protein
AT1G49570	-1,7474	/	/	8,89E-09	/	/	Peroxidase superfamily protein
AT1G49960	-1,8075	-1,3073	-1,3899	5,20E-07	6,53E-05	2,27E-05	Xanthine/uracil permease family protein

AT1G51402	/	/	-4,1441	/	/	0,009833241	hypothetical protein
AT1G51920	/	4,5968	4,5807	/	0,000314634	0,000329771	transmembrane protein
AT1G52410	/	1,4741	1,9347	/	5,80E-10	3,22E-16	TSK-associating protein 1 (TSA1)
AT1G53610	/	/	-2,0204	/	/	0,001651414	transmembrane protein
AT1G57560	/	/	1,1849	/	/	6,14E-18	myb domain protein 50 (MYB50)
AT1G58270	/	/	1,0284	/	/	1,08E-68	TRAF-like family protein (ZW9)
AT1G59620	/	4,808	/	/	0,004168299	/	Disease resistance protein (CC-NBS-LRR class) family (CW9)
AT1G60740	/	-1,6483	-1,4989	/	1,51E-19	7,35E-17	Thioredoxin superfamily protein
AT1G61065	/	/	1,215	/	/	0,000745802	1,3-beta-glucan synthase component (DUF1218)
AT1G61750	/	/	-2,5848	/	/	0,008607729	Receptor-like protein kinase-related family protein
AT1G62280	/	2,0043	3,0937	/	1,54E-05	2,02E-11	SLAC1 homologue 1 (SLAH1)
AT1G62510	/	-1,2294	-1,5713	/	1,58E-10	5,50E-16	Bifunctional inhibitor/lipid-transfer protein/seed storage 2S albumin superfamily protein
AT1G63580	/	/	1,1819	/	/	0,001326023	Receptor-like protein kinase-related family protein
AT1G63750	/	1,3541	1,7838	/	0,001199034	1,60E-05	Disease resistance protein (TIR-NBS-LRR class) family
AT1G64195	/	/	2,1269	/	/	0,00141553	Defensin-like (DEFL) family protein
AT1G64380	/	/	-1,2475	/	/	0,000372959	Integrase-type DNA-binding superfamily protein
AT1G65970	/	/	1,0996	/	/	7,35E-09	thioredoxin-dependent peroxidase 2 (TPX2)
AT1G66090	/	3,494	2,837	/	0,001378799	0,009980928	Disease resistance protein (TIR-NBS class)
AT1G66280	/	1,1847	1,7296	/	1,47E-111	8,70E-236	Glycosyl hydrolase superfamily protein (BGLU22)
AT1G67090	/	/	1,3243	/	/	2,67E-07	ribulose bisphosphate carboxylase small chain 1A (RBCS1A)
AT1G69150	/	/	1,251	/	/	1,15E-06	Cysteine/Histidine-rich C1 domain family protein
AT1G69890	-1,3409	/	/	7,18E-07	/	/	actin cross-linking protein (DUF569)
AT1G71050	/	/	1,1734	/	/	0,001729744	Heavy metal transport/detoxification superfamily protein (HIPP20)
AT1G73330	/	1,7243	2,2978	/	9,63E-13	1,89E-21	drought-repressed 4 (DR4)
AT1G75290	/	/	1,0034	/	/	0,000163233	NAD(P)-binding Rossmann-fold superfamily protein
AT1G75300	1,0892	/	/	0,000328865	/	/	NmrA-like negative transcriptional regulator family protein
AT1G77380	-1,5841	/	/	2,02E-07	/	/	amino acid permease 3 (AAP3)
AT1G78230	/	/	-1,1861	/	/	0,004067031	Outer arm dynein light chain 1 protein
AT1G78460	/	-1,1906	-1,5329	/	0,003348767	0,000201755	SOUL heme-binding family protein
AT1G79160	/	/	1,2249	/	/	6,91E-07	filamentous hemagglutinin transporter
AT1G79310	/	/	1,1589	/	/	8,90E-10	metacaspase 7 (MC7)
AT1G80840	/	/	1,3255	/	/	7,83E-07	WRKY DNA-binding protein 40 (WRKY40)
AT2G02120	-2,5365	-1,6141	-2,4565	3,81E-22	3,15E-12	1,26E-23	Scorpion toxin-like knottin superfamily protein (PDF2.1)
AT2G02450	/	/	4,6671	/	/	0,004526381	NAC domain containing protein 35 (LOV1)
AT2G02990	/	-1,5913	-2,0539	/	7,17E-05	7,93E-07	ribonuclease 1 (RNS1)
AT2G04050	/	4,574	/	/	0,000690336	/	MATE efflux family protein (DTX3)
AT2G05100	1,5078	/	1,7583	0,001865679	/	0,000132045	photosystem II light harvesting complex protein 2.1 (LHCB2.1)
AT2G05380	/	/	-2,2816	/	/	1,56E-05	glycine-rich protein 3 short (GRP3S)
AT2G11810	/	/	-1,0339	/	/	0,000162594	monogalactosyldiacylglycerol synthase type C (MGDC)

AT2G13810	/	-1,0602	-1,3092	/	0,002917298	0,000263107	AGD2-like defense response protein 1 (ALD1)
AT2G14247	2,7026	/	/	0,000284309	/	/	Expressed protein
AT2G15220	/	1,2699	1,4484	/	3,34E-05	2,03E-06	Plant basic secretory protein (BSP) family protein
AT2G15890	-1,6196	-1,3756	-1,2056	6,38E-16	2,71E-14	2,09E-11	maternal effect embryo arrest 14 (MEE14)
AT2G16005	/	1,7185	2,6217	/	7,71E-07	4,41E-14	MD-2-related lipid recognition domain-containing protein
AT2G16380	/	1,699	2,206	/	1,33E-16	2,67E-27	Sec14p-like phosphatidylinositol transfer family protein
AT2G18210	/	1,0294	1,6808	/	1,69E-07	5,01E-18	hypothetical protein
AT2G18620	/	1,3417	1,9165	/	5,85E-08	5,07E-15	Terpenoid synthases superfamily protein
AT2G18700	-1,0116	-1,0308	/	1,04E-06	3,60E-08	/	trehalose phosphatase/synthase 11 (TPS11)
AT2G19190	/	1,7257	1,2958	/	2,10E-10	2,11E-06	FLG22-induced receptor-like kinase 1 (FRK1)
AT2G22860	/	/	1,6115	/	/	1,57E-06	phytosulfokine 2 (PSK2)
AT2G23030	-2,6651	-1,5051	-1,7566	8,14E-20	1,12E-08	3,78E-11	SNF1-related protein kinase 2.9 (SNRK2.9)
AT2G23620	/	1,9695	2,3629	/	6,16E-64	4,08E-92	methyl esterase 1 (MES1)
AT2G24600	/	2,4863	2,4936	/	1,44E-09	1,26E-09	Ankyrin repeat family protein
AT2G24800	/	-5,9052	/	/	5,28E-05	/	Peroxidase superfamily protein
AT2G24850	/	/	4,8154	/	/	3,13E-30	tyrosine aminotransferase 3 (TAT3)
AT2G26380	/	/	3,0108	/	/	0,00084833	Leucine-rich repeat (LRR) family protein
AT2G26690	1,0518	/	/	0,000173544	/	/	Major facilitator superfamily protein
AT2G29340	/	1,1237	1,6855	/	0,003706022	1,09E-05	NAD-dependent epimerase/dehydratase family protein
AT2G30660	-3,7987	/	/	0,000520354	/	/	ATP-dependent caseinolytic (Clp) protease/crotonase family protein
AT2G30750	-1,7135	3,8215	3,3489	0,003110607	8,15E-15	1,03E-11	cytochrome P450 family 71 polypeptide (CYP71A12)
AT2G32510	/	1,0807	1,2477	/	0,000387177	3,93E-05	mitogen-activated protein kinase kinase kinase 17 (MAPKKK1)
AT2G34930	/	/	1,548	/	/	2,37E-18	disease resistance family protein / LRR family protein
AT2G35380	-1,6872	/	-1,2913	0,000643364	/	0,003701365	Peroxidase superfamily protein
AT2G36780	/	-5,7595	/	/	0,000271477	/	UDP-Glycosyltransferase superfamily protein
AT2G37770	/	-2,2148	-2,3526	/	2,88E-19	2,86E-21	NAD(P)-linked oxidoreductase superfamily protein (ChlAKR)
AT2G38750	/	1,1561	1,8555	/	6,31E-54	8,74E-137	annexin 4 (ANNAT4)
AT2G38760	/	/	1,3839	/	/	1,83E-74	annexin 3 (ANNAT3)
AT2G40340	-1,1335	/	-1,9445	9,32E-08	/	1,61E-22	Integrase-type DNA-binding superfamily protein (DREB2C)
AT2G41100	/	1,129	1,3663	/	9,29E-10	1,05E-13	Calcium-binding EF hand family protein (TCH3)
AT2G42980	/	1,3281	1,6866	/	5,99E-06	6,97E-09	Eukaryotic aspartyl protease family protein
AT2G43590	/	-1,0659	-1,5868	/	5,98E-10	4,40E-20	Chitinase family protein
AT2G46510	/	1,2353	2,0766	/	8,56E-06	2,80E-14	ABA-inducible BHLH-type transcription factor (AIB)
AT2G46680	/	/	-1,0467	/	/	1,15E-07	homeobox 7 (HB-7)
AT2G47010	/	/	1,2249	/	/	2,99E-12	calcium/calcium/calmodulin-dependent Serine/Threonine-kinase
AT2G47180	/	/	1,3974	/	/	0,005450228	galactinol synthase 1 (GolS1)
AT3G04070	/	-1,2202	-1,6144	/	5,29E-08	3,00E-12	NAC domain containing protein 47 (NAC047)
AT3G09390	-1,2782	/	-1,1553	1,66E-06	/	4,70E-06	metallothionein 2A (MT2A)
AT3G09940	/	1,1287	1,7448	/	4,55E-64	3,60E-151	monodehydroascorbate reductase (MDHAR)

AT3G10020	-1,3157	-1,1651	-1,2248	5,22E-10	1,35E-09	1,97E-10	plant/protein
AT3G10930	/	1,5942	1,6712	/	2,02E-05	7,53E-06	hypothetical protein
AT3G10986	/	/	1,3325	/	/	0,003368167	LURP-one-like protein (DUF567)
AT3G12500	/	-1,2804	-1,6429	/	1,62E-21	1,01E-33	basic chitinase (HCHIB)
AT3G12580	1,3407	/	/	3,35E-11	/	/	heat shock protein 70 (HSP70)
AT3G12820	-1,2865	/	/	0,001846109	/	/	myb domain protein 10 (MYB10)
AT3G14060	-1,5398	/	/	3,06E-05	/	/	hypothetical protein
AT3G14260	-1,3164	/	/	1,58E-08	/	/	LURP-one-like protein (DUF567)
AT3G16470	/	1,0351	1,2445	/	1,85E-10	1,77E-14	Mannose-binding lectin superfamily protein (JR1)
AT3G16690	/	1,2807	1,5719	/	3,24E-29	2,12E-43	Nodulin MtN3 family protein (SWEET16)
AT3G17880	/	3,9702	3,4239	/	0	0	tetraticopeptide domain-containing thioredoxin (TDX)
AT3G18930	-1,3143	/	/	0,001443971	/	/	RING/U-box superfamily protein
AT3G19200	/	/	1,5726	/	/	1,24E-08	hypothetical protein
AT3G22250	/	/	1,4665	/	/	4,25E-14	UDP-Glycosyltransferase superfamily protein
AT3G22415	/	-1,1199	/	/	0,00591159	/	hypothetical protein
AT3G22560	/	1,7655	2,1073	/	4,23E-08	4,15E-11	Acyl-CoA N-acyltransferases (NAT) superfamily protein
AT3G22830	-1,2989	-1,1378	-1,8798	1,60E-08	3,90E-08	4,69E-18	heat shock transcription factor A6B (HSFA6B)
AT3G23510	/	1,1284	1,5437	/	3,05E-10	6,87E-18	Cyclopropane-fatty-acyl-phospholipid synthase
AT3G25820	/	-1,5091	/	/	2,06E-05	/	terpene synthase-like sequence-1,8-cineole (TPS-CIN)
AT3G26450	/	1,2349	1,7249	/	1,50E-21	4,78E-41	Polyketide cyclase/dehydrase and lipid transport superfamily protein
AT3G26460	/	1,7256	2,2255	/	5,53E-10	1,12E-15	Polyketide cyclase/dehydrase and lipid transport superfamily protein
AT3G27416	/	/	1,0082	/	/	0,002639342	transmembrane protein
AT3G27650	/	/	-1,8324	/	/	0,001074086	LOB domain-containing protein 25 (LBD25)
AT3G28290	/	3,8063	4,7098	/	4,24E-05	3,10E-07	transmembrane protein, putative (DUF677) (AT14A9
AT3G29250	/	/	1,018	/	/	4,00E-83	NAD(P)-binding Rossmann-fold superfamily protein (SDR4)
AT3G29670	/	3,4468	4,1957	/	5,29E-06	2,41E-08	HXXXD-type acyl-transferase family protein (PMAT2)
AT3G30720	3,3257	4,5088	4,135	6,11E-08	2,32E-16	6,51E-14	qua-quine starch (QQS)
AT3G44260	/	2,7488	1,9784	/	9,98E-10	1,44E-05	Polynucleotidyl transferase, ribonuclease H-like superfamily protein (CAF1a)
AT3G44860	/	4,6136	7,2779	/	0,000231	5,18E-07	farnesoic acid carboxyl-O-methyltransferase (FAMT)
AT3G45070	/	1,0064	1,2359	/	1,72E-27	9,54E-41	P-loop containing nucleoside triphosphate hydrolases superfamily protein
AT3G45680	/	1,729	2,2214	/	1,99E-31	8,35E-52	Major facilitator superfamily protein
AT3G46700	/	1,0936	1,5628	/	1,13E-47	3,48E-96	UDP-Glycosyltransferase superfamily protein
AT3G46880	/	/	1,6686	/	/	0,00518417	hypothetical protein
AT3G47340	-1,511	/	1,3121	0,00183736	/	0,002439882	glutamine-dependent asparagine synthase 1 (ASN1)
AT3G49570	/	1,7436	2,1112	/	8,39E-11	1,93E-15	response to low sulfur 3 (LSU3)
AT3G49580	/	/	1,4439	/	/	0,005793983	response to low sulfur 1 (LSU1)
AT3G50310	/	/	-3,0806	/	/	0,002492003	mitogen-activated protein kinase kinase kinase 20 (MAPKKK20)
AT3G50460	-2,1752	/	/	0,001429705	/	/	homolog of RPW8 2 (HR2)
AT3G50610	1,4576	1,7849	1,7828	0,002742561	2,61E-05	2,66E-05	DNA-directed RNA polymerase II subunit RPB1-like protein

AT3G50930	/	/	1,2941	/	/	7,79E-21	cytochrome BC1 synthesi (BCS1)
AT3G50970	/	/	-1,0131	/	/	1,52E-27	dehydrin family protein (LTI30)
AT3G51570	/	1,72	/	/	2,53E-06	/	Disease resistance protein (TIR-NBS-LRR class) family
AT3G51960	/	/	1,1456	/	/	0,005239631	basic leucine zipper 24 (BZIP24)
AT3G53600	/	/	1,826	/	/	3,50E-07	C2H2-type zinc finger family protein
AT3G53830	/	1,0054	1,5484	/	6,57E-08	4,40E-17	Regulator of chromosome condensation (RCC1) family protein
AT3G54150	/	1,5902	1,2566	/	4,40E-08	1,68E-05	S-adenosyl-L-methionine-dependent methyltransferases superfamily protein
AT3G56080	/	/	1,4658	/	/	3,48E-11	S-adenosyl-L-methionine-dependent methyltransferases superfamily protein
AT3G56620	-1,8512	/	-1,231	0,000190523	/	0,006067421	nodulin MtN21 /EamA-like transporter family protein (UMAMIZ10)
AT3G56710	/	1,0043	/	/	0,000957464	/	sigma factor binding protein 1 (SIB1)
AT3G59340	/	/	1,1773	/	/	2,17E-13	solute carrier family 35 protein (DUF914)
AT3G59710	/	2,6591	3,8965	/	1,30E-156	0	NAD(P)-binding Rossmann-fold superfamily protein
AT3G59740	/	1,4519	1,7743	/	0,003811321	0,000349702	Concanavalin A-like lectin protein kinase family protein
AT3G59930	/	1,1571	1,004	/	8,27E-16	2,89E-12	defensin-like protein
AT3G60120	/	7,6646	7,3008	/	4,82E-09	2,58E-08	beta glucosidase 27 (BGLU27)
AT3G61280	/	3,0979	4,1984	/	0,002951641	4,56E-05	O-glucosyltransferase rumi-like protein (DUF821)
AT3G62680	/	1,0013	/	/	2,03E-13	/	proline-rich protein 3 (PRP3)
AT4G02330	/	2,411	2,0189	/	3,10E-10	1,40E-07	Plant invertase/pectin methylesterase inhibitor superfamily (ATPMEPCRB)
AT4G04840	/	/	1,1358	/	/	1,57E-24	methionine sulfoxide reductase B6 (MSBR6)
AT4G10500	/	/	1,7196	/	/	1,28E-23	2-oxoglutarate (2OG) and Fe(II)-dependent oxygenase superfamily protein
AT4G10780	/	/	1,1774	/	/	0,007481724	LRR and NB-ARC domains-containing disease resistance protein
AT4G11070	/	2,9182	2,5411	/	7,44E-05	0,000591541	WRKY family transcription factor (WRKY41)
AT4G11190	1,1095	1,6111	2,0233	7,48E-12	1,20E-29	7,51E-46	Disease resistance-responsive (dirigent-like protein) family protein
AT4G11211	/	/	1,0072	/	/	3,02E-09	hypothetical protein
AT4G11393	/	/	-1,2134	/	/	0,000580335	Defensin-like (DEFL) family protein
AT4G12470	-2,9416	/	/	2,19E-05	/	/	azelaic acid induced 1 (AZI1)
AT4G12480	-2,5288	-1,0294	-1,064	6,37E-17	0,000141691	8,40E-05	Bifunctional inhibitor/lipid-transfer protein/seed storage 2S albumin superfamily protein (EARLI1)
AT4G13300	/	/	1,8256	/	/	2,06E-12	terpenoid synthase 13 (TPS13)
AT4G13310	/	/	2,6223	/	/	8,25E-18	cytochrome P450, family 71, subfamily A, polypeptide 20 (CYP71A20)
AT4G14270	-1,3344	/	-1,4769	3,17E-07	/	2,84E-10	polyadenylate-binding protein interacting protein
AT4G14365	/	2,6287	2,2607	/	1,64E-09	2,45E-07	Putative E3 ubiquitin-protein ligase (XBAT34)
AT4G15236	/	/	-1,7948	/	/	0,005891197	ABC-2 and Plant PDR ABC-type transporter family protein (ABCG43)
AT4G15330	/	/	1,0595	/	/	4,49E-19	cytochrome P450, family 705, subfamily A, polypeptide 1 (CYP705A1)
AT4G15765	/	/	1,362	/	/	2,84E-08	FAD/NAD(P)-binding oxidoreductase family protein

AT4G16890	-1,055	/	/	0,000192072	/	/	TIR-NBS-LRR class disease resistance protein (SNC1)
AT4G19810	/	/	-1,1815	/	/	1,47E-06	Glycosyl hydrolase family protein with chitinase insertion domain-containing protein (ChiC)
AT4G20190	/	/	1,1508	/	/	3,48E-09	hypothetical protein
AT4G21840	/	1,1738	1,8928	/	3,27E-05	1,03E-11	methionine sulfoxide reductase B8 (MSRB8)
AT4G21920	/	5,0666	5,7179	/	0,00161343	0,00033391	hypothetical protein
AT4G22212	/	1,0674	1,4566	/	6,09E-15	1,67E-26	defensin-like protein
AT4G22214	/	2,2745	3,4378	/	3,98E-38	3,42E-85	Defensin-like (DEFL) family protein
AT4G22470	/	1,732	2,1131	/	1,13E-07	6,68E-11	protease inhibitor/seed storage/lipid transfer protein (LTP) family protein
AT4G22610	/	2,175	3,3699	/	2,36E-11	8,85E-26	Bifunctional inhibitor/lipid-transfer protein/seed storage 2S albumin superfamily protein
AT4G22960	/	/	1,6112	/	/	0,004667286	FAM63A-like protein (DUF544)
AT4G23420	/	/	1,1725	/	/	7,65E-40	NAD(P)-binding Rossmann-fold superfamily protein
AT4G23510	/	/	1,0725	/	/	1,03E-18	Disease resistance protein (TIR-NBS-LRR class) family
AT4G23670	/	1,5999	1,8773	/	9,34E-18	7,39E-24	Polyketide cyclase/dehydrase and lipid transport superfamily protein
AT4G23680	/	1,1857	1,8262	/	2,90E-05	8,83E-11	Polyketide cyclase/dehydrase and lipid transport superfamily protein
AT4G24340	/	1,6234	2,4508	/	7,18E-70	4,37E-160	Phosphorylase superfamily protein
AT4G25433	/	/	-2,2302	/	/	0,008173386	peptidoglycan-binding LysM domain-containing protein
AT4G25470	/	2,9183	/	/	0,002154299	/	C-repeat/DRE binding factor 2 (CBF2)
AT4G27450	-1,2582	/	/	3,58E-05	/	/	aluminum induced protein with YGL and LRDR motifs
AT4G27550	5,5595	/	/	0,001530362	/	/	trehalose-6-phosphatase synthase S4 (TPS4)
AT4G27654	/	1,8368	/	/	0,004623808	/	transmembrane protein
AT4G29780	/	1,1581	/	/	1,80E-06	/	nuclease
AT4G30140	-1,8746	/	/	2,81E-10	/	/	GDSL-like Lipase/Acylhydrolase superfamily protein (CDEF1)
AT4G30650	-1,0324	/	/	1,16E-14	/	/	Low temperature and salt responsive protein family
AT4G31330	/	/	1,0783	/	/	7,73E-06	transmembrane protein, putative (Protein of unknown function, DUF599)
AT4G31510	-1,1103	/	/	0,001676867	/	/	major centromere autoantigen B-like protein
AT4G33070	/	-1,1907	-1,7869	/	1,35E-05	7,27E-11	Thiamine pyrophosphate dependent pyruvate decarboxylase family protein
AT4G33220	/	-1,1621	-1,545	/	1,25E-07	4,66E-12	pectin methylesterase 44 (PME44)
AT4G33467	/	-2,7405	-2,1746	/	0,001343988	0,007119925	hypothetical protein
AT4G33666	/	-1,268	/	/	1,18E-08	/	hypothetical protein
AT4G33980	-1,829	/	-2,3365	1,93E-13	/	1,57E-23	hypothetical protein
AT4G34650	/	-2,9462	/	/	0,005106513	/	squalene synthase 2 (SQS2)
AT4G36600	/	/	5,0534	/	/	0,007369184	Late embryosis abundant (LEA) protein
AT4G37409	/	/	1,1987	/	/	3,22E-16	hypothetical protein
AT4G39950	/	1,0691	1,7898	/	1,83E-13	5,37E-35	cytochrome P450, family 79, subfamily B, polypeptide 2 (CYP79B2)
AT5G01200	1,1012	/	/	1,27E-06	/	/	Duplicated homeodomain-like superfamily protein
AT5G01540	/	1,2117	1,1703	/	0,003536182	0,004857497	lectin receptor kinase a4.1 (LECRKA4.1)
AT5G01660	/	/	-1,0212	/	/	0,001264434	influenza virus NS1A-binding protein

AT5G02230	/	/	1,0119	/	/	3,42E-35	Haloacid dehalogenase-like hydrolase (HAD) superfamily protein
AT5G02490	1,1451	/	/	8,38E-39	/	/	Heat shock protein 70 (Hsp 70) family protein (Hsp70-2
AT5G03570	-1,0594	/	/	0,000960409	/	/	iron regulated 2 (IREG2)
AT5G05390	2,217	/	/	0,000279652	/	/	laccase 12 (LAC12)
AT5G05410	/	/	-1,4125	/	/	1,42E-33	DRE-binding protein 2A (DREB2A)
AT5G06530	1,1974	/	/	6,94E-05	/	/	ABC-2 type transporter family protein (ABC22)
AT5G09980	/	/	1,3245	/	/	1,64E-30	elicitor peptide 4 (PROPEP4)
AT5G10140	/	1,5892	/	/	0,000373248	/	K-box region and MADS-box transcription factor family protein (FLC)
AT5G12020	/	/	4,2873	/	/	0,007636243	17.6 kDa class II heat shock protein (HSP17.6II)
AT5G13080	/	-1,2664	/	/	1,32E-05	/	WRKY DNA-binding protein 75 (WRKY75)
AT5G15970	/	1,0217	1,3404	/	2,81E-05	3,90E-08	stress-responsive protein (KIN2) / stress-induced protein (KIN2) / cold-responsive protein (COR6.6) / cold-regulated protein (COR6.6) (KIN2)
AT5G16080	/	3,7288	4,5006	/	0,006214856	0,000862311	carboxyesterase 17 (CXE17)
AT5G16340	1,197	/	/	0,000947052	/	/	AMP-dependent synthetase and ligase family protein
AT5G16970	/	/	-1,085	/	/	5,75E-05	alkenal reductase (AER)
AT5G16980	/	/	-2,6436	/	/	0,006699253	Zinc-binding dehydrogenase family protein
AT5G17960	/	/	-1,1464	/	/	0,007829173	Cysteine/Histidine-rich C1 domain family protein
AT5G19110	/	/	1,6579	/	/	1,52E-121	Eukaryotic aspartyl protease family protein
AT5G19140	-1,2661	/	/	1,02E-06	/	/	aluminum induced protein with YGL and LRDR motifs (AILP1)
AT5G20230	/	3,74	3,1394	/	5,33E-14	3,58E-10	blue-copper-binding protein (BCB)
AT5G20790	/	/	-1,3409	/	/	4,52E-11	transmembrane protein
AT5G21100	/	1,3586	1,5637	/	4,30E-06	1,00E-07	Plant L-ascorbate oxidase
AT5G22410	/	1,4581	1,6262	/	6,78E-19	3,91E-23	root hair specific 18 (RHS18)
AT5G22540	/	/	1,4102	/	/	0,003909038	transmembrane protein, putative (DUF247)
AT5G22570	/	1,1384	1,9901	/	8,31E-06	3,74E-15	WRKY DNA-binding protein 38 (WRKY38)
AT5G22860	/	-2,0809	-2,3313	/	2,06E-11	1,86E-13	Serine carboxypeptidase S28 family protein
AT5G23010	/	2,1584	3,1274	/	9,31E-05	1,38E-08	methylthioalkylmalate synthase 1 (MAM1)
AT5G23820	/	1,002	2,0656	/	5,11E-40	1,90E-165	MD-2-related lipid recognition domain-containing protein
AT5G24110	/	2,4314	2,188	/	7,63E-14	1,92E-11	WRKY DNA-binding protein 30 (WRKY30)
AT5G24660	/	1,3114	1,437	/	1,55E-09	3,24E-11	response to low sulfur 2 (LSU2)
AT5G25140	1,682	/	/	0,000444215	/	/	cytochrome P450, family 71, subfamily B, polypeptide 13 (CYP71B13)
AT5G25910	-1,3471	/	/	0,000290363	/	/	receptor like protein 52 (RLP52)
AT5G26260	/	/	1,5014	/	/	1,07E-208	TRAF-like family protein
AT5G26920	-1,9456	1,4641	1,2927	1,73E-07	3,95E-06	4,74E-05	Cam-binding protein 60-like G (CBP60G)
AT5G28770	-1,1092	-1,0346	/	0,000827652	0,000499596	/	bZIP transcription factor family protein (BZO2H3)
AT5G35940	/	/	2,0071	/	/	3,11E-35	Mannose-binding lectin superfamily protein (JAL41)
AT5G35940	/	1,0222	/	/	3,18E-10	/	Mannose-binding lectin superfamily protein
AT5G36220	/	/	1,2288	/	/	0,00190536	cytochrome p450 81d1 (CYP81D1)

AT5G37980	/	1,2318	1,5682	/	0,000155219	1,29E-06	Zinc-binding dehydrogenase family protein
AT5G38000	/	1,6623	2,2451	/	5,27E-24	6,09E-43	Zinc-binding dehydrogenase family protein
AT5G38700	/	1,3649	1,3187	/	1,22E-05	2,40E-05	cotton fiber protein
AT5G39050	/	-1,5277	-2,0535	/	1,19E-07	1,43E-12	HXXXD-type acyl-transferase family protein (PMAT1)
AT5G39580	/	/	1,009	/	/	0,001845448	Peroxidase superfamily protein
AT5G40210	/	1,3081	2,2723	/	2,31E-12	2,25E-35	nodulin MtN21 /EamA-like transporter family protein (UMAMIZ4)
AT5G41730	/	1,231	1,0085	/	1,19E-10	1,50E-07	Protein kinase family protein
AT5G42900	-1,6576	-1,8301	-2,4597	1,27E-07	2,09E-10	1,37E-16	cold regulated protein 27 (COR27)
AT5G42930	/	/	1,9558	/	/	2,29E-40	alpha/beta-Hydrolases superfamily protein
AT5G44050	/	2,6013	3,8849	/	0,002327533	3,71E-06	MATE efflux family protein
AT5G44550	-1,6955	/	-1,0058	7,63E-05	/	0,008935319	Uncharacterized protein family (UPF0497)
AT5G44568	/	2,3262	/	/	6,01E-05	/	transmembrane protein
AT5G44820	/	1,2464	1,3992	/	1,13E-16	9,57E-21	Nucleotide-diphospho-sugar transferase family protein
AT5G46050	/	1,372	1,2364	/	5,52E-14	1,32E-11	peptide transporter 3 (PTR3)
AT5G48250	/	/	-1,3607	/	/	1,27E-24	B-box type zinc finger protein with CCT domain-containing protein (BBX8)
AT5G49450	-1,4345	/	/	4,90E-05	/	/	basic leucine-zipper 1 (bZIP1)
AT5G49525	/	/	-1,4824	/	/	0,009070888	transmembrane protein
AT5G49850	/	-1,207	-2,011	/	1,90E-09	4,84E-22	Mannose-binding lectin superfamily protein
AT5G50630	2,1412	/	/	0,001858366	/	/	Major facilitator superfamily protein
AT5G51440	1,0646	/	/	0,00011173	/	/	HSP20-like chaperones superfamily protein
AT5G52330	-2,3481	/	/	0,000692094	/	/	TRAF-like superfamily protein
AT5G52750	/	1,5914	1,1928	/	6,61E-06	0,000811293	Heavy metal transport/detoxification superfamily protein
AT5G52760	/	5,3138	5,1741	/	0,001630707	0,002172721	Copper transport protein family
AT5G54470	1,2344	1,7371	1,9336	0,001825409	1,49E-06	7,48E-08	B-box type zinc finger family protein (BBX29)
AT5G54710	/	2,4683	2,155	/	1,69E-05	0,000184805	Ankyrin repeat family protein
AT5G54960	-1,0201	-1,2267	-1,7188	1,38E-09	4,26E-16	1,66E-29	pyruvate decarboxylase-2 (PDC2)
AT5G56160	/	1,0477	/	/	9,71E-05	/	Sec14p-like phosphatidylinositol transfer family protein
AT5G57190	/	/	1,1323	/	/	2,46E-08	phosphatidylserine decarboxylase 2 (PSD2)
AT5G58670	/	/	1,0769	/	/	0,004401892	phospholipase C1 (PLC1)
AT5G59080	-1,2882	/	/	0,002449584	/	/	hypothetical protein
AT5G59590	/	/	1,3038	/	/	4,35E-21	UDP-glucosyl transferase 76E2 (UGT76E2)
AT5G61590	-1,0085	-1,0466	-1,1556	0,000667169	9,02E-05	1,61E-05	Integrase-type DNA-binding superfamily protein
AT5G63450	/	1,2144	1,6832	/	1,53E-19	2,45E-36	cytochrome P450, family 94, subfamily B, polypeptide 1 (CYP94B1)
AT5G64110	/	1,1482	1,4111	/	7,63E-05	9,69E-07	Peroxidase superfamily protein
AT5G64260	/	-1,0194	-1,0591	/	2,21E-28	1,72E-30	EXORDIUM like 2 (EXI2)
AT5G64510	/	1,3308	1,4608	/	1,30E-06	9,69E-08	tunicamycin induced protein (TIN1)
AT5G64900	/	1,706	2,3281	/	3,34E-07	1,71E-12	of peptide 1 (PROPEP1)
AT5G65158	-2,23	/	/	0,000219209	/	/	Lipase/lipooxygenase, PLAT/LH2 family protein (PLAT3)

AT5G65207	-1,3891	/	-1,0907	4,72E-05	/	0,000351818	hypothetical protein
AT5G66640	/	2,7764	2,7633	/	4,46E-05	4,82E-05	DA1-related protein 3 (DAR3)
AT5G66815	1,7942	1,5373	1,4345	1,20E-11	2,54E-11	4,97E-10	transmembrane protein
AT5G66816	3,7444	1,975	1,7724	2,09E-05	0,00094068	0,003086466	DNA-directed RNA polymerase II subunit RPB1-like protein
AT5G67370	1,1863	/	/	1,68E-05	/	/	DUF1230 family protein (DUF1230) (CGLD27)
secondary metabolic processes							
AT1G01420	/	1,1586	1,1786	/	9,76E-05	7,25E-05	UDP-glucosyl transferase 72B3 (UGT72B3)
AT1G02920	-1,0535	1,5984	1,6216	2,49E-10	5,37E-28	8,54E-29	glutathione S-transferase 7 (GSTF7)
AT1G04330	/	/	1,4785	/	/	0,000786157	hypothetical protein
AT1G10370	/	/	1,1859	/	/	0,007489952	Glutathione S-transferase family protein (ERD9)
AT1G16400	/	/	1,3221	/	/	0,000171489	cytochrome P450, family 79, subfamily F, polypeptide 2 (CYP79F2)
AT1G18590	/	/	1,2331	/	/	8,93E-19	sulfotransferase 17 (SOT17)
AT1G21100	/	/	1,099	/	/	0,000687787	O-methyltransferase family protein (IGMT1)
AT1G27020	-1,3294	-1,2328	/	0,001040331	0,000785953	/	plant/protein
AT1G30530	1,6807	1,4682	3,5109	0,000270531	0,000337073	6,38E-18	UDP-glucosyl transferase 78D1 (UGT78D1)
AT1G35515	/	1,3053	1,342	/	1,79E-07	7,57E-08	high response to osmotic stress 10 HOS10)
AT1G52100	/	/	2,0538	/	/	9,75E-08	Mannose-binding lectin superfamily protein (JAIL11)
AT1G56160	/	-5,2929	/	/	0,002121113	/	myb domain protein 72 (MYB72)
AT1G60270	/	1,0562	1,0144	/	1,72E-07	5,20E-07	beta glucosidase 6 (BGLU6)
AT1G62560	/	/	4,3896	/	/	0,000166253	flavin-monooxygenase glucosinolate S-oxygenase 3 (FMO GS-OX3)
AT1G63295	/	/	1,4462	/	/	0,000227511	Remorin family protein
AT1G64670	/	/	-1,6825	/	/	0,00027508	alpha/beta-Hydrolases superfamily protein (BDG1)
AT1G65060	/	/	1,0803	/	/	1,16E-05	4-coumarate:CoA ligase 3 (4CL3)
AT1G65860	/	2,1073	3,6668	/	0,003744039	2,30E-07	flavin-monooxygenase glucosinolate S-oxygenase 1 (FMO GS-OX1)
AT1G66270	/	/	1,2904	/	/	7,12E-80	Glycosyl hydrolase superfamily protein (BGLU21)
AT1G69920	/	3,197	2,7364	/	1,56E-12	1,74E-09	glutathione S-transferase TAU 12 (GSTU12)
AT1G71030	-1,9726	/	/	0,001830368	/	/	MYB-like 2 (MYBL2)
AT1G73300	/	1,0693	1,5838	/	3,36E-09	8,80E-19	serine carboxypeptidase-like 2 (scpl2)
AT1G78370	/	/	1,2236	/	/	2,66E-06	glutathione S-transferase TAU 20 (GSTU20)
AT2G02930	/	5,0899	4,2212	/	0,00013589	0,001668254	glutathione S-transferase F3 (GSTF3)
AT2G03980	/	1,2422	1,7006	/	4,61E-08	5,30E-14	GDSL-like Lipase/Acylhydrolase superfamily protein
AT2G04080	/	2,119	2,7129	/	3,96E-05	1,12E-07	MATE efflux family protein (DTX2)
AT2G05440	-1,3285	/	/	0,000156828	/	/	GLYCINE RICH PROTEIN 9 (GRP9)
AT2G22330	/	/	1,4417	/	/	5,75E-22	cytochrome P450, family 79, subfamily B, polypeptide 3 (CYP79B3)
AT2G25820	/	5,527	5,3225	/	3,33E-06	7,71E-06	Integrase-type DNA-binding superfamily protein (ESE2)
AT2G29440	/	1,3725	2,1383	/	8,05E-57	6,28E-138	glutathione S-transferase tau 6 (GSTU6)
AT2G29450	/	/	1,1603	/	/	1,02E-33	glutathione S-transferase tau 5 (GSTU5)

AT2G31790	/	1,2779	1,9171	/	8,03E-11	9,68E-23	UDP-Glycosyltransferase superfamily protein
AT2G36650	/	/	1,2214	/	/	9,88E-15	CHUP1-like protein
AT2G38390	/	/	1,087	/	/	3,90E-05	Peroxidase superfamily protein
AT2G43000	/	1,2844	/	/	8,13E-05	/	NAC domain containing protein 42 (NAC042)
AT2G43100	/	/	1,6016	/	/	5,55E-05	isopropylmalate isomerase 2 (IPMI2)
AT2G43620	/	1,495	1,7781	/	4,12E-12	9,81E-17	Chitinase family protein
AT2G44940	/	/	1,1288	/	/	2,67E-13	Integrase-type DNA-binding superfamily protein
AT2G46650	/	/	1,2974	/	/	5,14E-08	cytochrome B5 (CB5-C)
AT2G46770	/	5,4079	5,8847	/	0,000373382	0,000103184	NAC (No Apical Meristem) domain transcriptional regulator superfamily protein (NST1)
AT3G02940	/	/	-2,419	/	/	3,94E-07	myb domain protein 107 (MYB107)
AT3G03190	-1,4227	/	1,2332	6,21E-05	/	5,31E-06	glutathione S-transferase F11 (GSTF11)
AT3G10450	/	4,2915	/	/	0,005475083	/	serine carboxypeptidase-like 7 (SCPL7)
AT3G12230	/	/	1,2024	/	/	0,00310375	serine carboxypeptidase-like 14 (scpl14)
AT3G19710	-1,9896	2,677	4,0622	0,003386322	6,61E-06	7,55E-12	branched-chain aminotransferase4 (BCAT4)
AT3G26200	/	3,4718	2,8756	/	3,26E-09	1,07E-06	cytochrome P450, family 71, subfamily B, polypeptide 22 (CYP71B22)
AT3G48450	-1,7317	/	/	3,23E-07	/	/	RPM1-interacting protein 4 (RIN4) family protein
AT3G53510	/	/	-1,3425	/	/	0,000946902	ABC-2 type transporter family protein (ABCG20)
AT3G54600	/	/	1,2113	/	/	6,80E-05	Class I glutamine amidotransferase-like superfamily protein (DJ1F)
AT3G55700	/	1,4083	1,3695	/	8,73E-05	0,000136203	UDP-Glycosyltransferase superfamily protein
AT3G58990	/	/	1,4496	/	/	6,35E-10	isopropylmalate isomerase 1 (IPM1)
AT4G04610	/	/	1,2521	/	/	7,40E-36	APS reductase 1 (APR1)
AT4G04810	/	/	1,1513	/	/	6,47E-06	methionine sulfoxide reductase B4 (MSRB4)
AT4G12030	/	/	1,2266	/	/	1,58E-10	bile acid transporter 5 (BAT5)
AT4G12440	/	1,2704	1,5399	/	1,68E-11	2,36E-16	adenine phosphoribosyl transferase 4 (APT4)
AT4G13770	-1,7319	/	1,8028	0,002622305	/	0,000410576	cytochrome P450, family 83, subfamily A, polypeptide 1 (CYP83A1)
AT4G15430	/	/	1,0263	/	/	7,78E-10	ERD (early-responsive to dehydration stress) family protein
AT4G16146	/	/	-1,1631	/	/	1,42E-08	cAMP-regulated phosphoprotein 19-related protein
AT4G17785	/	/	-1,0031	/	/	2,15E-06	myb domain protein 39 (MYB39)
AT4G19370	-1,5255	/	/	0,0009763	/	/	chitin synthase, putative (DUF1218)
AT4G29700	/	/	1,1594	/	/	3,14E-49	Alkaline-phosphatase-like family protein
AT4G31500	/	/	1,1179	/	/	2,72E-47	cytochrome P450, family 83, subfamily B, polypeptide 1 (CYP83B1)
AT4G37410	/	/	1,1445	/	/	3,18E-81	cytochrome P450, family 81, subfamily F, polypeptide 4 (CYP81F4)
AT4G37430	/	/	1,2748	/	/	6,25E-28	cytochrome P450, family 91, subfamily A, polypeptide 2 (CYP91A2)
AT4G39330	/	/	1,7989	/	/	0,003100264	cinnamyl alcohol dehydrogenase 9 (CAD9)
AT5G15360	/	/	-2,2374	/	/	0,001740086	transmembrane protein
AT5G23020	/	1,2326	1,7288	/	0,001054429	4,32E-06	2-isopropylmalate synthase 2 (IMS2)

AT5G26270	1,4134	1,6906	2,2922	4,31E-17	1,27E-30	5,37E-56	transmembrane protein
AT5G45095	/	-1,3743	-1,96	/	0,005456448	0,000140439	hypothetical protein
AT5G58860	-1,5357	-1,1399	/	0,000205917	0,002167755	/	cytochrome P450, family 86, subfamily A, polypeptide 1 (CYP86A1)
AT5G59580	/	1,3493	2,5514	/	0,00033654	2,32E-12	UDP-glucosyl transferase 76E1 (UGT76E1)
AT5G61290	/	/	1,919	/	/	4,58E-07	Flavin-binding monooxygenase family protein
AT5G63560	/	2,1081	1,6363	/	5,46E-06	0,00046563	HXXXD-type acyl-transferase family protein (FACT)
response to stimulus							
AT1G01190	/	/	1,4431	/	/	0,00967922	cytochrome P450, family 78, subfamily A, polypeptide 8 (CYP78A8)
AT1G02650	2,0001	/	/	0,003308482	/	/	Tetratricopeptide repeat (TPR)-like superfamily protein
AT1G03410	/	/	1,6275	/	/	8,19E-15	2-oxoglutarate (2OG) and Fe(II)-dependent oxygenase superfamily protein 2A6)
AT1G05560	/	-1,181	-1,5961	/	5,56E-07	1,47E-11	UDP-glucosyltransferase 75B1 (UGT75B1)
AT1G07690	/	/	-1,6607	/	/	6,81E-05	transmembrane protein
AT1G08430	-1,0047	-1,2259	-1,868	7,97E-05	8,16E-08	1,60E-15	aluminum-activated malate transporter 1 (ALMT1)
AT1G13420	/	/	1,2537	/	/	6,67E-18	sulfotransferase 4B (ST4B)
AT1G15630	/	/	1,0983	/	/	8,12E-05	transmembrane protein
AT1G19200	/	/	2,5466	/	/	1,69E-21	cyclin-dependent kinase, putative (DUF581)
AT1G19960	-1,2728	/	/	1,34E-07	/	/	transcription factor
AT1G21140	-1,159	/	-2,1492	4,14E-06	/	1,43E-20	Vacuolar iron transporter (VIT) family protein
AT1G21320	/	1,8472	/	/	0,0003018	/	nucleic acid/nucleotide binding protein
AT1G21680	/	/	-1,3306	/	/	1,49E-21	DPP6 N-terminal domain-like protein
AT1G22290	/	1,4093	1,5235	/	0,001556761	0,000611805	14-3-3 family protein
AT1G26210	/	/	-1,0616	/	/	0,000402798	SOB five-like 1 (SOFL1)
AT1G28330	-1,4644	/	/	6,42E-06	/	/	dormancy-associated protein-like 1 (DYL1)
AT1G29920	/	/	4,6869	/	/	0,004775906	chlorophyll A/B-binding protein 2 (CAB2)
AT1G31670	3,6812	2,7285	3,8934	0,003102055	0,002938142	1,47E-05	Copper amine oxidase family protein
AT1G33100	/	1,0168	/	/	0,000154	/	MATE efflux family protein
AT1G34670	-1,1416	/	/	0,000204331	/	/	myb domain protein 93 (MYB93)
AT1G44130	/	3,2228	2,5729	/	0,000423527	0,005228619	Eukaryotic aspartyl protease family protein
AT1G44350	/	/	1,0246	/	/	8,07E-12	IAA-amino acid hydrolase ILR1-like 6 (ILL6)
AT1G44575	1,1795	/	/	7,49E-06	/	/	Chlorophyll A-B binding family protein (NPQ4)
AT1G49720	-1,1549	/	-1,5849	2,83E-06	/	8,34E-13	abscisic acid responsive element-binding factor 1 (ABF1)
AT1G50280	/	/	1,9327	/	/	0,001701572	Phototropic-responsive NPH3 family protein
AT1G52342	/	-1,4821	/	/	0,00094431	/	hypothetical protein
AT1G54970	/	2,0991	2,3222	/	8,79E-41	1,42E-49	proline-rich protein 1 (PRP1)
AT1G56300	/	/	-1,396	/	/	1,59E-17	Chaperone DnaJ-domain superfamily protein
AT1G66800	/	/	1,4207	/	/	2,19E-48	NAD(P)-binding Rossmann-fold superfamily protei
AT1G67856	3,0652	/	/	0,00021213	/	/	RING/U-box superfamily protein
AT1G69570	/	1,2371	1,3702	/	6,48E-07	3,09E-08	Dof-type zinc finger DNA-binding family protein

AT1G70800	-1,2059	/	/	0,000781482	/	/	Calcium-dependent lipid-binding (CaLB domain) family protein (EHB1)
AT1G77880	/	/	-1,795	/	/	0,002536108	Galactose oxidase/kelch repeat superfamily protein
AT2G15960	/	/	-1,2552	/	/	0,0008525	stress-induced protein
AT2G18370	-1,6619	/	/	0,000156223	/	/	Bifunctional inhibitor/lipid-transfer protein/seed storage 2S albumin superfamily protein
AT2G21130	/	/	-1,1952	/	/	4,24E-12	Cyclophilin-like peptidyl-prolyl cis-trans isomerase family proteine
AT2G22460	/	/	-1,919	/	/	0,00072949	MIZU-KUSSEI-like protein (Protein of unknown function, DUF617)
AT2G22540	/	-2,1111	-2,3444	/	6,40E-11	9,56E-13	K-box region and MADS-box transcription factor family protein (SVP)
AT2G23180	/	1,7986	1,8869	/	0,000340353	0,000164304	cytochrome P450, family 96, subfamily A, polypeptide 1 (CYP96A1)
AT2G25130	/	1,0094	/	/	0,000117049	/	ARM repeat superfamily protein
AT2G26530	/	/	1,0723	/	/	9,86E-06	pheromone receptor-like protein (DUF1645) (AR781)
AT2G28210	/	-1,7005	-2,4341	/	3,40E-12	1,84E-21	alpha carbonic anhydrase 2 (ACA2)
AT2G29120	/	1,3977	/	/	0,002949563	/	glutamate receptor 2.7 (GLR2.7)
AT2G29630	-1,5277	-1,3587	-2,9576	0,000257731	0,000361535	1,32E-11	thiaminC (THIC)
AT2G29650	/	1,0392	/	/	1,54E-07	/	Sodium-dependent phosphate transport protein 1 (PHT4)
AT2G29710	/	/	1,1586	/	/	4,79E-06	UDP-Glycosyltransferase superfamily protein
AT2G31380	/	1,2146	1,4689	/	3,43E-06	1,64E-08	salt tolerance homologue (STH)
AT2G32487	/	4,5491	5,717	/	0,001697975	6,68E-05	hypothetical protein
AT2G32990	/	/	1,2701	/	/	7,11E-25	glycosyl hydrolase 9B8 (GH9B8)
AT2G33830	-1,8263	-1,3313	-1,3107	6,67E-05	0,001160087	0,001381706	Dormancy/auxin associated family protein
AT2G34350	/	1,2805	2,353	/	4,21E-18	7,62E-59	Nodulin-like / Major Facilitator Superfamily protein
AT2G36970	/	/	-4,7172	/	/	0,009171061	UDP-Glycosyltransferase superfamily protein
AT2G37280	/	/	1,0253	/	/	2,41E-11	pleiotropic drug resistance 5 (ABCG33)
AT2G37640	/	1,665	2,0173	/	5,74E-08	3,50E-11	Barwin-like endoglucanases superfamily protein (EXP3)
AT2G40080	-1,3797	-1,2279	-1,6874	2,76E-14	3,91E-14	3,93E-25	EARLY FLOWERING-like protein (DUF1313) (ELF4)
AT2G40100	/	/	-2,5196	/	/	0,001681133	light harvesting complex photosystem II (LHCB4.3)
AT2G40670	-4,5084	/	/	0,000217226	/	/	response regulator 16 (RR16)
AT2G42140	/	1,2556	1,1794	/	6,38E-05	0,000175971	VQ motif-containing protein
AT2G44130	/	1,0096	1,2887	/	0,001012717	2,40E-05	Galactose oxidase/kelch repeat superfamily protein
AT2G44340	/	/	1,0334	/	/	7,90E-07	VQ motif-containing protein
AT2G44840	/	/	2,2513	/	/	0,005766251	ethylene-responsive element binding factor 13 (ERF13)
AT3G01900	/	/	1,4589	/	/	2,17E-13	cytochrome P450, family 94, subfamily B, polypeptide 2 (CYP94B2)
AT3G07310	/	-1,1722	/	/	2,53E-06	/	phosphoserine aminotransferase, putative (DUF760)
AT3G14660	/	/	-1,0612	/	/	2,82E-08	cytochrome P450, family 72, subfamily A, polypeptide 13 (CYP72A13)
AT3G15510	/	/	1,0253	/	/	0,00025922	NAC domain containing protein 2 (NAC2)
AT3G15630	-1,555	/	/	4,53E-06	/	/	plant/protein
AT3G16450	/	/	1,3931	/	/	4,65E-93	Mannose-binding lectin superfamily protein (JAL33)

AT3G17690	/	2,0925	1,9305	/	6,78E-12	2,61E-10	cyclic nucleotide gated channel 19 (CNGC19)
AT3G21670	1,6122	1,5552	1,9457	3,97E-08	1,78E-09	3,08E-14	Major facilitator superfamily protein [Source:NCBI gene (formerly Entrezgene)
AT3G22420	/	-1,0377	/	/	0,005636587	/	with no lysine (K) kinase 2 (WNK2)
AT3G23080	-1,0501	/	/	1,89E-10	/	/	Polyketide cyclase/dehydrase and lipid transport superfamily protein
AT3G23110	/	/	2,4345	/	/	0,003643327	receptor like protein 37 (RLP37)
AT3G25190	/	/	-1,4798	/	/	5,67E-22	Vacuolar iron transporter (VIT) family protein
AT3G46650	/	1,2021	1,41	/	0,004297292	0,000773112	UDP-Glycosyltransferase superfamily protein
AT3G52840	/	-1,5928	/	/	1,25E-07	/	beta-galactosidase 2 (BGAL2)
AT3G55290	/	1,2382	1,2534	/	3,24E-06	2,41E-06	NAD(P)-binding Rossmann-fold superfamily protein
AT3G56380	-2,3942	1,6278	/	0,001605588	0,00615943	/	response regulator 17 (RR17)
AT3G57640	/	1,2919	1,8327	/	0,004657072	4,37E-05	Protein kinase superfamily protein
AT3G60160	/	-2,1094	-1,7319	/	0,001896905	0,009576387	multidrug resistance-associated protein 9 (ABCC9)
AT3G61390	/	-1,0933	-1,0495	/	5,39E-05	0,000101306	RING/U-box superfamily protein
AT3G61900	/	/	-1,2826	/	/	0,001010674	SAUR-like auxin-responsive protein family
AT4G01600	/	/	1,31	/	/	9,00E-05	GRAM domain family protein
AT4G04710	-1,1358	1,6124	2,6294	7,91E-05	1,06E-09	4,46E-24	calcium-dependent kinase-like protein (CPK22)
AT4G05100	/	/	1,0566	/	/	2,63E-11	myb domain protein 74 (MYB74)
AT4G12550	/	/	1,7352	/	/	7,28E-23	Auxin-Induced in Root cultures 1 (AIR1)
AT4G17030	-1,1194	/	-1,2965	9,34E-06	/	1,65E-08	expansin-like B1 (EXLB1)
AT4G18450	/	1,7901	1,4547	/	0,000198498	0,002729219	Integrase-type DNA-binding superfamily protein
AT4G21510	/	-1,0204	/	/	0,000389844	/	F-box family protein (FBS2)
AT4G22110	/	/	1,055	/	/	3,15E-24	GroES-like zinc-binding dehydrogenase family protein
AT4G23880	/	/	1,2501	/	/	0,002417198	hypothetical protein
AT4G25434	/	/	-1,261	/	/	7,36E-05	nudix hydrolase homolog 10 (NUDT10)
AT4G25810	1,0567	/	/	5,51E-12	/	/	xyloglucan endotransglycosylase 6 (XTR6)
AT4G27310	1,1956	1,352	1,7275	3,81E-06	4,36E-09	4,46E-14	B-box type zinc finger family protein (BBX28)
AT4G27440	/	-1,5037	-2,2041	/	3,34E-05	4,43E-09	protochlorophyllide oxidoreductase B (PORB)
AT4G30270	/	-1,1838	-1,3829	/	2,63E-14	1,16E-18	xyloglucan endotransglucosylase/hydrolase 24 (XTH24)
AT4G33120	/	/	2,0923	/	/	2,46E-20	S-adenosyl-L-methionine-dependent methyltransferases superfamily protein
AT4G35900	-1,7656	-1,378	-1,2443	1,07E-06	2,83E-05	0,000139682	Basic-leucine zipper (bZIP) transcription factor family protein (FD)
AT4G36410	-1,2851	/	/	4,16E-08	/	/	ubiquitin-conjugating enzyme 17 (UBC17)
AT4G37030	/	/	-1,1432	/	/	1,41E-06	membrane protein
AT4G37050	/	4,9845	/	/	0,001802346	/	PATATIN-like protein 4 (PLP4)
AT4G37220	/	2,5882	2,496	/	0,000252911	0,000417809	Cold acclimation protein WCOR413 family
AT4G37560	/	/	4,9876	/	/	0,005558614	Acetamidase/Formamidase family protein
AT4G38420	/	1,8206	1,414	/	5,13E-06	0,000421661	SKU5 similar 9 (sks9)
AT4G38860	/	/	-1,7568	/	/	0,005165423	SAUR-like auxin-responsive protein family
AT4G39830	/	1,4466	1,0022	/	1,56E-06	0,000947141	Cupredoxin superfamily protein

AT5G11180	/	/	-2,3933	/	/	0,002877761	glutamate receptor 2.6 (GLR2.6)
AT5G14360	1,1116	1,5492	1,5117	0,001451787	2,36E-07	4,60E-07	Ubiquitin-like superfamily protein
AT5G16530	/	/	1,1131	/	/	0,001060783	Auxin efflux carrier family protein (PIN5)
AT5G17350	/	1,2638	1,0767	/	3,58E-05	0,000448145	hypothetical protein
AT5G18240	/	/	1,1122	/	/	0,000377377	myb-related protein 1 (MYR1)
AT5G20690	/	4,0199	/	/	0,004963731	/	Leucine-rich repeat protein kinase family protein (PRK6)
AT5G21120	/	1,9362	2,4111	/	5,74E-11	2,06E-16	ETHYLENE-INSENSITIVE3-like 2 (EIL2)
AT5G23810	/	/	1,1099	/	/	3,56E-13	amino acid permease 7 (AAP7)
AT5G24490	-1,7503	-1,3629	-1,2084	5,31E-14	6,42E-11	5,89E-09	30S ribosomal protein
AT5G26220	/	1,9672	2,6919	/	0,000134674	1,30E-07	ChaC-like family protein
AT5G38030	/	/	1,4177	/	/	6,03E-57	MATE efflux family protein
AT5G42580	1,4664	2,0639	2,9139	2,42E-22	7,48E-79	6,24E-158	cytochrome P450, family 705, subfamily A, polypeptide 12 (CYP705A1)
AT5G43590	/	2,0534	2,5819	/	4,88E-06	8,46E-09	Acyl transferase/acyl hydrolase/lysophospholipase superfamily protein
AT5G45080	-2,2275	/	/	8,59E-07	/	/	phloem protein 2-A6 (PP2-A6)
AT5G47980	/	1,2375	2,0407	/	2,33E-41	2,83E-110	HXXXD-type acyl-transferase family protein
AT5G47990	/	1,3789	1,8406	/	3,67E-99	1,61E-175	cytochrome P450, family 705, subfamily A, polypeptide 5 (CYP705A5)
AT5G48010	/	1,278	1,6696	/	2,84E-91	1,25E-154	thalianol synthase 1 (THAS1)
AT5G48070	/	/	1,2161	/	/	5,95E-10	xyloglucan endotransglucosylase/hydrolase 20 (XTH20)
AT5G49130	/	-1,6977	-1,2985	/	4,41E-06	0,00031414	MATE efflux family protein
AT5G49770	-1,0611	/	/	0,000714082	/	/	Leucine-rich repeat protein kinase family protein
AT5G54930	/	/	-1,0585	/	/	2,17E-13	AT hook motif-containing protein
AT5G65980	/	2,1636	1,8327	/	1,84E-08	2,01E-06	Auxin efflux carrier family protein
AT5G66170	/	/	1,1762	/	/	2,53E-55	sulfurtransferase 18 (STR18)
regulation of development							
AT1G05577	/	/	1,1856	/	/	0,007310671	UPSTREAM OF FLC protein (DUF966)
AT1G06170	/	/	-2,2176	/	/	0,006075687	basic helix-loop-helix (bHLH) DNA-binding superfamily protein
AT1G16705	5,5179	/	/	0,001908317	/	/	p300/CBP acetyltransferase-related protein-like protein
AT1G17020	/	-1,0151	-1,0595	/	0,003521818	0,002337995	senescence-related 1 (SRG1)
AT1G26360	/	1,2704	1,1089	/	9,13E-12	2,85E-09	methyl esterase 13 (MES13)
AT1G34540	/	1,7358	2,1947	/	1,76E-07	3,03E-11	cytochrome P450, family 94, subfamily D, polypeptide 1 (CYP94D1)
AT1G47610	/	2,4303	2,2222	/	3,37E-06	2,26E-05	Transducin/WD40 repeat-like superfamily protein
AT1G55600	/	/	-5,447	/	/	0,001480615	WRKY DNA-binding protein 10 (WRKY10)
AT1G61450	/	/	-1,0111	/	/	0,000129245	CAP-gly domain linker
AT1G64370	/	/	1,3219	/	/	1,10E-05	filaggrin-like protein
AT1G67870	/	1,7603	2,6018	/	2,13E-09	3,34E-19	glycine-rich protein
AT1G75160	/	1,0701	/	/	1,64E-06	/	DUF620 family protein (DUF620)
AT1G79860	/	1,2353	1,3917	/	4,04E-10	1,60E-12	Rop guanin nucelotide exchange factor 12 (ROPGEF12)

AT2G15880	-1,5069	-1,2888	-1,214	1,46E-05	5,29E-05	0,000130812	Leucine-rich repeat (LRR) family protein
AT2G31081	/	/	-1,4374	/	/	0,000112666	CLAVATA3/ESR-RELATED 4 (CLE4)
AT2G31083	/	/	-1,3995	/	/	2,54E-07	CLAVATA3/ESR-RELATED 5 (CLE5)
AT2G33790	/	-2,3987	-2,6208	/	8,77E-16	1,64E-18	arabinogalactan protein 30 (AGP30)
AT2G35950	/	/	-5,1025	/	/	0,004627449	embryo sac development arrest 12 (EDA12)
AT2G38110	-1,5242	/	-1,0618	2,52E-05	/	0,001298907	glycerol-3-phosphate acyltransferase 6 (GPAT6)
AT2G38465	/	/	-1,6362	/	/	0,000476637	hypothetical protein
AT2G39510	-1,1329	-1,2055	-1,6669	1,20E-06	7,49E-09	1,48E-15	nodulin MtN21 /EamA-like transporter family protein (UMAMIT1)
AT2G42840	-3,0736	/	2,1366	0,001006259	/	0,000643893	protodermal factor 1 (PDF1)
AT2G46860	/	/	1,1846	/	/	1,72E-18	pyrophosphorylase 3 (PPa3)
AT3G05770	/	-4,2846	/	/	0,00172932	/	hypothetical protein
AT3G20557	/	1,0372	/	/	3,75E-06	/	hypothetical protein
AT3G51410	-2,7531	/	/	0,002295097	/	/	hypothetical protein
AT3G58770	/	/	2,0203	/	/	0,001255097	hypothetical protein
AT3G60470	/	3,7159	3,5986	/	5,75E-25	1,74E-23	transmembrane protein, putative (DUF247)
AT3G61880	1,0302	-1,2542	-1,4504	0,002733113	4,52E-05	3,04E-06	cytochrome p450 78a9 (CYP78A9)
AT4G01430	-1,1464	/	/	1,93E-05	/	/	nodulin MtN21 /EamA-like transporter family protein (UMAMIT29)
AT4G02850	/	/	1,1457	/	/	0,004508616	phenazine biosynthesis PhzC/PhzF family protein
AT4G04900	/	1,0448	/	/	5,66E-06	/	ROP-interactive CRIB motif-containing protein 10 (RIC10)
AT4G07960	/	1,2532	1,338	/	4,77E-24	2,99E-27	Cellulose-synthase-like C12 (CSLC12)
AT4G24265	/	/	-1,273	/	/	0,006694953	homeobox protein
AT4G36870	/	1,5701	2,1175	/	1,11E-06	3,33E-11	BEL1-like homeodomain 2 (BLH2)
AT4G38770	-1,5832	/	/	0,003070534	/	/	proline-rich protein 4 (PRP4)
AT4G39000	/	/	-1,1078	/	/	0,00016838	glycosyl hydrolase 9B17 (GH9B17)
AT5G04730	/	2,2821	2,6493	/	0,001022009	0,000128113	Ankyrin-repeat containing protein
AT5G10150	5,408	/	/	0,00267102	/	/	UPSTREAM OF FLC protein (DUF966)
AT5G21130	/	/	1,061	/	/	1,20E-06	Late embryosis abundant (LEA) hydroxyproline-rich glycoprotein family
AT5G44990	/	4,3184	4,0579	/	0,000135466	0,000343701	Glutathione S-transferase family protein
AT5G51750	/	/	-1,4692	/	/	0,000158496	subtilase 1.3 (SBT1.3)
AT5G54400	/	1,3838	1,6184	/	0,002179516	0,000310209	S-adenosyl-L-methionine-dependent methyltransferases superfamily protein
AT5G54700	-1,2011	/	-1,7521	0,00097724	/	4,90E-07	Ankyrin repeat family protein
AT5G55250	/	/	-1,0399	/	/	2,83E-13	IAA carboxylmethyltransferase 1 (IAMT1)
AT5G61650	/	1,1386	1,2231	/	1,75E-14	1,60E-16	Cyclin-U4-3 (CYCP4)
AT5G62165	/	-1,7421	-1,6805	/	3,06E-05	5,51E-05	AGAMOUS-like 42 (AGL42)
AT5G65070	/	1,0482	1,0843	/	7,83E-06	3,65E-06	K-box region and MADS-box transcription factor family protein (MAF4)
AT5G65080	/	2,3486	1,9853	/	9,05E-05	0,001009059	K-box region/MADS-box transcription factor family protein (MAF5)
circadian rhythm							

AT1G01060	2,2359	1,7792	2,6903	6,93E-19	3,96E-16	2,29E-35	Homeodomain-like superfamily protein (LHY)
AT1G68050	-2,2438	-1,5561	-2,5382	4,44E-16	2,78E-10	1,88E-23	flavin-binding, kelch repeat, f box 1 (FKF1)
AT2G21660	/	/	-1,2946	/	/	2,30E-33	cold, circadian rhythm, and rna binding 2 (GRP7)
AT2G37000	/	/	1,3003	/	/	0,004143202	TCP family transcription factor
AT2G46790	1,5916	1,1524	1,7756	1,42E-15	6,54E-11	3,35E-24	pseudo-response regulator 9 (PRR9)
AT2G46830	2,5244	2,8503	3,4509	8,26E-26	1,04E-36	5,57E-54	circadian clock associated 1 (CCA1)
AT3G01060	/	1,6435	1,8023	/	0,000728394	0,000198603	lysine-tRNA ligase
AT3G07650	-1,5973	-1,1827	-1,81	2,36E-19	1,43E-13	5,05E-28	CONSTANS-like 9 (COL9)
AT3G09600	1,6264	1,2889	2,0483	2,10E-11	3,08E-09	1,50E-21	Homeodomain-like superfamily protein (RVE8)
AT3G12320	2,528	1,2166	2,1528	3,37E-18	3,62E-07	3,24E-20	hypothetical protein
AT3G12700	/	/	-1,0706	/	/	1,80E-22	Eukaryotic aspartyl protease family protein (NANA)
AT3G20810	-2,9039	-2,488	-3,7603	7,09E-08	2,21E-07	1,55E-14	2-oxoglutarate (2OG) and Fe(II)-dependent oxygenase superfamily protein (JMJD5)
AT3G21890	1,7529	1,6688	1,8518	7,81E-05	1,46E-05	1,38E-06	B-box type zinc finger family protein (BBX31)
AT3G22231	/	-1,8162	/	/	0,001593676	/	pathogen and circadian controlled 1 (PCC1)
AT3G26740	/	/	-3,4108	/	/	0,000216161	CCR-like protein (CCL)
AT3G54500	1,6765	1,7192	2,2831	2,39E-08	1,61E-10	1,84E-17	agglutinin-like protein
AT3G63140	/	-6,3207	/	/	1,14E-05	/	chloroplast stem-loop binding protein of 41 kDa (CSP41A)
AT4G09970	/	/	1,3777	/	/	0,000274735	transmembrane protein
AT4G15248	4,9158	2,3419	2,6832	7,52E-08	3,25E-05	1,73E-06	B-box type zinc finger family protein (BBX30)
AT5G02120	/	/	1,1141	/	/	0,000757266	one helix protein (OHP)
AT5G06980	1,8975	1,7709	2,3442	9,39E-12	7,83E-13	1,03E-21	hypothetical protein
AT5G15850	/	1,746	1,5168	/	0,000948113	0,004317443	CONSTANS-like 1 (COL1)
AT5G24470	/	/	-1,0035	/	/	3,42E-05	two-component response regulator-like protein (PRR5)
AT5G59570	/	-1,4208	-1,2039	/	5,45E-07	1,79E-05	Homeodomain-like superfamily protein (BOA)
AT5G60100	-1,2943	/	-1,2251	4,36E-06	/	1,63E-06	pseudo-response regulator 3 (PRR3)
AT5G61380	/	/	-1,0014	/	/	1,06E-34	CCT motif -containing response regulator protein (TOC1)
AT5G64940	1,0127	/	1,0036	2,50E-17	/	3,11E-21	ABC2 homolog 13 (ATH13)
lipid metabolic processes							
AT1G61130	/	-1,3888	-1,9127	/	4,26E-08	3,38E-13	serine carboxypeptidase-like 32 (SCPL32)
AT1G77520	/	1,4071	1,3275	/	0,00074912	0,001486478	O-methyltransferase family protein
AT1G77860	-4,423	/	/	8,74E-05	/	/	Rhomboid-related intramembrane serine protease family protein (KOM)
AT5G24140	/	2,5398	2,9019	/	1,42E-44	1,11E-57	squalene monooxygenase 2 (SQP2)
AT5G42600	1,5677	1,8869	4,0117	1,83E-05	5,28E-10	5,11E-40	marneral synthase [Source:NCBI gene (MRN1)
AT5G48000	/	1,4986	1,9332	/	1,49E-87	1,21E-144	cytochrome P450, family 708, subfamily A, polypeptide 2 (CYP708A2)
AT5G52570	/	/	1,0029	/	/	0,000528101	beta-carotene hydroxylase 2 (BETA-OHASE 2)
AT5G54570	/	/	1,0805	/	/	0,005603983	beta glucosidase 41 (BGLU41)
AT5G55590	-2,2754	/	/	0,001158293	/	/	Pectin lyase-like superfamily protein (QRT1)

AT5G57530	/	1,163	/	/	3,49E-12	/	xyloglucan endotransglucosylase/hydrolase 12 (XTH12)
AT5G57540	1,0884	1,9228	1,6514	0,000209501	2,18E-13	3,00E-10	xyloglucan endotransglucosylase/hydrolase 13 (XTH13)
carbohydrate metabolic processes							
AT1G01453	/	1,3081	/	/	2,25E-14	/	late embryosis abundant hydroxyproline-rich glycoprotein family protein
AT1G04620	-1,2749	/	-2,0867	0,000124119	/	7,08E-11	coenzyme F420 hydrogenase family / dehydrogenase, beta subunit family (HCAR)
AT3G27620	/	/	-2,2638	/	/	0,000374663	alternative oxidase 1C (AOX1C)
AT4G29740	/	/	1,2673	/	/	0,001934901	cytokinin oxidase 4 (CKX4)
AT4G39770	/	1,9789	2,866	/	1,62E-10	7,53E-21	Haloacid dehalogenase-like hydrolase (HAD) superfamily protein (TPPH)
AT5G09730	/	3,5462	/	/	0,001768976	/	beta-xylosidase 3 (BXL3)
protein metabolic processes							
AT1G70220	-3,6446	/	/	0,002745192	/	/	RNA-processing, Lsm domain-containing protein
AT2G21140	/	-1,3016	-1,6948	/	1,31E-05	3,33E-08	proline-rich protein 2 (PRP2)
AT3G16150	/	/	1,0049	/	/	3,23E-11	N-terminal nucleophile aminohydrolases (Ntn hydrolases) superfamily protein (ASPGB1)
AT4G11320	/	1,8028	1,9112	/	4,39E-09	4,92E-10	Papain family cysteine protease
AT5G38020	/	1,6212	2,286	/	5,37E-36	5,68E-70	S-adenosyl-L-methionine-dependent methyltransferases superfamily protein
AT5G39220	/	1,3504	1,9257	/	0,006615437	8,26E-05	alpha/beta-Hydrolases superfamily protein
catabolic processes							
AT1G14240	/	1,0387	1,4293	/	1,67E-46	2,62E-87	GDA1/CD39 nucleoside phosphatase family protein
AT1G14520	/	/	-1,4807	/	/	0,000871719	myo-inositol oxygenase 1 (MIOX1)
AT1G16530	/	/	2,1481	/	/	0,009453963	ASYMMETRIC LEAVES 2-like 9 (ASL9)
AT1G32850	/	/	-2,4687	/	/	0,003474433	ubiquitin-specific protease 11 (UBP11)
AT1G33790	/	1,1589	1,0085	/	5,52E-08	2,41E-06	jacalin lectin family protein
AT1G49100	/	1,0678	/	/	0,003832292	/	Leucine-rich repeat protein kinase family protein
AT1G58684	/	-2,6518	-2,3245	/	0,001954693	0,006488583	Ribosomal protein S5 family protein
AT1G62290	/	/	1,1887	/	/	0,007988454	Saposin-like aspartyl protease family protein
AT1G67370	/	/	-1,079	/	/	0,003386292	DNA-binding HORMA family protein (ASY1)
AT1G68590	/	-1,0199	/	/	0,001191321	/	Ribosomal protein PSRP-3/Ycf65 (PSRP3/1)
AT1G78390	5,3642	/	/	0,000680765	/	/	nine-cis-epoxycarotenoid dioxygenase 9 (NCED9)
AT2G05330	/	-1,0116	/	/	0,003212482	/	BTB/POZ domain-containing protein
AT2G18720	/	1,4643	/	/	0,00598781	/	Translation elongation factor EF1A/initiation factor IF2gamma family protein
AT5G45670	/	/	1,6432	/	/	0,006088121	GDSL-like Lipase/Acylhydrolase superfamily protein
other metabolic processes							
AT1G11600	/	3,1272	/	/	0,005075663	/	cytochrome P450, family 77, subfamily B, polypeptide 1 (CYP77B1)
AT1G18870	1,2105	/	1,1794	4,61E-09	/	3,48E-13	isochorismate synthase 2 (ICS2)
AT1G33102	/	/	-1,1296	/	/	0,001458324	hypothetical protein

AT1G68880	/	/	-1,0678	/	/	1,90E-05	basic leucine-zipper 8 (bZIP8)
AT2G01880	/	/	1,5128	/	/	2,49E-85	purple acid phosphatase 7 (PAP7)
AT2G22890	-1,5482	/	/	0,001578675	/	/	Kua-ubiquitin conjugating enzyme hybrid localization domain-containing protein
AT2G47240	/	-1,2104	-2,3736	/	1,71E-11	3,07E-35	AMP-dependent synthetase and ligase family protein (LACS1)
AT3G01260	-1,0251	/	/	5,06E-05	/	/	Galactose mutarotase-like superfamily protein
AT3G02620	/	1,2227	1,8602	/	5,84E-05	8,86E-10	Plant stearoyl-acyl-carrier-protein desaturase family protein
AT3G16650	/	-1,0534	/	/	0,00562626	/	Transducin/WD40 repeat-like superfamily protein
AT3G44326	/	/	1,4906	/	/	4,55E-16	F-box family protein
AT3G44870	/	/	6,9294	/	/	1,69E-44	S-adenosyl-L-methionine-dependent methyltransferases superfamily protein (FAMT-L)
AT3G59130	/	/	1,0344	/	/	4,97E-14	Cysteine/Histidine-rich C1 domain family protein
AT4G20390	-1,3594	/	/	0,000484787	/	/	Uncharacterized protein family (UPF0497)
AT4G21326	/	1,2737	1,2198	/	0,006187417	0,008778771	subtilase 3.12 (SBT3.12)
AT4G34510	/	-1,3071	/	/	0,00679047	/	3-ketoacyl-CoA synthase 17 (KCS17)
AT5G12270	-1,4258	/	-1,013	0,000942135	/	0,008986324	2-oxoglutarate (2OG) and Fe(II)-dependent oxygenase superfamily protein
AT5G20710	/	-1,9002	-1,6444	/	5,24E-05	0,000349758	beta-galactosidase 7 (BGAL7)
AT5G36150	/	1,3069	1,2484	/	8,71E-07	2,63E-06	putative pentacyclic triterpene synthase 3 (PEN3)
AT5G37990	/	2,5218	2,6904	/	2,91E-17	1,94E-19	S-adenosyl-L-methionine-dependent methyltransferase superfamily protein
AT5G38100	/	1,7627	2,4272	/	1,53E-23	6,21E-44	S-adenosyl-L-methionine-dependent methyltransferases superfamily protein
AT5G42590	/	1,2542	1,7037	/	2,78E-80	9,11E-148	cytochrome P450, family 71, subfamily A, polypeptide 16 (CYP71A16)
cellular component organization							
AT1G24420	/	/	-3,7441	/	/	0,00429876	HXXXD-type acyl-transferase family protein
AT1G61080	-1,2889	1,463	1,4321	0,000140356	2,94E-08	5,72E-08	Hydroxyproline-rich glycoprotein family protein
AT1G64500	1,4426	/	1,0722	1,10E-05	/	0,00018452	Glutaredoxin family protein
AT2G22450	/	/	-1,1325	/	/	7,02E-13	riboflavin biosynthesis protein (RIBA2)
AT3G06390	/	/	-1,5697	/	/	0,000402359	Uncharacterized protein family (UPF0497)
AT4G23496	/	/	-1,2367	/	/	0,000115573	SPIRAL1-like5 (SP1L5)
AT4G24140	-1,047	/	/	0,003028351	/	/	alpha/beta-Hydrolases superfamily protein
AT4G29340	/	/	-1,0572	/	/	1,36E-05	profilin 4 (PRF4)
AT4G32200	/	/	1,2022	/	/	2,11E-12	DNA-binding HORMA family protein (ASY2)
AT5G37478	/	-1,0469	-1,1171	/	6,38E-05	2,04E-05	TPX2 (targeting protein for Xklp2) protein family
other cellular processes							
AT1G11920	/	1,176	1,058	/	7,35E-09	2,12E-07	Pectin lyase-like superfamily protein
AT1G26230	/	-1,3203	-1,5507	/	1,94E-05	6,66E-07	TCP-1/cpn60 chaperonin family protein (Cpn50beta4)
AT1G55940	-1,6585	/	/	0,002947626	/	/	cytochrome P450 family protein (CYP708A1)
AT1G58170	/	/	1,03	/	/	9,14E-06	Disease resistance-responsive (dirigent-like protein) family protein
AT1G62580	/	-1,615	-1,6796	/	7,72E-12	1,17E-12	flavin containing monooxygenase FMO GS-OX-like protein (NOGC1)

AT1G78970	/	-1,4738	-1,6177	/	0,000506235	0,000153606	lupeol synthase 1 (LUP1)
AT2G28860	/	/	2,7448	/	/	7,08E-07	cytochrome P450, family 710, subfamily A, polypeptide 4 (CYP710A4)
AT2G32530	/	/	-2,7003	/	/	0,006646041	cellulose synthase-like B3 (CSLB03)
AT2G33100	/	/	-1,7374	/	/	0,002577908	cellulose synthase-like D1 (CSLD1)
AT2G34490	/	1,0521	1,6145	/	0,000141427	3,91E-09	cytochrome P450, family 710, subfamily A, polypeptide 2 (CYP710A2)
AT2G36190	/	/	5,5573	/	/	0,001193088	cell wall invertase 4 (cwINV4)
AT2G42850	/	/	1,1398	/	/	1,05E-10	cytochrome P450, family 718 (CYP718)
AT3G07970	/	/	-1,6422	/	/	0,000660846	Pectin lyase-like superfamily protein (QRT2)
AT3G10710	/	/	1,0351	/	/	4,19E-37	root hair specific 12 (RHS12)
AT3G29430	/	/	-1,1358	/	/	4,33E-05	Terpenoid synthases superfamily protein
AT3G60140	/	/	1,4961	/	/	3,23E-05	Glycosyl hydrolase superfamily protein (DIN2)
AT4G01890	/	/	1,1304	/	/	1,18E-06	Pectin lyase-like superfamily protein
AT4G12290	/	-1,0377	-1,7865	/	0,00012754	4,07E-10	Copper amine oxidase family protein
AT4G13390	/	1,1803	1,1102	/	1,07E-11	1,63E-10	Proline-rich extensin-like family protein (EXT12)
AT4G15340	/	/	1,6323	/	/	4,37E-40	pentacyclic triterpene synthase 1 (PEN1)
AT4G15370	/	1,4661	/	/	5,80E-07	/	baruol synthase 1 (BARS1)
AT4G15396	/	2,0822	2,3903	/	0,002023698	0,000368242	cytochrome P450, family 702, subfamily A, polypeptide 6 (CYP702A6)
AT4G25220	/	1,4556	1,2569	/	8,48E-08	3,78E-06	root hair specific 15 (G3Pp2)
AT4G28420	/	6,4551	5,8788	/	3,02E-08	4,76E-07	Tyrosine transaminase family protein (TAT1)
AT4G28850	/	2,4708	2,7293	/	0,001230517	0,000355651	xyloglucan endotransglucosylase/hydrolase 26 (XTH26)
AT4G32950	/	-1,917	-2,5392	/	2,41E-05	3,46E-08	Protein phosphatase 2C family protein
AT4G36880	/	-1,4612	-1,9986	/	1,14E-09	2,73E-16	cysteine proteinase1 (CP1)
AT5G04120	1,7973	2,3132	3,8266	1,10E-11	2,66E-24	5,28E-64	Phosphoglycerate mutase family protein
AT5G15950	1,7409	1,4384	1,9903	3,36E-12	1,19E-10	4,69E-19	Adenosylmethionine decarboxylase family protein
AT5G25260	-1,9248	1,9695	/	0,000731146	2,67E-05	/	SPFH/Band 7/PHB domain-containing membrane-associated protein family
AT5G38450	/	/	1,0188	/	/	1,21E-05	cytochrome P450, family 735, subfamily A, polypeptide 1 (CYP735A1)
AT5G40040	/	-1,5852	-1,3369	/	0,001034588	0,004740435	60S acidic ribosomal protein family
AT5G63810	/	/	-1,1152	/	/	2,22E-60	beta-galactosidase 10 (BGAL10)
AT5G65580	/	/	-1,209	/	/	0,008090777	transmembrane protein
ATCG01020	/	/	2,5686	/	/	0,009076483	50S ribosomal protein L32 (rpl32)
transcription							
AT1G01030	/	1,7199	1,5401	/	0,001097791	0,003559067	AP2/B3-like transcriptional factor family protein (NGA3)#
AT1G14600	/	/	1,4317	/	/	2,79E-05	Homeodomain-like superfamily protein
AT1G29270	-1,3771	/	/	0,000321833	/	/	transcription factor bHLH35-like protein
AT1G35240	/	/	2,003	/	/	0,000331352	auxin response factor 20 (ARF20)
AT2G02060	/	2,0874	2,1404	/	0,001329729	0,000986256	Homeodomain-like superfamily protein

AT2G22760	/	/	2,4127	/	/	0,009787474	basic helix-loop-helix (bHLH) DNA-binding superfamily protein
AT2G34010	/	/	1,2774	/	/	1,64E-05	verprolin
AT3G15170	-3,7361	-2,5327	-2,5362	0,000121728	0,001550286	0,00149704	NAC (No Apical Meristem) domain transcriptional regulator superfamily protein (CUC1)
AT3G24310	-2,0997	/	-2,7398	0,002424903	/	0,000133841	myb domain protein 305 (MYB305)
AT3G47500	/	/	1,0038	/	/	4,01E-14	cycling DOF factor 3 (CDF3)
AT3G52540	/	-1,3529	-1,8445	/	0,003991235	0,000135699	ovate family protein 18 (OFP18)
AT4G00130	-2,3658	1,9315	/	2,51E-06	8,86E-06	/	DNA-binding storekeeper protein-related transcriptional regulator
AT4G14860	/	1,2957	1,1274	/	0,00089425	0,003969905	ovate family protein 11 (OFP11)
AT4G17600	/	/	-1,1866	/	/	0,002884451	Chlorophyll A-B binding family protein (LIL3:1)
AT4G28110	/	/	1,9606	/	/	1,44E-05	myb domain protein 41 (MYB41)
AT4G28530	/	-1,9525	-2,4812	/	6,71E-05	1,07E-06	NAC domain containing protein 74 (NAC074)
AT4G29930	/	/	1,1406	/	/	0,001165957	basic helix-loop-helix (bHLH) DNA-binding superfamily protein
AT4G37850	/	/	2,101	/	/	8,57E-12	basic helix-loop-helix (bHLH) DNA-binding superfamily protein
AT5G06500	/	/	-4,3555	/	/	1,96E-07	AGAMOUS-like 96 (AGL96)
AT5G43175	/	5,6126	5,7737	/	1,15E-05	6,31E-06	basic helix-loop-helix (bHLH) DNA-binding superfamily protein
AT5G58610	/	/	1,6274	/	/	0,003681654	PHD finger transcription factor
transferases							
AT1G21130	/	1,1488	/	/	3,56E-10	/	O-methyltransferase family protein (IGMT4)
AT1G35625	/	/	4,981	/	/	3,21E-07	RING/U-box superfamily protein
AT1G50090	/	1,6322	1,5497	/	5,17E-05	0,000123092	D-aminoacid aminotransferase-like PLP-dependent enzymes superfamily protein (BCAT7)
AT1G51620	/	1,3472	/	/	4,94E-05	/	Protein kinase superfamily protein
AT1G51870	/	1,5904	1,2671	/	0,000367532	0,004704244	protein kinase family protein
AT1G78360	/	1,2733	1,4564	/	1,46E-05	6,14E-07	glutathione S-transferase TAU 21 (GSTU21)
AT2G14510	-1,1992	/	/	0,002031894	/	/	Leucine-rich repeat protein kinase family protein
AT2G15350	/	/	1,0574	/	/	1,95E-06	fucosyltransferase 10 (FUT10)
AT2G19610	/	/	5,8592	/	/	0,003010633	RING/U-box superfamily protein
AT2G25150	/	2,1619	2,8673	/	3,59E-15	1,51E-25	HXXXD-type acyl-transferase family protein
AT2G29000	/	1,6964	1,5176	/	0,00024136	0,001048683	Leucine-rich repeat protein kinase family protein
AT3G02020	/	1,143	2,1361	/	0,003344382	3,86E-08	aspartate kinase 3 (AK3)
AT3G06640	/	/	1,7867	/	/	0,00102127	PAS domain-containing protein tyrosine kinase family protein
AT3G13640	/	/	-1,3089	/	/	8,05E-07	RNAse l inhibitor protein 1 (ABCE1)
AT3G23060	/	/	-1,5482	/	/	0,000378884	RING/U-box superfamily protein
AT3G45080	/	/	1,0794	/	/	3,04E-12	P-loop containing nucleoside triphosphate hydrolases superfamily protein
AT3G46340	/	1,7746	1,3122	/	2,53E-06	0,000541039	Leucine-rich repeat protein kinase family protein
AT4G00305	/	-2,7053	/	/	0,001298835	/	RING/U-box superfamily protein
AT4G09110	/	/	-2,7078	/	/	1,00E-05	RING/U-box superfamily protein
AT4G14780	/	/	-1,0566	/	/	4,26E-05	Protein kinase superfamily protein
AT4G18250	-3,0704	/	/	0,002659814	/	/	receptor Serine/Threonine kinase-like protein

AT4G35640	/	/	1,7225	/	/	0,00589815	Serine transferase 3 (SERAT3)
AT4G39110	-1,4576	/	/	0,001850141	/	/	Malectin/receptor-like protein kinase family protein
AT4G39940	/	1,4165	2,1624	/	1,70E-35	3,18E-81	APS-kinase 2 (AKN2)
AT5G37450	/	/	-2,092	/	/	0,000623131	Leucine-rich repeat protein kinase family protein
AT5G43690	/	2,1013	1,8567	/	7,90E-10	6,51E-08	P-loop containing nucleoside triphosphate hydrolases superfamily protein
AT5G65690	/	/	1,178	/	/	3,10E-07	phosphoenolpyruvate carboxykinase 2 (PCK2)
transport							
AT1G02440	/	1,066	1,0631	/	0,000412709	0,000424967	ADP-ribosylation factor D1A (ARFD1A)
AT1G02530	/	/	-1,1633	/	/	0,002334403	P-glycoprotein 12 (ABCB12)
AT1G05020	/	1,1048	1,4208	/	6,83E-05	2,35E-07	ENTH/ANTH/VHS superfamily protein
AT1G08090	/	-1,0389	-1,5365	/	0,004087665	2,22E-05	nitrate transporter 2:1 (NTR2:1)
AT1G22550	/	/	1,0729	/	/	1,15E-37	Major facilitator superfamily protein
AT1G25240	/	1,3119	1,3518	/	0,000195273	0,000121892	ENTH/VHS/GAT family protein
AT1G30220	/	/	-5,2626	/	/	0,003674526	inositol transporter 2 (INT2)
AT1G30560	/	1,6838	/	/	0,005113492	/	Major facilitator superfamily protein (G3Pp3)
AT1G45015	/	1,0365	1,6757	/	1,75E-10	3,04E-25	MD-2-related lipid recognition domain-containing protein
AT1G47603	/	1,0062	/	/	0,006348634	/	purine permease 19 (PUP19)
AT1G60050	-1,3842	1,4803	1,3919	0,00069277	7,63E-06	2,61E-05	Nodulin MtN21 /EamA-like transporter family protein (UMAMIT3)
AT1G72120	/	/	1,047	/	/	2,28E-07	Major facilitator superfamily protein
AT1G72140	/	/	1,2117	/	/	2,89E-37	Major facilitator superfamily protein
AT1G73220	/	/	-1,0702	/	/	0,00176516	organic cation/carnitine transporter1 (OCT1)
AT1G73655	/	-1,0634	/	/	0,0010149	/	FKBP-like peptidyl-prolyl cis-trans isomerase family protein
AT1G74810	/	-1,764	-1,2213	/	7,68E-09	2,46E-05	HCO3- transporter family [Source:NCBI gene (BOR5)
AT1G76530	/	/	-3,24	/	/	0,006476026	Auxin efflux carrier family protein
AT2G19910	/	/	3,1999	/	/	0,0048061	RNA-dependent RNA polymerase family protein
AT2G22950	/	3,6975	/	/	0,004870101	/	Cation transporter/ E1-E2 ATPase family protein (ACA7)
AT2G26370	/	2,2342	3,1793	/	1,33E-25	5,22E-51	MD-2-related lipid recognition domain-containing protein
AT2G33750	/	3,3099	/	/	0,000380016	/	purine permease 2 (PUP2)
AT3G04370	-1,1209	/	/	0,003076155	/	/	plasmodesmata-located protein 4 (PDLP4)
AT3G04440	-2,1074	/	1,973	0,002358701	/	0,001265595	Plasma-membrane choline transporter family protein
AT3G10290	1,7366	/	/	0,003073323	/	/	Nucleotide-sugar transporter family protein
AT3G22570	/	1,2303	1,6245	/	1,04E-46	1,23E-80	Bifunctional inhibitor/lipid-transfer protein/seed storage 2S albumin superfamily protein
AT3G26570	1,0551	/	1,0181	9,84E-17	/	2,20E-19	Inorganic phosphate transporter 2 (PHT2)
AT3G28380	/	1,4426	1,0321	/	1,22E-05	0,001926008	P-glycoprotein 17 (ABCB17)
AT3G28390	/	/	3,4409	/	/	0,001732074	P-glycoprotein 18 (ABCB18)
AT3G45060	/	/	2,0332	/	/	0,008145686	high affinity nitrate transporter 2.6 (RNT2.6)
AT3G45720	/	1,9493	2,3676	/	7,37E-06	4,16E-08	Major facilitator superfamily protein
AT3G47750	/	2,0024	2,9115	/	4,43E-09	5,51E-18	ATP binding cassette subfamily A4 (ABCA4)

AT3G51600	/	-1,8522	-2,163	/	0,00207851	0,000333113	lipid transfer protein 5 (LTP5)
AT3G54820	/	1,6197	2,0835	/	0,000696625	1,05E-05	PAMP-induced secreted peptide 2 (PIP2)
AT3G56290	1,2361	/	1,0945	6,62E-11	/	7,48E-11	potassium transporter
AT3G60540	/	1,1653	1,3676	/	0,001568117	0,000195423	Preprotein translocase Sec, Sec61-beta subunit protein
AT3G60970	-4,4351	/	/	0,000354303	/	/	multidrug resistance-associated protein 15 (ABCC15)
AT4G01580	/	/	-1,028	/	/	0,00609211	AP2/B3-like transcriptional factor family protein
AT4G01830	/	2,1598	2,2394	/	5,19E-09	1,38E-09	P-glycoprotein 5 (ABCB5)
AT4G04760	/	/	1,4112	/	/	1,39E-06	Major facilitator superfamily protein
AT4G08300	-1,5968	-1,3524	-1,355	4,75E-21	5,98E-19	4,69E-19	nodulin MtN21 /EamA-like transporter family protein (UMAMIZT17)
AT4G08620	/	2,1848	1,8619	/	3,31E-17	7,67E-13	Sulfate transporter 1 (SULTR1:1)
AT4G18197	-2,0256	/	/	0,000642902	/	/	purine permease 7 (PUP7)
AT4G19680	/	1,5529	1,7239	/	4,71E-14	5,55E-17	iron regulated transporter 2 (IRT2)
AT4G22600	/	1,7017	2,917	/	0,001205687	1,06E-08	transcription factor (INP1)
AT4G23700	-1,0964	-1,2565	-1,721	0,003690071	0,000220459	4,64E-07	cation/H+ exchanger 17 (CHX17)
AT4G25010	/	1,3511	1,2834	/	2,17E-11	2,07E-10	Nodulin MtN3 family protein (SWEET14)
AT4G27850	/	/	1,0175	/	/	6,64E-07	Glycine-rich protein family
AT5G02170	/	1,2643	2,2921	/	5,97E-27	6,31E-87	Transmembrane amino acid transporter family protein
AT5G15240	/	/	1,2145	/	/	0,00148452	Transmembrane amino acid transporter family protein
AT5G23830	/	/	1,6885	/	/	6,37E-38	MD-2-related lipid recognition domain-containing protein
AT5G23840	/	/	1,6212	/	/	1,11E-10	MD-2-related lipid recognition domain-containing protein
AT5G26250	/	1,7617	3,7707	/	4,87E-05	2,88E-19	Major facilitator superfamily protein
AT5G46240	/	/	4,8546	/	/	0,004113841	potassium channel 1 (KAT1)
AT5G46610	/	/	-2,6927	/	/	0,002394284	aluminum activated malate transporter family protein
AT5G47450	/	/	-1,2292	/	/	1,99E-08	TIR-domain containing protein 2 (TIP2)
AT5G62720	/	/	-1,1409	/	/	8,83E-17	Integral membrane HPP family protein
AT5G65990	/	/	1,2788	/	/	9,98E-27	Transmembrane amino acid transporter family protein
uncharacterized or unknown							
AT1G02070	/	/	-4,8408	/	/	0,002760098	zinc ion-binding protein
AT1G05990	/	1,4326	1,1783	/	4,13E-09	1,45E-06	EF hand calcium-binding protein family
AT1G11080	-1,8317	-1,3134	-1,2262	1,07E-20	7,70E-14	2,54E-12	serine carboxypeptidase-like 31 (scpl31)
AT1G11530	-1,354	/	/	3,18E-07	/	/	C-terminal cysteine residue is changed to a serine 1 (CXX1)
AT1G11655	/	1,0914	/	/	0,000207739	/	hypothetical protein
AT1G11690	/	2,6031	/	/	0,006103221	/	BRANCHLESS TRICHOME-like protein
AT1G13480	/	1,2506	/	/	1,85E-05	/	hypothetical protein
AT1G14120	/	/	1,7479	/	/	4,33E-18	2-oxoglutarate (2OG) and Fe(II)-dependent oxygenase superfamily protein
AT1G20490	/	1,1603	1,8212	/	2,76E-17	5,42E-41	AMP-dependent synthetase and ligase family protein
AT1G22340	/	/	2,743	/	/	3,35E-05	UDP-glucosyl transferase 85A7 (UGT85A7)
AT1G23170	/	/	-1,3373	/	/	2,57E-49	transmembrane protein (Protein of unknown function DUF2359, transmembrane)

AT1G24485	/	/	-1,124	/	/	0,000770242	ER protein carbohydrate-binding protein
AT1G26390	-5,6931	/	/	0,000214538	/	/	FAD-binding Berberine family protein
AT1G29000	-3,3242	/	/	0,000415406	/	/	Heavy metal transport/detoxification superfamily protein
AT1G29590	/	/	-1,5379	/	/	0,002999497	translation initiation factor (eIF4E3)
AT1G29600	/	/	-1,649	/	/	0,00012372	Zinc finger C-x8-C-x5-C-x3-H type family protein
AT1G33870	/	1,2662	1,1265	/	0,001208585	0,004052564	P-loop containing nucleoside triphosphate hydrolases superfamily protein
AT1G34520	/	2,5376	2,426	/	0,001472019	0,002368683	MBOAT (membrane bound O-acyl transferase) family protein
AT1G44030	/	/	-1,2659	/	/	0,000741478	Cysteine/Histidine-rich C1 domain family protein
AT1G51913	/	/	3,3753	/	/	0,008207747	transmembrane protein
AT1G52110	/	/	1,3026	/	/	0,00256831	Mannose-binding lectin superfamily protein
AT1G52120	-5,717	/	/	0,000431329	/	/	Mannose-binding lectin superfamily protein
AT1G53480	5,9522	10,3113	/	4,78E-05	1,32E-22	/	mto 1 responding down 1 (MDR1)
AT1G58320	/	1,3817	1,6004	/	1,44E-05	4,43E-07	PLAC8 family protein
AT1G59850	/	1,1239	/	/	1,27E-05	/	ARM repeat superfamily protein
AT1G60110	/	1,8476	1,5005	/	1,60E-11	5,34E-08	Mannose-binding lectin superfamily protein
AT1G63600	/	1,3229	1,1807	/	0,000544997	0,002040142	Receptor-like protein kinase-related family protein
AT1G67760	/	/	-1,2734	/	/	9,10E-06	TCP-1/cpn60 chaperonin family protein
AT1G67910	/	/	-1,3014	/	/	0,000533588	hypothetical protein
AT1G68350	/	/	-1,6431	/	/	1,74E-05	cotton fiber protein
AT1G70720	/	3,1817	4,301	/	5,71E-12	5,32E-21	Plant invertase/pectin methylesterase inhibitor superfamily protein
AT1G79780	/	2,3488	2,7628	/	0,002897803	0,000405063	Uncharacterized protein family (UPF0497)
AT2G02061	/	/	3,0951	/	/	0,000852477	Nucleotide-diphospho-sugar transferase family protein
AT2G05350	/	/	-1,4551	/	/	0,002285146	hypothetical protein
AT2G07774	/	/	-4,7646	/	/	0,00641489	hypothetical protein
AT2G10930	/	1,3461	/	/	0,004175882	/	transmembrane protein
AT2G15680	/	-1,117	/	/	0,001288606	/	Calcium-binding EF-hand family protein (CML30)
AT2G18680	-3,4898	/	/	0,003180494	/	/	transmembrane protein
AT2G20520	/	2,1415	2,0943	/	1,05E-07	1,99E-07	FASCICLIN-like arabinogalactan 6 (FLA6)
AT2G23540	-1,4231	-1,0986	/	0,001236846	0,005444375	/	GDSL-like Lipase/Acylhydrolase superfamily protein
AT2G28270	-2,1135	/	/	0,000330947	/	/	Cysteine/Histidine-rich C1 domain family protein
AT2G38600	/	-1,0483	-1,3465	/	6,39E-13	5,29E-20	HAD superfamily, subfamily IIIB acid phosphatase
AT2G40250	1,6606	/	/	6,19E-07	/	/	SGNH hydrolase-type esterase superfamily protein
AT2G45930	/	/	1,9341	/	/	0,006616415	hypothetical protein
AT2G47200	-1,7596	/	/	3,21E-06	/	/	hypothetical protein
AT2G47920	/	-1,0173	/	/	0,006627597	/	Kinase interacting (KIP1-like) family protein (NET3C)
AT3G01630	/	/	3,5525	/	/	0,009072787	Major facilitator superfamily protein
AT3G19430	/	-1,2184	/	/	2,01E-05	/	late embryosis abundant protein-related / LEA protein-like protein
AT3G20555	/	4,8021	4,8548	/	0,006405728	0,005790638	hypothetical protein

AT3G22210	/	/	-1,6341	/	/	0,001710843	transmembrane protein
AT3G22235	/	/	-1,0518	/	/	9,76E-07	cysteine-rich TM module stress tolerance protein
AT3G22770	/	/	-5,5068	/	/	0,001073941	F-box associated ubiquitination effector family protein
AT3G23930	/	/	-1,3036	/	/	0,000250056	troponin T, skeletal protein
AT3G24982	/	1,2221	2,7444	/	0,001698643	4,12E-13	receptor like protein 40 (RLP40)
AT3G27940	1,3523	/	-1,2486	2,71E-07	/	1,48E-06	LOB domain-containing protein 26 (LBD26)
AT3G28510	-2,0461	-1,5905	-2,1354	1,81E-05	0,00026821	1,26E-06	P-loop containing nucleoside triphosphate hydrolases superfamily protein
AT3G29000	/	1,2982	/	/	0,004294345	/	Calcium-binding EF-hand family protein
AT3G44790	/	/	-4,553	/	/	0,002100342	TRAF-like family protein
AT3G47480	/	1,9217	/	/	0,002287195	/	Calcium-binding EF-hand family protein
AT3G49380	/	/	1,0715	/	/	0,001294106	IQ-domain 15 (IQD15)
AT3G50180	/	/	2,3905	/	/	5,35E-05	transmembrane protein, putative (DUF247)
AT3G50290	/	/	1,239	/	/	0,001581154	HXXXD-type acyl-transferase family protein
AT3G53800	-1,5542	-1,2238	-2,2469	4,14E-06	4,49E-05	3,89E-12	Fes1B
AT3G55310	/	/	2,4241	/	/	1,89E-08	NAD(P)-binding Rossmann-fold superfamily protein
AT3G60280	/	1,1565	1,0962	/	3,62E-06	1,13E-05	Uclacyanin-3 (UCC3)
AT3G62430	/	-2,0638	-3,0963	/	0,001313627	2,06E-05	Protein with RNI-like/FBD-like domain
AT4G01390	/	/	1,1847	/	/	7,15E-06	TRAF-like family protein
AT4G07820	/	2,0567	1,9556	/	6,50E-11	5,46E-10	CAP (Cysteine-rich secretory proteins, Antigen 5, and Pathosis-related 1 protein) superfamily protein
AT4G08555	/	/	-1,3061	/	/	1,02E-08	hypothetical protein
AT4G09200	-3,3514	/	2,5901	0,001073221	/	0,004779633	SPla/RYanodine receptor (SPRY) domain-containing protein
AT4G09780	/	1,7251	2,2817	/	3,17E-06	4,68E-10	TRAF-like family protein
AT4G10640	/	2,4199	2,5954	/	1,19E-19	1,75E-22	IQ-domain 16 (IQD16)
AT4G10860	/	-3,9012	/	/	0,004105816	/	hypothetical protein
AT4G11950	/	/	1,2727	/	/	0,007328228	transmembrane protein, putative (DUF1191)
AT4G12170	2,8888	1,727	3,4575	0,001633586	6,57E-08	8,20E-29	Thioredoxin superfamily protein
AT4G12530	/	/	2,0184	/	/	0,00179919	Bifunctional inhibitor/lipid-transfer protein/seed storage 2S albumin superfamily protein
AT4G12545	/	/	1,4293	/	/	1,14E-23	Bifunctional inhibitor/lipid-transfer protein/seed storage 2S albumin superfamily protein
AT4G13290	3,2001	1,3366	2,3253	0,000952662	0,004297771	3,87E-07	cytochrome P450, family 71, subfamily A, polypeptide 19 (CYP71A19)
AT4G13860	/	1,0744	1,4216	/	2,32E-17	2,02E-29	RNA-binding (RRM/RBD/RNP motifs) family protein
AT4G14390	/	/	1,0454	/	/	1,92E-10	Ankyrin repeat family protein
AT4G15360	/	1,394	/	/	2,49E-07	/	cytochrome P450, family 705, subfamily A, polypeptide 3 (CYP705A3)
AT4G15990	/	/	3,1667	/	/	0,003110715	hypothetical protein
AT4G18510	/	/	1,0323	/	/	9,43E-14	CLAVATA3/ESR-related 2 (CLE2)
AT4G24890	/	/	-1,5471	/	/	0,005548922	purple acid phosphatase 24 (PAP24)
AT4G28405	/	/	-5,3376	/	/	0,003561999	Expressed protein

AT4G33145	/	/	-1,6002	/	/	0,009252518	hypothetical protein
AT4G39235	/	1,1147	/	/	0,002609576	/	hypothetical protein
AT4G39700	/	-1,1602	-1,4136	/	9,12E-05	2,50E-06	Heavy metal transport/detoxification superfamily protein
AT5G02390	/	1,0309	/	/	0,000522677	/	TRM32-like protein (DUF3741) (DAU1)
AT5G04210	/	-4,6948	/	/	0,004034912	/	CCCH-type zinc fingerfamily protein with RNA-binding domain-containing protein
AT5G09480	-1,5114	-1,128	/	7,42E-06	0,000202923	/	hydroxyproline-rich glycoprotein family protein
AT5G16330	-4,1981	/	/	0,002802004	/	/	NC domain-containing protein-like protein
AT5G17150	/	/	-2,7304	/	/	0,001832504	Cystatin/monellin superfamily protein
AT5G17720	/	3,589	4,6331	/	4,86E-06	2,50E-09	alpha/beta-Hydrolases superfamily protein
AT5G22555	/	/	2,0013	/	/	0,000645513	transmembrane protein
AT5G23240	-3,4477	/	-1,9419	3,41E-07	/	0,000587494	DNAJ heat shock N-terminal domain-containing protein
AT5G26300	/	1,3351	1,1507	/	6,81E-07	1,97E-05	TRAF-like family protein
AT5G26320	/	1,0277	1,0362	/	9,92E-08	7,63E-08	TRAF-like family protei
AT5G35525	/	/	-1,0367	/	/	5,31E-05	PLAC8 family protein
AT5G37240	/	/	-2,4312	/	/	0,001819905	hypothetical protein
AT5G37690	-1,6044	/	/	0,000250927	/	/	SGNH hydrolase-type esterase superfamily protein
AT5G38940	/	1,7406	1,7799	/	4,49E-23	4,62E-24	RmlC-like cupins superfamily protein
AT5G41280	/	1,2545	1,6015	/	2,53E-12	2,39E-19	Receptor-like protein kinase-related family protein
AT5G47600	1,329	/	/	0,00016503	/	/	HSP20-like chaperones superfamily protein
AT5G47950	/	/	1,2051	/	/	5,51E-66	HXXXD-type acyl-transferase family protein
AT5G48190	/	/	1,3664	/	/	5,13E-07	glycosyltransferase family protein (DUF23)
AT5G49350	-1,56	/	/	0,002952354	/	/	Glycine-rich protein family
AT5G52790	/	-1,0101	-1,4965	/	2,68E-09	2,91E-18	CBS domain protein with a domain protein (DUF21)
AT5G55770	/	/	1,43	/	/	1,66E-06	Cysteine/Histidine-rich C1 domain family protein
AT5G60350	/	/	-1,3839	/	/	0,008475498	hypothetical protein
AT5G62210	/	/	1,3971	/	/	0,000756759	Embryo-specific protein 3, (ATS3)
AT5G62360	-2,6907	-3,5346	-4,0334	0,000513755	2,79E-06	4,15E-07	Plant invertase/pectin methylesterase inhibitor superfamily protein
AT5G66610	/	1,0783	1,1755	/	1,84E-12	1,26E-14	DA1-related protein 7 (DAR7)

[A]Differentialy expressed genes (DEG) in *jaz2-6* (*jaz2*), *jaz2-6 jaz3-4* (*jaz2 jaz3*), and *jaz1-3 jaz2-6 jaz3-4* (*jazT*) root tips relative to WT samples. Each genotype was normalized to the WT (cutoff: Log2FC = ±1.0; p-value < 0,01). DEGs are organized by gene onthology (GO) functional classes and implemented manually. In many cases genes may fall into more than one category. Red highlighted Arabidopsis Genome Initiative codes (AGIs) depict genes in the cluster of stress response-related genes in *jaz2-6* that are particularly defense response-associated. Turquoise highlighted AGIs indicate genes in *jaz2-6* that are associated with water deprivation.

[B]Logarithmic Fold Change of the means of two biological replicated experiments. A negative number indicates down regulated genes.

[C]False Discovery rate (FDR) corrected p-value in comparison to WT.

/ = no significant fold change measured

FASTA sequences for gene synthesis

Capital letters indicate multisite GATEWAY attachment sites

>pASC021: pEN-R2-*UBQ10p*:*Ijas9*-*TOM**-L3

TACAGGTCACTAATACCATCTAAGTAGTTGATTCATAGTGACTGCATATGTTGTGTTTTACAGTATTATGTAGTCTG
TTTTTTATGCAAAATCTAATTTAATATATTGATATTTATATCATTTTACGTTTCTCGTTCAACTTTCTTGTACAAAGTG
Gagtctagctcaacagagcttttagtctagctcaacagagcttttaacccaaattggtacaatagaatacaactttagatcataattctcaaaagaaag
agattccttagctattctatctgccactccatttccttctcggcttgtatgcacaagcataaaatcctcaaacttgctaagtagatactttatgtcttggata
attggattgagacttgacaagcataactttcatgtaaccaaagacacaagttgctgagaatccacctcaaaaatgatcttcctataattgaatcgggat
aatgacagcacagcccatctaagagcctccacttctacttccagcacgcttcttacttttaccacagctcttgcacctaaccataacaccttccctgtatg
atcgcgaagcacccaccctaagccacattttaatccttctgttggccatgccccatcaaagttgcacttaacccaagattgtggtggagcttcccatgttt
ctcgtctgtcccgacggtgttgtggttggtgctttccttacattctgagcctctttccttctaatccactcatctgcatcttcttgtgtccttactaatacctca
ttggttccaaattccctcccctttaagcaccagctcgtttctgttcttccacagcctcccaagtatccaagggactaaagcctccacattcttcagatcagg
atattcttgtttaagatgttgaactctatggaggtttgtatgaactgatgatctaggaccggataagttcccttcttcatagcgaacttattcaaagaatgt
tttgtgtatcattcttgttacattgttattaatgaaaaaatattattggtcattggactgaacacgagtgttaaatatggaccaggccccaaataagatcc
attgatatatgaattaaataacaagaataaatcgagtcaccaaaccacttgccttttttaacgagacttgttcaccaacttgatacaaaagtcattatcc
tatgcaaatcaataatcatacaaaaatatccaataacactaaaaaattaaaagaaatggataatttcacaatatgttatacgataaagaagttacttttt
ccaagaaattcactgattttataagcccacttgcattagataaatggcaaaaaaaaacaaaaaggaaaagaaataaagcacgaagaattctagaaa
atacgaaatacgcttcaatgcagtgggacccacggttcaattattgccaattttcagctccaccgtatatttaaaaaataaaacgataatgctaaaaaa
atataaatcgtaacgatcgttaaatctcaacggctggatcttatgacgaccgttagaaattgtggttgtcgacgagtcagtaataaacggcgtcaaagt
ggttgcagccggcacacacgagtcgtgtttatcaactcaaagcacaaatacttttcctcaacctaaaaataaggcaattagccaaaaacaactttgcg
tgtaaacaacgctcaatacacgtgtcattttattattagctattgcttcaccgccttagctttctcgtgacctagtcgtcctcgtcttttcttcttcttcta
taaaacaatacccaaagagctcttcttcttcacaattcagatttcaatttctcaaaatcttaaaaactttctctcaattctctctaccgtgatcaaggtaaa
tttctgtgttccttattctctcaaaatcttcgattttgttttcgttcgatcccaatttcgtatatgttctttggtttagattctgttaatcttagatcgaagacga
ttttctgggtttgatcgttagatatcatcttaattctcgattagggtttcatagatatcatccgatttgttcaaataatttgagttttgtcgaataattactctt
cgatttgtgatttctatctagatctggtgttagtttctagtttgtgcgatcgaatttgtcgattaatctgagttttatgattccttcagtccctcaagctgctg
ctgcatccttggctcgggctttggagaagcgcaaagagaggcttatgagtgcaatgccatacaagaagatggggaaatccaactcaatactgaagct
atggctccaaagaagaagagaaaggtcatggtgagcaagggcgaggaggtcatcaaagagttcatgcgcttcaaggtgcgcatggagggctccat
gaacggccacgagttcgagatcgagggcgagggcgagggccgcccctacgagggcacccagaccgccaagctgaaggtgaccaagggcggccccc
tgcccttcgcctgggacatcctgtccccccagttcatgtacggctccaaggcgtacgtgaagcaccccgccgacatccccgattacaagaagctgtcct
tccccgagggcttcaagtgggagcgcgtgatgaacttcgaggacggcggtctggtgaccgtgacccaggactcctccctgcaggacggcacgctgatc
tacaaggtgaagatgcgcggcaccaacttcccccccgacggccccgtaatgcagaagaagaccatgggctgggaggcctccaccgagcgcctgtac
ccccgcgacggcgtgctgaagggcgagatccaccaggccctgaagctgaaggacggcggccactacctggtggagttcaagaccatctacatggcc
aagaagcccgtgcaactgcccggctactactacgtggacaccaagctggacatcacctcccacaacgaggactacaccatcgtggaacagtacgag
cgctccgagggccgccaccacctgttcctggggcatggcaccggcagcaccggcagcggcagctccggcaccgcctcctccgaggacaacaacatgg
ccgtcatcaaagagttcatgcgcttcaaggtgcgcatggagggctccatgaacggccacgagttcgagatcgagggcgagggcgagggccgccccta
cgagggcacccagaccgccaagctgaaggtgaccaagggcggccccctgccccttcgcctgggacatcctgtccccccagttcatgtacggctccaag
gcgtacgtgaagcaccccgccgacatccccgattacaagaagctgtccttccccgagggcttcaagtgggagcgcgtgatgaacttcgaggacggcg
gtctggtgaccgtgacccaggactcctccctgcaggacggcacgctgatctacaaggtgaagatgcgcggcaccaacttcccccccgacggccccgta
atgcagaagaagaccatgggctgggaggcctccaccgagcgcctgtacccccgcgacggcgtgctgaagggcgagatccaccaggccctgaagctg
aaggacggcggccactacctggtggagttcaagaccatctacatggccaagaagcccgtgcaactgcccggctactactacgtggacaccaagctgg
acatcacctcccacaacgaggactacaccatcgtggaacagtacgagcgctccgagggccgccaccacctgttcctgtacggcatggacgagctgta
caagtagaggtcactggattttggttttaggaattagaaattttattgatagaagtattttacaaatacaaatacatactaagggtttcttatatgctcaa
cacatgagcgaaaccctataagaaccctaattcccttatctgggaactactcacacattattctggagaaaaatagagagagatagatttgtagagag

agactggtgatttttgcggactctagCAACTTTATTATACAAAGTTGGCATTATAAAAAAGCATTGCTTATCAATTTGTTGCAA
CGAACAGGTCACTATCAGTCAAAATAAAATCATTATTT

>pASC011: pEN-L1-*JAZ1*-*CIT**-L2

CAAATAATGATTTTATTTTGACTGATAGTGACCTGTTCGTTGCAACAcATTGATGAGCAATGCTTTTTTATAATGCCA
ACTTTGTACAAAAAAGCAGGCTatgtcgagttctatggaatgttctgagttcgtcggtagccggagatttactgggaagaagcctagcttctc
acagacgtgtagtcgattgagtcagtatctaaaagagaacggtagctttggagatctgagcttaggaatggcatgcaagcctgatgtcaatggaactt
taggcaactcacgtcagccgacaacaaccatgagtttattcccttgtgaagcttctaacatggattccatggttcaagatgttaaaccgacgaatctgtt
tcctaggcaaccaagcttttcttcctcatcttcctctcttccaaaggaagatgttttgaaaatgacacagactaccagatctgtgaaaccagagtctcaa
actgcaccattgactatattctacgccgggcaagtgattgtattcaatgacttttctgctgagaaagccaaagaagtgatcaacttggcgagcaaaggc
accgctaatagcttagccaagaatcaaaccgatatcagaagcaacatcgctactatcgcaaaccaagttcctcatccaagaaaaaccacaacacaa
gagccaatccaatcctccccaacaccattgacagaacttcctattgctagaagagcttcacttcaccggttcttggagaagagaaaggacagagttac
gtcaaaggcaccataccaattatgcgatccagccaaagcgtcttcaaaccctcaaaccacaggcaacatgtcgtggctcggtttagcagctgaaatag
ggaaatccaactcaatactgaagcttatggctatggtgagcaagggcgaggagctgttcaccggggtggtgcccatcctggtcgagctggacggcga
cgtaaacggccacaagttcagcgtgtccggcgagggcgagggcgatgccacctacggcaagctgaccctgaagttcatctgcaccaccggcaagctg
cccgtgccctggcccaccctcgtgaccaccttcggctacggcctgatgtgcttcgcccgctaccccgaccacatgaagcagcacgacttcttcaagtcc
gccatgcccgaaggctacgtccaggagcgcaccatcttcttcaaggacgacggcaactacaagacccgcgccgaggtgaagttcgagggcgacacc
ctggtgaaccgcatcgagctgaagggcatcgacttcaaggaggacggcaacatcctggggcacaagctggagtacaactacaacagccacaacgtc
tatatcatggccgacaagcagaagaacggcatcaaggtgaacttcaagatccgccacaacatcgaggacggcagcgtgcagctcgccgaccactac
cagcagaacaccccccatcggcgacggccccgtgctgctgcccgacaaccactacctgagctaccagtccgccctgagcaaagaccccaacgagaag
cgcgatcacatggtcctgctggagttcgtgaccgccgccgggatcactctcggcatggacgagctgtacaagtagctagagtccgcaaaaatcaccag
tctctctctacaaatctatctctctctatttttctccagaataatgtgtgagtagttcccagataagggaattagggttcttatagggtttcgctcatgtgtt
gagcatataagaaacccttagtatgtatttgtatttgtaaaatacttctatcaataaaatttctaattcctaaaaccaaaatccagtgacctACCCAG
CTTTCTTGTACAAAGTTGGCATTATAAGAAAGCATTGCTTATCAATTTGTTGCAACGAACAGGTCACTATCAGTCAA
AATAAAATCATTATTTG

>pASC012: pEN-L1-*JAZ2*-*CIT**-L2

CAAATAATGATTTTATTTTGACTGATAGTGACCTGTTCGTTGCAACAcATTGATGAGCAATGCTTTTTTATAATGCCA
ACTTTGTACAAAAAAGCAGGCTatgtcgagtttttctgccgagtgttgggacttctctggtcgtaaaccgagctttcacaaacatgtactcga
ttgagtcgttacctgaaggagaagggtagttttggagatctgagcttagggatgacatgcaagcccgacgttaatggaggttcacgtcagcctacaat
gatgaatctgttcccttgtgaagcttcaggaatggattcttctgctggtcaagaagacattaaaccgaagactatgtttccgagacaatcaagcttttctt
cttcctcttcctctgggaccaaagaagatgtacagatgatcaaagagactactaaatctgtgaagccagagtctcaatctgctccgttgactatattcta
cggtggtcgagttatggtgtttgatgatttttctgctgagaaagctaaagaagtcattgatttggctaacaaaggaagtgccaaaagcttcacatgtttc
acagctgaagtaaacaataaccatagtgcttattctcaaaaagagattgcttctagcccaaatcctgtttgtagtcctgcaaaaaccgcagcacaaga
gccaattcagcctaacccggcctctttagcctgcgaactcccgattgcaagaagagcttcacttcatcggttccttgagaagaggaaggataggatcac
atcaaaggcaccataccaaatagacggttcagctgaagcgtcttccaagcctactaacccagcttggctcagttcacgggggaaatccaactcaatac
tgaagcttatggctatggtgagcaagggcgaggagctgttcaccggggtggtgcccatcctggtcgagctggacggcgacgtaaacggccacaagtt
cagcgtgtccggcgagggcgagggcgatgccacctacggcaagctgaccctgaagttcatctgcaccaccggcaagctgcccgtgccctggcccacc
ctcgtgaccaccttcggctacggcctgatgtgcttcgcccgctaccccgaccacatgaagcagcacgacttcttcaagtccgccatgcccgaaggctac
gtccaggagcgcaccatcttcttcaaggacgacggcaactacaagacccgcgccgaggtgaagttcgagggcgacaccctggtgaaccgcatcgag
ctgaagggcatcgacttcaaggaggacggcaacatcctggggcacaagctggagtacaactacaacagccacaacgtctatatcatggccgacaag

cagaagaacggcatcaaggtgaacttcaagatccgccacaacatcgaggacggcagcgtgcagctcgccgaccactaccagcagaacacccccatc
ggcgacggccccgtgctgctgcccgacaaccactacctgagctaccagtccgccctgagcaaagaccccaacgagaagcgcgatcacatggtcctgc
tggagttcgtgaccgccgccgggatcactctcggcatggacgagctgtacaagtagctagagtccgcaaaaatcaccagtctctctctacaaatctatc
tctctctatttttctccagaataatgtgtgagtagttcccagataagggaattagggttcttatagggtttcgctcatgtgttgagcatataagaaaccctt
agtatgtatttgtatttgtaaaatacttctatcaataaaatttctaattcctaaaaccaaaatccagtgacctACCCAGCTTTCTTGTACAAAGT
TGGCATTATAAGAAAGCATTGCTTATCAATTTGTTGCAACGAACAGGTCACTATCAGTCAAAATAAAATCATTATTT
G

>pASC013: pEN-L1-*JAZ3*-*CIT**-L2

CAAATAATGATTTTATTTTGACTGATAGTGACCTGTTCGTTGCAACAcATTGATGAGCAATGCTTTTTTATAATGCCA
ACTTTGTACAAAAAAGCAGGCTatggagagagattttctcgggttgggttcgaaaaattctccgatcactgtcaaggaggaaaccagcgaa
agctctagagattcagctcccaacagaggaatgaactggtctttctcaaacaaagtatcagcttcttcttctcagtttctatccttcaggccaactcaag
aagatagacatagaaagtctggaaattatcatcttcctcactctggttccttcatgccatcatcagtagctgatgtttatgattcaacccgcaaagctcct
tacagttctgtacagggagtgaggatgttccctaattccaatcaacacgaagaaactaacgcagtttccatgtcgatgccgggtttccagtctcatcatt
atgcaccaggaggaagaagcttcatgaacaataacaataactcacaacctttggtaggagttcctatcatggcacctccaatttcaatccttcctcctc
caggttccattgtagggactactgatattagatcttcttccaagccaataggttcacctgcgcagttgacgatcttttatgccggttcagtttgtgtttacg
atgacatatctcctgaaaaggcaaaggcgataatgttgctagctgggaacggttcctctatgcctcaagtcttttcgccgcctcaaactcatcaacaagt
ggtccatcatactcgtgcctctgtcgattcttcagctatgcctcctagcttcatgcctacaatatcttatcttagccctgaagctggaagtagcacaaacg
gactcggagccacaaaagcgacaagaggcttgacgtcaacatatcacaacaaccaagctaatggatccaatattaactgcccagtaccagtttcttgt
tctaccaatgtaatggctccaacagtggcattacctctggctcgcaaagcatccctggctaggtttttagagaaacgcaaagaaagggtcacgagcgt
atccccatattgcttagacaagaagtcatcgacagattgtcgcagatcaatgtctgaatgcattagttcttctctcagctctgcaaccgggaaatccaac
tcaatactgaagcttatggctatggtgagcaagggcgaggagctgttcaccggggtggtgcccatcctggtcgagctggacggcgacgtaaacggcc
acaagttcagcgtgtccggcgagggcgagggcgatgccacctacggcaagctgaccctgaagttcatctgcaccaccggcaagctgcccgtgccctg
gcccaccctcgtgaccaccttcggctacggcctgatgtgcttcgcccgctaccccgaccacatgaagcagcacgacttcttcaagtccgccatgcccga
aggctacgtccaggagcgcaccatcttcttcaaggacgacggcaactacaagacccgcgccgaggtgaagttcgagggcgacaccctggtgaaccg
catcgagctgaagggcatcgacttcaaggaggacggcaacatcctggggcacaagctggagtacaactacaacagccacaacgtctatatcatggc
cgacaagcagaagaacggcatcaaggtgaacttcaagatccgccacaacatcgaggacggcagcgtgcagctcgccgaccactaccagcagaaca
cccccatcggcgacggccccgtgctgctgcccgacaaccactacctgagctaccagtccgccctgagcaaagaccccaacgagaagcgcgatcacat
ggtcctgctggagttcgtgaccgccgccgggatcactctcggcatggacgagctgtacaagtagctagagtccgcaaaaatcaccagtctctctctaca
aatctatctctctctatttttctccagaataatgtgtgagtagttcccagataagggaattagggttcttatagggtttcgctcatgtgttgagcatataag
aaacccttagtatgtatttgtatttgtaaaatacttctatcaataaaatttctaattcctaaaaccaaaatccagtgacctACCCAGCTTTCTTGTA
CAAAGTTGGCATTATAAGAAAGCATTGCTTATCAATTTGTTGCAACGAACAGGTCACTATCAGTCAAAATAAAATC
ATTATTTG

>pASC014: pEN-L1-*JAZ4*-*CIT**-L2

CAAATAATGATTTTATTTTGACTGATAGTGACCTGTTCGTTGCAACAcATTGATGAGCAATGCTTTTTTATAATGCCA
ACTTTGTACAAAAAAGCAGGCTatggagagagattttctcgggctgggatcaaagttatctccgataactgtgaaggaggaaactaacgaa
gattcagccccaagtagaggtatgatggattggtcattctcaagcaaagtcggttctggtcctcagtttctttcttttgggacatcccaacaagaaacgc
gtgtaaacacagtcaatgatcatttgctttcttctgctgcaatggatcaaaaccagagaacttacttcagctcactacaggaagacagagtgttcccag
gttccagtcagcaagaccaaacaaccatcacagtctccatgtccgaaccaaactacatcaacagtttcataaaccaccaacatttaggaggatctcct
atcatggcacctccagtttcagtatttcctgctccaaccactattagatcttcttcaaaaccacttccccctcagttgacaatcttttatgccggttcagtat

tagtttaccaagacatagctcctgaaaaggcccaagctatcatgttgctagccggaaatggacctcatgctaaaccggtttcacaacctaaacctcaa
aaactggttcatcactctcttccaaccactgatcctccaactatgcctcctagtttcctgccttccatctcttacattgtctctgaaaccagaagtagtgga
tccaacggggttactggacttggaccaacaaaaacaaaggcgagtttagcatccacgcgcaacaaccaaactgctgccttctctatggctccaacagt
gggtttaccacaaacacgcaaagcatccttggctcggttcttagagaaacgcaaagaaagggtcattaacgtatcaccttattacgtagacaacaagt
catcaatagactgtagaacactgatgtctgaatgtgtaagctgtcctccagctcatcatctgcacgggaaatccaactcaatactgaagcttatggctat
ggtgagcaagggcgaggagctgttcaccggggtggtgcccatcctggtcgagctggacggcgacgtaaacggccacaagttcagcgtgtccggcga
gggcgagggcgatgccacctacggcaagctgaccctgaagttcatctgcaccaccggcaagctgcccgtgccctggcccaccctcgtgaccaccttcg
gctacggcctgatgtgcttcgcccgctaccccgaccacatgaagcagcacgacttcttcaagtccgccatgcccgaaggctacgtccaggagcgcacc
atcttcttcaaggacgacggcaactacaagacccgcgccgaggtgaagttcgagggcgacaccctggtgaaccgcatcgagctgaagggcatcgact
tcaaggaggacggcaacatcctggggcacaagctggagtacaactacaacagccacaacgtctatatcatggccgacaagcagaagaacggcatc
aaggtgaacttcaagatccgccacaacatcgaggacggcagcgtgcagctcgccgaccactaccagcagaacaccccccatcggcgacggccccgtg
ctgctgcccgacaaccactacctgagctaccagtccgccctgagcaaagaccccaacgagaagcgcgatcacatggtcctgctggagttcgtgaccg
ccgccgggatcactctcggcatggacgagctgtacaagtagctagagtccgcaaaaatcaccagtctctctctacaaatctatctctctctatttttctcc
agaataatgtgtgagtagttcccagataagggaattagggttcttatagggtttcgctcatgtgttgagcatataagaaacccttagtatgtatttgtatt
tgtaaaatacttctatcaataaaatttctaattcctaaaaccaaaatccagtgacctACCCAGCTTTCTTGTACAAAGTTGGCATTATAA
GAAAGCATTGCTTATCAATTTGTTGCAACGAACAGGTCACTATCAGTCAAAATAAAATCATTATTTG

>pASC016: pEN-L1-*JAZ6*-*CIT**-L2

CAAATAATGATTTTATTTTGACTGATAGTGACCTGTTCGTTGCAACAcATTGATGAGCAATGCTTTTTTATAATGCCA
ACTTTGTACAAAAAAGCAGGCTatgtcaacgggacaagcgccggagaagtccaatttttctcagagatgtagtctgctcagccggtacttga
aggagaagggaagttttgggaatattaatatggggttggctcgaaaatccgatcttgaactcgccggaaaattcgatctcaaaggacaacaaaatgt
gattaagaaggtagagacctcagaaactagaccgttcaagttgattcagaagttttctattggtgaggcctctacttctaccgaagacaaagccatata
tattgatctcagtgaaccggcaaaagtagcaccggagtctggaaattcacagttgaccatattctttggaggaaaagttatggttttcaacgagtttcct
gaagacaaagctaaggagataatggaagtagctaaagaagcgaatcatgttgctgttgattctaagaacagtcagagtcacatgaatcttgacaaaa
gcaacgtggtgattcccgatcttaacgagccaacgagttccgggaacaatgaagatcaagaaactgggcagcaacatcaggttgtggaacgcattgc
aagaagagcttctcttcatcgattctttgctaaacgaaaagacagggctgtggctagagctccatatcaagtgaaccaacacggtagtcatcttcctcc
caagccagagatggttgctccatcgataaagtcaggccaatcgtcgcaacacattgcaactcctccaaaaccaaaggcccataaccatatgccgatg
gaggtggacaagaaagaaggacaatcttccaaaaaccttgaactcaagcttgggaaatccaactcaatactgaagcttatggctatggtgagcaagg
gcgaggagctgttcaccggggtggtgcccatcctggtcgagctggacggcgacgtaaacggccacaagttcagcgtgtccggcgagggcgagggcg
atgccacctacggcaagctgaccctgaagttcatctgcaccaccggcaagctgcccgtgccctggcccaccctcgtgaccaccttcggctacggcctga
tgtgcttcgcccgctaccccgaccacatgaagcagcacgacttcttcaagtccgccatgcccgaaggctacgtccaggagcgcaccatcttcttcaagg
acgacggcaactacaagacccgcgccgaggtgaagttcgagggcgacaccctggtgaaccgcatcgagctgaagggcatcgacttcaaggaggac
ggcaacatcctggggcacaagctggagtacaactacaacagccacaacgtctatatcatggccgacaagcagaagaacggcatcaaggtgaacttc
aagatccgccacaacatcgaggacggcagcgtgcagctcgccgaccactaccagcagaacaccccccatcggcgacggccccgtgctgctgcccgac
aaccactacctgagctaccagtccgccctgagcaaagaccccaacgagaagcgcgatcacatggtcctgctggagttcgtgaccgccgccgggatca
ctctcggcatggacgagctgtacaagtagctagagtccgcaaaaatcaccagtctctctctacaaatctatctctctctatttttctccagaataatgtgt
gagtagttcccagataagggaattagggttcttatagggtttcgctcatgtgttgagcatataagaaacccttagtatgtatttgtatttgtaaaatactt
ctatcaataaaatttctaattcctaaaaccaaaatccagtgacctACCCAGCTTTCTTGTACAAAGTTGGCATTATAAGAAAGCATT
GCTTATCAATTTGTTGCAACGAACAGGTCACTATCAGTCAAAATAAAATCATTATTTG

>pASC017: pEN-L1-*JAZ9*-*CIT**-L2

CAAATAATGATTTTATTTTGACTGATAGTGACCTGTTCGTTGCAACAcATTGATGAGCAATGCTTTTTTATAATGCCA
ACTTTGTACAAAAAAGCAGGCTatggaaagagattttctgggtttgagcgacaagcagtatctaagtaataacgttaagcatgaggttaacg
atgatgctgtcgaagaacgagggttaagtacgaaggcagctagagaatgggggaagtcaaaggtttttgctacttcaagtttcatgccttcttcagatt
tccaggaggctaaggcgtttccgggtgcataccagtggggatcagtttctgcggccaatgttttccgcagatgccaatttggtggtgcgtttcaaaacgc
gacgccgcttttactaggcggttcagttcctttaccaactcatccttctcttgttccacgagtggcttcctccggatcatctcctcagctcacaatcttttat
ggcggaactataagcgtctttaatgacatatctcccgataaggctcaagccatcatgttatgcgccgggaacggtttgaaaggtgaaactggagatag
caaaccggttcgagaagctgaaagaatgtatggaaaacaaatccataacactgctgctacctcatcaagctctgccactcacactgataatttctcaa
ggtgtagggacacacccgttgctgcgactaatgcaatgagcatgatcgaatcattcaatgcagctcctcgtaacatgattccttcagtccctcaagctcg
gaaagcatccttggctcggttcttggagaagcgcaaagagaggcttatgagtgcaatgccatacaagaagatgcttcttgatttgtcgaccggagaat
ccagtggaatgaattactcttctacttctcctacagggaaatccaactcaatactgaagcttatggctatggtgagcaagggcgaggagctgttcaccg
gggtggtgcccatcctggtcgagctggacggcgacgtaaacggccacaagttcagcgtgtccggcgagggcgagggcgatgccacctacggcaagc
tgaccctgaagttcatctgcaccaccggcaagctgcccgtgccctggcccaccctcgtgaccaccttcggctacggcctgatgtgcttcgcccgctaccc
cgaccacatgaagcagcacgacttcttcaagtccgccatgcccgaaggctacgtccaggagcgcaccatcttcttcaaggacgacggcaactacaag
acccgcgccgaggtgaagttcgagggcgacaccctggtgaaccgcatcgagctgaagggcatcgacttcaaggaggacggcaacatcctggggcac
aagctggagtacaactacaacagccacaacgtctatatcatggccgacaagcagaagaacggcatcaaggtgaacttcaagatccgccacaacatc
gaggacggcagcgtgcagctcgccgaccactaccagcagaacaccccccatcggcgacggccccgtgctgctgcccgacaaccactacctgagctacc
agtccgccctgagcaaagaccccaacgagaagcgcgatcacatggtcctgctggagttcgtgaccgccgccgggatcactctcggcatggacgagct
gtacaagtagctagagtccgcaaaaatcaccagtctctctctacaaatctatctctctctatttttctccagaataatgtgtgagtagttcccagataagg
gaattagggttcttatagggtttcgctcatgtgttgagcatataagaaacccttagtatgtatttgtatttgtaaaatacttctatcaataaaatttctaatt
cctaaaaccaaaatccagtgacctACCCAGCTTTCTTGTACAAAGTTGGCATTATAAGAAAGCATTGCTTATCAATTTGTTG
CAACGAACAGGTCACTATCAGTCAAAATAAAATCATTATTTG

>pASC020: pEN-L1-*JAZ10*-*CIT**-L2

CAAATAATGATTTTATTTTGACTGATAGTGACCTGTTCGTTGCAACAcATTGATGAGCAATGCTTTTTTATAATGCCA
ACTTTGTACAAAAAAGCAGGCTatgtcgaaagctaccatagaactcgatttcctcggacttgagaagaaacaaaccaacaacgctcctaag
cctaagttccagaaatttctcgatcgccgtcgtagtttccgagatattcaaggtgcgatttcgaaaatcgatccggagattatcaaatcgctgttagcttc
cactggaaacaattccgattcatcggctaaatctcgttcggttccgtctactccgagggaagatcagcctcagatcccgatttctccggtccacgcgtct
ctcgccaggtctagtaccgaactcgtttcgggaactgttcctatgacgattttctacaatggaagtgtttcagttttccaagtgtctcgtaacaaagctgg
tgaaattatgaaggtcgctaatgaagcagcatctaagaaagacgagtcgtcgatggagacagatctttcggtaattcttccgaccactctaagaccaa
agctctttggccagaatctagaaggagatcttcccatcgcaaggagaaagtcactgcaacgttttctcgagaagcgcaaggagagattagtatcaaca
tctccttactatccgacatcggccgggaaatccaactcaatactgaagcttatggctatggtgagcaagggcgaggagctgttcaccggggtggtgcc
catcctggtcgagctggacggcgacgtaaacggccacaagttcagcgtgtccggcgagggcgagggcgatgccacctacggcaagctgaccctgaa
gttcatctgcaccaccggcaagctgcccgtgccctggcccaccctcgtgaccaccttcggctacggcctgatgtgcttcgcccgctaccccgaccacatg
aagcagcacgacttcttcaagtccgccatgcccgaaggctacgtccaggagcgcaccatcttcttcaaggacgacggcaactacaagacccgcgccg
aggtgaagttcgagggcgacaccctggtgaaccgcatcgagctgaagggcatcgacttcaaggaggacggcaacatcctggggcacaagctggagt
acaactacaacagccacaacgtctatatcatggccgacaagcagaagaacggcatcaaggtgaacttcaagatccgccacaacatcgaggacggca
gcgtgcagctcgccgaccactaccagcagaacaccccccatcggcgacggccccgtgctgctgcccgacaaccactacctgagctaccagtccgccct
gagcaaagaccccaacgagaagcgcgatcacatggtcctgctggagttcgtgaccgccgccgggatcactctcggcatggacgagctgtacaagtag
ctagagtccgcaaaaatcaccagtctctctctacaaatctatctctctctatttttctccagaataatgtgtgagtagttcccagataagggaattagggt
tcttatagggtttcgctcatgtgttgagcatataagaaacccttagtatgtatttgtatttgtaaaatacttctatcaataaaatttctaattcctaaaacc

aaaatccagtgacctACCCAGCTTTCTTGTACAAAGTTGGCATTATAAGAAAGCATTGCTTATCAATTTGTTGCAACGAA
CAGGTCACTATCAGTCAAAATAAAATCATTATTTG

Acknowledgment

I would like to extend my heartfelt gratitude to everyone who supported me throughout my journey as a PhD student and during the writing process.

First, I would like to convey my sincere appreciation to Dr. Debora Gasperini for providing me with the opportunity to contribute to this project. Inspired by her scientific acumen, I gained valuable insights into scientific thinking and practices. The scientific discussions with her not only offered encouragement but also served as a constant source of motivation. I am thankful for her open mind and the consistent opportunity to discuss various aspects with her at any time. Even when I was struggling with the project or with myself during my PhD journey, she unwaveringly offered support even beyond my research and maintained faith in my abilities.

Moreover, I would like to express my gratitude to the entire IPB and the DFG for making my PhD journey possible. A big thank you goes to my committee members, Prof. Dr. Steffen Abel, Dr. Luz Irina A. Calderón Villalobos, and Dr. Justin Lee, for providing valuable insights and feedback that have expanded my perspective and enriched my scientific thinking. I extend my appreciation to PD Dr. Susanne Berger, Prof. Dr. Sascha Laubinger, and Prof. Dr. Steffen Abel for reviewing my thesis. Furthermore, I want to thank Prof. Dr. Steffen Abel for affording me the opportunity to be a part of the MSV department. I would also like to acknowledge Prof. Dr. Bettina Hause and Hagen Stellmach for their gracious introduction to the LSM microscopes and their consistent assistance with technical and other related issues. I would like to express my thanks to Dr. Carolin Delker for her valuable statistical workshop, which greatly aided me in the analysis of my data. Additionally, I want to thank Dr. Martin Schattat for his comprehensive Fiji workshop, which proved me the instrumental knowledge to quantify my reporters.

I would also like to extend my thanks to everyone in the MSV department for their kindness and inclusion. Thank is especially owed to the former and current people from our neighbouring lab—Michael Niemeyer, Elena Moreno Castillo, and Tobias Wagner. Their openness to scientific discussions proved invaluable, contributing significantly to my diverse perspectives.

A big thank you goes also to all former and current members of our workgroup. I express gratitude to Adina Schulze and Henrikje Smits for their preliminary data contributions. Additionally, I want to give special thanks to Marlene Zimmer, who imparted her knowledge with passion and patience, particularly in guiding me through the technical aspects of the lab. Thanks for managing the lab; without your organizational efforts, we all would have been lost. A big acknowledgment goes to Verona Wilde, who

seamlessly took over all responsibilities after Marlene left. Her organizational and technical skills, as well as fresh insights have been instrumental in keeping the lab running smoothly. A big shoutout goes to Mukesh Meena, whose kindness and willingness to help have been invaluable. He not only assisted me with a friendly demeanour but also imparted a wealth of knowledge on genetic matters and more. Many thanks go to Yunjing Ma, whose invaluable companionship greatly enriched my time here. Her profound mental mindset imparted invaluable lessons, contributing significantly to my personal and intellectual growth. I would also like to thank Madalen Robert. Her perpetual cheerfulness brightened my time here and provided me encouragement. The insights she shared from her own research were consistently inspiring. I want to also thank Jhonny Oscar Figueroa Parra, who provided me valuable insights into biochemical aspects and offered a great introduction to GraphPad, which helped me with my analyses. Moreover, I thank our former Master student, Ronny Hennig. His precise work and encouraging manner were always very reliable. A big thank you goes to Stefan Mielke, who consistently had an open ear for both scientific and personal matters. He patiently taught me numerous technical aspects and was always there to talk to. I would also like to thank him for the preliminary data her provided. Thanks for the coffee breaks with you all; they greatly contributed to replenishing my energy and keeping me going. Thank you for assisting me with all my matters, extending your support beyond the scope of my project. Furthermore, I extend my thanks to Mariem Ben Sala, Udita Acharya, and Haojie Wang. Despite our relatively short acquaintance, I am grateful for your open and inclusive characters.

A big gratitude goes to my family and my friends. Especially, I want to say thank you to my father and my mother for consistently backing me up. Your unwavering support and belief in me, regardless of the circumstances, mean a lot to me. I would also to thank my sister, Antje, and my brother, Peter. Despite the physical distance that separates us, your unwavering mental support was precious.

My biggest thank goes to the most important people in my life: my incredible girlfriend, Anna, and my wonderful daughter, Viola. Your sacrifice for me is truly remarkable. The fact that you travelled all the way to Halle, dedicating your time and patience, is not taken for granted. You supported me mentally. Your encouragement has been invaluable, aiding in my personal growth. Your unwavering belief in me has never wavered. I am profoundly grateful for you being in my life, and words cannot adequately express my love for you. Without you, I wouldn't have made it. I dedicate this work to both of you.

Curriculum Vitae

Personal Details

Name: Andreas Schenke

Education, Research, and Work

Since 01/2024	**Teacher** Neustadt-Sekundarschule Weißenfels, Weißenfels
Since 01/2023	**Doctoral Student (Guest contract)** Leibniz-Institute for Plant Biochemistry, Halle (Saale) Department: "Molecular Signal Processing" Research Group: "Jasmonate Signaling" Supervisor: Dr. Debora Gasperini
11/2018 – 12/2022	**Doctoral Student** Leibniz-Institute for Plant Biochemistry, Halle (Saale) Department: "Molecular Signal Processing" Research Group: "Jasmonate Signaling" Supervisor: Dr. Debora Gasperini
10/2015 – 03/2018	**Master of Science in Biology** (completion) Albert-Ludwigs-University Freiburg Master-Thesis: "Interaction between Phytochrome A and Jasmonate Signalling"

02/2015 – 10/2018	**Laboratory Assistant** (in part time) Material Analytischer Service GmbH (M.A.S.), Freiburg (Breisgau)
10/2013 – 10/2014	**Social Care Worker** L'Arche Antigonish, Antigonish (Canada)
10/2012 – 09/2013	**Master of Science in Biology** Ludwig-Maximilian-Universität, München
10/2010 – 09/2012	**Bachelor of Science in Biology** (completion) Ludwig-Maximilian-Universität, München Bachelor-Thesis: "Diversität von Wildhundearten – Geometrisch morphometrische Analyse zur Ermittlung der Formveränderung des Schädels von Wildhunden im Vergleich zum Europäischen Wolf"
10/2009 – 09/2009	**Bachelor of Science in Biology** University of Hohenheim, Stuttgart
2006 – 2009	**Abitur** Käthe-Kollwitz-Schule (biotechnologisches Gymnasium) in Esslingen am Neckar
2000 – 2006	**Secondary School Leaving Certificate** (**Realschulreife)** Realschule Gerlingen, Gerlingen

Conference attendances during the time as Doctoral Student

-10/2019: 11th "International PhD School Plant Development" with oral presentation, Zellingen-Retzbach, Germany

- 06/2019: "Plant Science Student Conference" with oral presentation, Halle (Saale), Germany

Halle (Saale), February 2024

Andreas Schenke

Eidesstattliche Erklärung (Statutory declaration)

Hiermit erkläre ich an Eides statt, dass ich mich mit der vorliegenden wissenschaftlichen Arbeit erstmals um die Erlangung des Doktorgrades bewerbe, die Arbeit selbstständig und ohne fremde Hilfe verfasst, nur die angegebenen Quellen und Hilfsmittel genutzt und die den benutzten Werken wörtlich oder inhaltlich entnommenen Stellen als solche kenntlich gemacht habe.

Halle (Saale), den_____ _____

Andreas Schenke